1983

Synthesis of multidentate nitrile and isonitrile ligands and their transition-metal complexes

Daniel Tear Plummer
Iowa State University

8316332

Plummer, Daniel Tear

SYNTHESIS OF MULTIDENTATE NITRILE AND ISONITRILE LIGANDS AND THEIR TRANSITION-METAL COMPLEXES

Iowa State University PH.D. 1983

University
Microfilms
international 300 N. Zeeb Road, Ann Arbor, MI 48106

Synthesis of multidentate nitrile and isonitrile ligands and their transition-metal complexes

by

Daniel Tear Plummer

A Dissertation Submitted to the

Graduate Faculty in Partial Fulfillment of the

Requirements for the Degree of

DOCTOR OF PHILOSOPHY

Department: Chemistry
Major: Inorganic Chemistry

Approved:

Signature was redacted for privacy.

In Charge of Major Work

Signature was redacted for privacy.

For the Major Department

Signature was redacted for privacy.

For the Graduate College

Iowa State University
Ames, Iowa

1983

TABLE OF CONTENTS

LIST OF FIGURES

LIST OF TABLES

DEDICATION

To my mother and father

SYMBOLS AND ABBREVIATIONS

Ar	an aromatic radical
br	broad
Bu	butyl
COD	cycloocta-1,5-diene
Cy	cyclohexyl
Cp	cyclopentadienyl
d	doublet
diphos	1,2-bis(diphenylphosphino)ethane
Et	ethyl
L	a donor ligand
L-L	a symmetrical bidentate donor ligand
L-L'	an unsymmetrical bidentate donor ligand
m	multiplet (^{1}H NMR)
	medium (IR)
M	a metal atom or ion
Me	methyl
MLCT	metal-to-ligand charge transfer
nor	norbornadiene ([2.2.1]-bicyclohepta-2,5-diene)
p	pentet
ϕ or Ph	phenyl
Pr	propyl
R	an organic radical (usually H or alkyl)
s	singlet (^{1}H NMR)
	strong (IR)
sh	shoulder
t	triplet
THF	tetrahydrofuran
TLC	thin layer chromatography
vs	very strong
vw	very weak
w	weak
xcs	excess
X	an inorganic radical (usually halogen)
Y	an organic diradical

I. INTRODUCTION

A. General Comments

Synthetic chemistry involving chelating ligands dates back to the late 1880s, when Jörgensen prepared the first transition-metal complexes of ethylenediamine.[1,2] Several years later, Werner[3] suggested the correct structure for cis-$PtCl_2(H_2NCH_2CH_2NH_2)$. Soon thereafter, Ley[4] recognized that certain chelated complexes exhibited surprisingly lower reactivities than their parent aqueous ions. Work throughout the early 20th century continued to underscore the marked stability of complexes of chelating ligands with respect to those of monodentate ligands. An important report by Spike and Parry[5] in 1953 lent strong experimental evidence to the notion that this enhanced stability, or the so-called "chelate effect", was entropic rather than enthalpic in nature. In that work, it was shown that the displacement of two or more ligands by one chelating ligand took place with a large, positive entropy change. This entropy change arises from the fact that two particles react to give three; the total translational entropy in the latter case is suspected to be substantially higher.[6] The effect of a large ΔS as seen by the Gibbs-Helmholtz equation, $\Delta G = \Delta H - T\Delta S$, is to decrease ΔG greatly, assuming a relatively small ΔH. A more negative ΔG, of course, represents a larger equilibrium constant in favor of the chelated product. A rather recent investigation[7] into the thermodynamics of chelation supports the preceding classical view in essence, but

stresses that enthalpy changes for chelation reactions may be larger than previously assumed and that in systems deviating from ideality (that is, at high concentrations and/or under conditions of extensive hydrogen bonding), the observed thermodynamic results are not always readily predictable.

Manifestations of the chelate effect have held and continue to hold great interest for the chemist, both in theory and practice. Optimization of geometric and donor properties of chelating ligands has led to the development of potent metal-ion binders and sequestering agents. One well-known example is ethylenediaminetetraacetic acid and similar compounds, which have found many uses in the household, industry, and the chemical laboratory. Clinical medicine also finds use for such chelating agents; the recent development of the enterochelins by Raymond and coworkers[8,9] holds promise in the treatment of iron and plutonium poisoning. Because of their abilities to alter chemistry at metal center, a number of chelating ligands have had important applications in organometallic chemistry. In some cases, the ligand may serve only to alter the "natural" stereochemistry at a metal site with respect to monodentate ligands.[10] In other cases, the chelate effect may stabilize a certain structural type which is unknown for non-chelating ligands, as in $Cr(diphos)_3$.[11] The introduction of chiral diphosphine ligands into homogeneous catalysts has led to highly selective asymmetric synthesis of amino acids from prochiral substrates.[12] In theory, a properly constructed ligand system

might produce a highly destabilized metal center capable of carrying out an efficient catalytic reaction, in analogy to such "entatic states" in biological systems.[13]

B. The Present Research

Angelici, Quick, and Kraus reported the synthesis of two bidentate ligands containing the linear nitrile ("DiCN") and isonitrile ("DiNC") functional groups.[14] These ligands were shown to undergo reactions with

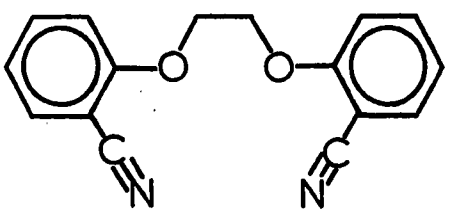

DiCN

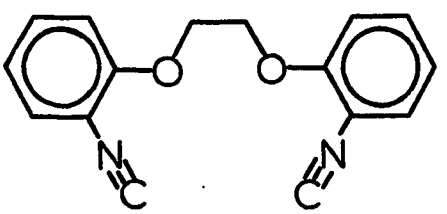

DiNC

organometallic substrates such as $Mn(CO)_5Br$, $[CpFe(CO)_2(CS)]PF_6$, and others to yield products $Mn(CO)_3(L\text{-}L)Br$ and $[CpFe(L\text{-}L)(CS)]PF_6$, respectively, where (L-L) represents either the DiCN or DiNC ligand. The mass spectrum of the complex $Mo(CO)_4$(DiNC) exhibited a parent ion as expected for the mononuclear product, providing strong evidence that a thirteen-member chelate ring had been formed. Assuming the corresponding nitrile complexes to be isostructural, the DiCN - containing complexes

appear to be the first examples of dinitrile ligands capable of chelation through the nitrogen lone pairs to a single metal center. The DiNC ligand joined several other ligands in the current literature as examples of chelating diisonitriles.[15,16]

The present research is concerned with extensions of the preceding work in several directions. It was first of interest to extend the chemistry of DiNC ligands to other pseudooctahedral metal systems with the idea of more fully characterizing such large-ring chelates and to attempt preparations of complexes containing metals in unusual oxidation states. Secondly, it was hoped that complexes with preferred ligand-metal-ligand angles of greater than 90° could be prepared. The scope of the present research also includes the design, synthesis, and reactivity of other nitrile and isonitrile ligands which might form chelate rings with fewer or greater than thirteen ring members, as well as ligands with three and four linear donor groups.

C. Principles of Ligand Design

Of all the chelating ligands to be studied since the days of Jörgensen and Werner, the vast majority have employed donor atoms with tetrahedral or trigonal-planar geometries. That is, a general chelating ligand of the type :A—X—$(Y)_n$—X—A: will bind to a metal M with an M—A—X angle, θ, where θ is something quite far from 180°. In most cases this angle will be somewhere between 105° and 120°, as with amines, phosphines, carboxylates, diolates, imines, etc. As an example, the structure of chelated ethylenediamine is shown in Figure 1.

ethylenediamine

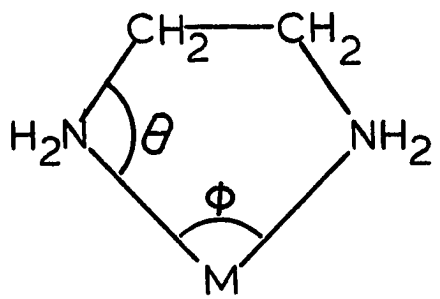

$\theta \cong 110^\circ$ $\Phi \cong 90^\circ$

succinonitrile

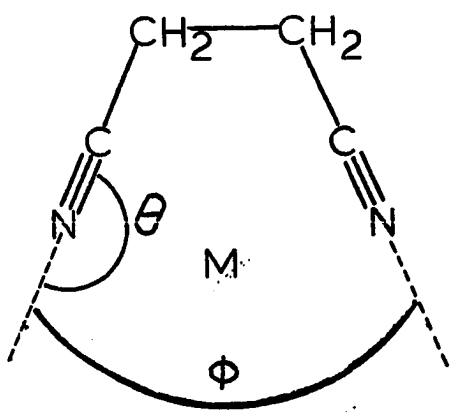

$\theta \cong 180^\circ$ $\Phi \cong 38^\circ$

Figure 1. Orientation of ethylenediamine and succinonitrile at a single metal center

Ligands such as acetylides,[17] nitriles,[18] and isonitriles,[19] however, usually bid to metals with an angle, Θ, of approximately 180° (Figure 2). Realization of this fact is quite important in the design of potentially chelating ligands with linear donor groups. Both chemical evidence and the construction of molecular models agree that ethylenediamine should chelate quite efficiently to a metal center while the analogous dinitrile, succinonitrile, won't. In fact, a simple calculation or molecular model shows that the -C≡N: groups in the latter case diverge away from the metal center at an angle of about 38° (see Figure 1). The desired situation is one in which these groups converge at an angle of about 90°.

It should be noted that metal complexes containing side-on bonded nitriles have been observed, but only in a small number of cases. These include the carbonitrile CF_3CN[20] and several N,N-disubstituted cyanamides.[21,22]

In order to achieve the desired end-on bonding in a bidentate ligand of the linear type, it is clear that the size of the potential chelate ring must be expanded. Space-filling molecular models suggest that such a system should contain at least twelve, and preferably, thirteen carbon, nitrogen and/or oxygen atoms. In this way, the metal-binding chelate groups can be directed toward the metal in an end-on fashion at an angle of 90°. The diisonitriles 1,7-diisocyanoheptane and 1,8-diisocyanooctane would then be expected to yield chelated complexes with twelve and thirteen ring members, respectively. In several

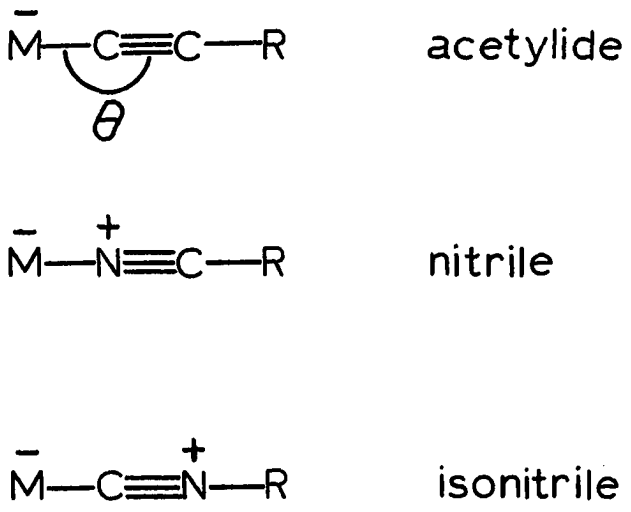

Figure 2. Representations of metal-bound acetylide, nitrile, and isonitrile ligands

studies[15,16] carried out with a series of α,ω-diisocyanoalkanes it was indeed found that the heptane and octane derivatives chelate to Rh(I), giving the structural unit $[Rh(CN-(CH_2)_n-NC)_2]^+$ (n = 7 or 8). With six or fewer methylene units, the ligands bridge two metal centers to form the binuclear structural units $[Rh_2(CN-(CH_2)_n-NC)_4]^{2+}$ (n = 3-6).

Based on these studies, as well as on investigations with molecular models and the preliminary results of Angelici et al.,[14] it seems fairly certain that successful chelating linear ligands will have at least twelve or thirteen total ring members (i.e. seven or eight atoms joining the chelating groups). Smaller rings would most likely be strained, at the expense of metal-ligand bonding. Hence, ligand geometry should be adjusted so as to allow for maximum overlap of ligand and metal bonding orbitals, and therefore, maximum ligand-metal bond energy.

Perhaps a secondary enthalpic consideration is important as well, involving ring strain not at the metal center, but within the organic portions of the chelate ring. It is known that "medium-sized" organic rings containing eight to eleven members suffer from enthalpic strains due to bond opposition forces, transannular van der Waal's interactions, and bond angle deformations. These factors are thought to be partially responsible for low synthetic yields and high strain energies for medium- to large-ring hydrocarbons[23,24] and metal chelate rings of diamino-alkanes.[25] Minor alterations of the chelate ring size and the introduction of heteroatoms can also affect the strain enthalpy in the organic ring.[26]

Were enthalpic considerations of singular importance in determining the free energy change for a chelation reaction, the design of bidentate ligands would be easier, since a number of ring sizes would be nearly equally effective once ligand-metal bonding was optimized. Experimentally, this is not so. In general, simple diaminoalkanes[22] and diphosphinoalkanes[24] function as effective chelating agents only for the ethane and propane derivatives. Higher homologues often show drastic drops in binding constants to the point that polymers are formed, rather than mononuclear chelate derivatives. The most likely explanation for these failures deals not with enthalpy, but with entropy.

Entropic considerations relating to chelate formation can be divided into two categories: translational entropy and conformational (or internal rotational) entropy. Translational entropy has long been thought to be of major importance in the chelate effect.[6,27] As mentioned earlier, a reaction of the type $ML_2 + L—L \rightleftharpoons M(L—L) + 2L$ takes place such that three particles are formed from two and on this basis, a large positive ΔS is expected. In addition, it has been suggested[28] that the ligand moiety (L—L) itself undergoes an increase in translational entropy upon binding since the compact chelate ring so formed undergoes fewer translation-inhibiting collisions with solvent molecules than does the unbound ligand. There appear to be no data or easy experiments, however, to support or discount this suggestion.

Nevertheless, considerations of translational entropy changes during chelation reactions are of great importance in explaining experimental evidence referred to collectively as "the chelate effect".

Translational entropy effects, however, do not account for certain other observations, namely the failure of large chelate rings to close. The explanation for this lies with conformational entropy effects. Consider that the greater the number of conformational degrees of freedom a free ligand has, the greater will be its conformational entropy. This applies as well to a bidentate ligand with one functional group bound to a metal. The ring closure or chelation process requires that many conformational degrees of freedom be lost, corresponding to a large entropy decrease. It appears that this is a factor in the failure of large chelate rings to close, despite favorable translational entropy effects. Schwarzenbach[29] described the same phenomenon in terms of the activity (i.e. effective concentration) of the free end of a singly-bound bidentate ligand. This activity is inversely proportional to the free volume swept out by the unbound donor group. The free volume is proportional to the length of the chain connecting the donor groups of interest. In addition, this volume can be seen by the use of molecular models to be greatest for highly flexible aliphatic chains and to decrease appreciably when the chain is restricted conformationally.

Consideration of such conformational entropy effects leads to several conclusions. First, a good chelating ligand will have the smallest number of ring members necessary for completion of the chelate

ring. Second, the ligand will not have free rotation around all bonds, but will instead possess a number of bonds around which rotation is restricted, so as to decrease its number of possible conformations and its molar entropy. In practice, this may be accomplished by the introduction of multiple bonds, ring structures and/or bulky substituents which inhibit free rotation around bonds. Successive modifications of a "floppy" ligand by these methods should converge at a free ligand structure which closely resembles the constrained ligand structure within the chelate complex. The ultimate result of such changes leads one conceptually to a macrocycle and the so-called "macrocyclic effect".[30,31] It is of note also that strain within the distal organic ring portion of a macrocycle or totally rigid open-chain ligand is of little consequence in the overall ΔG of a chelate-forming reaction since this strain would have been introduced prior to, rather than in concurrence with, the introduction of the metal.

A final point which has not been addressed up to this point is the influence of solvation effects. In solvents such as water, monodentate or open chain polydentate ligands are more highly solvated than their polydentate or macrocyclic counterparts, respectively. The breaking of fewer hydrogen bonds from the macrocyclic ligand tends to make ΔH and ΔS more negative than with more highly solvated displacing ligands.[30-32] As far as the present research is concerned, only relatively weak hydrogen bonds are expected between nitriles[33] or

isonitriles[34] and organic solvents and so solvation effects are not expected to be nearly as important in these systems as they are in aqueous systems.

Thus, the design of a chelating ligand requires attention to several factors. Perhaps most important is that the linear functional groups are allowed to interact comfortably with the metal. For linear nitrile or isonitrile chelating groups, the completed chelate ring should contain at least twelve members. Translational entropy considerations suggest that the larger the number of chelating groups, the more favorable the reaction since more unidentate ligands will be displaced in the chelation reaction. The minimization of conformational entropy loss can be accomplished by the introduction of ring structures or multiple bonds which restrict free rotation in the unbound ligand.

The ligands of interest in the present research have been designed with the preceding factors in mind. Figures 3-6 show structures for the dinitrile, diisonitrile, trinitrile and tetraisonitrile ligands upon which this research has focused. The molecules depicted in Figures 3 and 4 share a common structural feature, namely a dioxyalkylene unit connecting two aromatic rings. The metal-binding donor groups are attached to these aromatic nuclei.

As discussed earlier, the size of a chelate ring is expected to be of some importance in determining the binding properties of a multidentate ligand. For the series of ligands in Figures 3 and 4, the chelate ring size can be changed by varying n, the number of

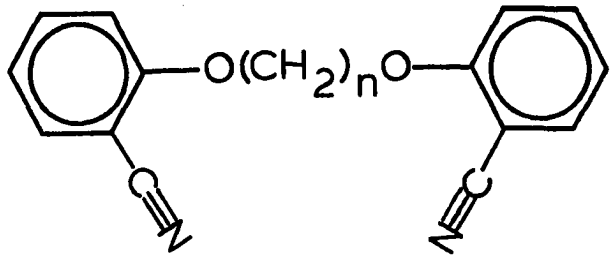

n = 2 DiCN-2

n = 3 DiCN-3

n = 4 DiCN-4

Figure 3. Structures of dinitrile ligands DiCN-n

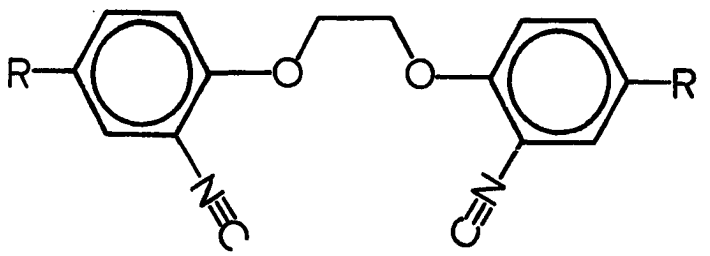

R = H DiNC

R = CMe_3 t-BuDiNC

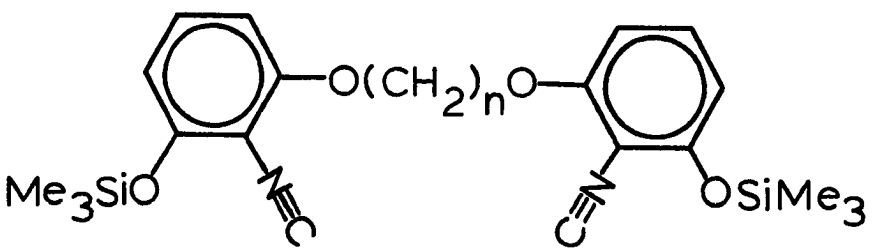

n = 2 SiNC - 2

n = 3 SiNC - 3

Figure 4. Structures of diisonitrile ligands DiNC, t-BuDiNC, and SiNC-n

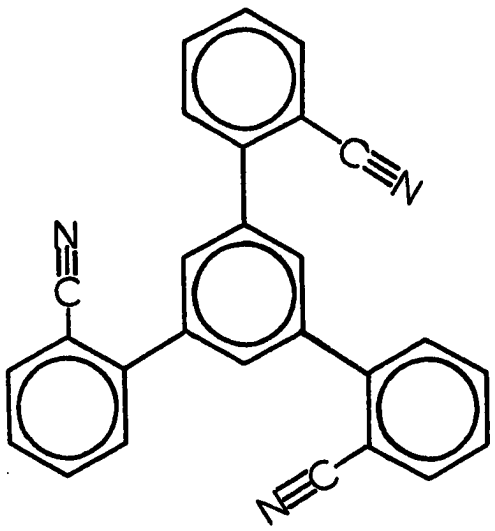

Figure 5. Structure of a trinitrile ligand, TriCN

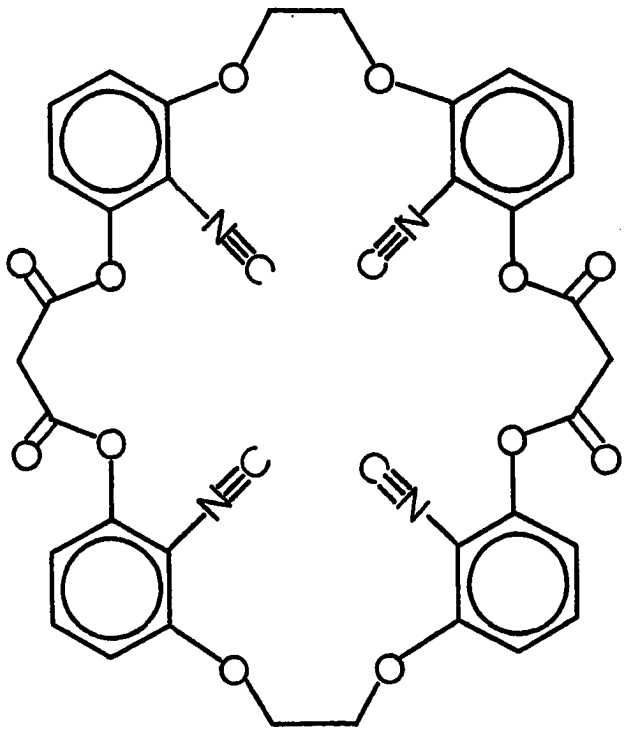

Figure 6. Structure of a potentially chelating macrocyclic tetrakis (isonitrile) ligand, MacNC

methylene groups in the dioxyalkylene units. When n=2, as in DiCN-2, DiNC, t-BuDiNC, and SiNC-2, the resulting chelate ring would contain thirteen members. While molecular models suggest that chelation would be possible with as few as twelve ring members, the thirteen-membered rings appear to contain considerably less strain than twelve-membered ones. This enthalpic factor is to be weighed against an expectedly larger (unfavorable) entropy change for closure of the larger rings. Internal rotation within the DiCN- and DiNC-type free ligands is worth comment as well. The aromatic ring, of course, restricts rotation around two bonds within each ligand framework, and results in the immobilization of two five-atom planes. In DiNC, for example, that plane contains the isocyanide carbon and nitrogen atoms, two aromatic carbon atoms and the oxygen atom. These planes should lend some rigidity to the uncomplexed ligands and work toward the desired situation in which the free ligand conformation is similar to that of the resulting metal chelate complex. Finally, the oxygen atoms might be expected to lower the strain enthalpy in the chelate ring relative to a case where these ring positions were occupied by methylene groups[26]; the oxy group is less sterically demanding than is the methylene group, due to its lack of hydrogens.

The tridentate ligand, TriCN, represents a much different structural class than the molecules just discussed. By adopting a C_{3v} or C_3 structure, the three nitrile groups should be able to chelate to a single metal center simultaneously, with N-M-N angles of approximately 90°. Molecular models suggest that a considerable deal of strain is

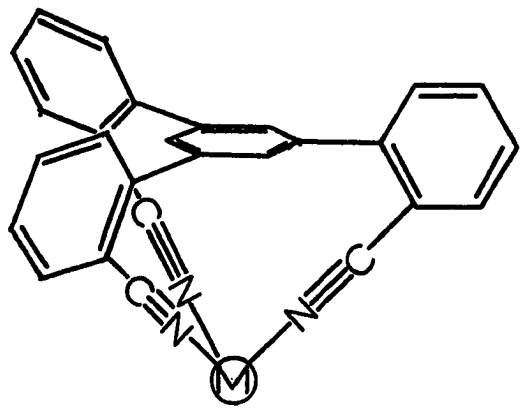

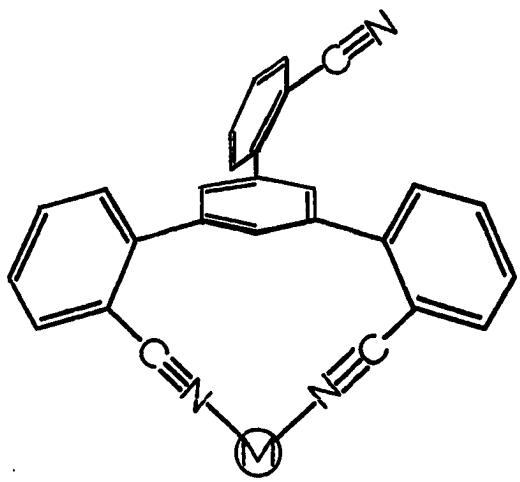

Figure 7. Possible conformations and chelating modes of the TriCN ligand

present in such an arrangement, but can be reduced by altering the N-M-N angles slightly or by increasing the size of the metal atom. A unique feature of this ligand is its high symmetry and concordant low conformational flexibility. Thus, TriCN would be expected to undergo chelation reactions with only marginal conformational entropy losses. Figure 7 shows the two possible conformations of the ligand and the modes (bidentate and tridentate) in which it might chelate to a metal from each of these conformations.

The design of macrocyclic tetrakis (isocyanide) ligands follows from principles applied to ligands of lower denticity. For an alicyclic tetraisocyanide ligand, it appears that at least 28 methylene units would be necessary to avoid undue strain in the chelate complex. For a ligand which contains four aromatic rings, such as MacNC (Figure 6), a total of 30 ring members is necessary. In either case, considerably larger rings would seem to be capable of chelating behavior though such rings might prove to be so conformationally "loose" as to prove detrimental to chelation on entropic grounds. Even the MacNC ligand in Figure 6 might be capable of considerable folding along either σ_v plane to yield a structure having two mutually parallel bidentate ligand planes.

D. Complexes Containing Dinitrile Ligands

To date, there appear to be no well-characterized examples of transition metal complexes containing chelating dinitrile ligands. As discussed in the last section, a chelating dinitrile ligand utilizing its N lone pair would need to contain seven or eight methylene units linking the —C≡N: donor groups. Unfortunately, the coordination chemistry of such potential ligands as 1,7-dicyanoheptane (nonanedinitrile) appears to be unexplored at this point.

On the other hand, some of the lower homologues have been examined in their reactions with transition metal salts and halides. For example, the adducts $AgClO_4 \cdot 2(NC(CH_2)_4CN)$ and $SnCl_4 \cdot (NC(CH_2)_3CN)$ have been examined by X-ray crystallography.[35,36] As expected, neither contains chelating dinitrile ligands. The former compound consists of a two-dimensional array of tetrahedrally coordinated Ag^+ ions, with bridging adiponitrile units.[35] Adiponitrile adducts of cobalt(II) halides have been investigated as well.[37] Structures and stoichiometries of these complexes vary according to the number of water molecules present and depending upon the identity of X (Cl, Br, or I). In no cases, however, is there any spectral evidence for either uncoordinated or π-bound adiponitrile ligands; infrared spectra of all the complexes consist of a single ν(N≡C) vibration shifted to a position 37 to 57 cm^{-1} higher than that in the free nitrile, as expected for end-on coordination.[38]

Similarly, the glutaronitrile ($NC(CH_2)_3CN$), adiponitrile, and pimelonitrile($NC(CH_2)_5CN$) derivatives of $Co(ClO_4)_2$ and $Ni(ClO_4)_2$ are nonchelated six-coordinate oligomers or polymers.[39]

In 1966 and in a later, fuller account, Farona and co-workers[40,41] reported the synthesis of a series of complexes of the general type $M(CO)_3(NCYCN)X$ (M = Mn, Re; Y = CH_2, C_2H_4, C_3H_6, o-C_6H_4; X = Cl, Br). In concordance with the apparent lack of coordinated or free ν(NC) bands in the infrared spectrum between 2250-2350 cm^{-1}, conductivity data, and an anomalous band at ~2070 cm^{-1}, these complexes were assigned structures in which the dinitriles chelated through their π bonds to the Mn or Re metal centers. The bands at 2070 cm^{-1} were assigned to the side-on bonded nitrile groups. Shifts to lower energy are expected and observed [17-19] for π-bound nitrile groups, though the confirmed cases of this bonding mode are characterized by much larger shifts.[17] Strong evidence presented by other workers,[42] however, seems to indicate that the assignments of π-chelation were in fact incorrect. In the solvent used for conductivity studies, Dunn and Edwards[42] demonstrated that considerable decomposition of $Mn(CO)_3(NC(CH_2)_2CN)Br$ occurred. Closer examination of the IR spectra of these compounds showed that ν(NC) absorptions, though weak, were indeed present; Raman spectra revealed strong bands due to N≡C stretching. Both observations are strong indications that σ-bound nitrile ligands are present in $Mn(CO)_3(NC(CH_2)_2CN)Br$. Accordingly, it is now well accepted that

infrared ν(NC) bands for coordinated nitrile ligands are in some cases very weak or unobservable.[18] Labelling studies employing $C^{18}O$ demonstrated that the proposed ν(NC) bands at ~2070 cm^{-1} were ν(CO) bands instead.[42] The data collected on these compounds seem to be consistent with a dinuclear, μ-dihalo-bridged structure[42] for which up to five infrared-active ν(CO) modes are expected (Figure 8). A later study by Dunn and Edwards[43] suggested as well that phthalonitrile derivatives contained only σ-bound nitrile ligands in the complexes $M(CO)_3[o\text{-}C_6H_4(CN)_2]_2Br$ (M = Mn, Re) and $Re_2(CO)_6X_2[o\text{-}C_6H_4(CN)_2]$ (X = Cl, I).

Unfortunately, the early reports of chelating short-chain dinitriles have prompted several other suggestions of chelation in similar systems which now appear to be questionable. For example, the ligand $(o\text{-}C_6H_4CN)P(C_6H_5)_2$ was proposed[44,45] to either bridge or chelate in a π-bonding fashion in $M(CO)_3(L\text{-}L')X$ complexes similar to those of Farona et al.[40,41] Raman spectroscopic investigations and molecular weight measurements by Storhoff,[46,47] however, strongly suggested that such complexes again were both end-on bonded and dinuclear. A number of investigations in the relatively recent literature[48-51] have dealt with organometallic derivatives of short-chain dinitrile ligands. In all of these cases, infrared spectral parameters are normal for end-on bonding in the particular system of interest, but mononuclear structures have been assigned or tacitly assumed.

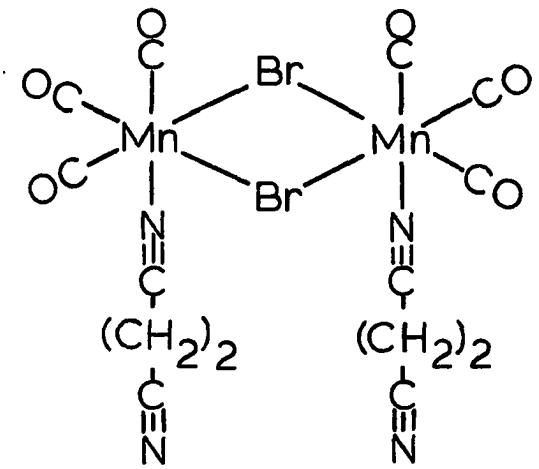

Figure 8. Likely structure of $Mn(CO)_3(NC(CH_2)_2CN)Br$ according to reference 38

E. Complexes of Diisonitrile Ligands

There has been considerable interest in the coordination behavior of α,ω-diisocyanoalkanes in the last six years. Much of this work has concentrated upon derivatives of rhodium, mainly because of the interesting chemical[52-55] and spectroscopic[56,57] properties of the complexes $[Rh(CNR)_4]^+$ and $[Rh_2(CNR)_8]^{2+}$ (Figure 9). The latter dinuclear structure is formed with the majority of diisocyanides studied so far. Ligands capable of such bridging behavior include the simple diisocyanides $CN(CH_2)_nNC$ (n = 3,[16,57] 4,[15,16,58] 5,[16] 6[15,16]) and the substituted analogs, 2,5-diisocyano-2,5-dimethyl hexane[58] (1), 1,3-and cis-1,2-diisocyanocyclohexanes[59] (2-4), and 1,8-diisocyanomethane[60] (5). Also expectedly, the ligands 1,3-bis(isocyanomethyl)benzene (6) and 1,4-bis(isocyanomethyl)benzene (7) form bridging compounds.[16]

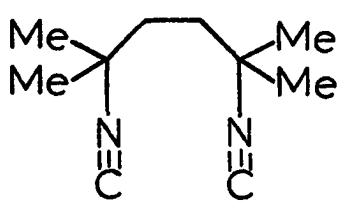

1

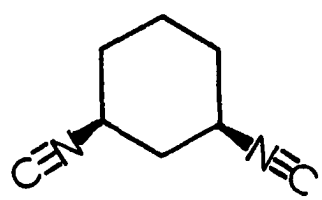

2

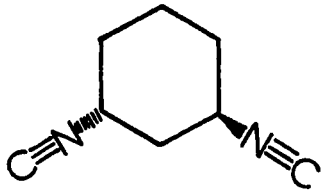

3

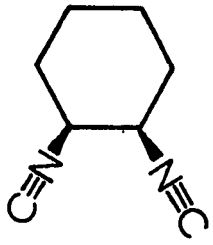

4

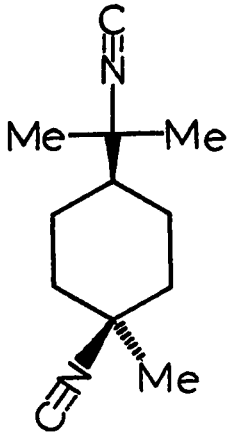

5

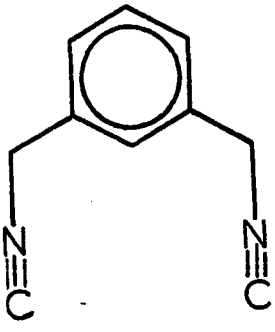

6

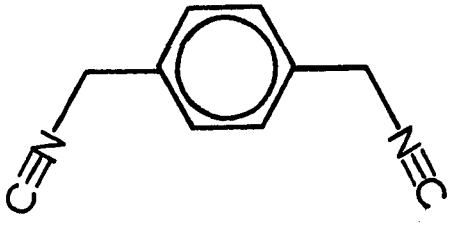

7

a

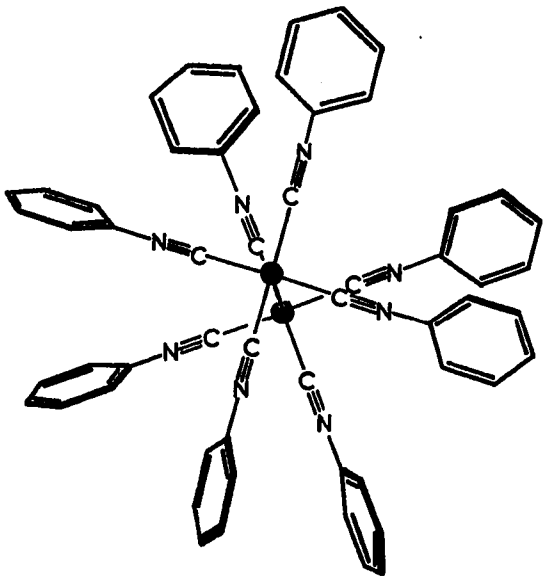

b

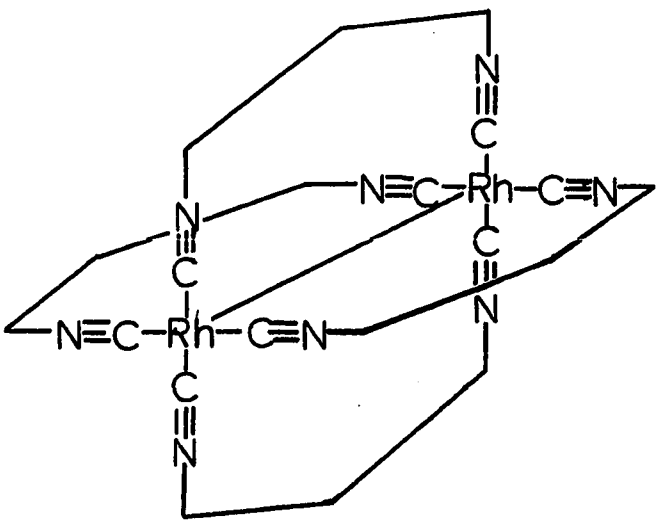

Figure 9. Structures of $[Rh_2(CNR)_8]^{2+}$, a) in $[Rh_2(CNPh)_8](BPh_4)_2$, reference 56; b) in $[Rh_2(CN(CH_2)_3NC)_4]$, reference 58

As mentioned earlier in this introduction, the only known chelating diisocyanides are 1,7-diisocyanoheptane[15] and 1,8-diisocyanooctane,[15,16] which form twelve- and thirteen-membered rings, respectively, in complexes of Rh(I).

The synthesis of these rhodium(I) monomers or dimers is straightforward, involving displacement of chloride and labile ligands from $[Rh(COD)Cl]_2$ or $[Rh(CO)_2Cl]_2$ in any one of a number of solvents. Metathesis with large anion-containing salts such as NH_4PF_6 or $NaBPh_4$ gives the corresponding PF_6^- or BPh_4^- salts. The isolated solid products are often dark blue to purple in color. The low energy band responsible for these deep colors is due to a transition from a metal d_{z^2} orbital perturbed by weak metal-metal bonding with an adjacent rhodium atom to the a_{2u} orbital, which is predominantly N-C antibonding in character. This weak metal-metal interaction is also responsible for the oligomerization of $[Rh(CNR)_4]^+$ (or $[Rh_2(CNR)_8]^{2+}$) units in solution.[56]

Efraty and his colleagues[61-63] have prepared extended two-dimensional polymers containing Rh(I) by the use of rigid bridging ligands (8-11). The formation of these extended structures provides an

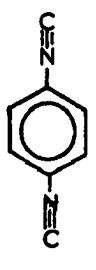

8

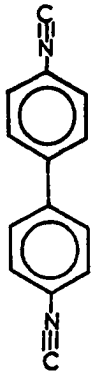

9

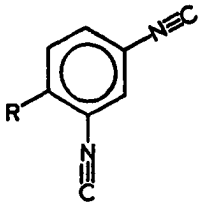

10

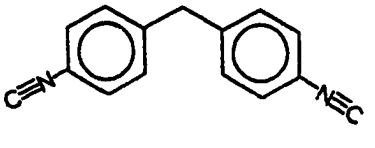

11

interesting example of "template polymerization".[61,62] The rigid linear ligand 4,4'-diisocyanobiphenyl (9) has also been shown[64] to form mixed-metal pentamers such as $Rh[CN(C_6H_4)(C_6H_4)NCMn(CO)_4Br]_4^+$.

Most of the examples above utilize diisocyanides as the sole ligand bound to the metal. A study by Howell and Rowan[65] in 1981 describes reactions between $Cp_2Fe_2(CO)_4$ and the diisonitriles $CN(CH_2)_nNC$ (n = 2, 3, 4, 6) in which one CO ligand from each iron complex is lost, giving exclusively bridging complexes $[Cp_2Fe_2(CO)_3]_2(CN-(CH_2)_n-NC)$. In these reactions, a given isocyano group of the ligand can be either terminally bound to a single metal center, or can bridge the two irons in a dimeric unit $Cp_2Fe_2(CO)_2(\mu-CO)(\mu-CNR)$. Reactions of diisocyanoethane and -hexane with $Fe_3(CO)_{12}$ gave no chelating products (as should be expected), but rather the dinuclear complexes $(OC)_4Fe-CN(CH_2)_nNC-Fe(CO)_4$ in which the isocyano groups occupy axial coordination sites.[65]

F. Ligands With More Than Two Isonitrile Groups

While not designed specifically for chelation to a single metal, the trifunctional ligand cis,cis-1,3,5-triisocyanocyclohexane (TriNC) (Figure 10) has been investigated as a potentially triply-bridging ligand at the face of a triangular metal cluster.[66] Unlike the diisocyanoalkanes discussed heretofore, this molecule has only two important conformations, all-axial and all-equatorial. In the former conformation, coordination to a triangular metal array should be possible. Unfortunately, reactions

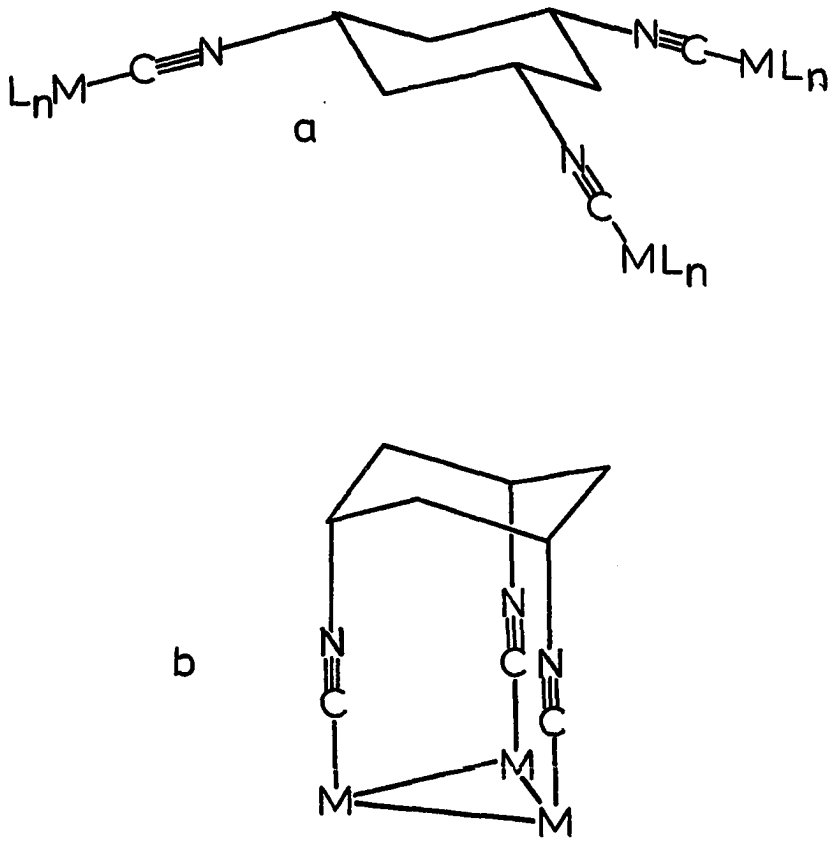

Figure 10. The TriNC ligand shown in a) all-equatorial and b) all-axial conformations

with the triangular clusters $Ru_3(CO)_{12}$ and $Os_3(CO)_{12}$ led only to polymers, while reactions with $Fe_3(CO)_{12}$ and $[M(CO)_5I]^-$ (M = Cr or W) yielded the derivatives $[Fe(CO)_4]_3$(TriNC) and $[M(CO)_5]_3$(TriNC), respectively. These complexes most likely involve the TriNC ligand in its all-equatorial form.[66] Such results suggest that obligate facial coordination might best be achieved by an endo-endo-endo-triisocyanoadamantane or similar structure.

Tetradentate isonitrile ligands, especially macrocyclic ones, would be of great interest because of the expected high stability of their metal complexes and also because of their resemblance to porphine ligands. The only known tetrakis(isocyanide) is cyclotetrakis (2-isocyano-1,3-xylenediyl) (12).[67] The ligand has been shown to undergo

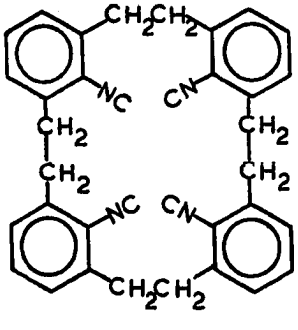

12

reactions with CuCl, $Ni(CO)_4$, and $CoCl_2$, but no experimental details are given. It is suggested[67] that this ligand chelates as a macrocycle to a single metal, but construction of molecular models, as well as

structural factors considered earlier in this introduction rule out such a structure. Full chelation such as this would require formation of four eleven-membered chelate rings, a situation which appears to be impossible. Rather, it seems from studies with molecular models that ligand 12 would form linear polymers in which alternate isocyanide groups bind to the same metal, forming sixteen-membered chelate rings. Such a structure is represented in Figure 11.

A final subject of some interest is the synthesis of macromolecular polyisocyanides. The anchoring of homogeneous catalysts or catalyst precursors is of some importance, since such catalysts might retain the specificity of their homogeneous precursors while enjoying the mechanical simplicity of heterogeneous catalysts. Interesting results have been obtained with optically active diphosphine-functionalized polymers.[68,69] Research involving polymer-supported isocyanides is also under way.[70-73] Recent results from the laboratory of Beck[74] have shown that "chelation", that is, disubstitution at a metal atom, can be effected by certain poly(isocyanoalkylstyrenes). The existence or extent of disubstitution by the functionalized polymer is affected by the chain length between the polymer network and the isocyanide donor groups, and therefore, by the distances between the donor groups themselves. In one sense, these polymers might be considered to be the largest chelating diisonitrile ligands known; on the other hand they are probably the most poorly characterized stereochemically. The

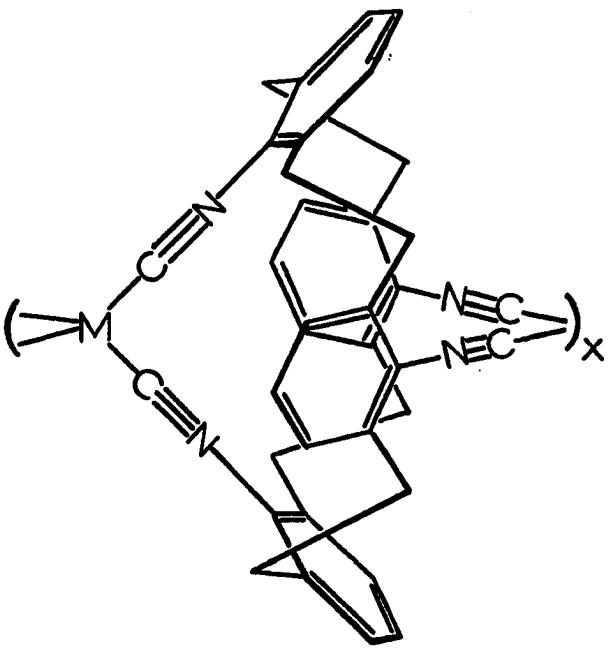

Figure 11. Possible polymeric structure of $\{[C_6H_3(CH_2)_2NC]_4M\}_x$

thought of these isocyanide groups converging across large pores (50-250 Å in the present case[74]) to bind a metal is interesting in its similarity to the general structural features of some metalloenzymes.

II. EXPERIMENTAL

A. Techniques

Unless stated otherwise, all manipulations were carried out under an inert atmosphere in 14/20 standard-taper Schlenk-type glassware or similar apparatus.[75] Solvents, solutions and suspensions were transferred using syringes or stainless steel transfer (cannula) tubes. The inert atmosphere consisted of Argon or N_2 gas which had been dried by passage through a 2.5 cm x 35 cm column of 4A molecular sieves. The sieves were periodically regenerated by heating to ca. 300°C in vacuo for several hrs. The generation of an inert atmosphere in a reaction vessel was accomplished by evacuating the apparatus to 0.02 torr, back-flushing with inert gas and repeating at least twice.

For reactions involving especially water-sensitive compounds, all glassware was dried by baking at 100°C or by flaming the evacuated apparatus. When encountered, air-sensitive solids were handled in an inert-atmosphere glove-box or polyethylene glove bag.

Recrystallizations of compounds were generally carried out by one of two methods. Recrystallization from a hot solvent involved the preparation of a saturated, near-boiling solution of the substance, which was allowed to cool to room temperature, then to -20°C. The product was then isolated by filtration and was washed with a small amount of the same cold solvent. Recrystallization from a mixed solvent system, for example $CHCl_3$/hexane, was effected as follows. First, a

concentrated solution of the compound (here, in $CHCl_3$) was prepared and filtered. Then, one to two volumes of the less polar solvent were very slowly added via syringe such that two separate layers were formed. The mixture was allowed to stand at the indicated temperature until the solution was homogeneous. If no solid had formed, a further aliquot of the less polar solvent was added and the solution was allowed to stand. This process was conveniently carried out in a Schlenk tube, or for smaller amounts, in a 2-dram vial fitted with a rubber septum.

B. Instrumental Techniques

1. Routine infrared spectra

Routine infrared (IR) spectra in the range 4000-600 cm^{-1} were determined with Perkin Elmer 281 or 681 grating infrared spectrophotometers. The calibration of each instrument was checked periodically by comparing observed and actual values for the frequencies of lines in the spectrum of CO gas (300 torr, path length = 4 cm) in the region 2242 - 2013 cm^{-1}. Below 2000 cm^{-1}, calibrations were checked against the 1944.0 cm^{-1} line of polystyrene film. Frequencies reported are accurate to $\pm$ 2 cm^{-1}.

The cells used for solution spectra consisted of two 19.5 x 38.5 mm NaCl plates separated by either 1 mm or 0.1 mm Teflon spacers. The short path cells were employed when monitoring reactions in ethereal solvents, which contain a band at ca. 1960 cm^{-1}. They were also used

when the solute concentration was so high as to prohibit the use of the larger path length. Solution IR spectra were always obtained in the double beam mode with pure solvent in a matched cell as reference.

Solid state IR spectra were measured as hydrocarbon oil (Nujol) mulls in which the mull was sandwiched between two circular 5 mm x 25 mm NaCl plates. Instruments were operated in the double beam mode with air as reference.

Low frequency IR spectra (below 600 cm^{-1}) were measured as Nujol mulls on an IBM IR 98 Fourier Transform spectrometer. A film of the Nujol mull on a single 1 mm x 18 mm polyethylene disc was found to be suitable for such measurements.

2. Infrared integrated intensity measurements

For air- and moisture-stable compounds, measurements were carried out on a Perkin Elmer Model 281 grating infrared spectrophotometer. The instrument was operated in the double-beam and absorbance modes with a slit width of approximately 1.4 cm^{-1}. Scans were made at the rate of 5 cm^{-1} min^{-1} with an abscissa scale of 5 cm^{-1} per linear cm.

An IBM IR 98 Fourier Transform infrared spectrometer was found to be more suitable for intensity measurements on all compounds, especially those exhibiting sensitivity to the atmosphere. The resolution of the instrument was set at 2 cm^{-1}, with a zero-filling factor of 2. Data were plotted as absorbance scans in which the reference file was obtained by scanning the pure solvent in the sample cell.

The cell used was of the same dimensions described earlier, and possessed a 1 mm Teflon spacer. The cell path (0.102 ± 0.001 cm) was determined by the interference fringe method.[76]

All solutions were made up with dry, degassed CH_2Cl_2 (Section II.C.). Samples (typically 1-3 mg) were weighed onto aluminum foil boats with the aid of a Perkin Elmer AD-2Z Autobalance. The boats were then inserted into small vials and the desired weight of solvent was introduced. For the air-sensitive solid $[Co(t\text{-}BuDiNC)_3]\ (PF_6)_3$, a tared, sealed ampule of the complex was opened under an inert atmosphere and the solvent was added from a tared syringe. After transfer of the solution to the cell, the ampule pieces were dried and reweighed to determine the sample weight.

Integrated intensities of the $\nu(C{\equiv}N)$ band of $[Co(t\text{-}BuDiNC)_3](PF_6)_3$ were estimated by the equation $A = (2.303\ c^{-1}\ \ell^{-1})\ \log\ (I_o/I)_{\nu max}\Delta\nu^t_{1/2}$ as outlined by Ramsay (Method I)[77] since an interfering solvent band (2305 cm^{-1}) and sample decomposition precluded direct measurement of the area beneath the peak. For the other complexes, areas under absorption bands were measured with a polar planimeter. Apparent integrated intensities, B, were then calculated as $B = (2.303\ c^{-1}\ \ell^{-1})\int \log\ (To/T)\ d\nu$. In all cases, wing corrections were applied according to Ramsay (Method II). Absolute integrated intensities, A, were determined[78] by extrapolation of B vs. log(To/T). Linear least squares analysis was used to carry out the extrapolations.

3. Nuclear magnetic resonance (NMR) spectra

Proton (89.55 MHz) and ^{13}C (22.50 MHz) NMR spectra were measured on a JEOL FX90Q spectrometer in deuterated (>99.5% D) solvents. Chemical shifts are reported in ppm downfield (i.e. ppm δ) from tetramethylsilane (TMS).

Solutions for ^{1}H NMR analysis contained internal TMS as the internal reference. Chemical shifts in ^{13}C NMR spectra were referenced indirectly to the chemical shift of the solvent signal: $CDCl_3$, 77.06 ppm; CD_2Cl_2, 53.80 ppm; $(\underline{C}D_3)_2CO$, 29.80 ppm. Solutions of metal complexes normally contained $Cr(acac)_3$ as a shiftless relaxation agent[79] to enhance the signal of quaternary carbons (e.g. in CO and CNR ligands). Carbon-13 chemical shift assignments for aromatic ring carbon atoms were made by calculating the spectrum empirically.[80,81]

4. Mass spectra

Mass spectra were determined on solid samples by Instrument Services personnel using either Finnegan 2000 or AEI MS902 mass spectrometers at ionization potentials of 70 or 20 eV.

5. UV-VIS spectra

Perkin Elmer Model 320 or Beckman DU-8 spectrophotometers were used for the measurement of electronic spectra. Solvents were purified as in section C. Rectangular quartz cells with 10 mm or 1 mm path lengths were employed. The positions of absorption maxima are given in nanometers (nm) and are accurate to $\pm$ 2 nm.

6. Conductivity data

Specific conductances, L, were measured directly with a Markson Model 4402 conductivity meter and dip cell. The meter was calibrated against a standard aqueous KCl solution at 25°C. Molar conductances, Λ_M, were calculated from the equation $\Lambda_M = 1000\ L/C$ where C is the molar concentration of analyte. Concentrations were approximately 1×10^{-3} M. Spectral grade nitromethane ($MeNO_2$) was employed as the solvent for all measurements.

7. Electrochemical measurements

The apparatus used for cyclic voltammetry studies was kindly provided by Dr. Robert E. McCarley. Current and potential functions were controlled by a Princeton Applied Research Model 173 potentiostat/galvanostat and Model 175 Universal Programmer. A three-electrode configuration was employed, consisting of a stationary Pt disc working electrode of area 0.45 cm^2, platinum wire counter electrode, and saturated calomel (aqueous KCl) reference electrode. Dry dichloromethane (Section II. C) was used as solvent and contained 0.1 M Bu_4NPF_6 as supporting electrolyte. The Bu_4NPF_6 was prepared by a literature method.[82] Analyte concentrations were 5×10^{-3} M, in a solution volume of ca. 3 mL. All measurements were carried out under an atmosphere of dry Ar gas.

8. Elemental analysis

Carbon, hydrogen, and nitrogen analyses were performed by Galbraith Laboratories, Inc., Knoxville, Tennessee.

9. Melting points

For metal complexes, melting or decomposition points were observed on a Thomas hot stage apparatus and are uncorrected. The melting points of organic compounds were measured with a Thomas-Hoover capillary melting point apparatus belonging to Dr. J. G. Verkade, and are uncorrected.

C. Solvents

Many of the solvents used were purified before use. All distillations were carried out under an atmosphere of dry N_2. Tetrahydrofuran (THF) was distilled from sodium/benzophenone. Anhydrous diethyl ether (Et_2O) was obtained similarly. When employed as an aqueous extractant, however, Et_2O was used as received without further treatment. Acetonitrile (CH_3CN) was stirred over CaH_2 overnight and distilled successively from P_4O_{10} and CaH_2. Pyridine was distilled from CaO. Triethylamine (Et_3N) was dried by distillation from KOH. Unless stated otherwise, N,N-dimethylformamide (DMF) was distilled from CaO. Dichloromethane (CH_2Cl_2) and 1,2-dichloroethane (1,2-$C_2H_4Cl_2$) were distilled from CaH_2. Hexane and pentane were distilled from $CaCl_2$ or P_4O_{10}. Benzene (C_6H_6) was stirred over H_2SO_4, then distilled. Methanol (MeOH) was AR grade and was simply purged with N_2 prior to use. All other solvents were AR grade and were stored over activated molecular sieves (4A) and purged with dry N_2 or Ar before being used.

D. Reagents

Acetic formic anhydride (AFA)[83] and the oxidant $(Bu_4N)_2Cr_2O_7$[84] were prepared by literature methods. Malonyl fluoride, $CH_2(COF)_2$[85] was prepared by reaction of malonyl chloride[86] with SbF_3. Chlorotrimethylsilane was distilled from CaH_2 prior to use.

Group VII pentacarbonyl halides $Mn(CO)_5Cl$,[87] $Mn(CO)_5Br$,[88] and $Re(CO)_5Br$[89] were prepared by halogen oxidation of the corresponding dimetal decacarbonyls by the cited procedures and were sublimed before use. The dinuclear complex $Mn_2(CO)_6(CH_3CN)_2Br_2$ was prepared by the procedure described by Dunn and Edwards.[90] The methods of Eisch and King[91] were used for the preparation of $Cr(CO)_4$(nor) and $Mo(CO)_4$(nor). The latter compound was generously provided by Mr. David E. Schiff. The complexes $Et_4N[M(CO)_5I]$ (M = Cr, W) were prepared by Dr. Michael H. Quick using the method of Abel et al.[92] Dr. Quick also supplied $[CpFe(CO)_2(CS)]PF_6$, which was prepared by the method of Busetto and Angelici.[93] The referenced methods were employed for the preparation of $[Cu(CH_3CN)_4]BF_4$[94] and $[Rh(COD)Cl]_2$.[95]

The ligands DiNC and DiCN-2, as well as $Mn(CO)_3$(DiCN)Br, were synthesized by the published method.[96] The complexes $Mo(CO)_4$(DiNC), $W(CO)_4$(DiNC), and $[W(CO)_4(pip)]_2$(μ-DiNC) were prepared according to the published procedures[96] by Dr. Michael H. Quick. All other reagents were purchased from commercial sources and were used without further purification.

E. Procedures

1. Synthesis and characterization of nitrile ligands

These compounds and their precursors have been characterized by elemental analysis (Table 1), infrared spectroscopy (Table 2), ^1H NMR (Tables 3 and 5) and ^{13}C NMR (Tables 4 and 6).

a. 1,3-bis(2-cyanophenoxy)propane, DiCN-3 A solution of 2-cyanophenol (4.78 g, 40.1 mmol) in 20 mL of DMF was added dropwise to a stirred suspension of NaH (0.96 g, 40 mmol) in 10 mL of DMF at 80°C under N_2. After several hours, most of the NaH had dissolved and 2.0 mL (4.0 g, 20 mmol) of 1,3-dibromopropane was added. The mixture was then heated to 120°C. This temperature was maintained for 6 h, and the reaction was cooled to room temperature. The mixture was poured into 100 mL of well-stirred ice water. The slurry was filtered, and the solid washed with water (6 x 30 mL), cold MeOH (3 x 10 mL), and dried in vacuo to give the product (3.0 g, 53%) as a white powder. An analytical sample, mp 113 - 115°C, was obtained by recrystallization from hot $CHCl_3$.

b. 1,4-bis(2-cyanophenoxy)butane, DiCN-4 In a procedure identical to that described for the synthesis of DiCN-3, 2-cyanophenol (4.8 g, 40 mmol), NaH (0.96 g, 40 mmol), and 1,4-dibromobutane (2.4 mL, 4.3 g, 20 mmol) yielded 2.5 g (43%) of the crude product. Recrystallization from hot $CHCl_3$ gave colorless crystals, mp 151 - 3°C.

c. 1,3,5-tris(2-methylphenyl)benzene, $TriCH_3$ The following method is essentially that described by Wirth et al.[97] The first step involves the conversion of 2-methylacetophenone to its diethyl ketal, which is accomplished as follows. To a solution of the ketone (25 g, 0.19 mol) and triethylorthoformate (52 g, 0.35 mol) in 52 mL of EtOH was added 10 drops of concentrated hydrochloric acid. The flask was stoppered and allowed to stand for 52 h, giving a red solution. Neutralization

was effected by the addition of a sodium ethoxide solution prepared by the dissolution of 0.11 g of Na in 8 mL of EtOH. Distillation of the resulting yellow solution under water aspirator vacuum (24 torr) gave a fraction boiling at 55°C which was primarily $HC(OEt)_3$, and a fraction at 122°C which was the desired ketal.

The isolated ketal was dissolved in 100 mL of dry benzene and HCl gas was introduced into the stirred solution in the apparatus represented below. A steady flow of HCl into the stirred solution was maintained for

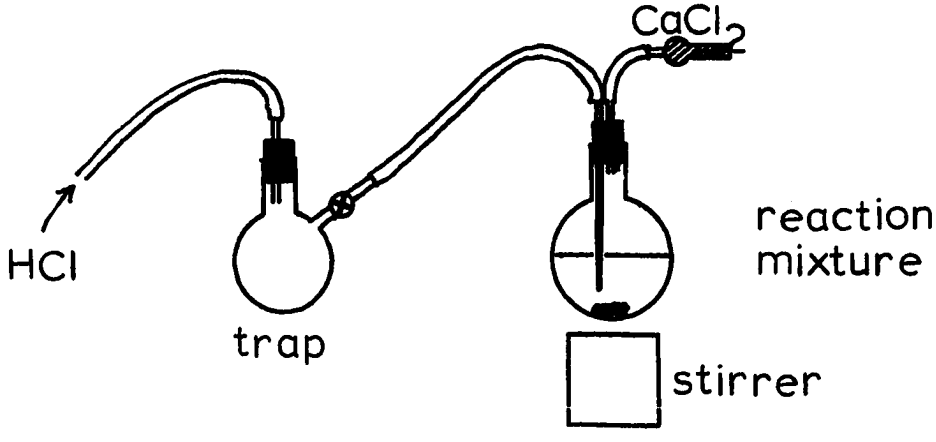

1 h, during which time the color of the reaction reached a very deep blue to purple color. Rotary evaporation of the reaction mixture gave a thick orange oil. This was diluted slightly with benzene and immediately chromatographed on a 44 mm x 80 cm silica gel column prepared with CCl_4/ Skelly C (2:1), eluting with the same solvent. The desired product eluted first, usually in a volume of ca. 2 liters after first detection. (The

product was easily detected by spotting the eluate onto a piece of indicating TLC plate and examining the plate under UV light.) After removal of the solvent by rotary evaporation, the crude product was purified by digestion in 150 mL of boiling EtOH for 1 h. The product was isolated by filtering the cooled (-20°C) mixture. Washing with EtOH at -20°C and drying in vacuo gave the compound as a colorless microcrystalline solid, mp 130-134°C (134-135°C, lit.).[97] Yield: 9.82 g, 45%.

d. 1,3,5-tris(2-bromomethylphenyl)benzene, TriBr The following reaction was carried out as for the reported bromination of 2,11-dimethylbenzo[C]phenanthrene.[98] In a typical preparation, 9.50 g (27.2 mmol) of $TriCH_3$ was dissolved in 200 mL of degassed CCl_4, N-Bromosuccinimide (15.10 g, 83.9 mmol) was added, and the mixture was heated to a gentle reflux. The addition of 0.1 g of benzoyl peroxide in 2 mL of $CHCl_3$ initiated the reaction. After refluxing for 1.5 h, the reaction mixture was cooled to room temperature, and the succinimide by-product was removed by filtration. Carbon tetrachloride was removed on a rotary evaporator to give a yellow oil. This oil was stirred for 1 h with 20 mL of CCl_4/C_6H_6 (9:1 by volume) to precipitate the product as a white powder. The mixture was cooled at -20°C overnight. The product was filtered off and washed with a small amount of the cold solvent mixture, then dried in vacuo. The yield was 9.28 g (58%), mp 133 - 9°C.

e. 1,3,5-tris(2-formylphenyl)benzene, TriAl A mixture consisting of 8.94 g (15.3 mmol) of TriBr, 21.52 g (30.74 mmol) of $(Bu_4N)_2Cr_2O_7$ and 35 mL of $CHCl_3$ was heated at reflux for 4 h. The green-black mixture was cooled to room temperature and poured onto 120 g of silica gel contained in a chromatography column 74 mm in diameter. The product was washed off the column with 2 L of Et_2O. Evaporation of the solvent and recrystallization of the residue from hot EtOH (washing with EtOH at -20°C) gave the product as a light yellow solid, mp 166 - 8°C. Yield: 3.72 g (62%). In Nujol mull, the product exhibits two ν(C=O) bands, rather than one, at 1706 cm^{-1} (s, sh) and 1690 cm^{-1} (s). A single, strong ν(C=O) absorbance is observed in $CHCl_3$ solution at 1695 cm^{-1}.

f. 1,3,5-tris(2-formylphenyl)benzenetrioxime, TriOx A solution of TriAl (3.47 g, 8.87 mmol) and $NH_2OH{\cdot}HCl$ (2.47 g, 35.5 mmol) in a mixture of EtOH (20 mL) and pyridine (20 mL) was refluxed for 6 h. The solvents were removed by a short-path distillation at atmospheric pressure, followed by vacuum drying of the residue. Trituration of the resulting pale yellow oil with 15 mL of cold H_2O gave a white solid, which was isolated by filtration, washed with cold H_2O (2 x 15 mL) and cold EtOH (2 x 10 mL). The product was dried in vacuo for 12 h. Yield: 3.80 g (98%), mp 222 - 8°C.

g. 1,3,5-tris(2-cyanophenyl)benzene, TriCN Methanesulfonyl chloride ($MeSO_2Cl$), a common dehydrating agent for the conversion of aldoximes to nitriles,[99] was employed for the conversion of TriOx to the trinitrile, TriCN. Thus, a solution of TriOx (3.66 g, 8.39 mmol)

in 55 mL of distilled pyridine was cooled to 0°C under N_2. The addition of $MeSO_2Cl$ (5.0 mL, 7.3 g, 64 mmol) caused a color change to yellow and the precipitation of a white solid. The mixture was stirred 12 h at 30°C, then cooled in ice to 0°C. Water (150 mL) was slowly added to the cool solution, precipitating the crude product as a tan powder. This solid was isolated by filtration and washed first with H_2O (3 x 20 mL) then with cold (0°C) EtOH (3 x 10 mL). After being dried in vacuo, the product was dissolved in $CHCl_3$, treated with activated charcoal and filtered through an 8 mm layer of silica gel in a 60 mL fritted funnel in air. The volume of the solution was reduced to 40 mL and ca. 40 mL of Et_2O was layered on the top of the solution, yielding, after 24 h, some yellowish crystals and a white solid. Another 20 mL of Et_2O was slowly added and the solution was allowed to stand at -20°C for 24 h. The resulting solids were filtered off, washed with 20 mL of Et_2O, and dried. Another recrystallization was carried out by slowly adding 80 mL of warm (45°C) EtOH to a warm $CHCl_3$ solution of the product, followed by slow cooling to -20°C. The final product was filtered off, washed with cold (0°C) EtOH and dried in vacuo. The yield of white to pale yellow microcrystals was 2.36 g (77%), mp 266 - 8°C. MS: M^+ m/e 381.1 (base).

Table 1. Analytical data for nitrile ligands and their precursors

Compound	Calculated %C	%H	%N	Found %C	%H	%N
DiCN-3	73.37	5.07	10.07	74.17	5.51	10.18
DiCN-4	73.95	5.52	9.58	74.27	5.89	9.48
TriBr	55.42	3.62	-	55.64	4.18	-
TriAl	83.06	4.65	-	83.27	4.97	-
TriOx	74.47	4.86	9.65	75.25	5.23	9.62
TriCN	85.02	3.96	11.02	84.88	4.06	10.93

Table 2. Infrared C≡N stretching frequencies of nitrile ligands, cm^{-1}

Compound	Nujol Mull	$CHCl_3$
DiCN-2	2229	2232
DiCN-3	2228	2231
DiCN-4	2223	2231
TriCN	2227	2228

Table 3. ^{1}H NMR data for DiCN ligands[a]

Compound	Ar-H	O-CH_2	CH_2
DiCN-2	7.67 - 7.04 m	4.54 s	-
DiCN-3	7.64 - 6.90 m	4.34 t[b]	2.39 p[b]
DiCN-4	7.62 - 6.90 m	4.21 m	2.12 m

[a]Spectra measured in $CDCl_3$ solvent.

[b]J = 5.8 Hz.

Table 4. ^{13}C NMR data for DiCN ligands[a]

Compound	1	2	3	4	5	6	CN	OCH_2	CH_2
DiCN-2	160.2	102.4	134.6	121.5	133.8	113.1	116.4	67.8	-
DiCN-3	160.2	101.8	133.4	120.8	134.4	112.3	116.3	64.7	28.6
DiCN-4	160.7	102.0	133.7	120.8	134.4	112.4	116.5	68.7	25.8

[a]In $CDCl_3$ solvent.

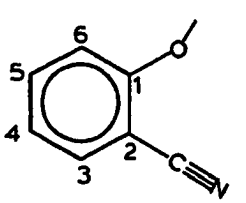

Table 5. ^{1}H NMR data for TriCN and precursors

Compound	Solvent	ArH	Other	
$TriCH_3$	$CDCl_3$	7.27 s, 7.26 s	CH_3	2.37 s
TriBr	$CDCl_3$	7.53-7.33 m	CH_2Br	4.58 s
TriAl	$CDCl_3$	8.04 m, 7.67-7.49 m	CHO	10.14 s
TriOx	CD_3CN	7.88 m, 7.51-7.28 m[a]	OH CH=N[b]	8.9 br, s 8.14 s
TriCN	CD_3CN	7.94 s, 7.89-7.50 m	-	-
	$CDCl_3$	7.89 s, 7.83-7.44 m	-	-

[a]Also includes CH=N of Z isomer (ref. 100).

[b]E isomer (ref. 100).

Table 6. ^{13}C NMR data for TriCN and precursors[a]

Compound	Observed Signals	Assignment[b]
$TriCH_3$	141.8, 141.6, 135.4	1,2,7
	130.4, 130.0, 128.6, 127.3, 125.9	3-6,8
	20.7	CH_3
TriBr	141.6, 140.4, 135.4	1,2,7
	130.9, 130.5, 128.7, 128.3	3-6,8
	32.3	CH_2Br
TriAl[c]	142.2, 136.4	1,2,7
	131.9, 129.4, 129.1, 126.5, 126.3	3-6,8
	189.8	CHO
TriCN	144.2	1
	111.3	2
	133.5	3
	130.6	4
	133.9	5
	129.5	6
	139.1	7
	128.2	8
	118.7	CN

[a]In $CDCl_3$ solvent unless stated otherwise.

[b]Where more than one number is listed on one line, the assignment could not be made with certainty.

[c]$CDCl_3/(CD_3)_2SO$ solvent. This compound exhibits only six lines in $CDCl_3$: 191.6, 144.1, 138.6, 133.8, 131.0, 128.5 ppm.

Table 6. Continued

Compound	Observed Signals	Assignment[b]
TriCN[d]	144.5	1
	111.8	2
	133.7	3
	130.8	4
	134.2	5
	129.9	6
	139.6	7
	128.7	8
	119.0	CN

[d] CD_2Cl_2 solvent.

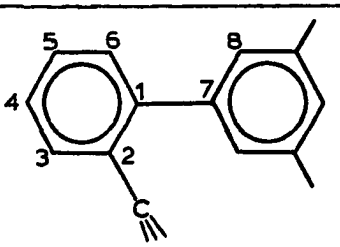

2. Preparation of nitrile complexes

Analytical data, IR spectra, ^{1}H NMR spectra, and ^{13}C NMR spectra for compounds of this type follow the preparative procedures in Tables 7 through 11. Complexes of the type $Mn(CO)_3(nitrile)_2Br$, as well as the complex $[Mn(CO)_3TriCN]PF_6$, were found to be photosensitive, even in the solid state. Thus, isolated samples were stored in foil-wrapped vials in the dark.

a. $Mn(CO)_3(DiCN\text{-}3)Br$ The reagents $Mn(CO)_5Br$ (0.104 g, 0.378 mmol) and DiCN-3 (0.105 g, 0.377 mmol) were dissolved in 10 mL of $CHCl_3$ and in darkness, the solution was refluxed for 1.3 h. After cooling the mixture, it was filtered with the apparatus being protected from light by aluminum foil. Solvent was removed at reduced pressure and the resulting yellow solid was triturated twice with 10 mL of Et_2O, followed each time by decantation of the Et_2O solution. The remaining solid was dried in vacuo and scraped from the Schlenk tube to give the pure product as a yellow microcrystalline solid, 0.087 g (46%), mp 100 - 110°C (decomp.).

b. $Mn(CO)_3(DiCN\text{-}4)Br$ In a procedure similar to that described for the DiCN-3 analog, DiCN-4 (0.175 g, 0.60 mmol) and $Mn(CO)_5Br$ (0.165 g, 0.60 mmol) were refluxed together in a CH_2Cl_2 solution (46 mL) in the dark for 9 h. (An IR spectrum of the solution after 1 h had revealed the presence of a small amount of $Mn(CO)_5Br$.) The cooled solution was taken to dryness and evaporated. Trituration with Et_2O (10 mL), then pentane (10 mL) gave the pure product as a yellow microcrystalline solid, 0.178 g (58%), mp. 122 - 5°C.

c. $Mn(CO)_3(TriCN)Br$ The trinitrile ligand TriCN (0.261 g, 0.681 mmol) and $Mn(CO)_5Br$ (0.252 g, 0.916 mmol) were refluxed together in CH_2Cl_2 solution (35 mL) for 3.5 h in subdued light. After cooling the reaction solution, it was filtered and evaporated to leave a yellow residue of the product and $Mn(CO)_5Br$. The latter was removed by four extractions with Et_2O (10 mL each), and the remaining solid was collected on a frit and dried in vacuo. This yielded 0.215 g (52%) of $Mn(CO)_3$-(TriCN)Br as a yellow powder, mp 159 - 162°C, which was analytically pure.

d. $[Mn(CO)_3TriCN]PF_6$ Halide abstraction from $Mn(CO)_3(TriCN)Br$ (0.067 g, 0.111 mmol) was accomplished by the addition of $AgPF_6$ (0.0282 g, 0.112 mmol) in 7 mL of 1,2-$C_2H_4Cl_2$ to a solution of the manganese complex in 3 mL of the same solvent. After stirring the mixture for 20 minutes, AgBr was filtered off. The volume of the now pale yellow solution was reduced to one-half, and Et_2O was added until slight turbidity developed. After standing at 0°C for 2 days, the mother liquor was decanted away and the product dried in vacuo giving 18 mg (24%). The product is a yellow microcrystalline solid which melts from 172 - 179°C, then loses CO and resolidifies at 189°C.

e. $Re(CO)_3(TriCN)Br$ TriCN (37.7 mg, 0.098 mmol) and $Re(CO)_5Br$ (40.8 mg, 0.100 mmol) were dissolved in 8 mL of 1,2-$C_2H_4Cl_2$ and the solution was refluxed for 5 h. Dichloroethane was removed at reduced pressure. Dichloromethane (2 mL) was added to the pale yellow gummy residue to dissolve it, then hexane was added with agitation until the

turbidity of the solution persisted. The solution was filtered and allowed to stand at -20°C for 3 days. This produced a single lump of light yellow crystals, which were washed with hexane and dried, and weighed 71.8 mg (89%). An analytical sample was obtained by preparative TLC (silica gel/$CHCl_3$) in air. The pure product was washed from the silica gel with CH_2Cl_2, precipitated from a concentrated CH_2Cl_2 solution with hexane, and dried for 24 h in vacuo. The colorless solid melted from 190 - 195°C. The mass spectrum of $Re(CO)_3$(TriCN)Br showed peaks assignable to the parent ion $[Re(CO)_3(TRiCN)Br]^+$ at m/e 729, 731 and 733, corresponding to $^{185}Re\ ^{79}Br$, $^{185}Re\ ^{81}Br$ (and $^{187}Re\ ^{79}Br$), and $^{187}Re\ ^{81}Br$, respectively.

f. $[Re(CO)_3(TriCN)]PF_6$ A solution of $Re(CO)_3$(TriCN)Br was prepared by heating TriCN (0.094 g, 0.246 mmol) and $Re(CO)_5Br$ (0.100 g, 0.246 mmol) in 40 mL of 1,2-$C_2H_4Cl_2$ at 75°C for 9.5 h. The volume of the solution was reduced to ca. 5 mL. While stirring, $AgPF_6$ (0.0645 g, 0.255 mmol) in 6 mL of CH_2Cl_2 was added, causing the precipitation of AgBr. Fifteen minutes later, an infrared spectrum showed the reaction to be complete (ν(C≡O) at 2060 s, 1958 s cm^{-1}) and the reaction mixture was filtered. Evaporation of the solvents gave a pale yellow gum. This residue was taken up in 3 mL of CH_2Cl_2, and 4 mL of hexane was layered on top of this. After standing for 5 days at -20°C, some white crystals and a dirty amorphous solid had precipitated. The crystals were easily isolated, washed with hexane and dried in vacuo for 6 days. The yield

of these white crystals was 0.084 g (43%), mp. 251 - 260°C. A further crop of the product (0.036 g, 18%) was obtained by addition of 13 mL of hexane to the mother liquor and storing the solution at -20°C for 5 days. Total yield: 0.120 g (61%).

3. Synthesis of a potentially chelating triamine ligand

a. 1,3,5-tris[2-(azidomethyl)phenyl]benzene, $TriN_3$ A mixture of NaN_3 (0.208 g, 3.20 mmol) and TriBr (0.498 g, 0.851 mmol) in 25 mL of absolute EtOH was refluxed for 24 h. The cooled solution was added to 50 mL of H_2O and the resulting suspension was extracted with Et_2O. The Et_2O solution was dried over $MgSO_4$ and evaporated to give a pale yellow oil, presumably the triazide, $(C_6H_4CH_2N_3)_3C_6H_3$. In CCl_4 the product exhibits characteristic absorbances of the azido group at 2087 cm^{-1} and 1302 cm^{-1}. An NMR spectrum in CCl_4 (Varian A-60 spectrometer) shows resonances at δ 7.37 s (ArH) and δ 4.35 s (CH_2-N_3), as expected.

b. 1,3,5-tris[2-(aminomethyl)phenyl]benzene, $TriNH_2$ The triazide was reduced by $LiAlH_4$ to the corresponding triamine as previously described for the synthesis of exo-bicyclo [3.2.1]-oct-3-en-2-yl amine.[101] Thus, the whole of the triazide obtained in the above reaction was dissolved in 8 mL of THF and slowly added dropwise to a suspension of 0.184 g of $LiAlH_4$ in 17 mL of THF. The mixture was then refluxed for 24 h under N_2. To the cooled, stirred solution, was carefully added H_2O (1 mL), 7% KOH solution (2 mL) and 2 mL more of H_2O. The resulting mixture was filtered and the solution dried over $MgSO_4$ and evaporated to an oil of the crude triamine. In $CDCl_3$ solution, the product exhibits resonances at 7.32 m

Table 7. Analytical data for nitrile complexes

Compound	Calculated			Found		
	%C	%H	%N	%C	%H	%N
$Mn(CO)_3(DiCN\text{-}3)Br$	48.23	2.84	5.63	48.14	3.09	5.50
$Mn(CO)_3(DiCN\text{-}4)Br$	49.34	3.15	5.48	48.96	3.34	5.35
$Mn(CO)_3(TriCN)Br$	60.02	2.52	7.00	59.64	3.03	6.88
$[Mn(CO)_3(TriCN)]PF_6$	54.15	2.27	6.32	53.12	2.58	6.12
$Re(CO)_3(TriCN)Br$	49.25	2.07	5.74	48.95	2.30	5.58
$[Re(CO)_3(TriCN)]PF_6$	45.23	1.90	5.27	45.34	2.02	5.21

Table 8. Infrared spectra of nitrile complexes, cm^{-1}

Compound	Medium	ν(C≡N)	ν(C≡O)
$Mn(CO)_3$(DiCN-2)Br	$CHCl_3$	2270 w	2044 s, 1968 s, 1938 s
$Mn(CO)_3$(DiCN-3)Br	$CHCl_3$	2272 w	2044 s, 1973 s, 1942 s
$Mn(CO)_3$(DiCN-3)Br	Nujol	2272 w	2042 s, 1960 s, 1936 s
$Mn(CO)_3$(DiCN-4)Br	$CHCl_3$	2272 w	2050 s, 1972 s, 1944 s
$Mn(CO)_3$(DiCN-4)Br	Nujol	2269 w	2044 s, 1974 ssh, 1959s, 1944 s, 1896 sh
$Mn(CO)_3$(TriCN)Br	$CHCl_3$	2267 vw 2228 w	2046 s, 1972 s, 1941 s
$[Mn(CO)_3(TriCN)]PF_6$	Nujol	2268 w	2066 s, 1986 s
$Re(CO)_3$(TriCN)Br	$CHCl_3$	2268 vw 2228 w	2039 s, 1950 s, 1916 s
$[Re(CO)_3(TriCN)]PF_6$	Nujol	2267 w	2052 s, 1951 sbr

Table 9. Low-frequency infrared data for dinitrile complexes in the range 700-100 cm^{-1}

Complex	Infrared data
$Mn(CO)_3(DiCN\text{-}3)Br$	676 s, 628 s, 590 wsh, 568 w, 525 m, 498 s, 464 msh, 402 w, br, 285 vw, br, 200 vw
$Mn(CO)_3(DiCN\text{-}4)Br$	678 s, 633 s, 626 s, 600 w, 594 w, 567 w, 526 m, 515 m, sh, 496 s, 478 m, 464 w, sh, 288 w, sh, 268 w, 198 w, sh, 186 w
$Mn_2(CO)_6(CH_3CN)_2Br_2$[a]	677 s, 634 s, 625 s, 601 w, 517 s, 488 w, sh, 463 m, 418 w, sh, 403 w, 363 w, 230 m, sh, 219 m, 193 m, 168 m

[a]Spectrum is virtually identical to the published spectrum (ref. 90).

Table 10. ^1H NMR data for TriCN complexes

Compound	Aromatic Protons
$Mn(CO)_3(TriCN)Br$[a]	7.99-7.36 m, br
$[Mn(CO)_3(TriCN)]PF_6$[b]	8.00-7.35 m, br
$Re(CO)_3(TriCN)Br$[a]	8.00-7.42 m
$[Re(CO)_3(TriCN)]PF_6$[b]	7.96-7.60 m, 7.39 s

[a]$CDCl_3$ solution.
[b]CD_2Cl_2 solution.

Table 11. ^{13}C NMR data for TriCN complexes[a]

Complex	1	2	3	4	5	6	7	8	CN	CO
free TriCN[b]	144.2	111.3	133.5	130.6	133.9	129.5	139.1	128.3	118.7	-
$Re(CO)_3(TriCN)Br$[b]	143.7 146.1	111.3 108.7	133.4 134.1	131.2	133.6 134.9	130.3	138.6 140.6	128.7	118.7 120.9	191.5
$[Re(CO)_3(TriCN)]PF_6$[c]	147.8	111.0	132.8	129.8	135.7	129.4	140.0	129.0	121.4	193.9
$Mn(CO)_3(TriCN)Br$[b,d]	143.7 145.4	111.1 109.6	133.3 133.6	130.8	133.6 134.3	130.0	138.6 140.1	128.4	119.3 126.2	219.6

[a]Where two data are presented for one C atom, the upper one is of lower intensity (usually 1:2) and is assigned to an atom associated with the uncoordinated portion of the ligand.

[b]$CDCl_3$ solvent.

[c]CD_2Cl_2 solvent.

[d]Assignments for carbons 3 and 5 are somewhat uncertain. The largest peak in the spectrum is at 133.6 ppm and is assigned to free C5 and coordinated C3. A peak of low intensity at 129.0 ppm remains unassigned.

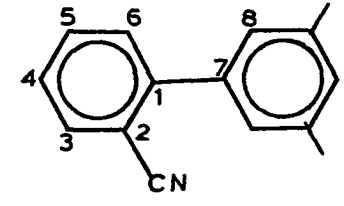

(ArH), 3.89 s (CH_2), and 1.85 br, s (NH_2). Addition of HCl(g) to a $CHCl_3$ solution of the triamine precipitated the hydrochloride salt as a white powder, 0.178 g (42%).

4. Synthesis of SiNC ligands and their rhodium complexes

The SiNC ligands and their precursors, and rhodium complexes have been characterized by elemental analysis (Table 12), infrared spectra (Table 13), ^{1}H NMR (Table 14) and ^{13}C NMR (Table 15) spectra. Electronic spectra of the rhodium complexes are presented in Table 16.

a. 2-aminoresorcinol The catalytic hydrogenation of 2-nitroresorcinol to 2-aminoresorcinol has been reported previously[102] without experimental details. In a 1-L, 3-neck flask equipped with an overhead stirrer, rubber septrum, and a 2-stemmed gas inlet tube fitted with a rubber balloon, 25.2 g (0.162 mol) of 2-nitroresorcinol and 1.3 g of 10% Pd/C catalyst under N_2 were dissolved in 300 mL of EtOH. The vessel was flushed with H_2 for 10 min and charged with H_2 to fill the balloon; the stirrer was then started. The flask was periodically charged to replace reacted H_2. After about 1 h, the mixture achieved a jet-black color and H_2 uptake ceased. The O_2-sensitive solution was filtered under N_2 and the solvent was removed at reduced pressure. Drying in vacuo gave 18.9 g (93%) of 2-aminoresorcinol as a light tan solid.

b. 4-hydroxybenzoxazole The following procedure is an adaptation of a literature method which has been applied to the synthesis of unsubstituted benzoxazole.[103] In a 100 mL flask fitted with a Claissen head and condenser, 18.0 g (0.144 mol) of 2-aminoresorcinol, 35 mL

(31.3 g, 0.212 mol) of $HC(OEt)_3$ and 0.30 mL of H_2SO_4 were combined, and the flask was immersed in an oil bath preheated to 120°C. Distillation of ethanol proceeded for ca. 20 min at which time the mixture solidified. The solid mass was heated for an additional 30 min at 155°C. The solid was cooled, crushed to a brown powder and sublimed (0.05 torr, 125°C) to give the product (14.8 g, 76%) as white crystals, mp 180 - 182°C (lit. 180-181°C,[102] 183°C[104]).

c. 1,2-bis(4,4'-benzoxazoloxy)ethane, Dibenz-2 In 20 mL of DMF under N_2, 4-hydroxybenzoxazole (6.75 g, 50.0 mmol), K_2CO_3 (7.00 g, 50.0 mmol), and 1,2-dibromoethane (2.15 mL, 4.70 g, 25.0 mmol) were heated at 65°C. After 25 h, an additional 1.0 mL of dibromoethane was added, and the mixture was heated for 22 h more. The reaction was cooled to 25°C and poured into 120 mL of rapidly stirred ice water. The resulting white powder was filtered, washed repeatedly with H_2O, and then dried in vacuo. Excess starting material (ca. 2.5 g) was removed via sublimation (0.05 torr, 125°C). The residue was decolorized with activated charcoal and recrystallized from hot acetone to give the product as colorless needles (3.07 g, 41%), mp 163 - 5°C. MS: M^+ (m/e 296, 0.6%); $(C_9H_8NO_2)^+$, (m/e 162, 100%).

d. 1,3-bis(4,4'-benzoxazoloxy)propane, Dibenz-3 A procedure analogous to that above, starting with 3.00 g (22.2 mmol) of 4-hydroxybenzoxazole, 3.00 g (21.4 mmol) of K_2CO_3 and 1.1 mL (2.2 g, 11 mmol) of 1,3-dibromopropane in 12 mL of DMF gave the product (3.34 g, 63%) as colorless needles, mp 128 - 9°C. MS: M^+ (m/e 310, 2.1%); $[C_{10}H_{10}NO_2]^+$ (m/e 176, 100%).

e. 1,2-bis-[2,2'-(isocyano)-3,3'-(trimethylsiloxy)phenoxy]ethane, SiNC-2 A sample of Dibenz-2 (1.91 g, 6.44 mmol) was suspended in 100 mL of THF under N_2, and the solution was cooled to -78°C. Over a period of five min, 5.90 mL (14.16 mmol) of a 2.4 M solution of n-BuLi in hexane was added, giving a yellow suspension. The mixture was stirred at -78°C for 20 min, then slowly warmed to 0°C, during which time a deep yellow-brown precipitate of the dianion formed. After stirring an additional 15 min at 0°C, 1.80 mL (1.54 g, 14.2 mmol) of $ClSiMe_3$ was added over a five minute period. The resulting yellow solution was stirred for 15 min at 0°C, then the solvent was removed at reduced pressure. The solid residue was treated with 10 mL of hexane at -10°C and the resulting suspension was transferred via a cannula tube to a frit and filtered. This procedure was repeated once. The resulting solid was washed twice with 4 mL of hexane and the washes were discarded. The remaining pale yellow solid was extracted with three 5 mL portions of Et_2O, leaving LiCl on the frit. The ether solution was taken to near dryness, treated with 10 mL of hexane and cooled to -20°C to give the product as an off-white microcrystalline solid (0.991 g, 35%) after decantation of the mother liquor and drying in vacuo. In air, the solid melts at 100 - 107°C, then resolidifies and melts again at 162°C (the melting point of Dibenz-2). MS: M^+ (m/e 440, 5.8%); $(C_9H_8NO_2)^+$ (m/e 162, 62%); $[Si(CH_3)_3]^+$ (m/e 73, 100%). Proton and ^{13}C NMR of the product (Tables 12, 13) showed it to contain 10 - 15% dibenzoxazole starting material.

f. 1,3-bis[2,2'-(isocyano)-3,3'-(trimethylsiloxy)phenoxy]propane, SiNC-3 This reaction was carried out as for SiNC-2 using 0.574 g (1.85 mmol) of Dibenz-3, 38 mL THF, 1.70 mL (4.07 mmol) of 2.4 M n-BuLi, and 0.52 mL (0.45 g, 4.1 mmol) $ClSiMe_3$. Upon workup of the dry reaction residue, a minimum amount of cold hexane was used to transfer the suspension of product and LiCl to a frit. The solid was washed with two 3 mL portions of cold hexane to remove impurities. The product was washed away from the LiCl with several portions of Et_2O into a clean Schlenk tube. The solvent was removed to give a yellow oil which crystallized upon addition of 1 mL of hexane. The mixture was cooled to -20°C, and the solution was decanted from the pale yellow solid. Washing of the solid with two 2 mL portions of cold hexane and drying in vacuo gave 0.45 g of the product (54%), mp 76 - 82°C. The SiNC-3 thus obtained had a purity of ca. 90%, as determined by ^1H NMR. MS: M^+ (m/e 454, 0.4%); $(C_{10}H_{10}NO_2)^+$ (m/e 176, 14.2%); $[Si(CH_3)_3]^+$ (m/e 73, 100%).

g. $[Rh(SiNC\text{-}2)_2]BPh_4$ A solution of SiNC-2 (0.159 g, 0.361 mmol) in 6 mL of C_6H_6 was added to a stirred solution of $[Rh(COD)Cl]_2$ (0.030 g, 0.061 mmol). The solution was stirred for 3.5 h. During this time, a blue-green precipitate of $[Rh(SiNC\text{-}2)_2]Cl$ formed. The solid was filtered off, washed twice with 5 mL of C_6H_6 and dried in vacuo. Dichloromethane (9 mL) was added to the solid to give a deep blue-green solution. After being filtered, the solution was treated with a filtered solution of $NaBPh_4$ (0.050 g, 0.15 mmol) in 5 mL of CH_3CN. The resulting solution was stirred for 30 min, and solvents were removed at reduced pressure. The deep blue-green product, $[Rh(SiNC\text{-}2)_2]BPh_4$, was extracted away from

precipitated NaCl with CH_2Cl_2. After filtration, the solvent was slowly removed at reduced pressure, yielding the pure product as a deep blue-green glass (0.140 g, 88%).

h. $[Rh(SiNC\text{-}2)_2]PF_6$ A sample of $[Rh(SiNC\text{-}2)_2]Cl$ was prepared from 0.565 g (1.28 mmol) of SiNC-2 (10 mL of C_6H_6) and 0.104 g (0.211 mmol) of $[Rh(COD)Cl]_2$ (15 mL of C_6H_6) as outlined for $[Rh(SiNC\text{-}2)_2]BPh_4$. A similar metathesis procedure employing 0.086 g (0.47 mmol) of KPF_6 gave $[Rh(SiNC\text{-}2)_2]PF_6$ as a deep blue-green solid, 0.335 g (70%).

i. $[Rh(SiNC\text{-}3)_2]PF_6$ A solution of $[Rh(COD)C]_2$ (0.091 g, 0.185 mmol) in 15 mL of benzene was treated dropwise with 0.501 g (1.10 mmol) of SiNC-3 in 20 mL of C_6H_6. The mixture was stirred overnight to give a yellow-green precipitate of $[Rh(SiNC\text{-}3)_2]Cl$ which was filtered, washed with C_6H_6, and dried in vacuo. This sample was dissolved in 8 mL CH_2Cl_2 to give a deep green solution. To this was added a filtered solution of KPF_6 (0.080 g, 0.43 mmol) in 8 mL of CH_3CN. The mixture was stirred 15 min, and the solvent was removed at reduced pressure. The dark green residue was extracted with CH_2Cl_2. Removal of KCl by filtration, evaporation of the CH_2Cl_2 at reduced pressure and drying in vacuo gave the product as a green microcrystalline solid, 0.137 g (32%).

j. Reaction of $[Rh(SiNC\text{-}2)_2]PF_6$ with I_2 Treatment of a solution of $[Rh(SiNC\text{-}2)_2]PF_6$ (0.0528 g, 0.0468 mmol) in 4 mL of CH_2Cl_2 with 0.94 mL of a 0.025 M solution (0.024 mmol) of I_2 in CH_2Cl_2 caused a rapid color change from blue to orange. After stirring for 5 min, the volume of the solution was reduced to 1 mL. Addition of 4 mL of hexane precipitated

an orange-brown tar. The solution was decanted away from the tar, which was then dried in vacuo. The residue was taken up in 2 mL of CH_2Cl_2 and 4 mL of Et_2O was carefully added. After standing for 3 days at 0°C, 0.022 g of rust-colored product was obtained by decantation of the mother liquor and vacuum drying. An additional 0.018 g of product was obtained by addition of Et_2O to the mother liquor and allowing the mixture to stand overnight at 0°C. The total yield was 0.040 g, representing a 68% yield as $[Rh_2(SiNC\text{-}2)_4I_2](PF_6)_2$. Analysis, calc'd. for $C_{88}H_{112}F_{12}I_2N_8O_{16}P_2Rh_2Si_8$: % C, 42.07; % H, 4.50; % N, 4.46; % I, 10.10; found: % C, 41.19; % H, 4.35; % N, 4.40; % I, 12.43.

k. Reaction of $[Rh(SiNC\text{-}3)_2]PF_6$ with I_2 A similar reaction to that described above was carried out between 0.0589 g (0.0582 mmol) of $[Rh(SiNC\text{-}3)_2]PF_6$ and 1.25 mL of 0.0273 M I_2 (0.034 mmol) in 6 mL of CH_2Cl_2. The reaction solution was filtered and reduced in volume to 4 mL. Et_2O (4 mL) was added to the solution, which was stored at 0°C for 6 h. A small amount (ca. 6 mg) of tan powder was removed by filtration. An 8 mL portion of Et_2O was added to the remaining solution, and after standing at 25°C overnight, 0.031 g of rust-colored microcrystals had formed. The solid was isolated by decantation of the mother liquor and was vacuum dried. Yield: 38% as $[Rh(SiNC\text{-}3)_2I_2](PF_6)$. Analysis, calc'd. for $C_{46}H_{60}F_6I_2N_4O_8PRhSi_4$: % C, 39.16; % H, 4.28; % N, 3.98; % I, 17.97; found: % C, 40.63; % H, 4.21; % N, 4.28; % I, 17.48.

Table 12. Analytical data for organic precursors and rhodium complexes of SiNC-2 and SiNC-3

Compound	Calculated %C	Calculated %H	Calculated %N	Found %C	Found %H	Found %N
Dibenz-2	64.86	4.08	9.45	64.75	4.08	9.35
Dibenz-3	65.80	4.55	9.03	65.66	4.63	8.99
$[Rh(SiNC\text{-}2)_2]BPh_4$	62.66	5.88	4.30	62.49	5.99	4.29
$[Rh(SiNC\text{-}2)_2]PF_6$	46.80	5.00	4.96	46.80	5.02	4.97
$[Rh(SiNC\text{-}3)_2]PF_6$	47.74	5.23	4.84	48.21	5.03	4.94

Table 13. Infrared data for SiNC ligands, precursors and rhodium complexes in Nujol mull, cm^{-1}[a]

Compound	Infrared data
Dibenz-2	3145 w, 1725 w, 1720 w, 1619 m, 1505 msh, 1497 s, 1482 s, 1430 m, 1351 m, 1317 s, 1276 s, 1248 w, 1239 w, 1206 w, 1104 ssh, 1096 s, 1078 msh, 1069 s, 1032 w, 869 w, 784 m, 749 msh, 741 s, 721 m, 630 m
Dibenz-3	3145 w, 1730 w, 1725 vw, 1620 s, 1499 s, 1470 s, 1432 m, 1361 wsh, 1352 m, 1315 s, 1277 s, 1249 m, 1205 m, 1110 s, 1094 ssh, 1081 s, 1067 s, 1038 m, 872 m, 864 w, 789 s, 750 s, 714 m, 632 m
SiNC-2	3100 vw, 2130 s(C≡N), 1611 wsh, 1588 s, 1492 msh, 1470-1400 ?, 1305 m, 1258 s, 1102 ssh, 1091 s, 1031 m, 910 w, 840 sbr, 773 m, 748 w, 715 m, 688 w
SiNC-3	3095 vw, 2126 s(C≡N), 1582 s, ~1460 s?, 1396 m, 1320 m, 1250 s, 1175 m, 1080 sbr, 1030 m, 990 w, 930 w, 836 sbr, 778 m, 754 m, 720 m, 675 w
$[Rh(SiNC\text{-}2)_2]BPh_4$	3053 w, 3030 w, 2200 wsh, 2162 vs(C≡N), 1590 s, 1580 s, 1472 s, 1422 w, 1305 w, 1255 s, 1171 w, 1112 m, 1087 s, 1073 m, 1028 m, 909 m, 840 s, 776 w, 740 wsh, 725 w, 711 wsh, 698 m
$[Rh(SiNC\text{-}2)_2]PF_6$	2200 wsh, 2160 vs(C≡N), 1595 s, 1588 s, 1475 s, 1420 w, 1311 w, 1260 s, 1177 w, 1119 m, 1094 s, 1032 m, 912 w, 835 sbr, 780 m, 774 msh, 755 wsh, 717 w, 680 vw br
$[Rh(SiNC\text{-}3)_2]PF_6$	~2200 wsh, 2159 vw(C≡N), 1582 s, 1470 s, 1255 s, 1095 s, 1074 ssh, 1030 wsh, 830 sbr, 775 m, 717 w, 670 vwbr

[a]Bands in the regions 3000-2800 cm^{-1}, 1380-1360 cm^{-1}, and 1365-1385 cm^{-1} are, in most cases, masked by Nujol absorptions.

Table 13. Continued

Compound	Infrared data
$[Rh_2(SiNC\text{-}2)_4I_2]PF_6$	2213 s(C≡N), 1590 m, 1585 m, 1478 s, 1310 w, 1261 s, 1177 vw, 1120 m, 1095 s, 1080 msh, 1031 w, 909 w, 838 vsbr, 774 w, 711 w, 663 vw, br
$[Rh(SiNC\text{-}3)_2I_2]PF_6$	2236 m(C≡N), 1596 m, 1588 m, 1487 s, 1265 s, 1105 s, 1076 m, 850 s, br, 788 m, 725 m

Table 14. ^1H NMR data for SiNC ligands, precursors, and rhodium complexes[a]

Compound	ArH	OCH_2	CH_2	Other
Dibenz-2[b]	7.37-6.97 m	4.82		OCH-N 8.35 s
Dibenz-3[c]	7.40-6.75 m	4.50 t (6.1)	2.48 p (6.1)	OCH=N 8.0 s
SiNC-2[c,d]	7.29-6.48 m	4.47 s	-	$OSiMe_3$ 0.33 s
SiNC-3[c,d]	7.17-6.45 m	4.29 t (5.9)	2.36 p (5.9)	$OSiMe_3$ 0.32 s
$[Rh(SiNC-2)_2]BPh_4$[e]	7.35-6.09 m	4.27 s	-	$OSiMe_3$ 0.13 s
$[Rh(SiNC-2)_2]PF_6$[f]	7.05-6.37 m	4.35 s	-	$OSiMe_3$ 0.11 s
$[Rh(SiNC-3)_2]PF_6$[e]	7.30 ps-t (8.4) 6.61 ps-t (7.9)	4.30 ps-t (4.8)	2.47 m	$OSiMe_3$ 0.26 s

[a]Coupling constants or apparent coupling constants (Hz) are given in parentheses; m = multiplet; ps-t = pseudotriplet; p = pentet; t = triplet; td = triplet of doublets.

[b]Acetone-d_6 solvent.

[c]$CDCl_3$ solvent.

[d]Also exhibits signals corresponding to a 10-15% impurity of the corresponding dibenzoxazole.

[e]CD_2Cl_2 solvent.

[f]CD_3CN solvent.

Table 14. Continued

Compound	ArH	OCH_2	CH_2	Other
$[Rh_2(SiNC\text{-}2)_4I_2](PF_6)_2$[f]	7.09, 6.99, 6.90, 6.47, 6.38	4.36 m	-	$OSiMe_3$ 0.17 s
$[Rh(SiNC\text{-}3)_2I_2](PF_6)_2$[f]	7.49 ps-t (8.5) 6.72 ps-td (7.6, 1.0)	4.34 ps-t (4.5)	2.57 m, br	$OSiMe_3$ 0.28 s

Table 15. ^{13}C NMR data for SiNC ligands and precursors

Compound	2	4	5	6	7	8	9	OCH_2	CH_2
4-hydroxybenzoxazole[a]	152.5	150.5[b]	111.1	127.1	102.7	150.5[b]	127.5	-	-
Dibenz-2[c]	151.0	151.8[b]	108.7	126.3	104.0	151.8[b]	_d	68.1	-
Dibenz-3[c]	150.9	151.4[b]	107.6	126.1	103.4	151.4	129.6	65.7	29.3
	NC	1	2	3	4	5	6	OCH_2	CH_2
SiNC-2[c]	170.6	152.7	113.1	129.7	106.0	155.3	_d	67.9	-
SiNC-3[c]	170.3	152.4	112.5	129.6	105.3	155.3	109.7	65.0	28.9

[a]Acetone-d_6 solvent.
[b]Single resonance assigned to both atoms.
[c]$CDCl_3$ solvent.
[d]Resonance not observed.

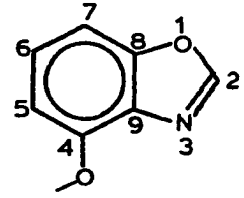

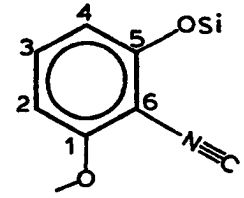

Table 16. Electronic spectra of SiNC-2 and SiNC-3 rhodium complexes in 1 mm cells

	10^4C, M	λ max, nm	$10^{-3}E$, $M^{-1}cm^{-1}$	
$[Rh(SiNC\text{-}2)_2]PF_6$ [a]	5.81	252	38.1	intraligand
		362	18.4	$^1A_{1g}\rightarrow{}^1E_u$
		607	0.22	$^1A_{1g}\rightarrow{}^1A_{2u}$
$[Rh(SiNC\text{-}3)_2]PF_6$ [a]	5.8	259	39	intraligand
		352	35	$^1A_{1g}\rightarrow{}^1E_u$
		406	2.8	$^1A_{1g}\rightarrow{}^1A_{2u}$
		463	0.58	$^1A_{1g}\rightarrow{}^3A_{2u}$
$[Rh_2(SiNC\text{-}2)_4I_2](PF_6)_2$ [b]	_c	365	_d	Rh(I) $^1A_{1g}\rightarrow{}^1E_u$?
		427	_d	$\sigma\rightarrow\sigma^*$
		478	_d	$d\pi\rightarrow\sigma^*$
$[Rh(SiNC\text{-}3)_2I_2]PF_6$ [b]	3.1	262	74	intraligand
		ca. 300, sh	30	
		400	9.1	

[a] CH_3CN solution. Band assignments follow those in ref. 56.

[b] CH_2Cl_2 solution.

[c] Concentration unknown. Band assignments follow ref. 105.

[d] Intensity ratios are 0.94: 1.00: 0.79 (in order of increasing wavelength).

5. Attempted preparation of a macrocyclic tetraisonitrile complex, $[Rh(MacNC)]BPh_4$

In a typical experiment, 0.067 g (0.051 mmol) of $[Rh(SiNC-2)_2]PF_6$ in 1 mL of CH_2Cl_2 was allowed to react with 8 μL (0.011 g, 0.102 mmol) of $H_2C(COF)_2$. After 1.5 h, the deep green precipitate which had formed was isolated, washed with CH_2Cl_2, and dried in vacuo, yielding 0.038 g (64% as the title compound). In Nujol mull, the product exhibited the following bands: 2200 m, sh, 2155 s, ν(C≡N); 1775 m, br, 1745 m, sh, ν(C=O). ^1H NMR (DMSO-d_6): 6.7 - 7.4 δ (m, br, 25H); 4.48 δ (m, br, 8H). The product is very slightly soluble in DMSO and insoluble in other common organic solvents. In DMSO solution, the two lowest-energy transitions were observed at 622 nm and 364 nm, with the latter one decreasing to half its original intensity in ca. 9 min. Analysis, calc'd. for $BC_{62}H_{44}N_4O_{12}Rh$: C, 64.71%; H, 3.85%; N, 4.87%; found: C, 56.62%; H, 3.82%; N, 5.02% (see Section III.B.3).

6. Synthesis of t-BuDiNC. Characterization of the synthetic precursors of DiNC and t-BuDiNC

Analytical and spectroscopic data for these compounds are presented in Tables 17-20.

a. 4-t-butyl-2-nitrophenol The reagents for this preparation were used as received, and the reaction was run under an air atmosphere. In a 2-L flask equipped with a thermometer, overhead stirrer, and dropping funnel, a solution of 100 g (0.67 mol) of 4-t-butylphenol in 350 mL of C_6H_6 was cooled to 10°C. With vigorous stirring, 225 mL of 6 M HNO_3 was

added dropwise such that the temperature stayed below 15°C. The solution was stirred for a total of 4 h at 15°C and was subsequently poured into 1 L of H_2O. The mixture was separated in a separatory funnel, and the aqueous layer was extracted with 200 mL of Et_2O. This ether extract was added to the C_6H_6 layer, and the resulting solution was washed three times with 200 mL of 5% aqueous NaCl, then dried over $CaSO_4$ for 12 h. The solvents were removed on a rotary evaporator; the crude product was distilled (b.p. 81°C, ca. 0.1 torr). The product is a bright yellow oily liquid, mp 10-15°C. Yield: 81.6 g (63%).

b. 1,2-bis-(4-t-butyl-2-nitrophenoxy)ethane, t-BuDiNO$_2$ Potassium carbonate (32 g, 0.23 mol) was added in portions of ca. 1 g over a period of 30 min to a hot (100°C) solution of 4-t-butyl-2-nitrophenol (81.6 g, 0.418 mol) in 270 mL of undistilled DMF. The resulting red solution was heated further to 130°C and with stirring, 18.0 mL (39.2 g, 0.209 mol) of 1,2-dibromoethane was added over a one-hour period. The mixture was stirred for an additional 24 h at 130°C, then cooled to room temperature. The mixture (now containing a large amount of precipitated KBr) was dumped into 3.5 L of stirred ice water, yielding a cloudy orange solution and a gummy tan solid. The majority of the solution was decanted away from the solid and discarded. The remaining slurry was extracted twice with 300 mL Et_2O. The combined ether extracts were washed successively with water (3 x 300 mL), 5% NaOH (3 x 400 mL), and water (3 x 300 mL). The resulting pale orange solution was dried 12 h over $CaSO_4$, filtered,

and the solvent removed by rotary evaporation. The crude product was purified by cooling a hot ethanolic solution slowly to 25°C, then to -20°C. Large, pale yellow needles of the product were removed by filtration, washed with cold ethanol (2 x 100 mL), then dried in vacuo overnight. The yield was 37.1 g (42.4%), mp 117.5-119.5°C.

c. 1,2,-bis-(2-amino-4-t-butylphenoxy)ethane, t-BuDiNH$_2$ This diamine was prepared by H_2 reduction of the corresponding nitro compound in a 3-liter, three-necked flask equipped with a gas-inlet tube, overhead stirrer and rubber balloon. Degassed ethanol (600 mL) was added to a mixture of t-BuDiNO$_2$ (34.3 g, 84.5 mmol) and 10% Pd/C catalyst (1.2 g). The apparatus was flushed several times with H_2, and the reaction was started by stirring the suspension rapidly. The balloon was refilled as necessary by introducing H_2 through the gas inlet tube. Stirring was continued until the mixture began to cool and hydrogen uptake ceased (ca. 1 h). The solution was heated to ~60°C, then the catalyst was removed by filtration in air. White needles of the product which precipitated upon cooling were redissolved by heating, then water was added until the solution reached the cloud point. The solution was chilled at 0°C for 6 h, and the product was filtered in air, washed with 1:1 EtOH/H_2O, the dried in vacuo for 12 h. The yield was 27.4 g (91%), of very pale pink needles, mp 120-123°C. An additional portion of less pure product (1.1 g), mp 117-120°C, was obtained by reducing the volume of the mother liquor. Total yield: 28.5 g (94.6%).

d. 1,2-bis-(4-t-butyl-2-formamidophenoxy)ethane, t-BuDiFor In a 250 mL, 3 neck flask equipped with a magnetic stir bar, thermometer, N_2 inlet, and rubber septum, 26 mL of AFA was cooled to 5°C. A solution of t-BuDiNH$_2$ (27.7 g, 77.7 mmol) in 90 mL of freshly distilled CH_2Cl_2 was cannulated into the flask, the reaction temperature being maintained at less than 20°C by immersion in an ice bath. The reaction was warmed to 25°C and stirred for 2 h. Extraction with water (2 x 100 mL) removed liberated acetic acid. The CH_2Cl_2 solution was dried over $MgSO_4$, then evaporated on a rotary evaporator to yield a pink syrup. Diethyl ether (80 mL) was added, and upon stirring, a white precipitate of the product formed. After stirring for 4 h, the product was filtered, washed with 30 mL Et_2O, and dried in vacuo. Yield: 28.1 g (87.7%), mp 138-130°C.

e. 1,2-bis-(4-t-butyl-2-isocyanophenoxy)ethane, t-BuDiNC The ligand, t-BuDiNC, was prepared by the phosgene dehydration of t-BuDiFor. Because of the toxic nature of phosgene ($COCl_2$), the reaction was carried out in an efficient fume hood. A 1.40 M solution of $COCl_2$ in 125 mL of CH_2Cl_2 was prepared by slowly passing $COCl_2$ (g) through a preweighed, ice-cooled flask of degassed CH_2Cl_2. Phosgene exhaust vapor was trapped by a concentrated aqueous ammonia solution. An aliquot of this solution (95 mL, 133 mmol) was added via a dropping funnel to an ice-cooled solution of t-BuDiFor (26.9 g, 65.2 mmol) and triethylamine (42.0 mL 30.5 g, 302 mmol) in 140 mL of dry, degassed CH_2Cl_2 over a ten-minute period. The mixture was stirred for 30 min at 0°C, warmed to 25°C, and 80 mL of water was added. After stirring 45 min, the layers were separated. The organic layer was washed with 80 mL of

water, 80 mL of 0.1 M HCl, and 80 mL of water, then dried over $MgSO_4$. Removal of the solvent by rotary evaporation gave a brown oil. The crude product was purified by chromatography on a 70 mm x 26 cm column of silica gel, eluting with $CHCl_3$/pentane (4:1). Evaporation of the eluate gave a pale yellow oil. Addition of 80 mL of pentane induced crystallization of the product as colorless needles, 8.08 g, mp 97.5-100°C. Three additional crops with similar melting points were obtained by evaporation and similar treatment of successive mother liquors. Total yield: 16.4 g (66.5%).

7. Preparation of complexes of DiNC and t-BuDiNC

Analytical and spectroscopic data are found in Tables 21-28.

a. cis-$Cr(CO)_4$(DiNC) A THF solution (50 mL) of DiNC (0.265 g, 1.00 mmol) and $Cr(CO)_4$(norbornadiene) (0.254 g, 0.99 mmol) was refluxed for 6 h. The solvent was removed in vacuo, and the residue was washed with three 5 mL portions of hexane. Recrystallization of the residue from $CHCl_3$/hexane at -20°C gave the product as yellow crystals (0.306 g, 72%); the mass spectrum showed a parent ion (M^+) at m/e 428, the $[M-n(CO)]^+$ ions (where n = 2,3,4), and the $[Cr(C_6H_4NCO)_n]^+$ ions for n = 1,2 at m/e 170 and 288, respectively. Traces of entrapped $CHCl_3$ in this complex were removed by recrystallization from hot hexane solution under N_2.

b. cis-$Cr(CO)_4$(t-BuDiNC) A solution of t-BuDiNC (0.0743 g, 0.197 mmol) and $Cr(CO)_4$(norbornadiene) (0.0493 g, 0.193 mmol) in 5 mL of THF was refluxed for 5 h. Evaporation of the solution, drying in vacuo, and recrystallization of the residue from $CHCl_3$/hexane at -20°C gave

Table 17. Analytical data for t-BuDiNC and precursors

Compound	Calculated %C	%H	%N	Found %C	%H	%N
t-BuDiNO$_2$	63.45	6.78	6.73	64.02	6.60	6.85
t-BuDiNH$_2$	74.12	9.05	7.86	73.11	9.05	7.72
t-BuDiFor	69.88	7.82	6.79	69.50	7.85	6.83
t-BuDiNC	76.55	7.50	7.45	76.64	7.57	7.38

Table 18. Infrared date for DiNC, t-BuDiNC and their precursors in Nujol mull, cm^{-1}[a]

Compound	Infrared Data
$DiNO_2$	1605 m, 1583 w, 1520 s (ν_s, NO_2), 1475 s, 1366 s (ν_a, NO_2) 1293 m, 1278 s, 1252 s, 1160 m, 1087 w, 1058 w, 1043 w, 937 m, 850 w, 769 m, 743 m
$DiNH_2$	3442 m [ν (NH)], 3360 [ν (NH)], 1610 m, 1505 m, 1341 w, 1275 m, 1244 w, 1212 s, 1143 w, 1081 w, 947 m, 923 w, 743 msh, 735 m
DiFor	3295 s [ν(NH)], 1673 vs [ν(C=O)], 1596 m, 1535 s, 1490 m, 1411 w, 1347 w, 1327 m, 1298 m, 1268 m, 1229 m, 1218 w, 1159 m, 1110 m, 1054 m, 1038 m, 942 w, 888 w, 923 m, 761 m, 745 s, 705 m, br
DiNC	3078 w, 2126 [ν(C≡N)], 1595 m, 1494 s, 1303 m, 1288 s, 1258 s, 1164 m, 1117 s, 1064 m, 1045 w, 950 m, 765 s, sh, 752 s
t-$BuDiNO_2$	1623 m, 1570 w, 1530 s [$\nu_s(NO_2)$], 1505 msh, 1382 msh, 1355 s [$\nu_a(NO_2)$], 1302 msh, 1270 s, 1257 s, sh, 1212 w, 1171 m, 1132 w, 1091 m, 1065 m, 949 m, 908 m, 900 m,sh, 838 m, 827 m, 807 w, 764 w, 729 m, 667 w
t-$BuDiNH_2$	3430 s, 3334 m [ν(NH)], 3065 w, 3050 w, 1629 m, 1606 m, 1524 s, 1514 ssh, 1432 m, 1496 w, 1371 m, 1368 m, 1297 s, 1256 m, 1215 s, 1208 ssh, 1164 s, 1094 m, 1069 m, 1044 m, 952 m, 928 m, 881 m, 802 s

[a]Bands in the regions 3000-2800 cm^{-1}, 1380-1360 cm^{-1} and 1365-1385 cm^{-1} are, in most cases, masked by Nujol absorptions.

Table 18. continued

Compound	Infrared Data
t-BuDiFor	3335 m, 3275 m [ν(NH)], 1682 s, 1669 s [ν(C=O)], 1615 w, 1594 m, 1538 s, 1497 msh, 1480 m, 1430 m, 1398 w, 1370 w, 1310 m, 1280 m, 1235 m, 1178 m, 1137 w, 1108 m, 1045 m, 933 w, 894 w, 859 m, 825 m, 768 w, 684 w, 640 w
t-BuDiNC	2126 s [ν(C≡N)], 1608 m, 1530 msh, 1502 s, 1408 w, 1366 w, 1270 s, 1255 s, 1140 s, 1105 m, 1067 m, 950 m, 904 w, 883 w, 810 m, 772 w, 720 w

Table 19. ^{1}H NMR data for DiNC, t-BuDiNC, and their precursors[a]

Compound	Ar-H	CH_2	t-Bu	Other
DiNC	7.50-6.84 m	4.51 s	-	-
DiNC[b]	7.56-6.93	4.62 s	-	-
t-BuDiNO$_2$	7.82 d(2.4), 7.63 dd(2.4, 8.8), 7.16 d(8.8)	4.50 s	1.33 s	-
t-BuDiNH$_2$	6.77 s	4.32 s	1.29 s	3.79 br, s NH$_2$
t-BuDiFor	7.25-6.79 m	4.37 s, 4.35 s	1.30 s	8.77-8.04 m NH, CHO
t-BuDiFor[c]	7.25-6.81 m	4.35 s	1.30 s	8.40 br,s CH 7.76 br,s NH
t-BuDiNC	7.48-7.01 m	4.47 s	1.28 s	-
t-BuDiNC[b]	7.56-7.19 m	4.58 s	1.30 s	-
t-BuDiNC[d]	7.47-7.01 m	4.48 s	1.28 s	-

[a]All spectra measured as $CDCl_3$ solutions unless noted otherwise.
[b]Acetone-d_6 solvent.
[c]Spectrum measured at 85°C.
[d]CD_2Cl_2 solution.

Table 20. ^{13}C NMR data for DiNC, t-BuDiNC, and t-BuDiNC precursors[a]

Compound	1	2	3	4	5	6	NC	OCH_2	$\underline{C}Me_3$	Me	Other
DiNC	153.9	116.6	127.7	121.3	130.5	113.6	167.7	67.9	-	-	-
DiNC[b]	155.1	116.7	128.5	122.0	131.6	114.6	169.7	68.8	-	-	-
t-$BuDiNO_2$	149.7	139.9	122.1	144.8	131.3	115.8	-	68.9	34.3	31.1	-
t-$BuDiNH_2$	144.2	136.2	112.3	144.9	115.0	113.0	-	67.7	34.1	31.5	-
t-BuDiFor[c]	_d	_e	118.6	_d	120.8	111.1	-	67.2	34.2	31.3	(C=O): 162.7(cis) 159.2(trans) (1:2)
t-BuDiNC	151.8	116.2	124.8	144.7	127.5	113.7	167.0	68.0	34.2	-	-
t-BuDiNC[f]	152.2	116.4	125.3	145.1	127.9	113.8	167.9	68.5	34.2	-	-

[a]Spectra run in $CDCl_3$ unless noted otherwise.

[b]Acetone-d_6 solvent.

[c]Exists in several diastereomeric forms resulting from cis-trans isomerism within the NHCHO (see ref. 106). Resonances given for C3, C5 and C6 are due to the transisomer. Unassigned resonances are at 122.2, 115.8, 113.4 and 112.5 ppm.

[d]Two of four lines at 146.1, 145.3, 144.9, and 144.7 ppm.

[e]Three lines at 126.7, 126.3, and 126.0 ppm.

[f]CD_2Cl_2 solvent.

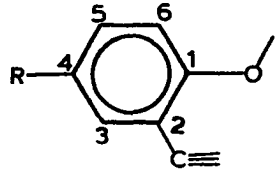

the product as opaque, pale yellow crystals (0.048 g, 46%); the mass spectrum showed M^+ at m/e 540 and $[M-n(CO)]^+$ ions for n = 3,4. Both the DiNC and t-BuDiNC derivatives oxidize to unknown products after several months in air.

c. cis-$Mo(CO)_4$(t-BuDiNC) A solution of t-BuDiNC (0.0715 g, 0.190 mmol) in 2 mL of Et_2O was added to a solution of $Mo(CO)_4$(norbornadiene) (0.057 g, 0.190 mmol) in 2 mL of Et_2O. After 10 min, needles of the product began to form, and the odor of norbornadiene could be detected. Solvent was removed under a slow N_2 stream until the volume was 0.5 mL. The remaining solution was decanted off, and the resulting pale yellow crystals were washed with two 1 mL portions of cold hexane and dried in vacuo. Yield: (0.075 g, 68%); the mass spectrum showed M^+ at m/e 586 (for ^{98}Mo) and peaks for $[M-n(CO)]^+$, n = 2-4. The complex decomposes to a tan solid in the solid state when exposed to air over a period of several months.

d. $[Cr(CO)_5]_2$(μ-DiNC) A solution of $AgPF_6$ (0.230 g, 0.909 mmol) in 5 mL of acetone was added over a period of 10 min to a rapidly stirred solution of $(Et_4N)[Cr(CO)_5I]$ (0.402 g, 0.895 mmol) in 35 mL of THF at 25°C. After stirring for an additional 20 min, the orange solution was filtered to remove precipitated AgI. A CH_2Cl_2 solution (6 mL) of DiNC (0.120 g, 0.455 mmol) was then added; the solution was stirred for 20 min and evaporated to dryness. The resulting yellow residue was taken up in 8 mL of $CHCl_3$ and eluted with 20 mL of $CHCl_3$

from a short column (1 x 7 cm) of silica gel to remove $(Et_4N)(PF_6)$. Evaporation of the $CHCl_3$ gave the product as a pale yellow powder, which was recrystallized from $CHCl_3$/hexane at -20°C to give pale yellow needles (0.201 g, 69%). The mass spectrum showed M^+ at m/e 648 as well as peaks for $[M-n(CO)]^+$ (n = 5-10), $Cr(DiNC)^+$, and $[Cr(C_6H_4NCO)]^+$

e. $[W(CO)_5]_2(\mu\text{-DiNC})$ An analogous procedure to that above, using 0.520 g (0.895 mmol) of $(Et_4N)[W(CO)_5I]$, 0.230 g (0.909 mmol) of $AgPF_6$, and 0.118 g (0.447 mmol) of DiNC gave the product (0.169 g, 41%) as colorless to pale yellow needles. Both the Cr and W derivatives are indefinitely stable in air in the solid state; solutions exposed to air undergo no detectable decomposition over a period of several days.

f. $Cr(t\text{-BuDiNC})_3$ A solution of $CrCl_3(THF)_3$ was prepared by stirring 0.023 g (0.145 mmol) of finely ground anhydrous $CrCl_3$ with 5 mg of Zn dust in 4 mL of THF until a homogeneous purple solution resulted. To this solution was added a solution of t-BuDiNC (0.167 g, 0.444 mmol) in 4 mL of THF, causing an immediate change in color to red-brown. The red-brown solution was transferred via a cannula tube to freshly prepared Na/Hg (0.045 g Na/2 mL of Hg). After stirring for 30 min, the resulting blood-red solution was transferred to a 15 mL centrifuge tube capped with a rubber septum, and the suspended NaCl was concentrated by centrifugation. The resulting solution was filtered, evaporated at reduced pressure, and the residue dried in vacuo overnight. The product is a deep red glassy solid. Yield: 0.112 g (65%),

mp 175°C. When exposed to air, the complex is slowly oxidized over a period of weeks. In chlorocarbon solutions, the complex is oxidized by air in a matter of hours to the monocation. The oxidation is complete within minutes when chlorocarbon solutions are chromatographed in air on alumina.

g. $[Cr(t\text{-}BuDiNC)_3]PF_6$ Acetone (3 mL) was added to a mixture of $Cr(t\text{-}BuDiNC)_3$ (0.050 g, 0.042 mmol) and $AgPF_6$ (0.012 g, 0.047 mmol). A deep red-black solution formed rapidly and a silver mirror was deposited on the walls of the flask. After stirring for 1 h, the solution was filtered to remove suspended silver. The reaction flask and frit were rinsed with acetone and the volume of the red-orange solution was reduced to 3 mL. Rapid addition of 10 mL of hexane gave an orange precipitate of the crude product, which was isolated by filtration, washed with ether, and dried. Yield: 0.052 g (83%). The product was recrystallized from CH_2Cl_2/hexane and obtained as an air-stable orange powder (0.038 g, 62%), mp 222°C, decomp.

h. $[Cr(t\text{-}BuDiNC)_3](PF_6)_2$ In a reaction similar to the one just described, $Cr(t\text{-}BuDiNC)_3$ (0.0538 g, 0.0455 mmol) and $AgPF_6$ (0.0225 g, 0.089 mmol) were allowed to react in 3 mL of acetone for 1.5 h. Workup of the reaction as before gave the crude product as a red powder (0.059 g, 90%). Recrystallization from acetone/hexane gave the product as an air-stable crystalline red solid (0.042 g, 64%), mp 260-280°C, decomp.

i. $[Mn(t\text{-}BuDiNC)_3]PF_6$ A solution of $Mn(CO)_5Cl$ (0.091 g, 0.39 mmol) and t-BuDiNC (0.453 g, 1.20 mmol) in 11 mL THF was heated to reflux. During the first few hours of reaction, a pale yellow precipitate of $[Mn(t\text{-}BuDiNC)_3]Cl$ formed. After 26 h, the mixture was cooled and filtered. The solid was washed with ether and dried in vacuo, giving 0.250 g (53%) of pale yellow $[Mn(t\text{-}BuDiNC)_3]Cl$. This salt was then metathesized to the PF_6^- salt as follows. The crude solid was dissolved in CH_2Cl_2, filtered, and the solvent was evaporated. The residue was treated with 35 mL of EtOH and heated to boiling, whereupon all the solid dissolved. A filtered solution of 0.130 g of NH_4PF_6 in 7 mL of EtOH was added to the hot solution, causing the desired product to precipitate from solution. The mixture was cooled to room temperature, filtered, and the product washed with Et_2O. The cream-colored product was then dried in vacuo. Yield: 0.255 g (49% from $Mn(CO)_5Cl$). The product turns yellow at ca. 200°C, but does not melt below 350°C. It appears to be quite stable to air as a solid and in solution.

j. $[Mn(t\text{-}BuDiNC)_3](PF_6)_2$ Concentrated HNO_3 (2 mL) was added to a stirred suspension of $[Mn(t\text{-}BuDiNC)_3]PF_6$ (0.0420 g, 0.032 mmol) in 4 mL of glacial acetic acid in air, yielding a deep blue solution. Having stirred for 10 min, the mixture was poured into a stirred, filtered solution of KPF_6 (0.33 g, 1.8 mmol) in 4 mL of H_2O. The deep blue precipitate which formed was isolated by filtration in air, washed with H_2O and dried in vacuo. Yield: 0.0434 g (93%). Infrared spectral analysis showed that some Mn(I) product was present. An

analytical sample was obtained by hexane precipitation from a CH_2Cl_2 solution containing a small amount of concentrated HNO_3. The complex decomposes slowly in $CHCl_3$ or CH_2Cl_2 solution to $[Mn(t\text{-}BuDiNC)_3]PF_6$, but as a solid, it is stable.

k. $[CpFe(CS)(t\text{-}BuDiNC)]PF_6$ A solution of $[CpFe(CO)_2(CS)]PF_6$ (0.0577 g, 0.158 mmol) and t-BuDiNC (0.0589 g, 0.157 mmol) in 12 mL of CH_3CN was stirred overnight. Evaporation gave a brown oil, which was washed with 5 mL of Et_2O and recrystallized twice from CH_2Cl_2/Et_2O at -20°C to give 0.0571 g (54%) of the product as brown crystals. The product hydrolyzes slowly in the solid state after prolonged exposure to air.

l. $cis\text{-}FeCl_2(t\text{-}BuDiNC)_2$ Anhydrous $FeCl_2$ (0.017 g, 0.131 mmol) was dissolved in 5 mL of CH_3OH and with stirring, was treated with 0.102 g (0.271 mmol) of solid t-BuDiNC. The color of the solution changed from pale yellow to deep orange within 10 s. After several min, a small amount of fine orange precipitate formed. The mixture was stirred a total of 15 min, filtered, and reduced in volume until more precipitate of the product formed. This suspension was treated with 7 mL of Et_2O and allowed to stand for 20 h. The resulting orange powder was collected by filtration, washed with Et_2O and dried in vacuo. Yield: 0.0842 g (73%). Orange microcrystals of the product were obtained by allowing a concentrated, filtered $CHCl_3$ solution of the complex to stand for 2 days at room temperature. These were isolated by decantation of the mother liquor, then vacuum dried for 2 days. Upon heating from 200°C, the compound turned black at 215°C and melted from ca. 245-255°C.

m. trans-$FeCl_2$(t-BuDiNC)$_2$ A solution of crude cis-$FeCl_2$(t-BuDiNC)$_2$ (0.101 g, 0.115 mmol) in 10 mL of CH_2Cl_2 was treated with $AlCl_3$ (0.005 g, 0.037 mmol). The solution was stirred for 15 min, then filtered to remove insoluble $AlCl_3$ hydrolysis products. After the solution stood for 15 days, the resulting lavender needles of the trans complex were collected by filtration, washed with CH_2Cl_2, then dried, yielding 0.0765 g (77%). The compound appears to be insoluble in all common solvents, including $(CH_3)_2SO$. Upon heating, the complex turns light brown at 235°C and melts with decomposition at ca. 255°C.

n. [Fe(t-BuDiNC)$_3$](PF_6)$_2$ A solution of cis-$FeCl_2$(t-BuDiNC)$_2$ (0.153 g, 0.174 mmol) in 6.0 mL of CH_2Cl_2 was treated with 0.0885 g (0.350 mmol) of $AgPF_6$ dissolved in 4 mL of CH_2Cl_2. This led to immediate precipitation of AgCl. The solution was stirred for 25 min, then filtered to remove the AgCl. To the resulting orange solution was added 0.0670 g of t-BuDiNC (0.178 mmol) in 4 mL CH_2Cl_2, causing a gradual color change to brown. This solution was stirred for 20 min and evaporated in vacuo. The resulting residue was dissolved in 3 mL of CH_2Cl_2, then treated with 9 mL of Et_2O to give a tarry yellow residue. The solvent was decanted off and the residue was triturated to a yellow powder with Et_2O. The product was filtered, washed with ether, and dried. Yield: 0.128 g (50%). Careful recrystallization from CH_2Cl_2/Et_2O gave the analytically pure compound as an off-white powder. The compound decomposed without melting from 335-350°C. In the solid state, the complex appears to be quite air stable. Solutions exposed to air turn noticeably yellow after 1 day.

o. $[Co_2(t\text{-}BuDiNC)_5](PF_6)_2$ The reagents t-BuDiNC (0.153 g, 0.406 mmol) and $CoCl_2 \cdot 6H_2O$ (0.036 g, 0.15 mmol) were dissolved in 5 mL of EtOH to give a brown-red solution. The addition of 0.015 g (0.23 mmol) of Zn dust caused a gradual color change to deep yellow. The mixture was stirred for 5.5 h, after which solid KPF_6 (0.050 g, 0.27 mmol) was added. After stirring an additional 1 h, the solution was filtered. Reduction of the volume at reduced pressure and ambient temperature was carried out until the product began to crystallize. The solution was cooled to -80°C and filtered. The resulting crude green-yellow product was washed with ether and dried. Yield: 0.062 g (36%). An analytically pure sample was obtained as yellow microcrystals by recrystallization from EtOH at -20°C, mp 206-213°C. The product is stable in air in the solid state, as well as in solution.

p. trans-$CoBr_2(t\text{-}BuDiNC)_2$ A relatively dilute solution of 0.500 g of t-BuDiNC (1.33 mmol) in 125 mL of acetone was treated with a solution of $CoBr_2 \cdot 6H_2O$ (0.210 g, 0.643 mmol) in 10 mL of acetone in air. A fine green precipitate of the product began to form after about 30 s. The reaction mixture was stirred for a total of 5 min, after which the product was filtered in air and washed with two 25 mL portions of acetone. The product was dried in vacuo to a very fluffy green powder, 0.486 g (78%), mp 254-263°C, decomp.

q. trans-$[CoBr_2(t\text{-}BuDiNC)_2]Br_3$ A stirred suspension of $CoBr_2(t\text{-}BuDiNC)_2$ (0.102 g, 0.105 mmol) in 4.5 mL of CH_2Cl_2 was treated slowly with Br_2 (8μL, 0.025 g, 0.157 mmol). Initially, a clear brown solution was formed. As the addition proceeded, a gelatinous precipitate

of orange-brown needles formed. The solvent was removed at reduced pressure, and the solid was dried in vacuo. The product was isolated without purification, yielding 0.113 g (89%), mp 248-258°C, decomp. The complex is stable in the solid state but is reduced by wet solvents to a deep brown compound with a $\nu(C{\equiv}N)$ value identical to that of trans-$CoBr_2$(t-BuDiNC)$_2$.

r. [Co(t-BuDiNC)$_3$](PF$_6$)$_3$ A suspension of $CoBr_2$(t-BuDiNC)$_2$ (0.198 g, 0.204 mmol) in 10 mL of CH_2Cl_2 was treated with Br_2 (5.4μL, 0.106 mmol) and the resulting clear brown solution was stirred for 20 min. Addition of $AgPF_6$ (0.158 g, 0.125 mmol) in 10 mL of CH_2Cl_2 caused precipitation of AgBr (91% of theoretical). The reaction mixture was stirred for 45 min, then filtered. A solution of t-BuDiNC (0.0775 g, 0.206 mmol) in 4 mL of CH_2Cl_2 was added, and after stirring an additional 30 min, the volume of the solution was reduced to 5 mL. The crude yellow-brown product was precipitated by rapid addition of 6 mL of Et_2O and was isolated by filtration. The final product was obtained by recrystallization from CH_2Cl_2/Et_2O (4 mL:6 mL) at -20°C, followed by filtration, washing with Et_2O, and vacuum drying. Yield: 0.0736 g (22%). The yellow product is quite sensitive to atmospheric moisture and slowly decomposes even after brief exposure to air in the solid state. Upon heating, the product melts with decomposition at 240-245°C.

s. Ni(CO)$_2$DiNC Caution: Ni(CO)$_4$ is extremely toxic. This and similar reactions should be carried out in an efficient fume hood. The cold trap of the vacuum system used for the following preparations

contained a frozen solution of several grams of I_2 in ca. 15 mL of CH_2Cl_2 to destroy trapped $Ni(CO)_4$. Approximately 0.12 mL (0.16 g, 0.93 mmol) of $Ni(CO)_4$ was condensed into a frozen (-196°C) solution of DiNC (0.336 g, 1.27 mmol) in 11 mL of CH_2Cl_2. Upon warming to room temperature, the solution began turning yellow as CO evolution commenced. After 15 min, a yellow precipitate began to form. The reaction was stirred for one more hour and the solid was filtered off, washed with 5 mL of CH_2Cl_2 at 0°C, and vacuum dried. The product is a light yellow microcrystalline solid. Yield: 0.213 g (44% based on DiNC), mp 140°C (decomp). Exposure to air for a period of a month or more leads to darkening of the solid sample. In solution, the product is easily decomposed by air.

t. $Ni(CO)_2$(t-BuDiNC) In a procedure similar to the one above, approximately 0.1 mL (0.13 g, 0.76 mmol) of $Ni(CO)_4$ was condensed into a frozen solution of t-BuDiNC (0.240 g, 0.638 mmol) in 5 mL of CH_2Cl_2. After warming to room temperature, the reaction mixture was stirred for 1 h. The mixture was taken to near dryness and 3 mL of hexane was added to precipitate the product as pale yellow microcrystals, which were filtered off, washed with hexane and dried. Yield: 0.190 g, 61%. Upon heating, the complex turns brown at ca. 140°C. A vapor pressure osmometry study of $Ni(CO)_2$(t-BuDiNC) in the concentration range 0.01-0.02 M showed the complex to be mononuclear, with the experimentally determined molecular weight being 475 g mol^{-1} (491 g

mol^{-1} theoretical). These yellow solutions and others in chlorocarbon solvents decompose over a period of hours to a deep brown color by the influence of either heat or air.

u. $Ni(t\text{-}BuDiNC)_2$ Approximately 0.08 mL (0.10 g, 0.6 mmol) of $Ni(CO)_4$ was condensed into a frozen solution of t-BuDiNC (0.377 g, 1.00 mmol) in 10 mL of Et_2O, and the mixture was warmed to 20°C. The yellow product began to precipitate from solution soon after the onset of CO evolution. When gas evolution had ceased, the volume of the solution was reduced to 2 mL and 5 mL of pentane was added with stirring. The yellow residue was filtered off, washed with pentane, and dried in vacuo. Yield: 0.406 g (90%). Air-exposed samples are decomposed either as solids or in solution. Even under N_2, samples appear to darken noticeably at ambient temperatures in the laboratory. The sample decomposes quickly at ca. 120°C.

v. $[Cu(t\text{-}BuDiNC)_2]BF_4$ A solution of $[Cu(CH_3CN)_4]BF_4$ (0.041 g, 0.130 mmol) and t-BuDiNC (0.102 g, 0.271 mmol) in 10 mL of CH_2Cl_2 was stirred for 50 min. Evaporation of the solvent gave a clear oil. This was washed twice with 10 mL of Et_2O to remove excess ligand and CH_3CN. Drying in vacuo gave an off-white solid which was scraped out of the reaction vessel. Yield: 0.080 g (68%), mp 190-200°C. The product is air-stable.

Table 21. Analytical data for DiNC and t-BuDiNC complexes

Compound	Calculated %C	Calculated %H	Calculated %N	Found %C	Found %H	Found %N
cis-$Cr(CO)_4$(DiNC)	56.08	2.82	-	56.21	2.91	_a
cis-$Cr(CO)_4$(t-BuDiNC)	62.22	5.22	5.18	61.78	5.39	5.09
cis-$Mo(CO)_4$(t-BuDiNC)	57.54	4.83	4.79	58.07	4.47	4.85
$[Cr(CO)_5]_2$(μ-DiNC)	48.16	1.87	4.32	47.60	1.83	4.15
$[W(CO)_5]_2$(μ-DiNC)	34.24	1.33	3.07	34.06	1.34	3.14
$Cr(t\text{-}BuDiNC)_3$	73.19	7.17	7.11	72.69	7.31	6.92
$[Cr(t\text{-}BuDiNC)_3]PF_6$	65.20	6.38	6.34	65.18	6.52	6.10
$[Cr(t\text{-}BuDiNC)_3](PF_6)_2$	58.77	5.75	5.71	59.45	6.26	5.44
$[Mn(t\text{-}BuDiNC)_3]PF_6$	65.05	6.37	6.32	64.51	6.33	6.28
$[Mn(t\text{-}BuDiNC)_3](PF_6)_2$	58.66	5.74	5.70	58.03	5.78	5.64
cis-$FeCl_2(t\text{-}BuDiNC)_2$	65.53	6.42	6.37	62.67	6.54	5.98
trans-$FeCl_2(t\text{-}BuDiNC)_2$	65.53	6.42	6.37	65.21	6.18	6.31

[a]Not determined.

Table 21. Continued

Compound	Calculated %C	Calculated %H	Calculated %N	Found %C	Found %H	Found %N
$[Fe(t\text{-}BuDiNC)_3](PF_6)_2$	58.62	5.74	5.70	58.93	5.90	5.70
$[Co_2(t\text{-}BuDiNC)_5(PF_6)_2$	62.93	6.16	6.12	62.87	6.59	6.17
trans-$CoBr_2(t\text{-}BuDiNC)_2$	59.33	5.81	-	58.88	5.78	-a
trans-$[CoBr_2(t\text{-}BuDiNC)_2]Br_3$	47.59	4.66	4.62	47.91	4.89	4.65
$[Co(t\text{-}BuDiNC)_3](PF_6)_2$	54.23	5.88	5.44	53.27	5.22	5.18
$Ni(CO)_2DiNC$	57.02	3.19	7.39	56.74	3.05	7.24
$Ni(CO)_2(t\text{-}BuDiNC)$	63.57	5.75	-	63.42	5.78	-a
$Ni(t\text{-}BuDiNC)_2$	71.03	6.95	6.90	69.91	7.20	6.83
$[Cu(t\text{-}BuDiNC)_2]BF_4$	63.82	6.25	6.20	63.96	6.44	6.21

Table 22. Infrared spectra of DiNC and t-BuDiNC complexes, cm^{-1}

Compound	Medium	$\nu(C\equiv N)$, cm^{-1}	$\nu(C\equiv O)$, cm^{-1}	Other, cm^{-1}
cis-$Cr(CO)_4$(DiNC)	$CHCl_3$ hexane	2142 w, 2091 w 2135 w, 2076 w	2009 s, 1932 vs, br 2008 m, 1955 s, 1942 s, 1936 sh	
cis-$Cr(CO)_4$(t-BuDiNC)	$CHCl_3$	2143 w, 2089 w	2010 s, 1934 vs, br	
cis-$Mo(CO)_4$(t-BuDiNC)	$CHCl_3$	2143 w, 2092 w	2014 s, 1935 vs, br	
$[Cr(CO)_5]_2$(μ-DiNC)	$CHCl_3$	2146 w	2059 s, 1998 m, sh, 1952 vs, br	
$[W(CO)_5]_2$-(μ-DiNC)	$CHCl_3$	2146 w	2060 s, 1992 w, sh, 1950 vs, br	
Cr(t-BuDiNC)$_3$	CH_2Cl_2 Nujol	1958 vs, br 1940 vs, br		
$[Cr(t\text{-}BuDiNC)_3]PF_6$	CH_2Cl_2 Nujol	2056 vs, 2050 vs		ν(P-F) 848 s[a]
$[Cr(t\text{-}BuDiNC)_3](PF_6)_2$	CH_2Cl_2 Nujol	2153 s 2155 s		ν(P-F) 844 vs[a]

[a]Taken in Nujol mull.

Table 22. continued

Compound	Medium	$\nu(C\equiv N)$, cm^{-1}	$\nu(C\equiv O)$, cm^{-1}	Other, cm^{-1}
$[Cr(t\text{-}BuDiNC)_3](SbCl_6)_3$[b]	CH_2Cl_2	2206 m		
$[Mn(t\text{-}BuDiNC)_3]PF_6$	CH_2Cl_2 Nujol	2082 vs, 2071 vs		$\nu(P\text{-}F)$ 848 s[a]
$[Mn(t\text{-}BuDiNC)_3](PF_6)_2$	CH_2Cl_2 Nujol	2162 s 2162 s		$\nu(P\text{-}F)$ 847 vs[a]
$[CpFe(CS)(t\text{-}BuDiNC)]PF_6$	CH_2Cl_2	2179 sh, 2159 m		$\nu(C\equiv S)$ 1310[a]
cis-$FeCl_2(t\text{-}BuDiNC)_2$	CH_2Cl_2 Nujol	2200 w, sh, 2154 vs, br, 2126 s, sh, 2190 w, sh, 2147 vs, 2131 s, sh		
trans-$FeCl_2(t\text{-}BuDiNC)_2$	Nujol	2146 vs		$\nu(Fe\text{-}Cl)$ 338 m
$[Fe(t\text{-}BuDiNC)_3](PF_6)_2$	CH_2Cl_2 Nujol	2194 s, 2195 s		$\nu(P\text{-}F)$ 847 vs[a]
$[Co_2(t\text{-}BuDiNC)_5](PF_6)_2$	Nujol	2150 s, sh, 2108 vs		$\nu(P\text{-}F)$ 846 s[a]

[b]Generated by addition of $SbCl_5$ to a CH_2Cl_2 solution of $Cr(t\text{-}BuDiNC)_3$ at -20°C.

Table 22. continued

Compound	Medium	$\nu(C{\equiv}N)$, cm^{-1}	$\nu(C{\equiv}O)$, cm^{-1}	Other, cm^{-1}
trans-$CoBr_2$(t-BuDiNC)$_2$	Nujol	2188 s, 2109 wsh		ν(Co-Br) 158 s[a]
trans-[$CoBr_2$(t-BuDiNC)$_2$]Br_3	Nujol	2227 m		
[Co(t-BuDiNC)$_3$](PF_6)$_3$	CH_2Cl_2 Nujol	2258 w, 2259 w		ν(P-F) 845 vs[a]
Ni(CO)$_2$(DiNC)	$CHCl_3$	2146 s, 2092 s	2014 s, 1972 s	
Ni(CO)$_2$(t-BuDiNC)	$CHCl_3$	2145 s, 2094 s	2014 s, 1975 s	
Ni(t-BuDiNC)$_2$	$CHCl_3$ Nujol	2040 vs, br, 2160 wsh, 2020 vs, br		
[Cu(t-BuDiNC)$_2$]BF_4	$CHCl_3$ Nujol	2169 vs, 2165 vs		ν(B-F) 1047 s, br[a]

Table 23. ^1H NMR data for DiNC and t-BuDiNC complexes[a]

Compound	Solvent	Ar-H	CH_2	t-Bu	Other
cis-$Cr(CO)_4$DiNC	$CDCl_3$	7.42-6.90 m	4.42	-	
cis-$Cr(CO)_4$(t-BuDiNC)	$CDCl_3$	7.35-7.22 m; 6.98-6.88 m	4.37	1.29	
cis-$Mo(CO)_4$(t-BuDiNC)	$CDCl_3$	7.35-7.25 m; 7.00-6.89 m	4.38	1.30	
cis-$Mo(CO)_4$(DiNC)	$CDCl_3$	7.43-6.91	4.43	-	
cis-$W(CO)_4$(DiNC)	$CDCl_3$	7.41-6.91 m	4.43	-	
$[Cr(CO)_5]_2$(μ-DiNC)	$CDCl_3$	7.46-6.90 m	4.50	-	
$[W(CO)_5]_2$(μ-DiNC)	$CDCl_3$	7.47-6.93 m	4.51	-	
$[W(CO)_4(pip)]_2$(μ-DiNC)	$CDCl_3$	7.57-6.98 m	4.56	-	_b
$Cr(t\text{-}BuDiNC)_3$	C_6D_6	7.17-6.57 m	3.78	1.04	
$[Mn(t\text{-}BuDiNC)_3]PF_6$	CD_2Cl_2	7.41-7.29 m; 7.10-6.90 m	4.41	1.26	

[a]Coupling constants for doublets (d) and doublets of doublets (dd) are given in parenthesis. Where more than one signal is observed, the approximate ratio is given in brackets.

[b]Piperidine (pip) ligand signals: 3.28 m; 2.62 m; 1.50 m.

Table 23. continued

Compound	Solvent	Ar-H	CH_2	t-Bu	Other
$[CpFe(CS)(t\text{-}BuDiNC)]PF_6$	$(CD_3)_2CO$	7.67-7.25 m	4.53	1.30	Cp 5.58 s
$cis\text{-}FeCl_2(t\text{-}BuDiNC)$	$CDCl_3$	7.71-6.85 m	4.39 br	1.31, 1.23, [1:1]	
$[Fe(t\text{-}BuDiNC)_3](PF_6)_2$	CD_2Cl_2	7.60-7.50 m; 7.23-7.13 m	4.50	1.30	
$[Co_2(t\text{-}BuDiNC)_5](PF_6)_2$	CD_2Cl_2	7.50-6.94 m	4.51, 4.15, [4:1]	1.24, 1.16, [4:1]	
$[CoBr_2(t\text{-}BuDiNC)_2]Br_3$	CD_3CN	7.95 d (2.4); 7.67 dd (2.4, 8.8); 7.19 d (8.8)	4.54	1.35	
$Ni(CO)_2(DiNC)$	$CDCl_3$	7.40-6.92 m	4.41		
$Ni(CO)_2(t\text{-}BuDiNC)$	CD_2Cl_2	7.44-7.31 m; 7.08-6.97 m	4.36	1.30	
$Ni(t\text{-}BuDiNC)_2$	$CDCl_3$	7.33-6.86 m	4.35	1.25	
$[Cu(t\text{-}BuDiNC)_2]BF_4$	CD_2Cl_2	7.61-7.15 m	4.50	1.30	

Table 24. ^{13}C NMR data for DiNC and t-BuDiNC complexes

Compound	1	2	3	4	5	6
DiNC[a]	153.9	116.6	127.7	121.3	130.5	113.6
t-BuDiNC[a,b]	151.8	116.2	124.8	144.7	127.5	113.7
$Cr(CO)_4$(DiNC)[a]	154.2	120.1	126.2	122.1	129.0	114.8
$Cr(CO)_4$(t-BuDiNC)[a]	151.7	119.3	123.0	145.2	125.6	114.3
$Mo(CO)_4$(DiNC)[a]	154.1	119.3	126.4	122.0	129.3	114.7
$Mo(CO)_4$(t-BuDiNC)[a]	152.1	119.0	123.8	145.7	126.4	114.7
$[Cr(CO)_5]_2$(μ-DiNC)[a]	154.6	117.8	126.3	121.2	130.1	112.4
$[W(CO)_5]_2$(μ-DiNC)[a]	154.7	117.2	126.6	121.3	130.4	112.4
$Cr(t\text{-}BuDiNC)_3$[f]	152.0	–[g]	124.6	144.4	127.2	113.6
$[Mn(t\text{-}BuDiNC)_3]PF_6$[h]	152.6	120.1	123.4	145.8	126.7	115.3
$[CpFe(CS)(t\text{-}BuDiNC)]PF_6$[i]	153.3	119.0	124.5	146.0	129.1	116.1
$[Fe(t\text{-}BuDiNC)_3](PF_6)_2$[h]	152.8	117.1	124.1	146.0	126.7	115.0
$Ni(CO)_2(t\text{-}BuDiNC)$[h]	152.1	119.5	123.4	146.0	126.7	115.5
$Ni(t\text{-}BuDiNC)_2$[h]	151.6	121.1	122.5	145.4	124.4	115.3
$[Cu(t\text{-}BuDiNC)_2]BF_4$[h]	152.9	116.4	124.1	146.1	129.5	115.8

[a] $CDCl_3$ solvent.

[b] ^{13}C spectral data in DC_2Cl_2 solvent presented in Table 20.

[c] trans CO.

[d] cis CO.

[e] $J_{^{183}W-^{13}C} = 127\ s^{-1}$.

[f] C_6D_6 solvent.

[g] Resonance not observed.

[h] CD_2Cl_2 solvent.

[i] Acetone-d_6 solvent.

[j] Questionable assignment.

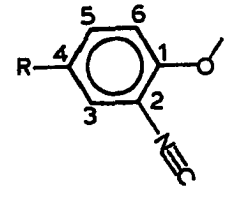

NC	OCH_2	$C(CH_3)_3$	$C(CH_3)_3$	Other
167.7	67.9	--	--	
167.0	68.0	34.6	31.4	
182.2	67.8	--	--	CO: 220.1, 216.1
180.9	68.0	34.0	31.0	CO: 220.1, 217.0
171.2	67.8	--	--	CO: 209.7, 205.8
170.4	68.3	34.4	31.3	CO: 210.2, 206.0
175.5	66.8	--	--	CO: 216.8[c], 214.6[d]
155.6	66.9	--	--	CO: 196.4[c], 194.0[d,e]
170.2	67.8	38.8	30.9	
_[g]	68.6	34.6	31.4	
162.3	69.2	34.7	31.5	Cp 90.0, CS 322.6
153.4[j]	67.8	34.5	31.0	
166.4	69.4	34.4	31.2	CO: 197.8
158.8	69.4	34.0	30.9	
_[g]	69.1	34.6	31.2	

Table 25. Electronic spectra of some homoleptic t-BuDiNC complexes

Complex	Solvent	λ_{max};nm($10^{-3}\varepsilon$)	Assignment[a]
$Cr(t\text{-}BuDiNC)_3$	THF	468 sh (44.1)	$d\pi \rightarrow \pi_v^*$
		420 (47.2)	$d\pi \rightarrow \pi_v^*$
		320 sh (32.3)	$d\pi \rightarrow \pi_h^*$
		300 (32.7)	$d\pi \rightarrow \pi_h^*$
		286 (37.1)	intra-ligand
$[Cr(t\text{-}BuDiNC)_3]PF_6$	CH_2Cl_2	443 sh (30.9)	$d\pi \rightarrow \pi_v^*$
		365 (49.6)	$d\pi \rightarrow \pi_v^*$
		276 (36.3)	intraligand
$[Mn(t\text{-}BuDiNC)_3]PF_6$	CH_2Cl_2	341 (60.9)	$d\pi \rightarrow \pi_v^*$
		249 sh (47.1)	intraligand
$[Mn(t\text{-}BuDiNC)_3](PF_6)_2$	CH_2Cl_2	684 br (4.4)	?
		481 br (3.3)	?
		355 sh (8.9)	?
		303 (42.4)	$d\pi \rightarrow \pi_v^*$
		282 sh (37.3)	$d\pi \rightarrow \pi_v^*$
		246 sh (54.3)	intraligand
$[Fe(t\text{-}BuDiNC)_3](PF_6)_2$	CH_2Cl_2	298 (30)	$d\pi \rightarrow \pi_v^*$
		258 (64)	$d\pi \rightarrow \pi_v^*$
		247 sh (56)	intraligand
$[Co(t\text{-}BuDiNC)_3](PF_6)_3$	CH_2Cl_2	307 (29)	$d\pi \rightarrow \pi_v^*$
		255 (77)	$d\pi \rightarrow \pi_v^*$
		248 sh (71)	intraligand

[a]Assignments made as in reference 107.

Table 26. Conductivity data for some t-BuDiNC complexes[a]

Compound	Concentration x 10^3, M	Λ_M, $ohm^{-1}cm^2mol^{-1}$
$[Cr(t\text{-}BuDiNC)_3]PF_6$	1.01	83.1
$[Cr(t\text{-}BuDiNC)_3)(PF_6)_2$	0.99	157
$[Mn(t\text{-}BuDiNC)_3]PF_6$	1.00	84.8
$[Fe(t\text{-}BuDiNC)_3](PF_6)_2$	1.02	156
$[Co_2(t\text{-}BuDiNC)_5](PF_6)_2$	1.03	148
$[CoBr_2(t\text{-}BuDiNC)_2]Br_3$	1.03	79.7
$[Co(t\text{-}BuDiNC)_3](PF_6)_3$	1.10	229
$[Cu(t\text{-}BuDiNC)_2]BF_4$	0.97	84

[a]Expected ranges for Λ_M in CH_3NO_2: (1:1), 75-95; (2:1), 150-180; (3:1), 220-260 (ref. 108).

Table 27. Linear intensities (ε) and integrated intensities (A) of the ν(CN) bands in t-BuDiNC and homoleptic d^6 complexes in CH_2Cl_2

Compound	ν(C≡N)	ε_{total} [a]	A_{total} [b] (no. of points)	$A_{specific}$ [b,c]
t-BuDiNC[d]	2130	676	2.86×10^4 (7)	1.43×10^4
t-BuDiNC[e]	2129	603	2.22×10^4 (1)	1.11×10^4
$[Co(t\text{-}BuDiNC)_3](PF_6)_3$[e]	2258	3.6×10^2	2.9×10^4 (2)	0.5×10^4
$[Fe(t\text{-}BuDiNC)_3](PF_6)_2$[d]	2194	3.77×10^3	29.9×10^4 (6)	4.98×10^4
$[Fe(t\text{-}BuDiNC)_3](PF_6)_2$[e]	2188	3.58×10^3	27.7×10^4 (1)	4.61×10^4
$[Mn(t\text{-}BuDiNC)_3]PF_6$[d]	2082	1.01×10^4	$147. \times 10^4$ (7)	24.5×10^4
$[Mn(t\text{-}BuDiNC)_3]PF_6$[e]	2982	9.05×10^3	$118. \times 10^4$ (4)	19.7×10^4
$Cr(t\text{-}BuDiNC)_3$[e]	1958	7.77×10^3	$203. \times 10^4$ (2)	33.8×10^4

[a] Units of $M^{-1}cm^{-1}$.
[b] Units of $M^{-1}cm^{-2}$.
[c] $A_{specific} = \frac{A\ total}{\#(CN)\ groups}$ (ref 109).
[d] PE 681 instrument.
[e] IBM IR 98 instrument.

Table 28. Cyclic voltammetric data[a]

Complex	Scan rate, mVs^{-1}	$1/2[E_{p,a}+E_{p,c}]$,V	$[E_{p,c}-E_{p,a}]$V	Couple
$[Cr(t\text{-}BuDiNC)_3]PF_6$	20	- 0.50	0.18	Cr/Cr^+
	20	+ 0.10	0.19	Cr^+/Cr^{2+}
	20	+ 0.99	0.19	Cr^{2+}/Cr^{3+}
	100	- 0.54	0.61	Cr/Cr^+
	100	+ 0.16	0.61	Cr^+/Cr^{2+}
	100	+ 1.05	0.57	Cr^{2+}/Cr^{3+}
$[Mn(t\text{-}BuDiNC)_3]PF_6$	20	+ 0.86	0.46	Mn^+/Mn^{2+}
	20	+ 2.00	0.51	Mn^{2+}/Mn^{3+}
	100	+ 0.85	0.60	Mn^+/Mn^{2+}
	100	+ 1.92	0.61	Mn^{2+}/Mn^{3+}

[a]In CH_2Cl_2 solution, 0.1 M Bu_4NPF_6 supporting electrolyte. Other experimental parameters as defined in section II.B.7.

III. RESULTS AND DISCUSSION

A. Nitrile Ligands and their Complexes

1. General

Before embarking upon a discussion of the multidentate nitrile ligands of the present research, it is appropriate to first discuss in a general way the coordination behavior of nitrile ligands; two extensive reviews on this subject are available.[18,38] Nitriles are known to form a very large number of stable, and in most cases, well-characterized complexes with Lewis-acidic main-group halides (e.g. $BF_3 \cdot NCR$),[110] transition-metal halides (e.g. $TiBr_4 \cdot NCR$),[111] and transition-metal salts (e.g. $[Mn(NCR)_6](SbCl_6)_2$).[112] Without exception, the nitrile ligands of such complexes bind through the nitrogen lone pair of electrons to the metal, and infrared spectra of such complexes exhibit higher $\nu(N{\equiv}C)$ frequencies than those found in the spectra of the free nitrile ligand.[38]

There also exists a large number of nitrile-transition metal complexes in which the metal is "electron-rich" by virtue of its low oxidation state and/or the presence of strong σ-donor ligands, for example, $(\eta^6C_6Me_6Cr(CO)_2(NCPh)$[113] and $[Ru(NH_3)_5(NCPh)]^{2+}$.[114] In these cases, the nitrile $\nu(NC)$ absorbance(s) may appear at either higher or lower frequency than that of the free ligand. Decreases in $\nu(NC)$ upon coordination may be taken as evidence of π-donation from the metal into the nitrile π^* system, but in general, nitriles are considered to be

poor π-acceptors relative to CO, isonitriles, phosphites, and phosphines.[18] In contrast to the complexes of the "harder" metal halides and salts referred to in the last paragraph, these "electron-rich" complexes sometimes exhibit two ν(NC) bands when more than one nitrile is bound to the metal, as for the cis-acetonitrile ligands of $Mo(CO)_2(PBu_3)_2(NCCH_3)_2$.[48]

Homoleptic nitrile complexes of the general formula $[M(NCR)_6]^{2+}$ are well-known (M = Mg, Cd, Mn, Fe, Co, Ni, Cu),[112,115] as mentioned earlier. These complexes are usually quite sensitive to atmospheric moisture, and aside from the iron(II) complexes, do not obey the "eighteen-electron" rule, as do many organometallic complexes. Other homoleptic nitrile complexes include the cations, $[Cu(NCCH_3)_4]^{2+}$,[116] $[Cu(NCCH_3)_4]^{+}$,[94,116] $[Ag(NCCH_3)_4]^{+}$,[116] and $[Pd(NCCH_3)_4]^{2+}$.[116,117] Eighteen-electron organometallic complexes containing three nitrile groups are less common, and include the air-sensitive complexes fac-$M(CO)_3(NCCH_3)_3$[118,119] (M = Cr, Mo, W), and the more stable derivatives $[M(CO)_3(NCCH_3)_3]^{+}$[120] (M = Mn, Re), $[CpRu(NCCH_3)_3]^{+}$,[121] $[(\eta^5\text{-}C_5Me_5)M(NCCH_3)_3]^{2+}$ (M = Co,[122] Rh or Ir)[123], and $[(\eta^6\text{-}C_6H_6)Ru(NCCH_3)_3]^{2+}$.[124] Organometallic compounds containing one or two nitriles coordinated to a single metal center are quite common and are far too numerous to be listed here. One reason perhaps for the abundance of nitrile complexes, especially those of acetonitrile, is that nitriles are often good solvents, in addition to being suitable ligands. Thus, reactions which open coordination sites at metal centers, such as

thermal or photochemical elimination of neutral ligands, halide abstraction, and oxidative metal-metal bond cleavage, will often yield nitrile complexes when carried out in a nitrile solvent. Conversely, the ease with which nitriles are displaced from metal centers in non-coordinating solvents often makes such complexes useful as precursors to complexes containing other, stronger ligands.

2. Synthesis of nitrile ligands

The dinitrile ligands DiCN-3 and DiCN-4 are prepared simply by displacement of bromide ion from 1,3-dibromopropane or 1,4-dibromobutane, respectively, by sodium 2-cyanophenoxide in hot (120°C) DMF solutions. Yields in these reactions (53% and 43%) are similar to that

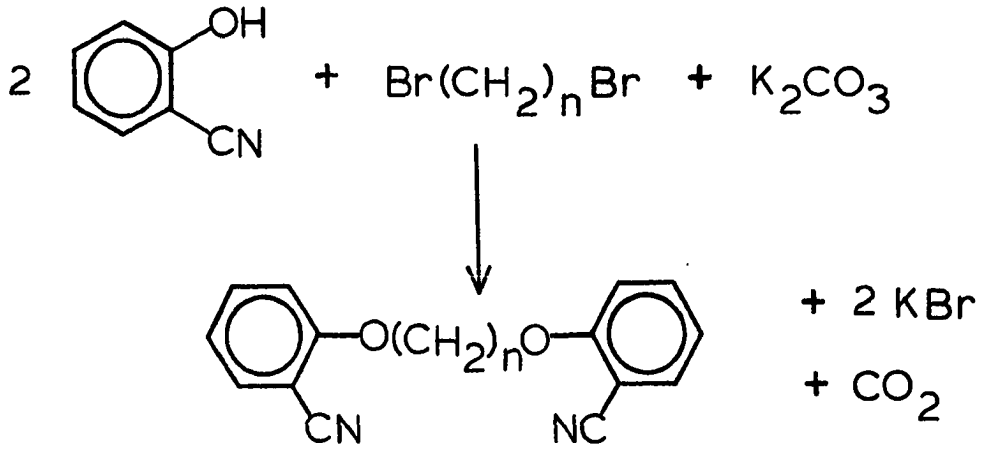

(I)

obtained in the synthesis of DiCN-2 by reaction of sodium 2-cyanophenoxide with 1,2-dichloroethane.[14,96] Deviations from 100% yields are probably a result of incomplete reaction, as well as a side reaction in which HX is eliminated from the dihaloalkane; upon aqueous workup, the odor of

2-cyanophenol is easily detected. This coupling reaction is simple in both concept and practice and provides easy access to the simple framework of these dinitrile ligands (and others in section B of this discussion).

All three dinitrile ligands are colorless, odorless solids. The ligands DiCN-2 and -4 have moderate solubility in chlorinated hydrocarbons and low solubility in nonpolar solvents such as ether, benzene, or hexane. DiCN-3 has considerably greater solubility (ca. ten times) in chlorinated solvents, but still very low solubilities in the less polar solvents mentioned above. Infrared stretching frequencies of the three ligands at 2231-2232 cm^{-1} ($CHCl_3$ solution) are slightly lower than that of benzonitrile (2235 cm^{-1}) in the same solvent.

The TriCN ligand is synthesized by the six-step reaction sequence shown in Scheme I. In the first step, 2-methylacetophenone is converted

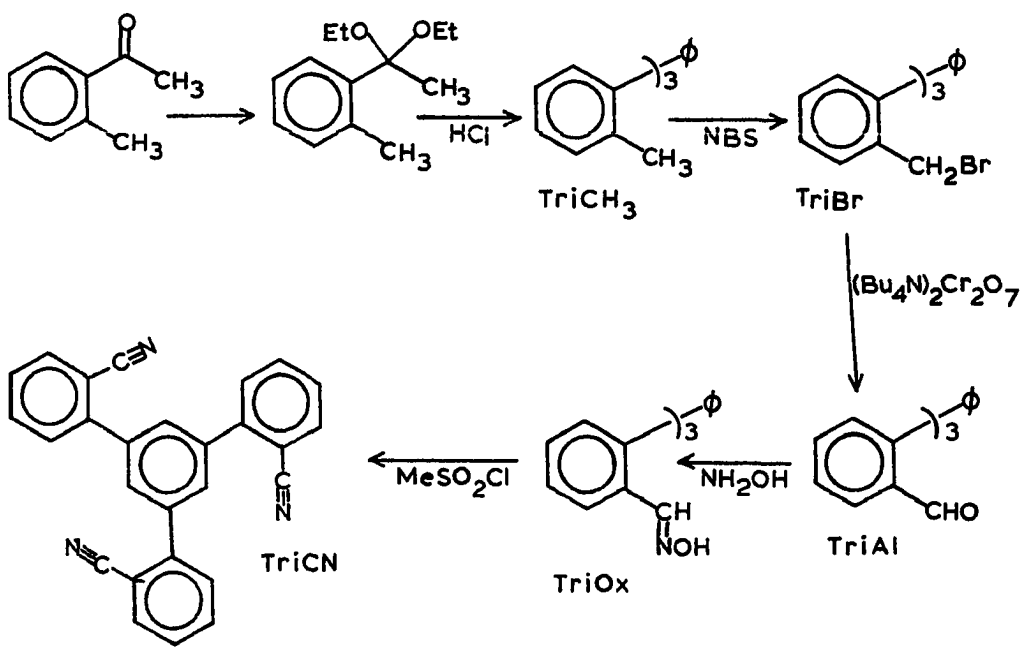

Scheme I

to its diethyl ketal by reaction with triethylorthoformate. Subsequent treatment with HCl(g) leads to $TriCH_3$, which has been previously synthesized by this route.[97] The yield of $TriCH_3$ from the ketone is 45% after chromatography. This cyclization of an acetophenone can be considered an aldol condensation, where the carbonyl and α-carbon atoms of the methyl ketone end up in the central phenyl ring of the product. In the present case, the reaction is thought to proceed via 2-methyl-α-ethoxystyrene as an intermediate[97] (α-Methoxystyrene has been converted to 1,3,5-triphenyl benzene under similar conditions).[125] An interesting side-product (ca. 0.1%) isolated from one of these reactions is the tetramer, 1,3,5,7-tetrakis(2-methyl phenyl)cycloctatetraene, which was identified by its ^1H NMR and mass spectra.

With the structural framework of the desired ligand established, a series of functional group interconversions is carried out to reach the desired product. Most of these reactions are straightforward and proceed in moderate yields. Bromination with N-Bromosuccininide gives the useful intermediate, TriBr in 58% yield. Further oxidation with the $CHCl_3$-soluble $(Bu_4N)_2\ Cr_2O_7$[84] gives the aldehyde, triAl, in 62% yield. Oximation with $NH_2OH{\cdot}HCl$ in pyridine (98%), followed by dehydration with methanesulfonyl chloride[99] gives TriCN in 77% yield (12% overall). The ligand is a colorless, odorless, crystalline solid which melts at 266°C and can be sublimed in vacuo at temperatures near its melting point.

The TriBr intermediate deserves comment here as a possible precursor to other interesting tridentate ligands. It does react with sodium azide to give "$TriN_3$" which can be reduced with $LiAlH_4$ to form the triamine, 1,3,5-tris[2-(aminomethyl)phenyl]benzene ("$TriNH_2$") 13, in 42% yield. In preliminary infrared studies, this ligand was found to react with $Mn(CO)_5Br$ to give the neutral complex $Mn(CO)_3(TriNH_2)Br$ [ν(CO) at 2028, 1931, 1906 cm^{-1}, CH_2Cl_2]. Treatment of this complex with $AgPF_6$ gave, along with decomposition products, an infrared spectrum [ν(CO) 2040, 1929 cm^{-1}, CH_2Cl_2] consistent with the formation of a cationic, tris-chelated product, $[Mn(CO)_3(TriNH_2)]PF_6$. This infrared spectrum can be compared to that of $[Mn(CO)_3(NH_2Cy)_3]^+$, which exhibits bands at 2032 and 1936 cm^{-1} [126]. Preliminary studies have also shown that a different

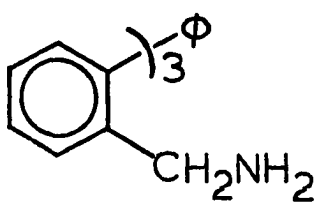

13

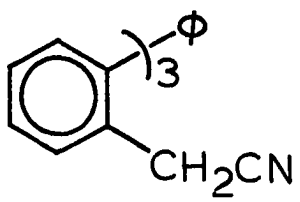

14

trinitrile ligand, 14, can be formed by substitution of the bromide ions in TriBr by cyanide ion (KCN, refluxing CH_3CN). Finally, reaction of TriBr with $LiPR_2$[127] might be expected to yield a phosphorous analog of $TriNH_2$ shown below (15). A structurally similar ligand, 1,3,5-tris[2-(difluorophosphito)ethyl]benzene (16) has been shown by Nesmeyanov and coworkers[128] to coordinate through all three phosphorous atoms and the phenyl ring simultaneously to a single chromium atom.

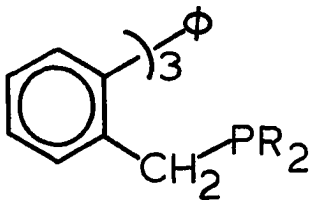

15

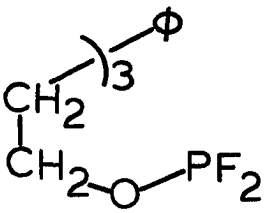

16

3. Complexes of DiCN ligands

DiCN-3 and DiCN-4 react with $Mn(CO)_5Br$ over a period of hours in refluxing $CHCl_3$ or CH_2Cl_2, respectively, with the liberation of CO gas to yield the derivatives fac-$Mn(CO)_3$(DiCN-n)Br, (eq. II). The same type

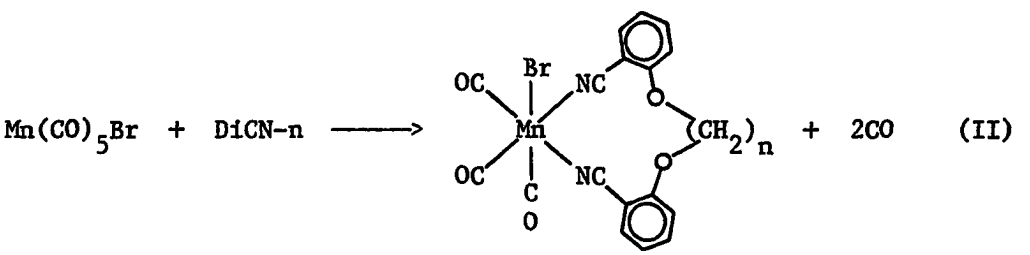

of reaction takes place between DiCN-2 and $Mn(CO)_5Br$.[14,96] The facial geometry of the complexes is supported by the characteristic infrared pattern of three strong $\nu(C{\equiv}O)$ absorptions as expected for complexes such as these with C_s symmetry. Carbonyl stretching frequencies of the DiCN derivatives are observed at 2042-2050, 1968-1973, and 1938-1944 cm^{-1} in $CHCl_3$, close to the values reported for fac-$Mn(CO)_3(CH_3CN)_2Br$[41] at 2043, 1957, and 1934 cm^{-1}. These DiCN complexes are also analogous to fac-$Re(CO)_3(C_6H_5CN)_2Br$.[18] In the region 2300-2200 cm^{-1}, the complexes exhibit a single, weak $\nu(N{\equiv}C)$ band at 2270-2272 cm^{-1} assigned to the

coordinated nitrile group. The lack of an appreciable ν(N≡C) band at the free nitrile frequency indicates that both nitrile groups are coordinated to the metal, ruling out a structure such as 17. Also arguing

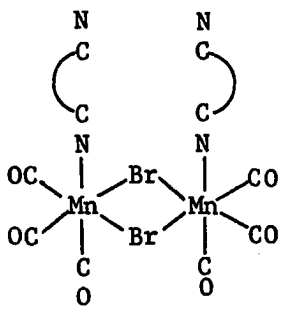

17

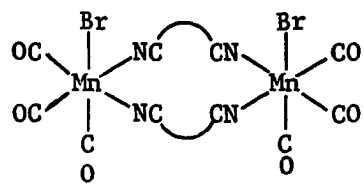

18

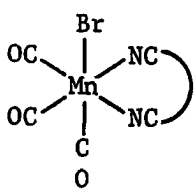

19

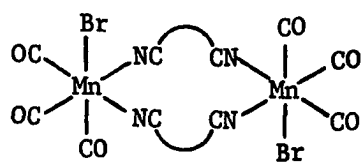

20

against structure 17 is the absence of a ν(MnBr) doublet in the low-frequency solid state IR spectra of the DiCN-3 and DiCN-4 derivatives. This doublet, however, is quite apparent in the IR spectrum of $Mn_2(CO)_6(CH_3CN)_2(\mu\text{-}Br)_2$ [90] (see Table 9).

While the solution infrared spectra of all three complexes are very similar, there are some differences between the solid state spectra of $Mn(CO)_3$(DiCN-4)Br and those of the other two complexes. These differences might be due either to different molecular or crystal structures for the DiCN-4 derivative. In the $\nu(C\equiv O)$ region, $Mn(CO)_3$ (DiCN-4)Br exhibits "extra" shoulders at 1974 and 1896 cm^{-1}, for a total of five $\nu(C\equiv O)$ bands. For structure 18, which has C_{2v} symmetry, five IR-active $\nu(C\equiv O)$ bands ($2A_1 + 2B_1 + 1B_2$) are predicted, but for the C_{2h} structure 20, $4\nu(C\equiv O)$ are predicted ($2\ A_g + 2\ B_u$). In the low-frequency IR spectra of $Mn(CO)_3$ (DiCN-3)Br and $Mn(CO)_3$(DiCN-4)Br, the latter shows eleven bands in the region 680-460 cm^{-1}, while the former shows eight bands. Whether these extra bands of the DiCN-4 complex are required by molecular symmetry or are due to simple solid state splitting cannot be determined with certainty, though the observation of similar solution spectra for all the complexes suggest that solid state splitting might be responsible. For the dinuclear complexes $M_2(CO)_6(CH_3CN)_2\ (\mu\text{-}X)_2$, splitting in the $\nu(C\equiv O)$ region is seen in the solid state but not in solution (the complexes are thought to have C_{2h} symmetry).[90] It may be that solid-state splitting is characteristic of these dinuclear structures in general and if so, might argue for structure 20 for $Mn(CO)_3$(DiCN-4)Br. On the other hand there are no data to suggest dinuclear structures for $Mn(CO)_3$(DiCN-2)Br or $Mn(CO)_3$(DiCN-3)Br.

In ambient room light, $CHCl_3$ or CH_2Cl_2 solutions of $Mn(CO)_3(DiCN)Br$ complexes begin to precipitate a white solid within minutes of preparation. Concurrently, the intensity of the coordinated DiCN ν(CN) peak decreases, as does the ν(CO) band of $Mn(CO)_3(DiCN)Br$ at ca. 1940 cm^{-1}. New ν(CO) bands appear at ca. 2112 cm^{-1}, 2066 cm^{-1}, and ca. 2015 cm^{-1}, which might be assigned to a mixture of $Mn(CO)_5X$ (X = Br; 2146 (m), 2060 (s), 2016 (s) cm^{-1}) and $Mn_2(CO)_6(\mu\text{-}X)_2$ (X = Br; 2099 (m), 2042 (s), 2011 (m), 1975 (m) cm^{-1} [129]). Exhaustive photolysis of $Mn(CO)_3(DiCN\text{-}4)Br$ in $CHCl_3$ solution by direct sunlight under N_2 requires less than 20 minutes, forming DiCN-4 as the only IR-observed product and a copious white precipitate, presumably MnX_2 (X = Br, Cl) (vide infra). Bamford and coworkers[130] have previously described this chemistry for $Mn(CO)_3L_2Br$ complexes (L = CO, CH_3CN). In the case of L = CH_3CN, the first step is a thermal or photochemical reaction, forming the dimer $Mn_2(CO)_6(CH_3CN)_2(\mu\text{-}Br)_2$ (eq. III). Subsequently, the $Mn_2(\mu Br)_2$ linkage is photolytically cleaved to produce $MnBr_2$, CO, CH_3CN, and an unsaturated Mn(0) radical which can undergo further reaction with itself, liberated CO, and/or organic halides (eq. IV). In the case of the $Mn(CO)_3(DiCN\text{-}n)Br$ complexes in $CHCl_3$, it is

$$2\ Mn(CO)_3(\text{nitrile})_2Br \longrightarrow Mn_2(CO)_6(\text{nitrile})_2(\mu\text{-}Br)_2 + 2\ \text{nitrile} \qquad \text{(III)}$$

$$Mn_2(CO)_6(\text{nitrile})(\mu\text{-}Br)_2 \xrightarrow{h\nu} MnBr_2 + 1/2\ Mn_2(CO)_{10} + 2\ \text{nitrile} + \text{other products} \qquad \text{(IV)}$$

possible that the Mn(0) fragment, initially $Mn(CO)_3$, picks up CO from solution and a chlorine atom from $CHCl_3$, then dimerizes to $Mn_2(CO)_8(\mu\text{-}Cl)_2$. The latter is then photolyzed further in a similar cycle until all the manganese has precipitated out as Mn(II) salts.

When dissolved in neat acetone, the DiCN complexes are rapidly decomposed to $[Mn(CO)_3(acetone)_3]Br$, identified by its infrared spectrum,[131,132] and free DiCN ligand. Thus, solution of these complexes are stable only in non-coordinating solvents, and only in the absence of light.

Because of these limitations, some investigations which might more firmly distinguish between mono- and dinuclear structures for the pure $Mn(CO)_3(DiCN\text{-}n)Br$ complexes were not possible. While ^1H NMR spectra of certain DiNC complexes (section III.E) are useful in assigning bridged versus chelated structures, line broadening due to Mn(II) precluded the observation of suitably well-resolved spectra in these systems. Presumably, molecular weight determinations by vapor-pressure osmometry would be affected by photodecomposition as well and were not attempted.

If indeed the DiCN ligands chelate to Mn(I), one might expect to observe some chelate effect in competition experiments with monodentate nitriles. While it proved to be difficult to ascertain an absolute measure of the chelate effect in the system studied, it is possible to obtain a relative measure of the chelating abilities of the three DiCN ligands. The reaction of interest is represented in equation V. In

$$2\ \mathrm{DiCN} + \mathrm{Mn_2(CO)_6(CH_3CN)_2(\mu\text{-}Br)_2} \rightleftharpoons 2\ \mathrm{Mn(CO)_3(DiCN)Br} + 2\ \mathrm{CH_3CN} \qquad \text{(V)}$$

chloroform solution in the dark, this equilibrium was found to be rapidly established. To carry out such experiments, a known amount of the manganese dimer was dissolved in a standard $CHCl_3$ solution of the DiCN ligand, such that the Mn/DiCN ratio was near unity. By measuring the absorbance of the DiCN nitrile stretching band before and after addition of the manganese dimer, it was possible to observe the fraction of free DiCN nitrile groups remaining at equilibrium. The results of these experiments are represented in Table 29. DiCN-3 and DiCN-4 appear to be

Table 29. Results of competition experiments between DiCN ligands and $Mn_2(CO)_6(CH_3CN)_2(\mu\text{-}Br)_2$[a,b,c]

DiCN-2			DiCN-3			DiCN-4		
expt.	Mn/L	Ce/Co	expt.	Mn/L	Ce/Co	expt.	Mn/L	Ce/Co
1	1.06	.07	1	1.10	.14	1	1.11	.11
2	1.05	.08	2	1.05	.14	2	1.03	.14
3	1.06	.08	3	1.01	.16			

[a] $\mathrm{Mn/L} = \dfrac{[\text{Mn dimer}]_o}{2\ [\mathrm{DiCN}]_o}$; values are accurate to $\pm$ 3%.

[b] $\mathrm{Ce/Co} = \dfrac{\nu(\mathrm{N{\equiv}C})\ \text{absorbance at equilibrium}}{\nu(\mathrm{N{\equiv}C})\ \text{absorbance initially}}$

[c] $[\text{Mn dimer}]_o \cong 0.014$ M.

nearly equal in their abilities to bind to manganese as shown by their similar ratios of final to initial free nitrile group concentration. DiCN-2, however, appears to be significantly better. Assuming the reaction to take place as written in equation V, these results are consistent with the operation of a stronger chelate effect for DiCN-2 than either of the other ligands, as would be expected, based on entropy considerations discussed in Section I.C.

In summary, there are no data which argue strongly against chelated structures for the pure compounds $Mn(CO)_3$(DiCN-2)Br and $Mn(CO)_3$(DiCN-3)Br. Competition studies between DiCN ligands and $Mn_2(CO)_6(CH_3CN)_2(\mu\text{-}Br)_2$ bear out the expected relationship between DiCN-2 and the other two ligands, namely, that DiCN-2 is a more efficient chelator. The solid state infrared spectrum of the DiCN-4 complex leaves some question about the structure of this compound, however.

4. Complexes of the TriCN ligand

a. Complexes with group VII carbonyls The neutral six-coordinate complex $Mn(CO)_3$(TriCN)Br is formed upon reaction of TriCN and $Mn(CO)_5Br$ in refluxing chlorocarbon solvents, in much the same way that the DiCN complexes are prepared (eq. VI). Though the TriCN ligand is potentially

$$Mn(CO)_5Br + TriCN \longrightarrow Mn(CO)_3(TriCN)Br + 2CO \qquad (VI)$$

tridentate, the structure is certainly one in which the ligand acts as a bidentate ligand as shown in Figure 7. This structure is supported by infrared spectroscopy; a pattern of three strong $\nu(C{\equiv}O)$ bands at 2046, 1972, and 1941 cm^{-1} is observed in $CHCl_3$ solution. In the $\nu(N{\equiv}C)$ region of the spectrum, two bands are observed. The weaker, high-frequency band (2267 cm^{-1}) is assigned to the coordinated groups while the somewhat stronger band at 2228 cm^{-1} corresponds to the free nitrile group.

The conversion of $Mn(CO)_3(TriCN)Br$ to $[Mn(CO)_3(TriCN)]^+$ is carried out by treatment with a silver salt such as $AgPF_6$ (eq. VII). As the

$$Mn(CO)_3(TriCN)Br + AgPF_6 \longrightarrow [Mn(CO)_3(TriCN)]PF_6 + AgBr \quad (VII)$$

coordinated bromide is removed by Ag^+, the third and uncoordinated nitrile group swings in to bind to the manganese, forming the tris-chelate structure in Figure 7. As this happens, the symmetry of the complex increases to C_{3v} and accordingly the $\nu(C{\equiv}O)$ pattern simplifies to two strong bands at 2066 and 1986 cm^{-1} (of A_1 and E symmetry, respectively). In the $\nu(N{\equiv}C)$ region, a single band at 2268 cm^{-1} is observed; the low frequency absorbance seen in $Mn(CO)_3(TriCN)Br$ at 2228 cm^{-1} is no longer apparent. Treatment of the cation with an equimolar amount of Et_4NBr in CH_2Cl_2 leads to quantitative conversion back to $Mn(CO)_3(TriCN)Br$, as one nitrile group is displaced from the manganese center by Br^-.

The equilibrium between bis-nitrile and tris-nitrile chelated forms (eq. VIII), if existent, must lie far to the left, since no

$$Mn(CO)_3(TriCN)Br \rightleftharpoons [Mn(CO)_3(TriCN)]Br \qquad \text{(VIII)}$$

IR bands due to $[Mn(CO)_3(TriCN)]^+$ are observed in the spectrum of $Mn(CO)_3(TriCN)Br$ in solution.

Like its DiCN analogs, $Mn(CO)_3(TriCN)Br$ decomposes photochemically in non-coordinating solvents, ultimately yielding TriCN and precipitated manganous halides. This process appears to take place somewhat more slowly for the present compound, although a direct comparison of the rates of decomposition in the two systems has not been made. Accordingly, it is possible to obtain ^1H NMR (Table 10) and ^{13}C NMR (vide infra and Table 11) spectra of $Mn(CO)_3(TriCN)Br$ which are not severely broadened by the presence of Mn(II).

The TriCN ligand reacts with $Re(CO)_5Br$ over a 5h period in refluxing 1,2-dichloroethane (b.p. 85°C) to yield $Re(CO)_3(TriCN)Br$ (eq. IX). The product is initially obtained as a light yellow crystalline

$$Re(CO)_5Br + TriCN \longrightarrow Re(CO)_3(TriCN)Br + 2\ CO \qquad \text{(IX)}$$

substance, though a yellow impurity can be removed by chromatography to give the pure complex as colorless microcrystals. The pattern of $\nu(C{\equiv}O)$ bands in $CHCl_3$ solution is similar to the manganese analog (2039, 1950, 1916 cm^{-1}), though the bands are all shifted to significantly lower

frequency, as is often observed when comparing spectra of first- and third-row transition metals. The coordinated nitrile frequency of 2268 cm^{-1} is nearly identical to that of the manganese complex. Again, the intensity of the coordinated nitrile band is lower than that of the single free nitrile group. Unlike $Mn(CO)_3(nitrile)_2Br$ complexes, this neutral rhenium complex is stable in solutions exposed to room light, making it a much easier compound to study.

Silver ion removes coordinated bromide ion from $Re(CO)_3(TriCN)Br$ to give the cationic C_{3v} complex $[Re(CO)_3(TriCN)]PF_6$ (eq. X). This is a

$$Re(CO)_3(TriCN)Br + AgPF_6 \longrightarrow [Re(CO)_3(TriCN)]PF_6 + AgBr \quad (X)$$

colorless crystalline complex exhibiting one $\nu(N{\equiv}C)$ band (2267 cm^{-1}) and two $\nu(C{\equiv}O)$ absorbances (2052, 1951 cm^{-1}) as would be expected. The stability of both rhenium TriCN complexes allowed the measurement of well-resolved ^1H NMR (Table 10) and ^{13}C NMR (Table 11) spectra. Some interesting comparisons and contrasts can be pointed out in these spectra. The ^1H NMR spectrum of free TriCN (Table 5) includes a sharp low field singlet at 7.94 ppm (CD_3CN). This signal integrates to roughly three protons and is assigned to the three equivalent protons residing on the central phenyl ring of the ligand. Expectedly, these three protons are the only ones within the ligand which are not split by coupling to adjacent ring protons. In the complex $Re(CO)_3(TriCN)Br$, the NMR spectrum consists

of a multiplet from which the previously observed spike is absent. Upon removal of Br^- and coordination of the last nitrile moiety, the sharp three-proton spike reappears as a high field singlet at 7.45 ppm (CD_3CN). These spectra are shown in Figure 12. The low field position of this resonance in the free ligand is most likely due to magnetic anisotropy within the nitrile and peripheral phenyl groups. Assuming a time-averaged conformation of C_3 symmetry something like that in 21, the protons of interest lie in regions deshielded by a phenyl ring and a nitrile group. In the other limiting case, that of full chelation to $Re(CO)_3^+$, 22, the nitrile groups are no longer able to affect those

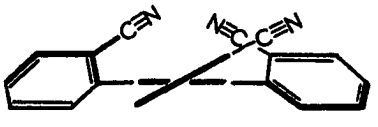

21

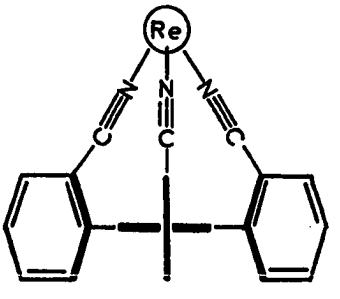

22

protons. At the same time, they are now considerably less deshielded by the phenyl rings and their chemical shift from TMS decreases.

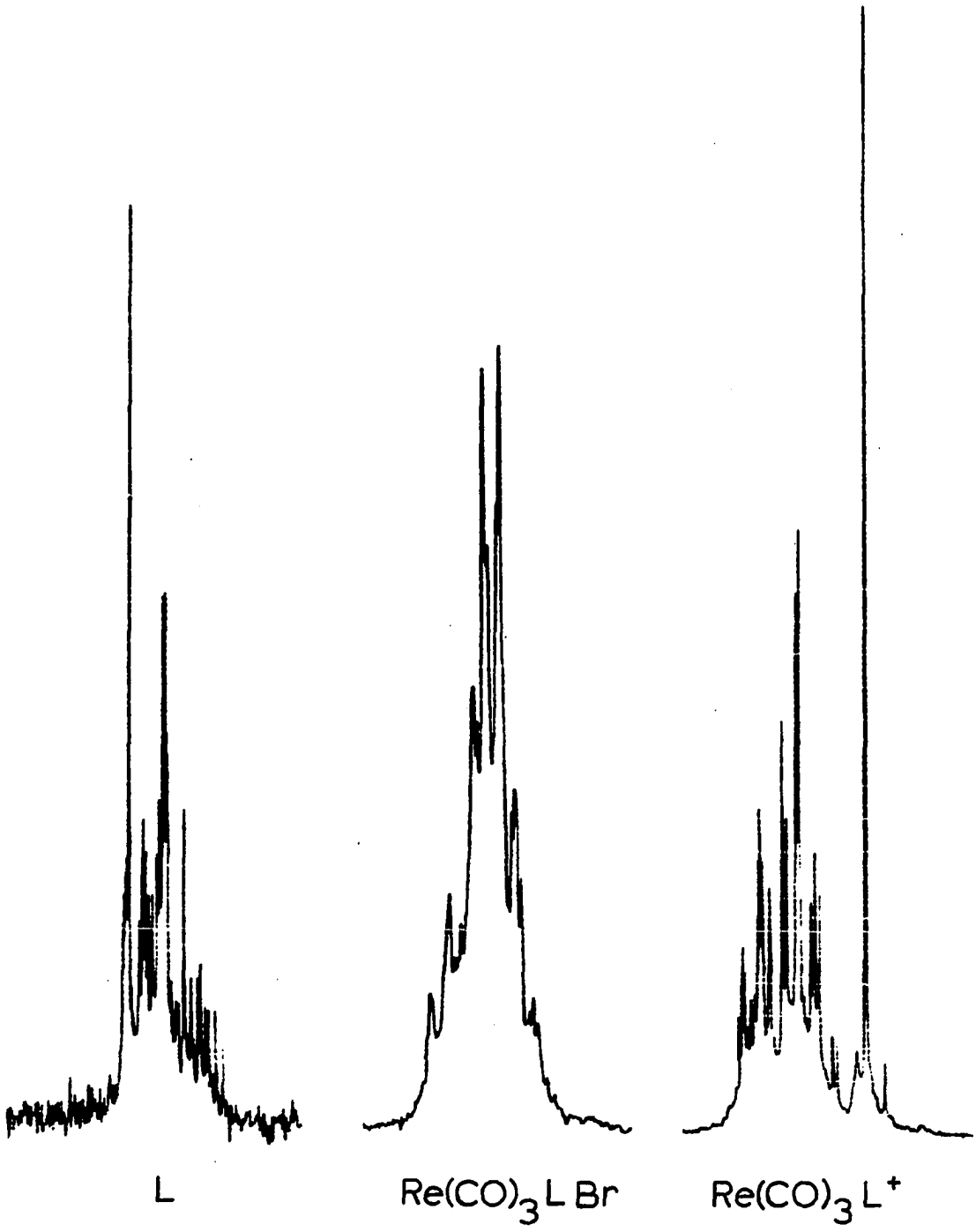

Figure 12. ^{1}H NMR spectra of aromatic protons in TriCN (L) and its Re complexes in CD_3CN solution

Studies of the rhenium TriCN complexes by ^{13}C NMR are also informative (Table 11). The free TriCN ligand exhibits nine signals, one for each group of three symmetry-related carbon atoms (23).

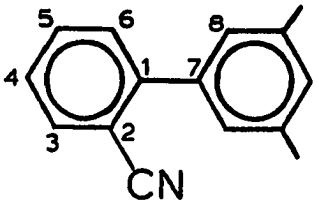

23

When complexed as a bidentate ligand to rhenium in $Re(CO)_3(TriCN)Br$, fifteen signals are observed. Here, all but three of the ligand carbon resonances are split into two signals with a 1:2 intensity ratio. Furthermore, each of those with the lower intensity has a chemical shift which falls within 0.5 ppm of the chemical shift for the corresponding carbon atom in the free ligand. The other signal is shifted by 0.7 to 2.4 ppm from the corresponding resonance in free TriCN. A logical interpretation of these results is that the coordination of two nitrile groups leads to a relatively large change in the chemical shifts of the nitrile carbon atoms, four of the phenyl ring carbons associated with those nitrile groups, and the two central phenyl ring carbons bound to the complexed C_6H_4CN groups. Electronic effects are most likely responsible for shifts within the peripheral phenyl rings (23);

carbons 4 and 6, which are meta to the NC group, have the same chemical shift in complexed and free rings of $Re(CO)_3(TriCN)Br$. In the tris-chelated complex $[Re(CO)_3(TriCN)]PF_6$, the ^{13}C NMR pattern is seen as another simple nine-line pattern as is required by either C_3 or C_{3v} symmetry in this complex.

The ^{13}C NMR spectrum of $Mn(CO)_3(TriCN)Br$ was obtained, but the pattern of signals corresponding to C3 and C5 is not as easily interpreted as for the rhenium complex, and one signal in the spectrum cannot be explained. Thus, the assignments for C3 and C5 are still questionable. Other resonances, however, are readily assigned by comparison of the two spectra. Unfortunately, the cationic complex $[Mn(CO)_3(TriCN)]PF_6$ gave an uninterpretable ^{13}C NMR spectrum, due to decomposition or the presence of impurities. Resonances of the ^{13}CO ligands were observed as weak singlets in the three compounds investigated. Though two ^{13}CO signals are expected for the neutral complexes, it should be born in mind that room temperature ^{13}C spectra of CO ligands bound to such quadrupolar nuclei (^{55}Mn, I = 5/2; ^{185}Re, I = 5/2; ^{187}Re, I = 5/2) often show broadened signals and/or fewer CO signals than expected on the basis of symmetry[133,134]. The chemical shifts of the CO ligands in the manganese (219.6 ppm) and rhenium complexes (191.5 ppm for $Re(CO)_3(TriCN)Br$; 193.9 ppm for $Re(CO)_3(TriCN)^+$) are well within ranges defined by other organometallic manganese and rhenium

complexes.[135] The large chemical shift difference between the analogous manganese and rhenium complexes is a trend commonly observed as a transition metal triad is descended.[135] Also to be noted is the slight increase in chemical shift (2.4 ppm) upon gaining a positive charge in the rhenium system.

b. Complexes with other metals TriCN reacts with $CrCl_3(THF)_3$[136] under anhydrous conditions to yield a lavendar solid thought to be $CrCl_3$(TriCN) [ν(C≡N) 2278 cm^{-1}, 2228 cm^{-1}, w]. This complex is analogous to the known purple-black complexes[137] $CrCl_3(NCC_2H_5)_3$ and $CrCl_3(NCC_2H_3)_3$, which show shifts in their nitrile stretching frequencies similar to that in the TriCN complex. When exposed to air, the presumed $CrCl_3$(TriCN) decomposes to form $CrCl_3 \cdot 6H_2O$ and free TriCN.

Under a variety of experimental conditions, TriCN reacts with $SnCl_4$. The observed infrared spectra of reaction products vary widely depending upon the reaction conditions employed, with bands at 2271 cm^{-1}, 2266 cm^{-1}, 2255 cm^{-1}, and 2228 cm^{-1} having been observed. This system is no doubt complex because of the presence of three nitrile groups and the possibility of forming acid/base (A/B) adducts of the types AB[138,139], AB_2[110,139], or $(AB)_2$[110,140].

An attempt to prepare fac-$RuCl_3$(TriCN) by the reaction of TriCN with $RuCl_3 \cdot xH_2O$ in CH_3OH gave a very air-sensitive yellow product of unknown formulation. This result contrasts sharply with the known reaction

between o-tolylnitrile and $RuCl_3 \cdot XH_2O$, which gives red, air stable <u>mer</u>-$RuCl_3(NC\text{-}tol)_3$ under the same reaction conditions[141]. This reaction was not investigated further, however.

B. Isonitrile Ligands and Their Complexes

1. General

A great deal could be said about both the organic chemistry and coordination properties of isonitriles. However, there are a number of reviews on the subject which provide a strong background on this subject,[142-145] the latest one having been published in 1980.[19] Isonitrile complexes of metals have been known for well over 100 years.[146] A common early method for their preparation was the alkylation of cyanometallates. In the last 30 years, preparative methods for isonitriles have been improved[142] and accordingly, a large number of isonitrile complexes have been synthesized by addition of isonitriles to metal salts and halides, and by substitution of CO or more labile ligands from organometallic complexes.

The metal-binding properties of isonitriles most closely resemble those of CO; both possess a σ-donating lone pair localized on carbon and relatively low-lying π^* orbitals which can accept π-electron density from otherwise non-bonding orbitals of the metal atom. In general, isonitriles are somewhat better σ-donors and worse π-acceptors than the carbon monoxide ligand.[19] Aromatic isonitriles are considered better

π-acceptors than alkyl isonitriles, due to conjugation of the vertical π^* orbitals of the isonitrile group with π-antibonding orbitals of the phenyl group.[147,148] Experimentally, this concept is supported by electrochemical and spectroscopic studies. The vast majority of isonitrile complexes prepared and isolated to date are those of formally zero-, mono-, and divalent metals, though isonitrile complexes of monoanionic[149] to tetravalent metals[150,151] are known. The stretching frequency of the coordinated isonitrile group depends upon the metal, its oxidation state, and the nature of other ligands. Fundamentally, these parameters determine the relative importance of σ-bonding vs. π-bonding in the complex. Because the carbon lone pair is antibonding with respect to C and N, σ-donation from this orbital raises the isonitrile stretching frequency.[144,148] Donation of electron density into the isonitrile π^* orbitals lowers the stretching frequency. In practice, ν(CN) may appear at higher or lower energies than that of the free ligand, with higher frequencies associated with greater formal positive charge or the presence of stronger π-acid ligands in the complex. Also, where more than one ν(CN) band is expected on the basis of symmetry (as for cis-$ML_4(CNR)_2$), these bands are usually observed and are useful in determining the structure of the complex.

2. Synthesis of siloxylated diisonitriles

The initial interest in ortho-siloxylated isonitriles was to use them as precursors for the synthesis of macrocyclic tetradentate isonitrile ligands. It was anticipated that a scheme to obtain these large ligands

would first entail the synthesis of a bidentate isonitrile ligand with an additional functional group ortho to each isonitrile. The second step would be that of chelating two such ligands at a square planar metal center, forming a template for the third step, coupling of the ortho-functional groups with an appropriate bifunctional bridge. Scheme II shows a series of reaction which yield the functionalized

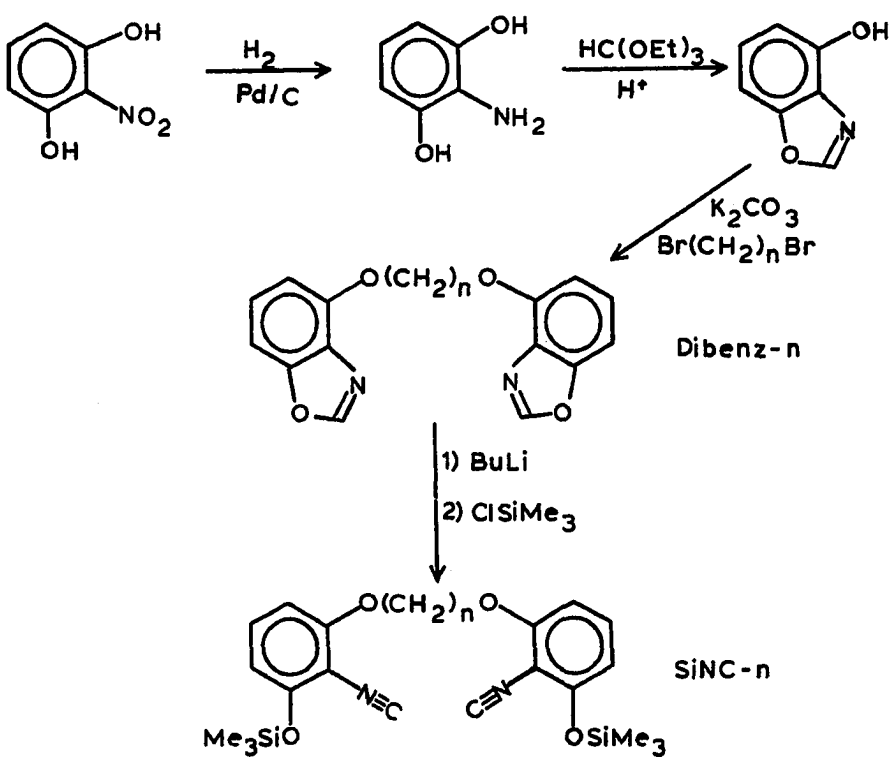

Scheme II

diisonitriles SiNC-2 and SiNC-3. The scheme is simple in that the two important functional groups, $-OSiMe_3$ and $-N{\equiv}C$, are generated in a single reaction. Furthermore, the whole sequence involves only four steps from commercially available 2-nitroresorcinol.

In ethanol, 2-nitroresorcinol is reduced by hydrogen with a palladium catalyst quantitatively to air-sensitive 2-aminoresorcinol.[102] Treatment with triethylorthoformate and a catalytic amount of sulfuric acid at 120-155°C gives 4-hydroxybenzoxazole in 76% yield.[103] By coupling two 4-hydroxybenzoxazoles with either 1,2-dibromoethane or 1,3-dibromopropane, the "Dibenz" ligand precursors are obtained in yields of 41% and 63%, respectively. Though the yield is rather low for Dibenz-2, several grams of 4-hydroxybenzoxazole can be sublimed from the crude reaction product, bringing the effective yield to ca. 65%. Schröder et al.[152] have reported the conversion of 4,5-diphenyloxazole to cis- and trans-1,2-diphenyl-2-trimethylsiloxyvinyl isonitriles, and by a similar reaction, the SiNC ligands were prepared. At -78°C, butyllithium metallates the benzoxazole ring at position 2 (the CH), and in the next step, chlorotrimethylsilane is attacked by the isocyanophenoxide tautomer to give the final products (eq. XI). Application of this reaction to the model systems benzoxazole and 4-hydroxybenzoxazole gives, as the major products, 2-trimethylsiloxyphenylisocyanide (**24**) and 2,6-bis(trimethylsiloxy)phenylisocyanide (**25**), respectively, which were characterized by NMR and mass spectra. These simple derivatives might be interesting to study as ligands and multidentate ligand precursors.

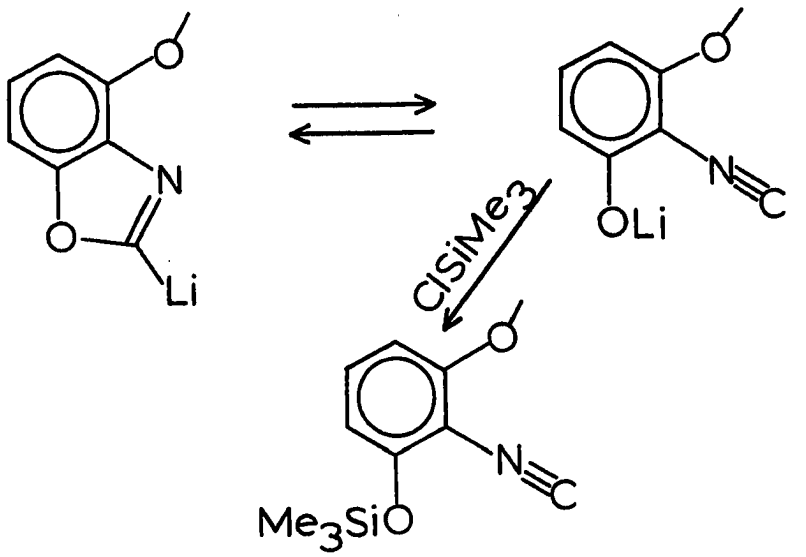

(XI)

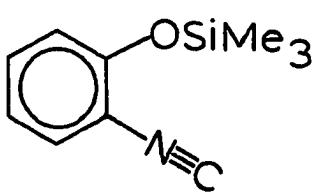

24

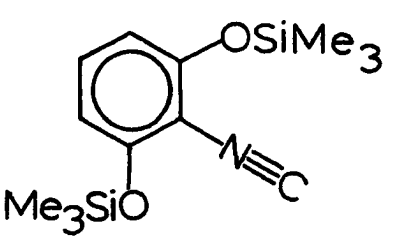

25

The ligands SiNC-2 and SiNC-3 are obtained in overall yields of 10% and 24%, respectively. Analysis of the products by ^{1}H or ^{13}C NMR shows that each usually contains about a 10% impurity of the benzoxazole functionality due to either incomplete reaction or hydrolysis of the silyl ether by adventitious water (vide infra). However, products of this quality were suitable for the preparation of metal complexes without further purification. SiNC-2 and SiNC-3 are pale yellow, odorless solids. As such, they react slowly with atmospheric moisture via hydrolysis of the silyl ether to regenerate the benzoxazole functional group and hexamethyldisiloxane. In $CDCl_3$ solution, a similar decomposition reaction takes place with excess CH_3OH over a period of about 8 hours, giving the dibenzoxazole and $MeOSiMe_3$ (Eq. XII). Thus, metal complex-

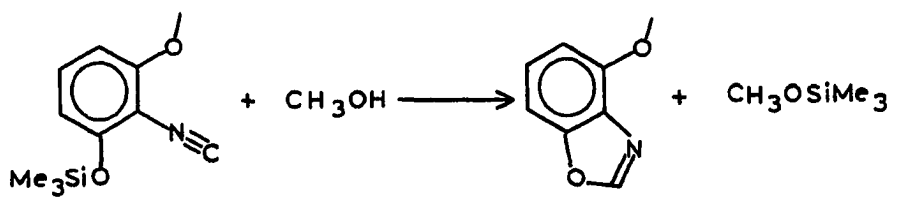

(XII)

forming reactions with SiNC-2 and SiNC-3 were carried out in non-hydroxylic solvents and in the absence of water.

The ligands are slightly soluble in saturated hydrocarbons; the solubility of SiNC-3 is noticeably greater than that of SiNC-2 in these solvents. Both are moderately soluble in Et_2O and C_6H_6, and are

quite soluble in $CHCl_3$ and CH_2Cl_2. The greater solubility of SiNC-3 noted above is parallelled in the Dibenz precursors as well. It is thought that the higher yield in the formation of SiNC-3 vs. SiNC-2 from the dibenzoxazoles is due in part to the greater solubilities of Dibenz-3 and its dianion in THF.

Interestingly, the DiCN-2 ligand (Section III.A.2) is considerably less soluble than DiCN-3, just as SiNC-2 is less soluble than SiNC-3. It is noted that the less soluble ligands also have higher melting points than their more soluble analogs. This trend holds within the DiCN series (DiCN-2, mp 175-7°C[96]; DiCN-3, mp 113-115°C; DiCN-4, mp 151-3°C), as well as the SiNC pair (SiNC-2, mp 100-7°C; SiNC-3, mp 76-82°C). Thus, the melting points of closely-related ligands may indicate their relative solubilities.

3. Rhodium complexes of siloxylated diisonitriles

a. Rhodium(I) complexes The ligands SiNC-2 and SiNC-3 react at room temperature in benzene solution with $[Rh(COD)Cl]_2$ to precipitate the hygroscopic blue-green (SiNC-2) and yellow-green (SiNC-3) chloride salts, $[Rh_n(SiNC)_{2n}]Cl_n$, (Eq. XIII). Metathesis with $NaBPh_4$ or KPF_6 in

$$2\ \text{SiNC-n} + 1/2[Rh(COD)Cl]_2 \longrightarrow [Rh(\text{SiNC-n})_2]Cl + COD \qquad \text{(XIII)}$$

CH_3CN/CH_2Cl_2, evaporation, extraction of the dry residue with CH_2Cl_2, and re-evaporation of the solutions gives the products $[Rh(\text{SiNC-2})_2]X$

($X = BPh_4$, PF_6) and $[Rh(SiNC\text{-}3)_2]PF_6$ in analytically pure form. In the solid state, complexes containing the ethylene-bridged ligand are deep blue-green while the SiNC-3 complex is green in color.

Gray and others have extensively studied the solution behavior and electronic spectra of many complexes of the type $[Rh(CNR)_4]^+$ in their monomeric forms.[56-58,105,153,154] These cations usually exhibit three metal-to-ligand charge transfer (MLCT) bands assigned as $^1A_{1g} \longrightarrow {}^3A_{2u}$ ($2a_{1g} \longrightarrow 2a_{2u}$), $^1A_{1g} \longrightarrow {}^1A_{2u}$ ($2a_{1g} \longrightarrow 2a_{2u}$) and $^1A_{1g} \longrightarrow {}^1E_u$ ($2e_g \longrightarrow 2a_{2u}$). These transitions can be seen in part a of Figure 13, which shows appropriate molecular orbital diagrams adapted from those of Geoffroy et al.[153] and Mann et al.[154] Many of the known $[Rh(CNR)_4]^+$ compounds associate through weak Rh-Rh bonding interactions in solution to form dimers, and sometimes higher oligomers. These species exist in equilibrium with one another and the concentrations of oligomeric species depend upon the total rhodium concentration and the equilibrium constants for the system.[56] Part b of Figure 13 shows the perturbation of the d_{z^2} ($2a_{1g}$) and $\pi^*_{CN}(2a_{2u})$ orbitals attendant to dimer formation. Such dimers and the obligate dinuclear complexes such as $[Rh_2(CN(CH_2)_nNC)_4]^{2+}$ show a low energy band assigned as $^1A_{1g} \longrightarrow {}^1A_{2u}(1a_{2u} \longrightarrow 2a_{1g})$, a higher energy band assigned as $^1A_{1g} \longrightarrow {}^1E_u(d_{xz},d_{yz} \longrightarrow \pi^*_{CN})$, and sometimes a triplet component, $^1A_{1g} \longrightarrow {}^3E_u$ of the latter band.[58] Oddly, the energies of the $^1A_{1g} \longrightarrow {}^1E_u$ transitions in monomers ($2\ e_g \longrightarrow 2a_{2u}$) and analogous dimers ("$d_{xz},d_{yz} \longrightarrow \pi^*_{CN}$") are nearly the same, despite the observations that 1) the π^*_{CN} orbital of initially a_{2u} symmetry is significantly

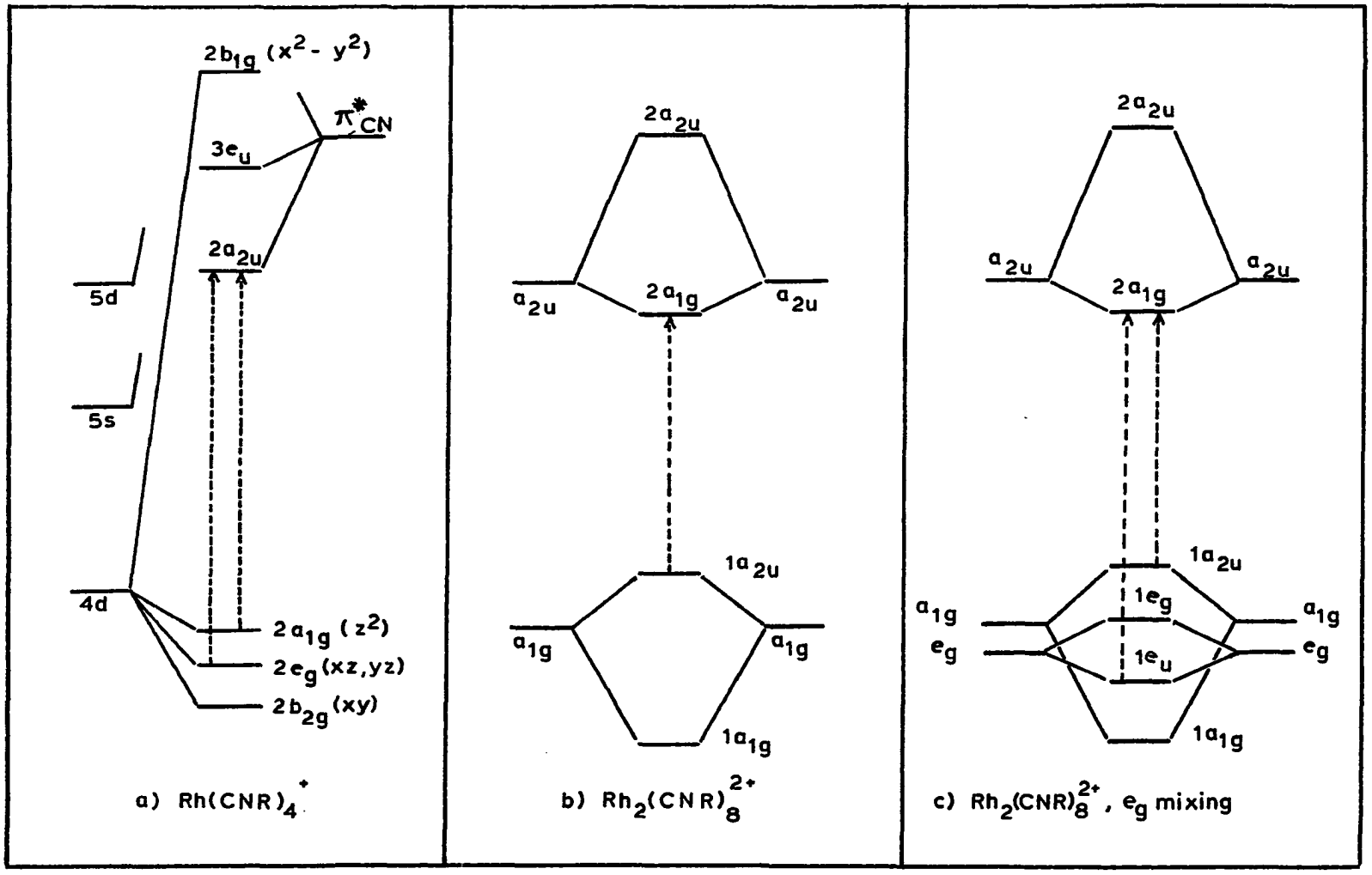

Figure 13. Molecular orbital diagrams for $[Rh(CNR)_4]^+$ (a) and $[Rh_2(CNR)_8]^{2+}$ (b,c)

split to a_{1g} and a_{2u} components in the dimer; 2) a transition from the unsplit d_{xz},d_{yz} (e_g) pair to the $2a_{1g}$ orbital would be of much lower energy than in the monomer and would also be electric dipole-forbidden; and 3) the electric dipole-allowed transition $^1A_{1g} \longrightarrow {}^1E_u$ ($2e_g \longrightarrow 2a_{2u}$ in Figure 13b) in the dimer would be of much higher energy than in the corresponding monomer. These inconsistencies could be accounted for by allowing the d_{xz} and d_{yz} orbitals of the two rhodium centers to mix, just as the d_{z^2} and π^*CN (a_{2u}) do. This gives rise to a set of stabilized e_u and destabilized e_g orbitals, as shown in part c of Figure 13. From this configuration, the $^1A_{1g} \longrightarrow {}^1E_u$ ($1e_u \longrightarrow 2\ a_{1g}$) transition is fully allowed, and should now be similar in energy to the $^1A_{1g} \longrightarrow {}^1E_u$($2e_g \longrightarrow 2a_{2u}$) transition of the monomer.

The solution structures of the SiNC complexes can now be analyzed in terms of their electronic spectra. $[Rh(SiNC\text{-}3)_2]PF_6$ (26) has an

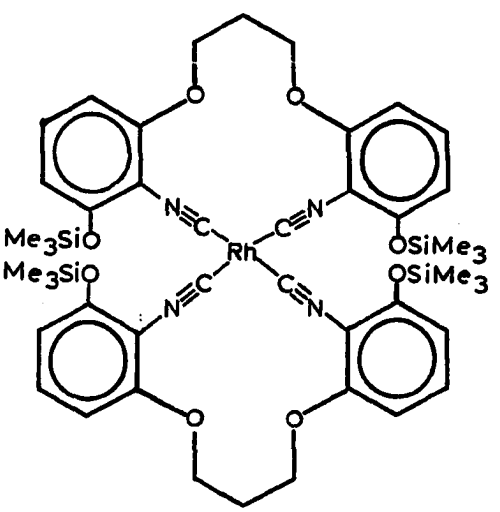

26

electronic spectrum comparable to those of other $[Rh(CNAr)_4]^+$ complexes. In CH_3CN solution, three bands are observed: 352 nm ($^1A_{1g} \longrightarrow {}^1E_u$), 406 nm ($^1A_{1g} \longrightarrow {}^1A_{2u}$), and 463 nm ($^1A_{1g} \longrightarrow {}^3A_{2u}$). The energies of these bands are similar to those of other $[Rh(CNAr)_4]^+$ monomers, as shown in Table 30. At concentrations as high as 3×10^{-3} M, $[Rh(SiNC\text{-}3)_2]^+$ shows no tendency to dimerize, as evidenced by a lack

Table 30. Electronic absorptions of $[Rh(CNAr)_4]^+$ monomers, nm

Compound	$^1A_{1g} \longrightarrow {}^1E_u$	$^1A_{1g} \longrightarrow {}^3E_u$	$^1A_{1g} \longrightarrow A_{2u}$	$^1A_{1g} \longrightarrow {}^3A_{2u}$
$[Rh(SiNC\text{-}3)_2]^+$ [a]	352	b	406	463
$[Rh(DiNC)_2]^+$ [c]	357	415 sh	427	472
$[Rh(t\text{-}BuDiNC)_2]^+$ [c]	361	413 sh	421	472
$[Rh(CNPh)_4]^+$ [d]	335	b	411	463

[a] CH_3CN solution.

[b] Not observed.

[c] DMF solution, from ref. 155.

[d] CH_3CN solution, from ref. 56.

of low energy bands at ca. 600 nm. Thus, even concentrated solutions of this complex are green in color, as is the complex in the solid state. This contrasts with the blue to violet colors characteristic of

$[Rh_2(CNR)_8]^{2+}$ solids.[52,56,58,155,156] The low tendency of $[Rh(SiNC\text{-}3)_2]^+$ to dimerize is attributed to unfavorable steric interactions among trimethylsiloxy, phenyl, and propylene units in the perhaps hypothetical $[Rh_2(SiNC\text{-}3)_4]^{2+}$ dimer. Steric interactions between other $[Rh(CNR)_4]^+$ units have been shown previously to affect oligomerization behavior, as with tetrakis (2,4,6-tri-t-butylphenylisonitrile) rhodium(I), which shows no tendency to dimerize.[157]

Acetonitrile solutions of "$[Rh(SiNC\text{-}2)_2]PF_6$" (and the BPh_4^- salt) are blue-green in color and exhibit two visible absorption bands at 607 and 362 nm. The low energy band at 607 nm is assigned to the $^1A_{1g} \longrightarrow {}^1A_{2u}$ ($1a_{2u} \longrightarrow 2a_{1g}$) transition in a $[Rh_2(SiNC\text{-}2)_4]^{2+}$ dimer (see Fig. 13c), and the higher energy band at 362 nm could be due to an $^1A_{1g} \longrightarrow {}^1E_u$ transition in either a dimer or monomer. There are no bands at all between these two, though monomer transitions of the type $A_{1g} \longrightarrow {}^{1,3}Eu$ ($2e_g \longrightarrow 2a_{2u}$) would be expected around 425 and 480 nm, as for $[Rh(SiNC\text{-}3)_2]^+$ and others (Table 30). Qualitatively, it is observed that even very dilute solutions of the complex are a blue-green color, indicating that a dimeric species (λ_{max} 607 nm) is present. The apparent omnipresence of a dimeric species suggests that one of two sets of circumstances obtains for the complex. The first would be that the equilibrium constant for the dimerization reaction $2[Rh(SiNC\text{-}2)_2]^+ \overset{K}{\rightleftharpoons} [Rh_2(SiNC)_4]^{2+}$ is very large. The other would be that "$[Rh(SiNC\text{-}2)_2]^+$" exists a dimer containing four bridging SiNC-2 ligands, as shown in 27. At a concentration of 5.8×10^{-5} M, where no "monomer" bands are observed

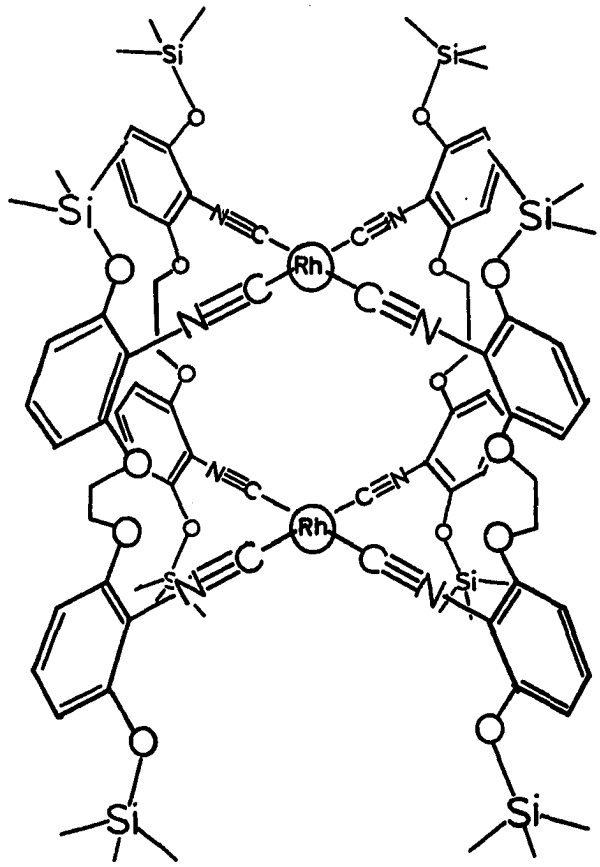

27

(i.e. at ca. 410 and 470 nm), the maximum concentration of such a monomer which could avoid detection would be roughly 10^{-6} M, assuming an ε_{410} of ca. 35000. This yields a K value of ca. 6 x 10^{7} M^{-1}, which is very, very large considering that $[Rh(CNPh)_4]^+$, with its sterically less-demanding ligands, has a K value of roughly 35 M^{-1}.[56] On this basis (which assumes that a $[Rh(SiNC\text{-}2)_2]^+$ monomer would absorb energy at ca. 410 and 470 nm), it is proposed that the complexes "$[Rh(SiNC\text{-}2)_2]X$"

($X^- = PF_6^-$, BPh_4^-) do indeed exist in the obligate dinuclear form as shown in 27. In terms of this dinuclear structure, the dication's $^1A_{1g} \longrightarrow {}^1E_u$ band at 362 nm is assigned as the $1e_u \longrightarrow 2a_{1g}$ transition as shown in Figure 13c. Its ε value calculated per Rh_2 unit is $36.4 \times 10^3\ M^{-1}\ cm^{-1}$, comparable to ε values for the same transition in $[Rh_2(CN(CH_2)_3NC)_4]^{2+}$ and similar molecules, which range from 31.5×10^3 to $43.3 \times 10^3\ M^{-1}\ cm^{-1}$.[58] The molar extinction coefficient for the 607 nm band calculates to ca. 4400 $M^{-1}\ cm^{-1}$, compared to a value of 8500 - 12500 $M^{-1}\ cm^{-1}$ estimated for $[Rh_2(CNPh)_8]^{2+}$.[56] It is to be pointed out here that $[Rh_2(SiNC\text{-}2)_4]X_2$ decomposes slowly in solution, as indicated by a decrease in the intensities of both visible bands, and also by a drop in the intensities of ^1H NMR signals of the samples in CD_2Cl_2 solution with respect to an internal standard such as $CDHCl_2$ or added cyclohexane. The decomposition is probably due to reaction of the silyl ether with adventitious water (vide supra). In light of this decomposition, the ε values given above are to be considered lower limits, and the actual extinction coefficients could be larger.

An interesting question concerns the very different structures 26 and 27 which arise from reactions of the similar ligands SiNC-3 and SiNC-2 with $[Rh(COD)Cl]_2$ under nearly identical conditions. In the absence of concrete structural data on these two compounds, this discussion necessarily relies upon information made available by molecular models and an X-ray crystallographic study of $[Rh(t\text{-}BuDiNC)_2]BPh_4 \cdot 1.5\ CH_3CN$.[158] In the hypothetical cation $[Rh(SiNC\text{-}2)_2]^+$, the range of possible ring-RhC_4 interplanar angles is more constricted than in the SiNC-3 analog,

due to the tighter 13-membered chelate ring. In $[Rh(t\text{-}BuDiNC)_2]^+$, which also contains a 13-membered t-BuDiNC chelate ring, these angles range from 6° to 31°.[158] Accordingly, steric interactions between facing pairs of bulky trimethylsiloxy groups in the hypothetical $[Rh(SiNC\text{-}2)_2]^+$ chelate would certainly be greater than in the known cation $[Rh(SiNC\text{-}3)_2]^+$. Energetically, this would have several consequences. In terms of ΔH for the chelate-forming reaction, more energy is stored in the $[Rh(SiNC\text{-}2)_2]^+$ structure in the form of van der Waal's repulsions between the crowded trimethylsilyl groups and/or in strain energy within the chelate rings as these groups attempt to avoid one another. Such interactions also may reduce the amount of conformational flexibility within the chelate ring and reduce ΔS for the chelate-forming reaction in $[Rh(SiNC\text{-}2)_2]^+$ vs. $[Rh(SiNC\text{-}3)_2]^+$, also disfavoring the former structure. The dinuclear structure 27, on the other hand, would appear by molecular models to possess no drastic steric interactions at all between neighboring trimethylsiloxy groups and appears to be favored over the chelated structure.

Infrared spectra of the square-planar rhodium(I) complexes $[Rh_2(SiNC\text{-}2)_4]^{2+}$ and $[Rh(SiNC\text{-}3)_2]^+$ exhibit one strong $\nu(CN)$ band of E_u symmetry at a position ca. 30 cm^{-1} higher than that observed in the corresponding free ligand. Increases in $\nu(CN)$ upon coordination to positively charged metal centers are very common due to σ-donation from the slightly C-N antibonding lone electron pair of the isocyanide carbon.

The values of 2160 cm^{-1} and 2159 cm^{-1} observed for the SiNC-2 and SiNC-3 complexes compare closely to the value of 2160 cm^{-1} reported for $[Rh(CNPh)_4]^+$ [56] and are 10-20 cm^{-1} higher than stretching frequenices reported for Rh(I) complexes of some other substituted aromatic isocyanides.[52] In addition to the strong band at 2160 cm^{-1}, each complex exhibits a weak shoulder at 2200 cm^{-1}, probably due to a weakly allowed mode of A_{1g} or B_{1g} symmetry.[52] Other characteristic infrared bands include the strong ν(SiO) absorbance of the silyl ether of the SiNC ligands at ca. 840 cm^{-1}. In the PF_6^- salts, this band is coincident with the T_{1u} ν(PF) mode of the anion.

Proton NMR spectra of the SiNC-2 and SiNC-3 complexes are similar to spectra of the free ligands themselves. The single CH_2 resonance of the SiNC-2 ligand in $[Rh_2(SiNC\text{-}2)_4]^{2+}$ is slightly broadened relative to the uncomplexed ligand. The $[Rh_2(SiNC\text{-}2)_4]^{2+}$ unit probably has an instantaneous solution structure of D_4 symmetry, since the weak Rh-Rh interaction should pull the Rh atoms to a bonding distance of ca. 3.3 Å.[158] In this structure, the CH_2CH_2 protons should fall into an AA'BB' spin system as represented for the Δ isomer of D_4 symmetry in **28**. As long as the conversion between forms **28** (Δ) and **29** (Λ) takes place on the time scale of several hundred Hz or faster, only a time averaged signal should be observed, and the single CH_2 resonance indicates that this is the case.

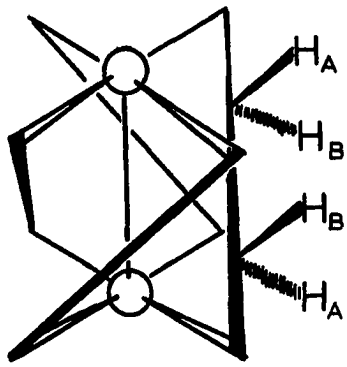

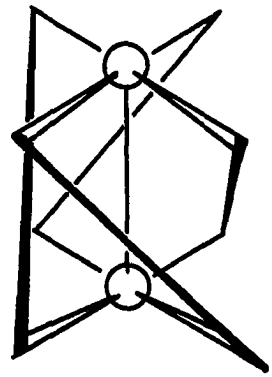

28 29

The methyl protons of the $SiMe_3$ group appear also as a singlet at 0.11 - 0.13 ppm, with the chemical shift depending slightly upon the solvent and counterion. No splitting would be expected, since the $SiMe_3$ groups are interconvertible by the C_4 operation in D_4 symmetry.

In NMR spectra of $[Rh(SiNC\text{-}3)_2]PF_6$, the OCH_2 signal of the propylene unit is found as a pseudotriplet at the same chemical shift as in the free ligand, while the central CH_2 multiplet is at slightly lower field than in SiNC-3. Winzenburg et al.[155] have observed that the structurally similar $[Rh(t\text{-}BuDiNC)_2]^+$ complexes show two separate CH_2 resonances corresponding to monomeric species and dimeric species in solution. The monomeric cation's CH_2 chemical shift is at roughly the same postion as for free t-BuDiNC, while the oligomer signal is shifted upfield. Here,

in the case of $[Rh(SiNC\text{-}3)_2]^+$, the OCH_2 and CH_2 resonances are near those of free SiNC-3, which supports the contention that this cation does not dimerize in solution.

b. Oxidative addition reactions Oxidative addition reactions (Eq. XIV) and the reverse reaction, reductive elimination, are of

$$L_nM + X\text{-}Y \rightleftharpoons L_nMXY \qquad \text{(XIV)}$$

both practical and theoretical interest because of their importance in many catalytic processes. Tetrakis(isonitrile)rhodium(I) complexes exhibit a rich and varied oxidative addition chemistry with halogens and alkyl halides. In many cases, the products are of the type trans-$[Rh(CNR)_4XY]^+$.[159] In some systems, Rh(II), rather than Rh(III) complexes result, as in the halogen oxidation of the dinuclear, diisocyanide-bridged complex $[Rh_2(CN(CH_2)_3NC)_4]^{2+}$.[105] Balch and Olmstead[53,54,160] have described solvent-dependent equilibria of the type in equation XV.

$$Rh(CNR)_4^+ + Rh(CNR)_4X_2^+ \rightleftharpoons Rh_2(CNR)_8X_2^{2+} \qquad \text{(XV)}$$

Deep blue CH_2Cl_2 solutions of $[Rh_2(SiNC\text{-}2)_4]X_2$ ($X^- = PF_6^-$, BPh_4^-) react rapidly with added I_2 to give orange solutions. Addition of hexane or ether gives orange solids formulated as $[Rh_2(SiNC\text{-}2)_4I_2]X_2$ ($X^- = PF_6^-$, BPh_4^-) (30). Infrared spectra of the isolated products include a single, strong $\nu(CN)$ mode at 2211 cm^{-1} (CH_2Cl_2) or 2213 cm^{-1}

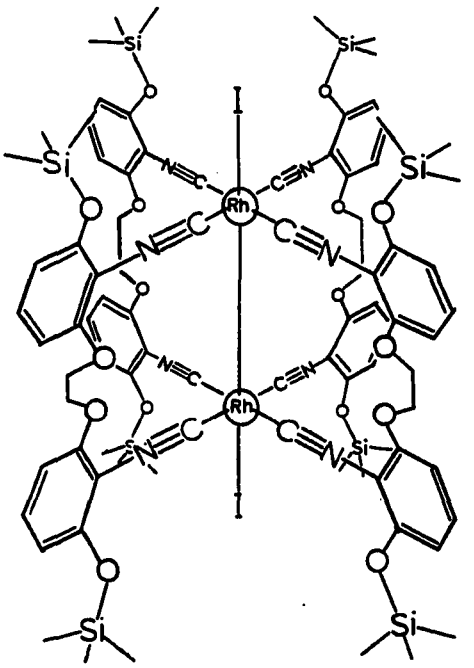

30

(Nujol mull). The observed shift in the isocyanide stretching frequency with respect to that of the Rh(I) complex (51 cm^{-1}) is within the range of 39-55 cm^{-1} expected for such diiodo-Rh(II) dimers based on other examples in the literature.[53,54,105,155] The composition of $[Rh_2(SiNC\text{-}2)_4I_2](PF_6)_2$ is supported fairly well by elemental analysis (Sec. II.E.4.j). The BPh_4^- salt, however, gave analyses with a much lower carbon content than expected (43.40% found; 57.10% calc'd.). This is probably related to an interesting photodecomposition of $[Rh_2(SiNC\text{-}2)_4I_2](BPh_4)_2$ back to $[Rh_2(SiNC\text{-}2)_4]^{2+}$ (identified by IR), and an unknown counterion. It seems that the counterion could be I^- and that the BPh_4^- ion is partially decomposed to volatile products, thus accounting for the low C analysis.

In CD_3CN solution, both the PF_6^- and BPh_4^- salts of the $[Rh_2(SiNC\text{-}2)_4I_2]^{2+}$ dication give ^1H NMR spectra in which the ethylene group of the ligand appears as a complex multiplet, rather than the slightly broadened singlet characteristic of the Rh(I) monomer (Figure 14). This splitting is a result of coupling among diastereotopic ethylene protons in an AA'BB' pattern. The chemical shift inequivalence results from the fact that there are now two sets of symmetry-unrelated protons in the closely bonded Rh-Rh dimer as represented in Figure 14. Unlike the Rh(I) dimer, $[Rh_2(SiNC\text{-}2)_4]^{2+}$, where the formal Rh-Rh bond order is zero, $[Rh_2(SiNC\text{-}2)_4I_2]^{2+}$ has a formal Rh-Rh bond of order one. This bond must slow the interconversion of Δ and Λ enantiomers sufficiently to allow the observation of the ethylene multiplet, in contrast to the Rh(I) dimer, for which the ethylene group appears as a singlet.

The visible spectrum of $[Rh_2(SiNC\text{-}2)_4I_2](BPh_4)_2$ in CH_2Cl_2 exhibits three prominent bands of nearly equal intensity at 365, 427, and 478 nm. The latter two bands may be assigned as $\sigma \rightarrow \sigma^*$ and $d\pi \rightarrow \sigma^*$ transitions, respectively, by analogy with $[Rh_2(CN(CH_2)_3NC)_4I_2]^{2+}$.[105] The absorption at 365 nm is very close to the $^1A_{1g} \longrightarrow {}^1E_u$ transition of the Rh(I) dimer $[Rh_2(SiNC\text{-}2)_4]^{2+}$ and may be due to the presence of such, having been formed by the aforementioned solid state photodecomposition reaction.

The oxidation of $[Rh(SiNC\text{-}3)_2]PF_6$ by I_2 in CH_2Cl_2 solution proceeds differently than for the SiNC-2 derivative. The addition of 0.47 mole of I_2 to one mole of $[Rh(SiNC\text{-}3)_2]^+$ leads to an infrared spectrum with a new ν(CN) band at 2231 cm^{-1} and a weak shoulder at 2162 cm^{-1} due to

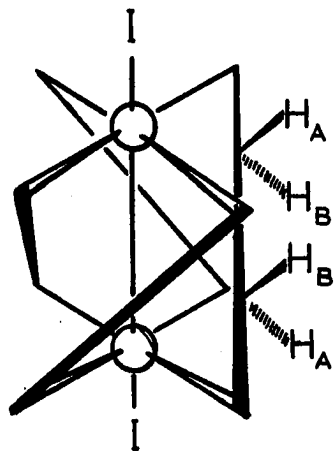

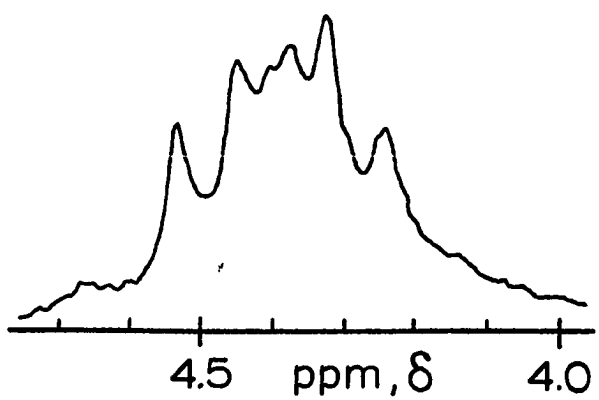

Figure 14. Schematic representation and ^1H NMR pattern of ethylene protons of $[Rh_2(SiNC\text{-}2)_4I_2]^{2+}$

remaining Rh(I) starting material. Addition of 0.12 mole more of I_2 consumes the remaining Rh(I) compound but causes no change in the frequency of the new, higher frequency band. From the solution is isolated a compound formulated as $[Rh(SiNC\text{-}3)_2I_2](PF_6)$ in 37% yield. This is a Rh(III) product, as suggested by the rather high ν(CN) value of 2231 cm^{-1} in CH_2Cl_2 (2236 cm^{-1} in Nujol mull). A broad absorption band ($\varepsilon \cong 9000\ M^{-1}\ cm^{-1}$) at 400 nm also is consistent with a Rh(III) formulation.[160,161] The simple ^1H NMR spectrum of the complex (Table 14) suggests a mononuclear Rh(III) structure as well. The product's elemental analysis is consistent with the proposed composition as far as the iodine content is concerned (17.97% calc'd.; 17.48% found), but the carbon content is significantly high (39.16% calc'd.; 40.63% found). It can only be said at this point that the major product is $[Rh(SiNC\text{-}3)_2I_2]PF_6$, which provides a contrast to the Rh(II) complexes formed exclusively by the reactions of halogens with $[Rh(DiNC)_2]^+$.[155] The formation of this Rh(III) product, rather than a Rh(II) complex, is most likely a result of the steric bulk of the $[Rh(SiNC\text{-}3)_2]^+$ cation noted earlier; the same interactions which prevent the Rh(I) complex from dimerizing in solution would also be expected to destabilize a Rh(II)-Rh(II) bonded system.

Preliminary studies indicate the $[Rh_2(SiNC\text{-}2)_4]^{2+}$ cation to undergo oxidative addition reactions with a number of halogen-containing molecules. Reaction of the BPh_4^- salt with excess Br_2 in CH_2Cl_2 yields a yellow-orange compound with a solid state ν(CN) value of 2214 cm^{-1}, indicative

of a Rh(II) product. Methyl iodide gives a green product with ν(CN) at 2200 cm^{-1} (Nujol mull). Both complexes are photosensitive, as is $[Rh_2(SiNC\text{-}2)_4I_2](BPh_4)_2$. The photosensitivity of the CH_3I adduct, however, appears to be independent of the anion (i.e. BPh_4^- or PF_6^-). Other substrates were observed to react quickly (in less than 5 min) with the cation in CH_2Cl_2. They include (color, ν(CN) of product): $ClCH_2CH_2Cl$ (yellow, 2215 cm^{-1}); $CHCl_3$ (yellow-green, 2210 cm^{-1}); CCl_4 (yellow, 2215 cm^{-1}); HCl(g) (Violet ⟶ yellow-green, 2213 cm^{-1}), and allyl bromide (yellow, 2205 cm^{-1}). The most surprising reactions are those involving $CHCl_3$ and CCl_4, with which $[Rh(CNR)_4]X$ complexes do not undergo facile reactions. McCleverty and coworkers[52] have determined NMR spectra for $[Rh(CN\text{-}i\text{-}Pr)_4]^+$ and $[Rh(CN\text{-}p\text{-}anisyl)_4]^+$ in $CDCl_3$, apparently without reaction. Also reported was the chlorination of $[Rh(CNCH_3)_4]^+$ by CCl_4 to the Rh(III) product, but under the stringent conditions of 5 hours in refluxing CCl_4/CH_2Cl_2 (2:1), with a yield of 52%. In contrast, the reaction between $[Rh_2(SiNC\text{-}2)_4](BPh_4)_2$ and CCl_4 (a 40-fold excess compared to 380-fold above) took place quantitatively at room temperature in less than one minute. The $[Rh(SiNC\text{-}3)_2]^+$ cation reacts with CCl_4 at a rate similar to that of $[Rh_2(SiNC\text{-}2)_4]^{2+}$, to form a Rh(III) product with a ν(CN) of 2235 cm^{-1} in CH_2Cl_2. The reasons for the high reactivity of the SiNC complexes of Rh(I) are not known at this time.

c. Attempted preparation of a macrocyclic tetraisonitrile complex

As mentioned in Section III.B.1, it was anticipated that SiNC-2 and SiNC-3 complexes of Rh(I) might be convertible into macrocyclic tetraisonitrile complexes. This goal was of interest for several reasons. First, it was hoped that the planarity of the macrocyclic rhodium complex would promote stronger metal-metal interactions, both in solution and in the solid state, possibly giving rise to interesting physical and chemical properties. Second, if a general synthetic scheme could be developed for such a ligand, a series of square planar tetraisonitrile complexes of many different metals might be obtainable. The chemistry of such complexes would be interesting for systems not yet known to adopt square-planar geometries with isonitrile ligands.

The macrocyclic complex whose preparation was attempted is shown in 31. It had been anticipated that an appropriate coupling reagent,

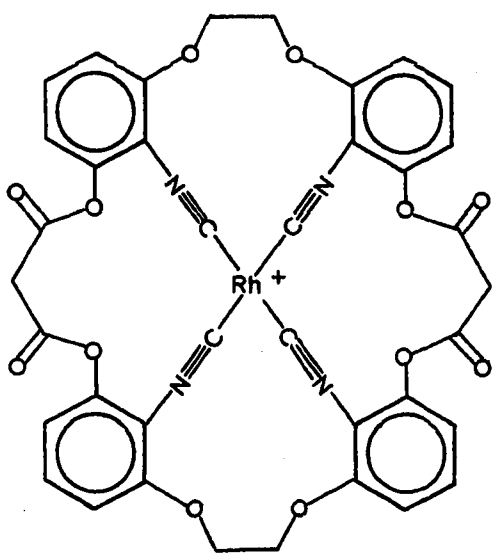

31

here containing the malonyl unit, might react with adjacent phenol oxygens in the $[Rh(SiNC-2)_2]^+$ monomer to yield the macrocycle. Unfortunately, it was not realized until some time after this experimental work was finished that "$[Rh(SiNC-2)_2]^+$" has a dinuclear structure (vide supra) and would thus have yielded dinuclear structures employing bridging cyclic tetradentate 32 or octadentate ligands 33. However,

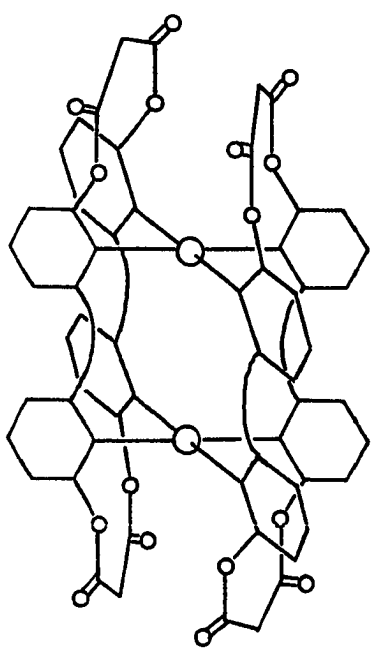

32

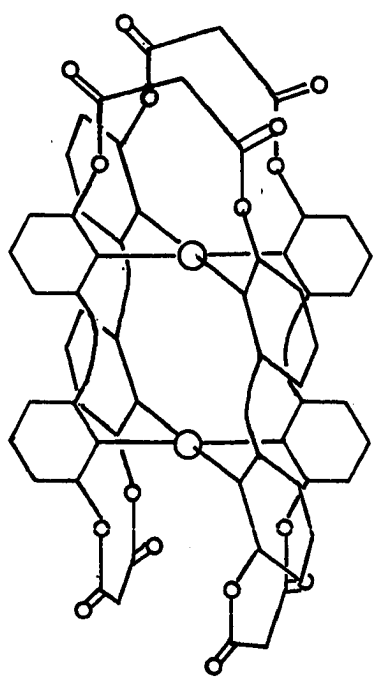

33

the synthetic and spectroscopic techniques outlined during this work may be useful in further attempts to create such macrocycles. Thus, the results and discussion of experiments intended to give the macrocyclic complex 31 follow.

Attempts to carry out a stepwise synthesis, comprised of deprotection of the phenol group of the SiNC ligand in a "$[Rh(SiNC)_2]^+$" cation, followed by coupling with a malonyl dihalide proved to be fruitless. Treatment of $[Rh_2(SiNC\text{-}2)_4](BPh_4)_2$ with Bu_4NF[162] in THF leads to rapid silyl ether cleavage and benzoxazole ring formation. That this reaction takes place is not surprising; hydrolysis of the silyl ether in the free ligand leads to benzoxazole formation. Also, it is well-known that coordination of isonitrile groups to transition metals can promote attack by many nucleophiles,[144,145] including alcohols.[163]

Because of this unwanted cyclization, a concerted coupling reaction was sought. Acyl fluorides are known to condense with silyl ethers[164] and this was attempted. Thus, the treatment of $[Rh_2(SiNC\text{-}2)_4](BPh_4)_2$ with four molar equivalents of malonyl difluoride in CH_2Cl_2 solution over a period of 1-2 h liberates $FSiMe_3$, identified by its characteristic ^1H NMR doublet.[165] Concurrently, the ligand $OSiMe_3$ resonance decreases in intensity and eventually the remaining ligand signals diminish as a blue-green solid precipitates from solution. Monitoring of reactions by infrared spectroscopy reveals a decrease in the intensity of the malonyl fluoride $\nu(CO)$ band at 1845 cm^{-1} and the growth of two new bands at ca. 1775 and 1740 cm^{-1}. No change in the position or relative intensity of the $\nu(CN)$ band is observed. Solid state infrared spectra of the isolated blue-green precipitate show similarly that the isonitrile groups are intact and that no oxidation of the Rh(I) center has taken place; a single $\nu(CN)$ is observed at 2158 - 2160 cm^{-1}. The two $\nu(C{=}O)$ bands

at ca. 1780 and 1740 cm^{-1} are similar in frequency to those reported for a number of diarylmalonate esters.[166] In most of these molecules, coupling of the two ν(C=O) modes through the central methylene unit is observed. The initially intense ν(SiO) band of the silyl ether is no longer apparent, indicating that the reaction proceeds to completion.

The isolated solid is insoluble in all common solvents except DMSO. UV-visible spectra ($C \cong 10^{-5}$ M) reveal a low energy dimer band initially at 622 nm which loses intensity with a $t_{1/2}$ of ca. 8 min. This apparent deoligomerization behavior is much like that observed for dilute solutions of $[Rh(DiNC)_2]^+$ and $[Rh(t\text{-}BuDiNC)_2]^+$.[155] Such deoligomerization would be consistent with the presence of weakly Rh-Rh-bound dimers of monomeric "$[Rh(SiNC\text{-}2)_2]^+$" units. However, the observed deoligomerization and certainly the product's low solubility could also be consistent with a structure in which SiNC-2 ligands had been linked randomly among themselves to give an extended or polymeric structure. The ^1H NMR spectrum of the product in DMSO-d_6 confirms the absence of the silyl ether functionality and shows broad resonances assignable to aromatic and ligand methylene hydrogens. The resonance of the malonyl CH_2 group expected at 3.4-3.7 ppm is unobservable, possibly being masked by H_2O in the solvent. Integration of the spectrum indicates that approximately 35% of the expected BPh_4^- is absent. Elemental analysis of the same sample gives values of % C and % N consistent with loss of 38% of the theoretical BPh_4^-. Thus, in this reaction as in oxidative addition

reactions (vide supra), anion variability seems to be a problem. The successful completion of this project would first require the investigation of a known mononuclear Rh(I) system such as $[Rh(SiNC\text{-}3)_2]^+$. The anion variability problem above would also require attention, in order to get salts of known composition. Also important would be further characterization of the product(s) by NMR methods, osmometry, and ideally, X-ray crystallography.

4. Synthesis of t-BuDiNC

The t-BuDiNC ligand is synthesized in a manner very similar to that in which the DiNC ligand was prepared.[96] Scheme III outlines the synthesis. Commercially available 4-t-butylphenol is easily nitrated by 6 M HNO_3 to 4-t-butyl-2-nitrophenol.[167] In a coupling step very much like that employed for the preparation of the DiCN ligands and the Dibenz precursors, the nitrophenoxide anion (generated by the action of K_2CO_3) reacts with 1,2-dibromoethane to produce t-BuDiNO$_2$. The procedure used in this reaction is nearly identical to that reported by Cannon et al[168] for the preparation of 1,2-bis(2-nitrophenoxy)ethane, though with a somewhat lower temperature and longer reaction time. Catalytic hydrogenation of the nitro group[169] gives the free diamine in high yield. Formylation of the diamine with acetic formic anhyride[83,170] gives the diamide, t-BuDiFor, in excellent yield. It is noted here that both the ^{13}C and room-temperature ^{1}H NMR spectra of t-BuDiFor (Tables 19 and 20) are complicated by the existence of syn - anti isomerism within the amide group.[106,171] That the

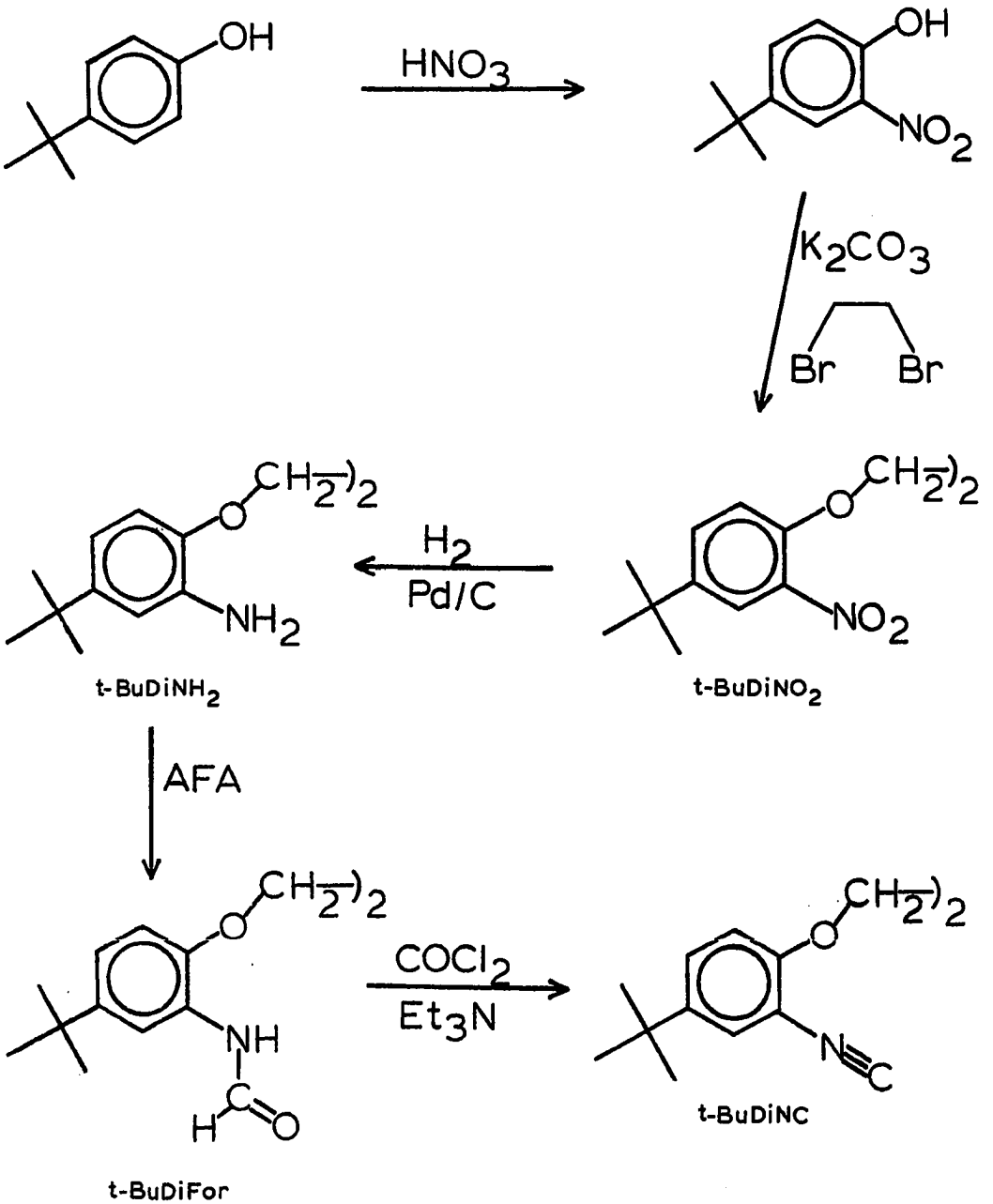
OH
HNO3
OH
NO2
K2CO3
Br
Br
CH2)2
O
H2
Pd/C
NH2
NO2
t-BuDiNH2
t-BuDiNO2
AFA
NH
C
O
H
COCl2
Et3N
N≡C
t-BuDiFor
t-BuDiNC

Scheme III

complications are due to isomerism and not a mixture of products is shown by the high-temperature (85°C) ^{1}H NMR spectrum, in which separate CH and NH resonances are observed, rather than the overlapping AB patterns seen in the ambient temperature spectrum[171] (Table 19). Dehydration of formanilides is a common route to aromatic isocyanides.[172] The use of a phosgene/Et_3N mixture, as outlined by Ugi and coworkers,[172] works considerably better than the bulky PPh_3/CCl_4 reagent[173] used earlier in the syntheses of DiNC and t-BuDiNC;[96] removal of excess PPh_3 and $OPPh_3$ proved to be somewhat of a problem when using PPh_3/CCl_4 in those syntheses. After chromatography on silica gel, t-BuDiNC is obtained as an odorless, colorless, air-stable crystalline solid in 67% yield (15% overall from 4-t-butylphenol).

The butylated ligand is much more soluble than DiNC itself, and has a melting point (98-100°C) ca. 50°C lower than DiNC. This melting point/solubility relationship was pointed out earlier for the DiCN and SiNC ligands as well (Section III.B.2). The ν(CN) frequencies of DiNC and t-BuDiNC are both 2126 cm^{-1} in the solid state. In $CHCl_3$ solution, the stretching frequencies are observed at 2128 cm^{-1} and 2126 cm^{-1}, respectively. These compare rather closely with the value of 2132.5 cm^{-1} reported for phenylisocyanide in $CHCl_3$ solution.[143]

5. Complexes of DiNC and t-BuDiNC

a. Complexes containing CO ligands A variety of substituted complexes of chromium, molybdenum, and tungsten having the general formulae $M(CO)_{6-n}(CNR)_n$ (n = 1-3) have been prepared by reactions between

isonitriles and the metal hexacarbonyls,[174-176] amine derivatives,[177] olefin derivatives,[176,178,179] and halopentacarbonyl metallates.[179,180] More recently, high yield syntheses from the metal carbonyl, isonitrile, and a transition-metal catalyst ($CoCl_2 \cdot 2H_2O$[181] or PdO[182]) have been developed.

The cis-disubstituted complexes $Cr(CO)_4$(DiNC), $Cr(CO)_4$(t-BuDiNC), and $Mo(CO)_4$(t-BuDiNC) are most conveniently prepared by displacement of norbornadiene from $Cr(CO)_4$(norbornadiene) or $Mo(CO)_4$(norbornadiene)[91] (eq. XVI). The DiNC and t-BuDiNC complexes of chromium are obtained in

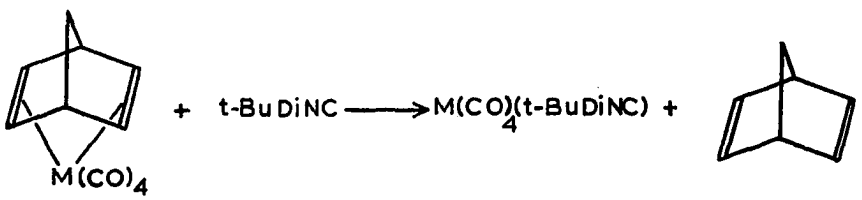

(XVI)

72% and 46% yields, respectively, by refluxing a THF solution of the diisonitrile and $Cr(CO)_4$(norbornadiene) for 5 or 6 h. The molybdenum complex cis-$Mo(CO)_4$(t-BuDiNC) is obtained in 68% yield after a reaction time of ca. 15 min in an ether/hexane mixture at room temperature. The shorter reaction time and lower temperature in this case reflect the greater lability of $Mo(CO)_4$(norbornadiene) with respect to the chromium analog.[183] The complex cis-$Mo(CO)_4$(DiNC) has been previously prepared in 64% yield by M. H. Quick through the reaction of DiNC with cis-$Mo(CO)_4(piperidine)_2$[184] after six hours' reaction time at room temperature.[14,96] The present method involving $Mo(CO)_4$(norbornadiene), which presumably could be applied to the $Mo(CO)_4$(DiNC) synthesis, would

appear to be an improvement over that employing $Mo(CO)_4(piperidine)_2$ because the required reaction time is considerably shorter, though $Mo(CO)_4(nor)$[91] is more difficult to prepare than $Mo(CO)_4(piperidine)_2$.[184]

Complexes containing a single bridging DiNC ligand are readily prepared by the reaction of 1 mole of DiNC with 2 moles of $M(CO)_5(acetone)$, where M is Cr or W, generated by the addition of $AgPF_6$ to $Et_4N[M(CO)_5I]$ in THF/acetone solvent (eq. XVII). These reactions take place by

$$2\ M(CO)_5(acetone) + DiNC \longrightarrow [M(CO)_5]_2(\mu\text{-DiNC}) \qquad \text{(XVII)}$$

displacement of the labile acetone ligand from the chromium or tungsten atoms, with isolated yields of 69% and 41%, respectively.

The $M(CO)_4(L\text{-}L)$ and $[M(CO)_5]_2(\mu\text{-DiNC})$ complexes are characterized by their elemental analyses (Table 21), infrared (Table 22), ^1H NMR (Table 23), ^{13}C NMR (Table 24) spectra, and mass spectra (in the Experimental section). The infrared spectrum of cis-$Cr(CO)_4$DiNC in the $\nu(CN)$ and $\nu(CO)$ regions includes two $\nu(CN)$ bands at 2142 cm^{-1} (A_1) and 2091 cm^{-1} (B_1), indicative of cis-coordination of the isonitrile groups. In $CHCl_3$ solution, two $\nu(CO)$ bands are seen at 2009 and 1932 cm^{-1}, though the lower frequency band at 1932 cm^{-1} probably consists of three unresolved bands. In hexane solution, the expected four $\nu(CO)$ bands are observed at 2008, 1955, 1942 and 1936 (sh) cm^{-1}. The hexane solution spectrum of cis-$Cr(CO)_4$(DiNC) is similar to that of cis-$Cr(CO)_4$-$(CN\text{-}p\text{-}tolyl)_2$[179] (cf. 2136, 2081, 2011, 1955, 1944 cm^{-1}). Infrared

spectra of cis-$Cr(CO)_4$(t-BuDiNC) and cis-$Mo(CO)_4$(t-BuDiNC) are nearly identical to that of cis-$Cr(CO)_4$(DiNC). Both monosubstituted complexes $[M(CO)_5]_2$(μ-DiNC) exhibit a single ν(CN) band at 2146 cm^{-1} and three ν(CO) bands, observed at 2059 cm^{-1} (s), 1998 cm^{-1} (m, sh), and 1952 cm^{-1} (vs, br) for M = Cr. These spectra closely resemble those of $Cr(CO)_5$-(CN-p-tol)[179] and $Mo(CO)_5$(CN-p-anisyl).[178]

Carbon-13 NMR spectra of the complexes also confirm the proposed structures. The cis-complexes each show two ^{13}CO resonances of roughly equal intensity, one for the mutually cis CO ligands trans to isonitrile groups and one for the pair of mutually trans CO ligands. The monosubstituted complexes show two ^{13}CO peaks in an approximate 1:4 ratio, the former being assigned to the single CO ligand trans to the isonitrile group. Chemical shifts of the carbonyl ligands range from 220 and 217 ppm in the $Cr(CO)_4$(L-L) derivatives to 196 and 194 ppm for $[W(CO)_5]_2$(μ-DiNC); the isonitrile carbon resonances range from 182 ppm in $Cr(CO)_4$(DiNC) to 156 ppm for $[W(CO)_5]_2$(μ-DiNC) and are normally of very low intensity due to the lack of nuclear Overhauser enhancement and broadening by the quadrupolar ^{14}N nucleus. The CO and CN resonances of the chromium complexes are ca. 10 ppm downfield of those in the analogous molybdenum complex; those of $[Cr(CO)_5]_2$(μ-DiNC) are ca. 20 ppm downfield of the isostructural W complex. Similar trends were noted for the $M(CO)_3(TriCN)^+$ system (M = Mn, Re) and have been observed in other isonitrile derivatives of the group VI carbonyls.[185]

To help establish the mononuclear nature of the cis-$M(CO)_4(L-L)$ complexes, their mass spectra were determined. In all cases, a + 1 parent ion of weak to medium intensity is observed, corresponding to the molecular weight of the mononuclear complex; no peaks at higher m/e values are seen. Additional peaks are observed for the loss of up to four CO ligands as well. The detection of a + 1 parent ion for $[Cr(CO)_5]_2(\mu\text{-DiNC})$ at m/e 648 establishes it as the expected binuclear complex. The analogous W complex shows ions corresponding to $[W(CO)_4DiNC]^+$ and $[W(CO)_6]^+$, apparently due to thermally-induced disproportionation during heating of the sample, and no signals assignable to dinuclear species. This process might be related to the partial decomposition of $Mo(CO)_4(CNR)_2$ complexes to $Mo(CO)_5(CNR)$ and $Mo(CO)_3(CNR)_3$ during heating in mass spectral investigations.[179]

It was hoped that chelating and bridged DiNC ligands could also be distinguished by ^1H NMR studies of the CH_2 groups in the ligand since such a method would provide a readily accessible evaluation of the ligand's binding mode. The CH_2 groups might be held in a significantly different chemical environment in the fairly rigid chelate than in the flexible bridging DiNC ligand. For the neutral Cr, Mo, and W complexes, as well as fac-$Mn(CO)_3(DiNC)Br$,[96] it is found that the chemical shifts of the CH_2 ligand are all at slightly higher field (0.07 - 0.10 ppm) than in free DiNC. In complexes containing the bridging DiNC ligand, however, the CH_2 chemical shifts are at the same, or slightly lower, field relative to free DiNC. This trend appears to be valid only for neutral complexes; charged complexes containing one chelating

DiNC or t-BuDiNC ligand, e.g. $CpFe(CO)(DiNC)^+$,[96] $CpFe(CS)(DiNC)^+$,[96] and $CpFe(CS)(t\text{-}BuDiNC)^+$ show CH_2 resonances at either higher or lower field than that of the free ligand in the same solvent.

b. Derivatives of iron and cobalt halides Like many isonitriles, DiNC and t-BuDiNC react with a variety of transition metal halides, giving isolable products in most cases. Kargol and Angelici[186] have reported previously the preparation of cis- and trans-$FeCl_2(DiNC)_2$, obtained by direct reaction between the diisocyanide and $FeCl_2$ in alcoholic solution. It is found that t-BuDiNC reacts with $FeCl_2$ in CH_3OH at room temperature after several minutes' time to give orange cis-$FeCl_2$-$(t\text{-}BuDiNC)_2$ as the only product, which is isolated from solution; (eq. XVIII). A small amount of the product also precipitates from the

$$FeCl_2 + 2\ t\text{-}BuDiNC \xrightarrow[25^\circ]{CH_3OH} \xrightarrow{Et_2O} cis\text{-}FeCl_2(t\text{-}BuDiNC)_2 \qquad (XVIII)$$

reaction. When carried out at -10°C, the reaction yields a very small amount of lavendar trans-$FeCl_2(t\text{-}BuDiNC)_2$ as an insoluble powder, with the orange cis complex being again the predominant product. These complexes are analogous to derivatives of monodentate isonitriles of the type cis- and trans- $FeCl_2(CNR)_4$, which have been the subjects of a number of investigations.[187-191] The complex cis-$FeCl_2(t\text{-}BuDiNC)_2$ is orange in color, as is often observed for the monodentate complexes. In $CHCl_3$ solution, ν(CN) bands at 2200 w, sh, 2154 s, and 2126 s, sh are observed, similar to those of cis-$FeCl_2(CN\text{-}p\text{-}anisyl)_4$[188] at 2196 w,

sh, 2160 vs, 2154, sh, and 2134 s; four infrared-active bands of $A_1(2)$, B_1, and B_2 symmetry are expected. The fourth band of cis-$FeCl_2$(t-BuDiNC)$_2$ is most likely hidden within the broad manifold below 2160 cm^{-1}.

In $CDCl_3$ solution, the ^1H NMR spectrum of cis-$FeCl_2$(t-BuDiNC)$_2$ shows a multiplet for the aromatic protons, a broad hump for the CH_2 protons, and two lines of equal intensity for the t-Bu groups. No change in the spectrum is observed upon heating to 80°C. A broad CH_2 peak was reported for the analogous complex cis-$FeCl_2$(DiNC)$_2$ by Kargol and Angelici.[186] It is due, most likely, to extensive coupling within the CH_2-CH_2 unit, which can be described as an ABCD spin system; each cis-$FeCl_2$(t-BuDiNC)$_2$ molecule exists as either a Λ or Δ enantiomer (Figure 15) having only C_2 symmetry and no two protons within the CH_2CH_2 unit

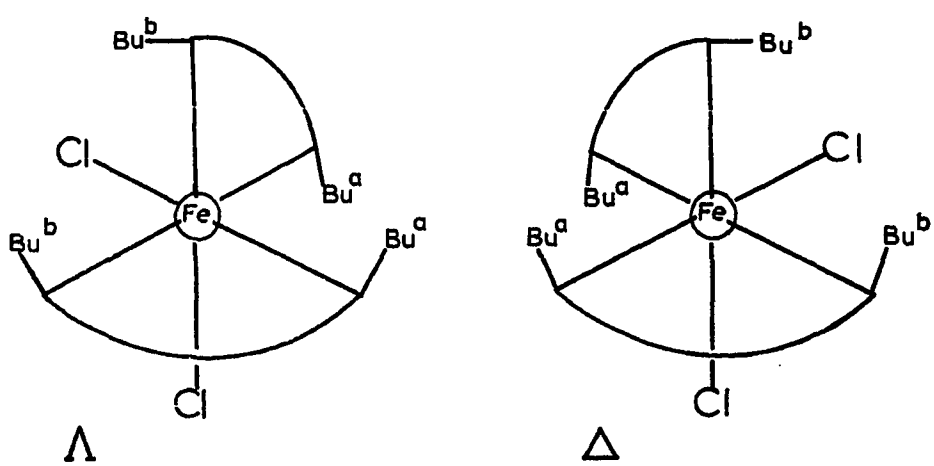

Figure 15. Schematic representations of Λ- and Δ- cis-$FeCl_2$(t-BuDiNC)$_2$

are chemical-shift equivalent. Similarly, there are two inequivalent sets of "inner" and "outer" t-Bu groups. The members of each pair are C_2-related and are labelled "a" and "b" in Figure 15.

The initially-isolated cis product is a fine orange powder, obtained by addition of ether to the reaction solution. Concentrated solutions of the product in $CHCl_3$ precipitate orange microcrystals having the same spectral characteristics as the powder. However, when this microcrystalline cis complex is dissolved in $CHCl_3$ or CH_2Cl_2, purple needles of the trans complex begin to form within several hours, (eq. XIX).

$$\underline{cis}\text{-}FeCl_2(t\text{-}BuDiNC)_2 \xrightarrow[(AlCl_3)]{CHCl_3 \text{ or } CH_2Cl_2} \underline{trans}\text{-}FeCl_2(t\text{-}BuDiNC)_2 \quad \text{(XIX)}$$

crystalline

The trans complex was also obtained in good yield after 10 days when a catalytic amount of $AlCl_3$ was added to a CH_2Cl_2 solution of the "crude" (powder) cis complex; isomerization of these crude samples was not observed otherwise. It has been suggested[189] for other $FeCl_2(CNR)_4$ systems that the stable but soluble cis form undergoes ionization in solution to a five-coordinate cation which can isomerize to the metastable, insoluble trans form (eq. XX). Certainly, the addition of

$$\underline{cis}\text{-}FeCl_2(CNR)_4 \rightleftharpoons [FeCl(CNR)_4]Cl \rightleftharpoons \underline{trans}\text{-}FeCl_2(CNR)_4 \quad \text{(XX)}$$

$AlCl_3$ would tend to generate this intermediate, and thus, promote the isomerization. It is not clear why some samples of cis-$FeCl_2$(t-BuDiNC)$_2$ isomerize more quickly than others, however. The cis-complex was not

sufficiently soluble in nitromethane or acetone to determine its conductivity. In CH_2Cl_2 solution, its conductivity was ca. 0.3 Ω^{-1} cm^2 mol^{-1}, which is essentially negligible. Conductivity studies on cis-$FeCl_2$(CN-p-tolyl)$_4$ in acetone and nitrobenzene showed this complex to undergo appreciable ionization involving ca. 50% and 13% of the material in solution for the respective solvents.[189]

The complex trans-$FeCl_2$(t-BuDiNC)$_2$ forms long lavender needles which appear to be deep purple when wet with solvent. It is virtually insoluble in most common solvents, though an orange (cis) solution can be obtained by allowing a crystal of the trans complex to stand in $CHCl_3$ for several days. The infrared spectrum of trans-$FeCl_2$(t-BuDiNC)$_2$ in the solid state exhibits a single, strong ν(CN) peak at 2146 cm^{-1}, as observed for trans-$FeCl_2$(CN-p-anisyl)$_4$ at 2144 cm^{-1};[188] a single band of E_u symmetry is expected for these D_{4h} complexes. In the low-frequency infrared spectrum of trans-$FeCl_2$(t-BuDiNC)$_2$, the ν(Fe-Cl) absorption is assigned to a band at 338.5 cm^{-1}. A nearby band at 356 cm^{-1} is ruled out because of its presence in the spectrum of isostructural trans-$CoBr_2$(t-BuDiNC)$_2$ (vide infra). Also, the ν(Fe-Cl) mode of trans-$FeCl_2$(CN-p-anisyl)$_4$ is observed at 324 cm^{-1}.[188] The low-frequency infrared spectrum of cis-$FeCl_2$(t-BuDiNC)$_2$ showed only very broad bands and the ν(FeCl) band(s) could not be assigned unambiguously in that case.

Dilute acetone solutions of t-BuDiNC (0.01 M) react with added $CoBr_2 \cdot 6H_2O$ to yield a fine, light green precipitate of trans-$CoBr_2$-(t-BuDiNC)$_2$, (eq. XXI). Much like trans-$FeCl_2$(t-BuDiNC)$_2$, the complex

$$CoBr_2 \cdot 6H_2O + 2\text{t-BuDiNC} \longrightarrow \text{trans-}CoBr_2(\text{t-BuDiNC})_2 \quad 78\% \qquad \text{(XXI)}$$

is only sparingly soluble in common organic solvents, and is totally insoluble in H_2O. A single, strong ν(CN) band is observed in its solid-state infrared spectrum at 2188 cm^{-1}, along with a weak shoulder of unknown origin at 2109 cm^{-1}. The assigned trans stereochemistry is also supported by the presence of a strong band at 158 cm^{-1}, which is assigned to the IR-allowed ν(Co-Br) mode of A_{2u} symmetry. The complex is similar to the previously reported trans-$CoBr_2(CNPh)_4$, which is also green in color and has a ν(CN) value of 2190 cm^{-1}.[192] Unlike trans-$FeCl_2$-(t-BuDiNC)$_2$ which is a diamagnetic, 18-electron complex, trans-$CoBr_2$-(t-BuDiNC)$_2$ is a 19-electron species and is presumably paramagnetic, though this was not verified experimentally. The addition of 1/2 mole of Br_2 to a suspension of one mole of trans-$CoBr_2$(t-BuDiNC)$_2$ rapidly yields a deep brown solution, presumably of the 18-electron Co(III) complex, trans-[$CoBr_2$(t-BuDiNC)$_2$]Br. Addition of one more mole of Br_2 leads to the precipitation of a deep red-brown microcrystalline substance which analyzes as $CoBr_5$(t-BuDiNC)$_2$, and is formulated as the Br_3^- salt, trans-[$CoBr_2$(t-BuDiNC)$_2$]Br_3 (eq. XXII). Similar oxidations of Co $X_2(CNR)_4$

$$\text{trans-}CoBr_2(\text{t-BuDiNC})_2 + 1.5\ Br_2 \longrightarrow \text{trans-}[CoBr_2(\text{t-BuDiNC})_2]Br_3 \quad 89\% \qquad \text{(XXII)}$$

derivatives containing monodentate isonitriles are known, but relatively little has been published on the subject.[143,193] The complex $[CoBr_2(CNPh)_4]Br$, prepared by bromine oxidation of $CoBr_2(CNPh)_4$, is reported[193] to be red-violet in color, and diamagnetic. Similarly, trans-$[CoBr_2(t\text{-}BuDiNC)_2]Br_3$ is diamagnetic and exhibits a single $\nu(CN)$ band at 2227 cm^{-1}, an increase of 39 cm^{-1} from the neutral Co(II) derivative. The single $\nu(CN)$ band supports the trans-assignment, as do the presence of sharp singlets for CH_2 and t-Bu protons in the ^1H NMR spectrum of the complex (see Table 23). That the complex is dissociated in solution as $[CoBr_2(t\text{-}BuDiNC)_2]^+$ and Br_3^- ions is supported by its molar conductance of 79.7 Ω^{-1} cm^2 mol^{-1} in CH_3NO_2. This value falls within the range of 75-95 Ω^{-1} cm^2 mol^{-1} expected for a 1:1 conductor.[108]

The simple Br^- salt, $[CoBr_2(t\text{-}BuDiNC)_2]Br$, could not be isolated in pure form. Attempts to obtain the compound by addition of Et_2O to Br_2-generated solutions of $[CoBr_2(t\text{-}BuDiNC)_2]Br$ led to the preferential precipitation of the Br_3^- salt instead. Attempts to metathesize the Br_3^- salt in an acetone/KPF_6/H_2O system gave a darker red-brown solid with $\nu(CN)$ values of 2184 m, 2115 w, indicative of a Co(II) product. A similar result is obtained with acetone/H_2O alone. The reductant in these cases may be H_2O itself, (yielding O_2 and HBr), or the isocyanide, to produce HBr and an isocyanate derived from t-BuDiNC.

The reaction between $CoCl_2 \cdot 6H_2O$ and 2 t-BuDiNC in acetone gives a pale green precipitate which looks much like trans-$CoBr_2(t\text{-}BuDiNC)_2$, with yields ranging from 86-98%. In the solid state, the complex has a

strong ν(CN) band at 2195 cm^{-1} and a weak shoulder at 2015 cm^{-1}, supporting a tentative formulation as trans-$CoCl_2$(t-BuDiNC)$_2$. An isostructural complex, trans-$CoCl_2$(CN-2,6-xylyl)$_4$, is reported to form under similar experimental conditions.[194] Elemental analysis of several samples, however, showed the products to have a formulation closer to $CoCl_2$(t-BuDiNC)$_2$·H_2O and the presence of H_2O in the samples is verified by a ν(OH) band at 3240 cm^{-1} (broad). This water is not removed to any appreciable extent by vacuum drying for 2 d at room temperature.

Sixteen-electron complexes of rhodium and iridium are quite common, and are often active catalysts for organic transformations such as olefin hydrogenation or hydroformylation. On the other hand, stable 16-electron cobalt complexes are rather scarce, but examples include $Co(PMe_3)_3X$,[195] $[Co(PMe_3)_4]BPh_4$,[195] and $Co(P\phi_3)_3Cl$.[196] It was thought that t-BuDiNC might be capable of stabilizing a coordinatively unsaturated cobalt(I) center such as [Co(t-Bu-DiNC)$_2$]X. More reasonably, the stabilization of a neutral, 18-electron Co(I) center such as Co(t-BuDiNC)$_2$-Cl might also be postulated. Neither has an analog in monodentate isonitrile chemistry. Unfortunately, no evidence could be obtained for the existence of any unsaturated species. The following paragraphs describe the course of the investigation, and its final results.

A number of coordinatively saturated, 18-electron cobalt(I) complexes of the general formula $[Co(CNR)_5]^+$ are known, and can be obtained by reactions of isocyanides with Co(II) salts in the presence of N_2H_4,[197] pyridine,[198] Zn,[199] or excess isocyanide.[143] In the chemistry of

t-BuDiNC, a structural analog would be $[Co_2(t\text{-}BuDiNC)_5]^{2+}$, in which one t-BuDiNC ligand is terminally bound to each of two $[Co(t\text{-}BuDiNC)_2]^+$ units. Reductions of $CoCl_2(t\text{-}BuDiNC)_2 \cdot H_2O$ with Zn/Hg or $N_2H_4 \cdot H_2O$ in CH_2Cl_2 or EtOH, respectively, give deep yellow solutions from which dirty yellow solids are isolated. Infrared spectra of the solids show bands at 2142-2150 s, sh and 2105-2112 vs, which are strongly suggestive of a $[Co(CNR)_5]^+$ structure having local D_{3h} symmetry (cf. $[Co(CN\text{-}p\text{-}tol)_5]^+$ 2148, 2105 cm^{-1}).[199] Only one band would be expected for either square-planar or tetrahedral $[Co(t\text{-}BuDiNC)_2]^+$, but two bands of A_1 and E symmetry would be consistent with a C_{4v} structure such as $Co(t\text{-}BuDiNC)_2Cl$. Reactions between cobalt(II) salts and t-BuDiNC in the presence of a reducing agent appear to yield the same product as that obtained by reduction of $CoCl_2(t\text{-}BuDiNC)_2 \cdot H_2O$. As detailed in section II.E.6, the reaction between $CoCl_2 \cdot 6H_2O$ and 2.5 mol of t-BuDiNC in EtOH in the presence of Zn dust, followed by metathesis with KPF_6, gives a yellow solid with IR bands at 2150 cm^{-1} s, sh and 2108 s. Elemental analysis supports the structure $[Co_2(t\text{-}BuDiNC)_5](PF_6)_2$. This is confirmed by conductivity measurements in CH_3NO_2, which reveal a molar conductance of 148 Ω^{-1} cm^2 mol^{-1} at a concentration of 1.03×10^{-3} M. In addition, a study of the conductivity over the concentration range 1.03×10^{-3} M to 2.08×10^{-5} M yields an Onsager plot[200] with a "B" value of 352, which is close to the typical value of ca. 400 for 2:1 electrolytes.[200]

Because of the chirality at each Co atom, the complex should exist as a mixture of up to six stereoisomers shown schematically in Figure 16.

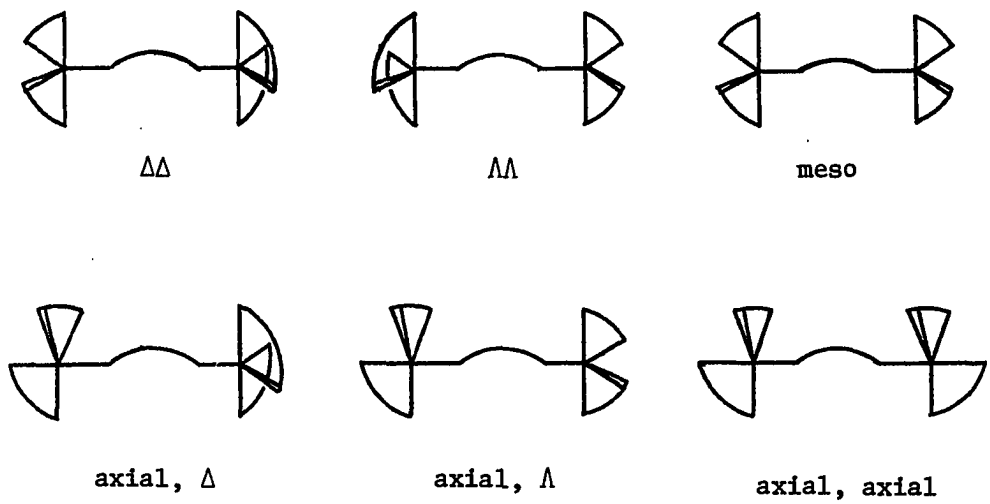

Figure 16. Possible stereoisomers of $[Co_2(t\text{-BuDiNC})_5]^{2+}$

The ^1H NMR spectrum of $[Co_2(t\text{-BuDiNC})_5](PF_6)_2$ exhibits two CH_2CH_2 resonances at 4.51 and 4.15 ppm in a ratio of 4:1, respectively. The t-butyl group resonance also appears as two lines at 1.24 and 1.16 ppm, again in a ratio of approximately 4:1, respectively. These observations are consistent with the proposed structure(s) if the upfield CH_2CH_2 and t-Bu resonances are assigned to the bridging t-BuDiNC. Regarding the stereochemical rigidity of the complex, it seems that at room temperature in solution, the t-BuDiNC ligands undergo a relatively rapid intramolecular exchange. Two things suggest this. First, each CH_2CH_2 resonance is observed as a relatively sharp singlet, whereas a very broad resonance is observed for <u>cis</u>-$FeCl_2$(t-BuDiNC), which is stereochemically

similar to the $Co(t\text{-}BuDiNC)_2$ unit and is non-fluxional. If $[Co_2(t\text{-}BuDiNC)_5]^{2+}$ was not fluxional, one would certainly expect to observe more complex CH_2 resonances due to spin-spin coupling (as with the iron complex) and the presence of up to six diastereomers. Also, it is known that other pentakis (isonitrile) cobalt(I) complexes are stereochemically non-rigid. For example, $[Co(t\text{-}BuNC)_5]PF_6$ exhibits a temperature-dependent ^1H NMR spectrum consisting of a single resonance at ambient temperature and two resonances of unequal intensity at -30°C or below, due to intramolecular exchange of t-BuNC ligands.[201] Similarly, $[Co(CN\text{-}p\text{-}tolyl)_5]ClO_4$ exhibits one methyl signal at room temperature.[198] These observations suggest that the separation of the many stereoisomers of $[Co_2(t\text{-}BuDiNC)_5](PF_6)_2$ would be impossible at room temperature.

c. Nickel and copper complexes Isonitrile complexes of zerovalent nickel have been known for over 30 years, having been first prepared by Hieber and Böckly[202] and Klages and Mönkemeyer[203] through reactions of aromatic isonitriles with $Ni(CO)_4$. The products from such reactions possess the general formulae $Ni(CO)_{4-n}(CNAr)_n$ (n = 1-4). Tetrakis (isonitrile) nickel complexes have also been obtained via the reaction of isonitriles with $Ni(COD)_2$,[204,205] Cp_2Ni,[206] or via equation XXIII.[207] Zerovalent

$$K_4[Ni_2(CN)_6] + 4\ RNC \xrightarrow{NH_3} K_2[Ni(CN)_4] + Ni(CNR)_4 + 2\ KCN \quad (XXIII)$$

nickel clusters such as $Ni_4(CN\text{-}t\text{-}Bu)_7$, $Ni_8(CN\text{-}i\text{-}pr)_{12}$ and $Ni_4(CNCH_2Ph)_4$ have been obtained by reactions between isonitriles and $Ni(COD)_2$;[205] $Ni_4(CN\text{-}t\text{-}Bu)_7$ has been shown to be an effective catalyst precursor for

oligomerization of acetylenes and dienes, and for the hydrogenation of acetylenes, nitriles, and isonitriles.[205,208] In view of the often rapid polymerization of isonitriles by Ni(II) salts,[143,209] stable derivatives of divalent nickel are rather uncommon, and include $NiCl_2(EtOH)(CN\text{-}t\text{-}Bu)$,[210] $[Ni(CN\text{-}t\text{-}Bu)_4](ClO_4)$,[211] $[Ni(CNMe)_4](PF_6)_2$,[212] $[NiX(DMB)_4](PF_6)_3$ (X = Cl, Br; DMB = 1,8-diisocyanomenthane),[60] $NiI_2(CN\text{-}t\text{-}Bu)_2$[204] and several others.[213,214]

All the complexes of DiNC and t-BuDiNC discussed heretofore employ the diisonitrile as a bridging ligand, or as a ligand which chelates to a pseudooctahedral metal center to form complexes in which the C-M-C angle is nearly 90°. The latter mode is that for which these ligands were specifically designed. Molecular models have suggested that chelation of DiNC (or t-BuDiNC) to a pseudotetrahedral metal, where the C-M-C angles would be roughly 109°, is much less favorable. Indeed, space-filling models having normal bond lengths and angles will come together to form a chelate ring only with great difficulty. The following studies with zerovalent nickel and Cu(I) (vide supra) were undertaken to determine whether the diisonitriles DiNC and t-BuDiNC can form chelate rings at tetrahedral metal centers, and if so, what effects this would have upon the spectroscopic and physical properties of the complexes.

The reaction between equimolar amounts of $Ni(CO)_4$ and DiNC (or t-BuDiNC) in CH_2Cl_2 solution is complete after ca. 1 h, and produces the products $Ni(CO)_2(DINC)$ or $Ni(CO)_2(t\text{-}BuDiNC)$ (eqs. XXIV, XXV).

$$Ni(CO)_4 + DiNC \longrightarrow Ni(CO)_2(DiNC) + 2\ CO \qquad (XXIV)$$

$$Ni(CO)_4 + t\text{-}BuDiNC \longrightarrow Ni(CO)_2(t\text{-}BuDiNC) + 2\ CO \qquad (XXV)$$

In the case of $Ni(CO)_2(DiNC)$, the product is isolated in 44% by filtering the precipitated product from the reaction mixture. The $Ni(CO)_2(t\text{-}BuDiNC)$ product is isolated in 61% yield after addition of hexane to the near-dry reaction residue. Both are pale yellow solids which are slightly air-sensitive in the solid state, and much more so in solution. The compositions of these two isostructural complexes are supported by elemental analysis. Two structures, 34 and 35, are possible.

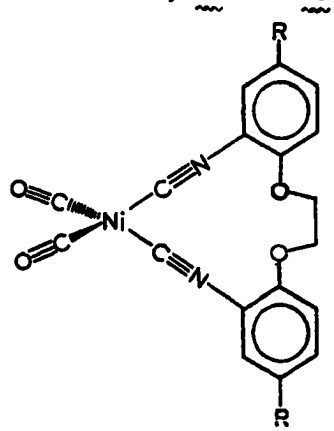

34

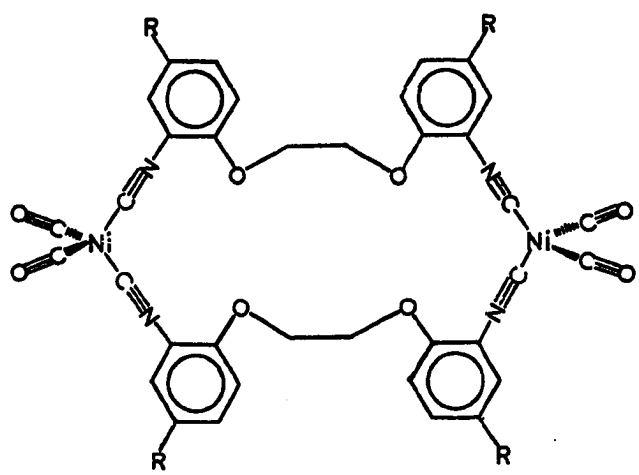

35

The mononuclear structure 34 contains the chelated DiNC (or t-BuDiNC) ligand, while structure 35 shows the diisonitriles functioning as bridging ligands. The infrared spectra of the two complexes are quite similar to one another, showing two ν(CN) absorptions at 2146 and 2092 cm^{-1} (DiNC complex) or 2145 and 2094 cm^{-1} (t-BuDiNC complex) and two ν(CO) bands at 2014 and 1972 or 2014 and 1975 cm^{-1} in $CHCl_3$ solution. The IR band positions of these complexes are close to those for $Ni(CO)_2$-$(CNPh)_2$ in $CHCl_3$, observed at 2146, 2095, 2018, and 1976 cm^{-1} by Bigorgne,[175] and at 2142, 2085, 2016, and 1963 cm^{-1} by van Hecke and Horrocks.[215] The IR data observed for the DiNC and t-BuDiNC complexes are certainly consistent with their proposed formulations, but still cannot distinguish between structures 34 and 35. Unfortunately, both complexes decompose at *ca.* 140°C and as a result, their mass spectra showed no fragments which contained both Ni and the ligand. However, a vapor pressure osmometric study of $Ni(CO)_2$(t-BuDiNC) in 1,2-dichloroethane at concentrations of 0.01 - 0.02 M yielded an experimental molecular weight of 475 g mol^{-1}, compared wih the theoretical value of 491.2 g mol^{-1} for mononuclear $Ni(CO)_2$(t-BuDiNC). Thus, the t-BuDiNC complex is certainly mononuclear in solution and by analogy, $Ni(CO)_2$(DiNC) is presumed to be mononuclear as well. The positions of the CH_2 resonances in the ^1H NMR spectra of these complexes fit in with the trend outlined in section III.5.a for other zerovalent complexes; these resonances are observed at positions 0.10 and 0.12 ppm lower (i.e. toward higher field) than are the CH_2 resonances of DiNC and t-BuDiNC, respectively, in the same solvents. This high field shift is consistent

with the proposed chelate structure 34. The ^{13}C NMR spectrum of $Ni(CO)_2$(t-BuDiNC) clearly shows resonances assignable to coordinated CO (197.8 ppm) and the isocyano group (166.4 ppm), as well as signals assignable to the nine other ligand resonances (Table 24). Interestingly, the CO and CN resonances are at considerably higher field in $Ni(CO)_2$-(t-BuDiNC) than in cis-$Cr(CO)_4$(t-BuDiNC) (cf. CO: 220, 217 ppm; CN: 182 ppm), despite the fact that the ν(CN) values of the two complexes are nearly coincident. Others have attempted to make such correlations between ν(CN) or ν(CO) and the corresponding ^{13}C NMR chemical shifts, but the nature of the metal has a large effect which is not fully understood.[185]

The reaction between t-BuDiNC and $Ni(CO)_4$ in a 2:1 molar ratio leads to the formation of a yellow complex, presumably $Ni(t\text{-}BuDiNC)_2$, in 90% yield, (eq. XXVI). This product is obtained also upon Na/Hg reduction

$$Ni(CO)_4 + 2\ t\text{-}BuDiNC \longrightarrow Ni(t\text{-}BuDiNC)_2 + 4CO \qquad \text{(XXVI)}$$

of $[Ni(t\text{-}BuDiNC)_2](BF_4)_2$ (vide infra) and by reaction of t-BuDiNC with $Ni(CO)_2$(t-BuDiNC). In the solid state, the compound exhibits a strong, broad ν(CN) band at 2020 cm^{-1} (Figure 17). In $CHCl_3$ solution, the band is shifted to 2040 cm^{-1} and a weak shoulder of unknown origin is observed at 2160 cm^{-1}. Cotton and Zingales[178] have reported bands for the monodentate analog, $Ni(CNPh)_4$, at 2050 (s) and 1990 (s) cm^{-1}; Bigorgne[175] gives the values 2136 (w), 2045 (s), 2019 (m), and 1993 (m) cm^{-1} in $CHCl_3$ and 2029 (s), 2013 (s, sh), and 1988 (m, sh) cm^{-1} in the solid state.

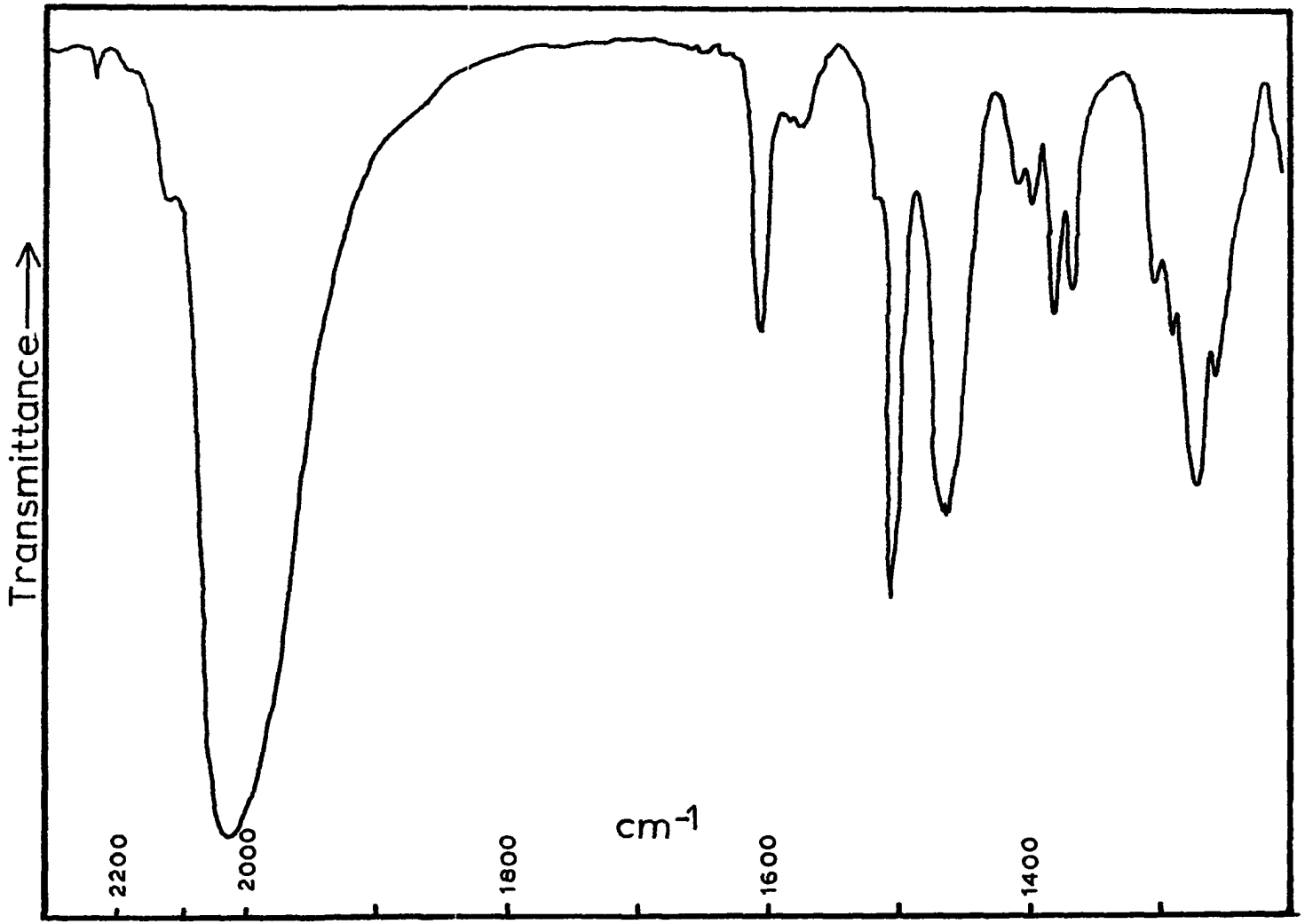

Figure 17. Infrared spectrum of $Ni(t\text{-}BuDiNC)_2$ between 2300 cm^{-1} and 1200 cm^{-1} in Nujol mull

According to Cotton and Zingales[178] the "extra" bands might arise as a result of distortion away from ideal T_d symmetry, due to bending of the C-N-C unit. However, $Cr(CNPh)_6$, for which this argument was also made, has been shown to have essentially linear C-N-C linkages by an X-ray crystallographic study,[216] and it is debatable whether Cotton's argument obtains in either case. Whatever the explanation, $Ni(t\text{-}BuDiNC)_2$ has only one major ν(CN) band, as would be expected for a complex having local T_d symmetry. Significant distortions from T_d toward C_{2v} symmetry should complicate the spectrum somewhat, since four infrared-active ν(CN) bands ($2A_1$, B_1, and B_2) are expected for molecules of C_{2v} symmetry.

The proton NMR spectrum of $Ni(t\text{-}BuDiNC)_2$ is very much like that of $Ni(CO)_2(t\text{-}BuDiNC)$ (Table 23). The ligand CH_2 group resonates at 4.35 ppm, very close to the value of 4.36 ppm for the dicarbonyl derivative. As with the dicarbonyls, this relatively high-field resonance is consistent with the presence of chelating t-BuDiNC ligands as shown in 36.

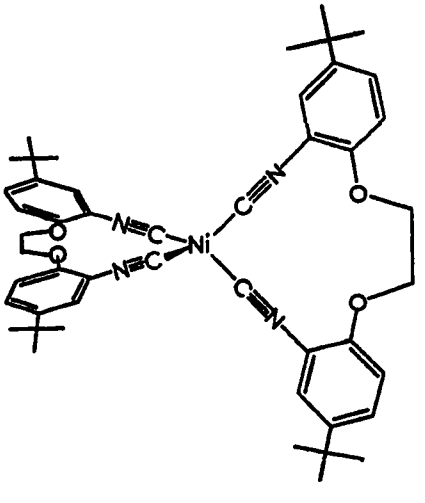

36

Like its dicarbonyl analog, $Ni(t\text{-}BuDiNC)_2$ decomposes thermally upon heating. Its decomposition point of ca. 120°C is 20°C lower than that of $Ni(CO)_2(t\text{-}BuDiNC)$. In contrast, $Ni(CNPh)_4$ melts without decomposition at 202-204°C.[203] It may be that the strained t-BuDiNC chelate rings facilitate the thermal cleavage of the Ni-C bonds and open the way to further decomposition of the complex. The mass spectrum of the compound shows fragments at m/e values as high as 605, but none in the region of the expected molecular ion around m/e 810. The most prominent peaks in the mass spectrum appear to result from reaction of t-BuDiNC with O_2 to give the diisocyanate (m/e 408, v. low intensity) which loses fragments such as NC(→ m/e 382, 5.2%), CO(→ m/e 364, 5.3%), and N_2C_2(→ m/e 356, 7.0%). The base peak in the mass spectrum is at m/e 191, probably corresponding to the fragment $[C_6H_3(t\text{-}Bu)(OH)(NCO)]^+$. Elemental analysis of $Ni(t\text{-}BuDiNC)_2$ would also be consistent with the presence of some oxygen in the sample, as the observed %C is somewhat lower than expected, vis. 69.91 obs. vs. 71.03 calc'd. Also in support of this idea is the known catalytic oxidation of isonitriles to isocyanates by $Ni(CNR)_4$ and $Ni(C_8H_{12})_2$.[217]

As pointed out earlier, there exist relatively few stable complexes containing isonitriles coordinated to divalent nickel. It seemed quite possible that $[Ni(t\text{-}BuDiNC)_2]^{2+}$ might be more stable toward isonitrile polymerization than would complexes containing monodentate isonitriles. The addition of solid $Ni(BF_4)_2 \cdot 6H_2O$ to a CH_3OH solution of t-BuDiNC causes the immediate precipitation of impure yellow-brown

$[Ni(t\text{-}BuDiNC)_2](BF_4)_2$ in yields of 25-40%. A similar result is obtained when solid t-BuDiNC is added to the Ni(II) solution, or if an EtOH solution of $(Et_4N)_2NiCl_4$[218] is treated with an EtOH solution of t-BuDiNC and KPF_6. The BF_4^- salt has ν(NC) at 2234 cm^{-1}, m, and 2190 cm^{-1}, w, sh in Nujol mull, and the following ^1H NMR spectrum (CD_3CN): ArH, 7.86 - 7.25, m; CH_2, 4.51, s; t-Bu, 1.34 s. Elemental analysis, however, shows the product to be impure, and the high values of carbon, hydrogen, and nitrogen are consistent with a formulation closer to $Ni(t\text{-}BuDiNC)_{2.5}(BF_4)_2$. The excess ligand might be incorporated as the polymer $(t\text{-}BuDiNC)_x$ or as coordinated t-BuDiNC oligomers of some kind. The presence of a weak, broad manifold in the IR spectrum between 1700 and 1600 cm^{-1} might be assignable to the C=N stretches of the alkylimino units resulting from isonitrile oligomerization. Such bands are seen in IR spectra of polymers of isonitriles[209] and for mononuclear complexes containing oligomers of t-butylisonitrile, 37 and 38, generated by the addition of

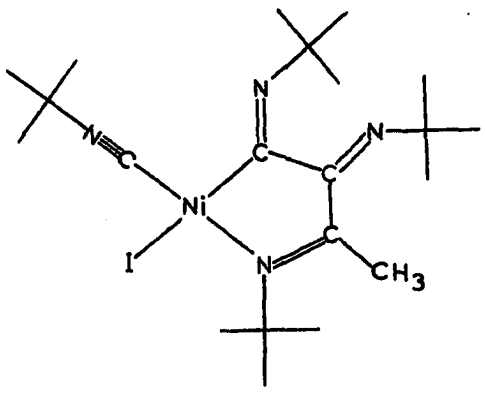

37

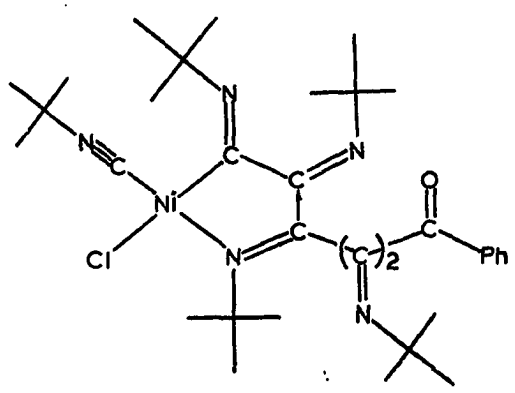

38

CH_3I or PhCOCl to $Ni(CN\text{-}t\text{-}Bu)_4$.[219] On the other hand, ^1H NMR spectra of $[Ni(t\text{-}BuDiNC)_2]^{2+}$ samples exhibit single resonances for the t-BuDiNC CH_2 and t-butyl protons, rather than more complicated patterns which would be expected if oligomers or soluble polymers of the ligand were present.

It is possible to reduce $[Ni(t\text{-}BuDiNC)_2](BF_4)_2$ to $Ni(t\text{-}BuDiNC)_2$ with 1% sodium amalgam in THF solution (eq. XXVII). The reaction takes

$$[Ni(t\text{-}BuDiNC)_2](BF_4) \xrightarrow{Na/Hg} Ni(t\text{-}BuDiNC)_2 + 2\ NaBF_4 \qquad \text{(XXVII)}$$

approximately 1 h and produces the desired compound in yields of 60-74%, along with a deep green impurity which is removed from the filtered, dry reaction residue by extraction with Et_2O. The product has spectroscopic properties (IR and NMR) identical to that of $Ni(t\text{-}BuDiNC)_2$ synthesized from $Ni(CO)_4$. This reaction appears to be the first example of the reduction of a homoleptic Ni(II) salt to its Ni(0) analog, though reductions of Ni(II) salts with hydrazine in the presence isonitriles have led to $Ni(CNR)_4$ compounds.[143]

Copper complexes of isonitriles form an interesting class of compounds. Derivatives of Cu(I) salts exhibit a variety of stoichiometries and coordination numbers, as represented by this series of stable complexes: $Cu(RNC)Cl$, $Cu(RNC)_2Cl$, $Cu(RNC)_3Cl$ and $[Cu(RNC)_4]Cl$ where R = p-tolyl,[220] and a similar series involving p-anisylisonitrile.[221] Two oxidation states are available to such complexes, as in the pair

$[Cu(CN\text{-}t\text{-}Bu)_4(H_2O)_2](ClO_4)_2$ and $[Cu(CN\text{-}t\text{-}Bu)_4]ClO_4$,[222] though the Cu(II) compounds are certainly less common. In addition, Cu(I)/isonitrile systems can be active catalysts for a variety of organic chemical transformations which includes the α-addition of alcohols to isonitriles,[142] the cyclization of α-hydrogen-containing isonitriles with α,β-unsaturated carbonyl and nitrile compounds,[223] olefin dimerization,[224] and the condensation of cyclopentadiene or indene with carbonyl compounds to yield substituted fulvenes and alkylideneindenes.[225] The present interest in derivatives of Cu(I) is not so much concerned with their reactivities but rather with their structures.

Displacement of the labile acetonitrile ligands from $[Cu(CH_3CN)_4]BF_4$[94] by two t-BuDiNC ligands takes place readily at room temperature over a period of 30 min, giving $[Cu(t\text{-}BuDiNC)_2]BF_4$ in 68% yield (eq. XXVIII).

$$[Cu(CH_3CN)_4]BF_4 + 2\ t\text{-}BuDiNC \longrightarrow [Cu(t\text{-}BuDiNC)_2]BF_4 + 4\ CH_3CN \qquad \text{(XXVIII)}$$

The formulation of the complex is supported by a molar conductance of 84 Ω^{-1} cm^2 mol^{-1} and by elemental analysis (Table 21). The isoelectronic complex $[Cu(CNCH_3)_4]BF_4$ has been recently subjected to an X-ray crystallographic study, showing the molecule to possess tetrahedral symmetry.[226] By analogy, the t-BuDiNC complex is expected to have near-tetrahedral symmetry at the Cu center. Two limiting structures of $[Cu(t\text{-}BuDiNC)_2]BF_4$ would be the bis-chelated form 39 or the polymeric form

40. The latter would be expected to be less soluble than the mononuclear

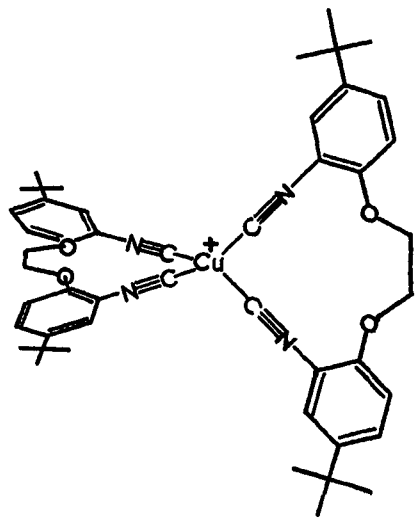

39

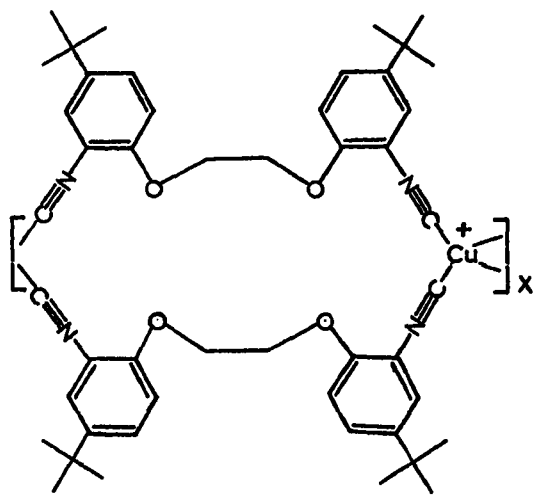

40

complex. In fact, the isolated complex is quite soluble in solvents such as CH_2Cl_2 and $CHCl_3$, suggesting it to be mononuclear. Its infrared spectra contain a single, symmetric ν(CN) band at 2169 cm^{-1} in $CHCl_3$

and 2165 cm^{-1} in Nujol Mull (Figure 18), similar to the ν(CN) absorption of the mononuclear analog $[Cu(CN\text{-}p\text{-anisyl})_4]PF_6$, at 2169 cm^{-1}.[221] That only one ν(CN) band is observed in solution indicates that $[Cu(t\text{-}BuDiNC)_2]^+$ undergoes little, if any, dissociation to complexes of lower coordination number, and as with $Ni(t\text{-}BuDiNC)_2$, indicates that there is little distortion of the local symmetry toward C_{2v}. Comparison of the infrared spectra of the isoelectronic and presumably isostructural complexes $Ni(t\text{-}BuDiNC)_2$ (Figure 17) and $[Cu(t\text{-}BuDiNC)_2]BF_4$ (Figure 18) shows several interesting trends. The frequency difference between the ν(CN) values (2020 cm^{-1} vs. 2165 cm^{-1}) in the two complexes is 145 cm^{-1}. The higher ν(CN) in the Cu(I) complex reflects the greater importance of σ-donation vs. π-acceptance in this complex relative to the zerovalent Ni analog. Also to be noted is the much greater integrated intensity of the ν(CN) band in $Ni(t\text{-}BuDiNC)_2$, as indicated qualitatively by its higher linear intensity with respect to other bands in the spectrum, and the larger band width. Reflected in the integrated intensity is the degree of π-backbonding from the metal to the ligand π^* orbitals; from the intensities in these cases, it is again obvious that there is more back-bonding in the Ni(0) complex than in the Cu(I) complex, as would be expected in comparing a neutral molecule to a cationic one. The integrated intensities of other homoleptic t-BuDiNC complexes are discussed in greater depth in the following section.

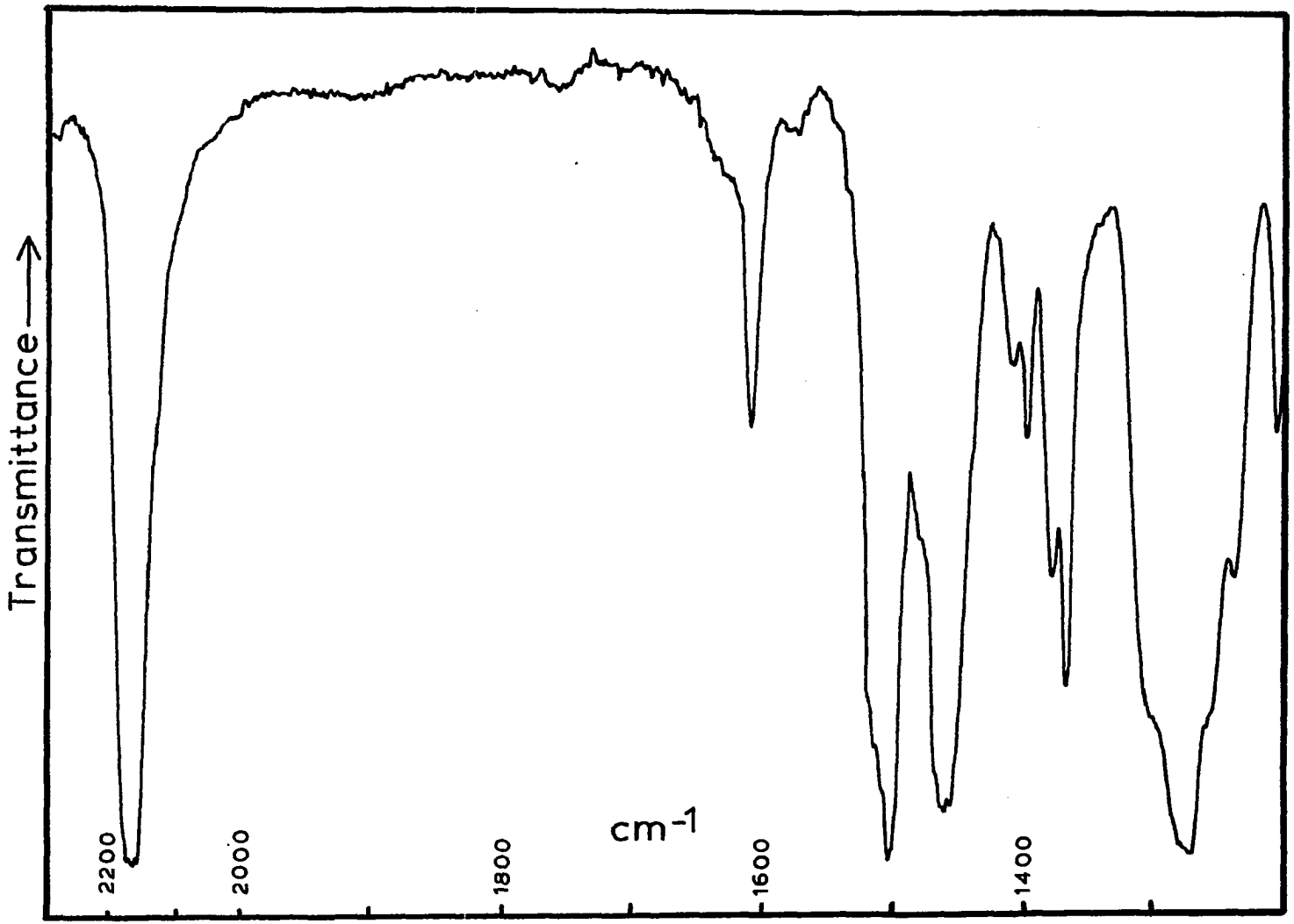

Figure 18. Infrared spectrum of $[Cu(t\text{-}BuDiNC)_2]BF_4$ between 2300 cm^{-1} and 1200 cm^{-1} in Nujol mull

The proton NMR spectrum of $[Cu(t\text{-}BuDiNC)_2]BF_4$ in CD_2Cl_2 solution consists of a multiplet of aromatic protons at 7.61 - 7.15 ppm, a sharp CH_2 singlet at 4.50 ppm, and a sharp t-Bu singlet at 1.30 ppm. That the CH_2 signal comes at lower field in this compound than in $Ni(t\text{-}BuDiNC)_2$ (4.35 ppm) reflects the charge on the Cu(I) complex, much as the cationic chelate complexes $[CpFe(CX)(L\text{-}L)]^+$ (X = O, S; L-L = DiNC, t-BuDiNC) show lower-field CH_2 signals than neutral chelate complexes (vide supra).

d. Homoleptic six-coordinate t-BuDiNC complexes Homoleptic isonitrile complexes, $[M(CNR)_{6\ or\ 7}]^{Z+}$, have received a good deal of attention in the recent literature. Such compounds, most notably those of the Cr group, exhibit interesting electrochemical,[227-233] spectroscopic[107,147] and photochemical[234-236] behavior. Hexakis(arylisonitrile) complexes of Cr, Mo, and W show activity as initiators of free radical polymerization of methyl methacrylate in the presence of CCl_4,[237] and upon reaction with AlR_3, certain chromium complexes form Ziegler-Natta type catalysts for the production of isotactic and/or syndiotactic poly-1,2-butadienes.[238] All told, there exists a wide variety of homoleptic six- and seven-coordinate complexes containing metals of the V, Cr, Mn, and Fe groups. Table 31 includes a listing of such compounds and their methods of synthesis.

As can be seen in Table 31, the group VI metals form the largest class of homoleptic six- and seven-coordinate isonitrile complexes. Variations in oxidation state, electron count, and the number and nature (alkyl or aryl) of the isonitriles are all factors which contribute

Table 31. Homoleptic six- and seven-coordinate isonitrile complexes

Compound Type	Electron Count	Mode of Synthesis	Comments	Reference
$[V(CNR)_6]^{2+}$	15	VCl_3 + xcs RNC $[V(CO)_6]^-$ + xcs RNC + $PhICl_2$	R=t-Bu	239, 240
$Cr(CNAr)_6$	18	$Cr_2(OAc)_4 \cdot 2H_2O$ + ArNC	Ar=phenyl, substituted phenyl	227, 228, 241
"	"	$Cr(CO)_6$ + PhNC	PdO catalyst required	182
$[Cr(CNAr)_6]^{+,2+}$	17, 16	Ag^+ oxidation of $Cr(ArNC)_6$	Ar=phenyl, substituted phenyl	229
$Cr(CNR)_6$	18	$Cr_2(C_8H_8)_3$ + RNC	R=t-Bu	242
"	"	$Cr(i\text{-}pr)_4$ + RNC	R=n-Bu, Cy	243
$[Cr(CNR)_6]^{2+}$	16	$CrCl_2$ + RNC	R=t-Bu, Cy	230
$[Cr(CNR)_7]^{2+}$	18	$[Cr(CNR)_6]^{2+}$ + RNC(neat)	R=t-Bu, Cy	230
$M(CNAr)_6$	18	reduction of $MoCl_3$ or WCl_6 in presence of ArNC	M=Mo, W, Ar=phenyl, substituted phenyl	244, 245
$Mo(CNAr)_6$	18	$Mo_2(OAc)_4$ + ArNC	Ar=Ph	107

Table 31. Continued

Compound Type	Electron Count	Mode of Synthesis	Comments	Reference
$W(CNAr)_6$	18	ArNC + $W_2(dmhp)_4$[a] ArNC + $W_2(mhp)_4$[b]	Ar=Ph	246
$[M(CNAr)_7]^{2+}$	18	Ag^+ oxidation of $M(CNAr)_6$	Ar=Ph, M=Mo, W	246
$[M(CNR)_7]^{2+}$	18	$M(CO)_3(CNR)_3$ + CNR + $PhICl_2$	M=Mo, W, R=t-Bu, Cy	247
$[Mo(CNR)_7]^{2+}$	18	RNC + $K_4Mo_2Cl_8$ RNC + $Mo_2(OAc)_4$	R=Me, t-Bu, Cy	248
$[W(CNR)_7]^{2+}$	18	RNC + $W_2(mhp)_4$[b]	R=t-Bu, Cy	249
$[Mn(CNAr)_6]^+$	18	xcs ArNC + MnI_2	R=Ph, substituted Ph	250
"	"	ArNC + $Mn(CO)_5X$	X=Cl, Br, Ar=Ph, substituted Ph	231, 251
$[Mn(CNAr)_6]^{2+}$	17	$[Mn(CNAr)_6]^+$ + HNO_3(or Br_2)	Ar=Ph, substituted Ph	147, 252, 253

[a]dmhp is the anion of 2,4-dimethyl-6-hydroxypyrimidine.

[b]mhp is the anion of 2-hydroxy-6-methylpyridine.

Table 31. Continued

Compound Type	Electron Count	Mode of Synthesis	Comments	Reference
$[Mn(CNR)_6]^+$	18	$RNC + MnI_2$	R=Me, Et, Cy, Bz	147, 252, 253
$[Mn(CNR)_6]^{2+}$	17	$[Mn(CNR)_6]^+ + HNO_3$	R=Me, Et, Cy, Bz	147, 253, 254
$[Re(CNR)_6]^+$	18	xcs $RNC + ReI_3$	R=Et, p-tolyl	255
$[Re(CNAr)_6]^+$	18	xcs $ArNC + Re(CO)_5Br$	Ar=p-tdyl	256
$[Re(CNR)_6]^+$	18	$RNC + Re_2(OAc)_4Cl_2$	R=t-Bu	257, 258
$[Fe(CNAr)_6]^{2+}$	18	xcs $ArNC + Fe(ClO_4)_2$	Ar=p-tolyl, 2% yield	189
$[Fe(NCR)_6]^{2+}$	18	$Ag_4[Fe(CN)_6]$ + xcs RI $K_4[Fe(CN)_6] + Me_2SO_4$ (or RX)	R=Me, Et, Bz	259-261
$[Ru(CNR)_6]^{2+}$	18	$K_4[Ru(CN)_6] + (CH_3O)_2SO_2$	R=Me	262
"	"	$K_4[Ru(CN)_6] + (CH_3)_3OBF_4$ + acetone	R= 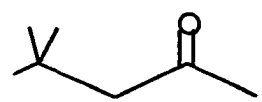	263

to the large number of known compounds. A relatively limited number of manganese complexes is known, all having six (never seven) ligands and existing in the mono- or divalent state. While hexakis (alkylisonitrile)iron(II) complexes are relatively abundant (a result of rather simple synthetic methodologies), only a single aromatic isonitrile derivative is known, and this is prepared in quite low yield from the reaction of neat p-tolylisonitrile with $Fe(ClO_4)_2$. Thus, there do exist stable d^6, 18-electron, homoleptic aromatic isonitrile complexes of Cr(0), Mn(I), and Fe(II), but no examples of either alkyl or aryl isonitrile analogs of Co(III) are known. The goal of the following research was to prepare a series of d^6 homoleptic complexes of the general formula $[M(t\text{-BuDiNC})_3]^{Z+}$ for M = Cr; Z = 0 through M = Co; Z = 3. Such a series encompasses metals in four different oxidation states and provides a number of interesting comparisons in the spectroscopic (IR, UV-Vis, ^1H NMR), chemical, and electrochemical properties within the series and with respect to known monodentate analogs.

The first member of the series, $Cr(t\text{-BuDiNC})_3$, 41, is prepared most conveniently by reducing a mixture of $CrCl_3(THF)_3$ and t-BuDiNC in THF solution with 1% sodium amalgam (eq. XXIX); the reaction is complete in

$$CrCl_3(THF)_3 + 3\ t\text{-BuDiNC} \xrightarrow{Na/Hg} Cr(t\text{-BuDiNC})_3 + 3\ NaCl \qquad (XXIX)$$

30 min. After centrifugation of the blood-red solution to remove the NaCl by-product, the solvent is evaporated to give the analytically pure product in 65% (isolated)yield. Interestingly, the product can also be obtained, albeit in low yield (27%), by the photolysis of a solution of

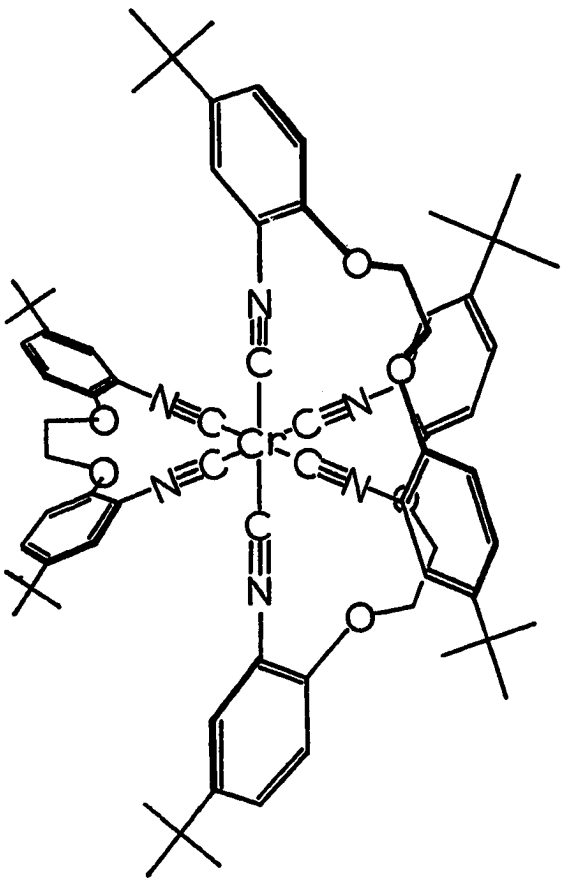

41

$Cr(CO)_6$ and t-BuDiNC in Et_2O at 254 nm for ca. 48 h. A large amount of insoluble orange material is produced in this reaction as well. There are relatively few ligands which will form homoleptic complexes through the photolysis of $Cr(CO)_6$; these include $CH_3N(PF_2)_2$, n-$PrOPF_2$, and $(MeO)_2$-PF.[264a] The "classical" synthesis of $Cr(CNAr)_6$ complexes is carried out by addition of an excess of isonitrile to a suspension of $Cr_2(OAc)_4 \cdot 2H_2O$

in an alcohol solvent.[227,228,241] While both DiNC and t-BuDiNC undergo rapid reactions with $Cr_2(OAc)_4 \cdot 2H_2O$, no pure samples of $Cr(DiNC)_3$ or $Cr(t\text{-}BuDiNC)_3$ have been obtained by this method; these reaction mixtures typically contain Cr(0) and Cr(I) products, free ligand, and other Cr salts. Thus, the use of $Cr_2(OAc)_4 \cdot 2H_2O$ appears to be far less satisfactory than the method employing $CrCl_3$, Na/Hg, and t-BuDiNC.

In the solid state, $Cr(t\text{-}BuDiNC)_3$ (ν(CN) 1940 cm^{-1}) reacts slowly with atmospheric oxygen to yield $[Cr(t\text{-}BuDiNC)_3]^+$ $(anion)^-$, identified by its $\tilde{\nu}$(CN) band in the infrared spectrum at ca. 2050 cm^{-1}. This oxidation is much more rapid in solution. The 17-electron Cr(I) complex $[Cr(t\text{-}BuDiNC)_3]PF_6$ can be prepared independently in 62% yield by the method of Treichel and Essenmacher[229] through the reaction of $AgPF_6$ with the zerovalent complex. Two equivalents of $AgPF_6$ produce the 16-electron Cr(II) species (ν(CN) 2153 cm^{-1}) in high yield. Both reactions are well-established for a large number of $Cr(CNAr)_6$ complexes.[229] A species presumed to be the 15-electron trication, $[Cr(t\text{-}BuDiNC)_3]^{3+}$, is generated chemically by the addition of $SbCl_5$ to a CH_2Cl_2 solution of $Cr(t\text{-}BuDiNC)_3$ at -20°C.[264b] Infrared spectra of such solutions show a single ν(CN) band at 2206 cm^{-1}.

Infrared spectra of pure $Cr(t\text{-}BuDiNC)_3$ samples in CH_2Cl_2 solution exhibit a broad, nearly symmetrical band at 1956 cm^{-1} assignable to the T_{1u} ν(NC) mode (see Figure 19). A very weak hump at ca. 2100 cm^{-1} might be due to a mode of disallowed symmetry; the peak at ca. 2125 cm^{-1} in Figure 19 could be due to a small amount of free t-BuDiNC. In contrast to the one major ν(CN) band observed for $Cr(t\text{-}BuDiNC)_3$, $Cr(CNPh)_6$ and related

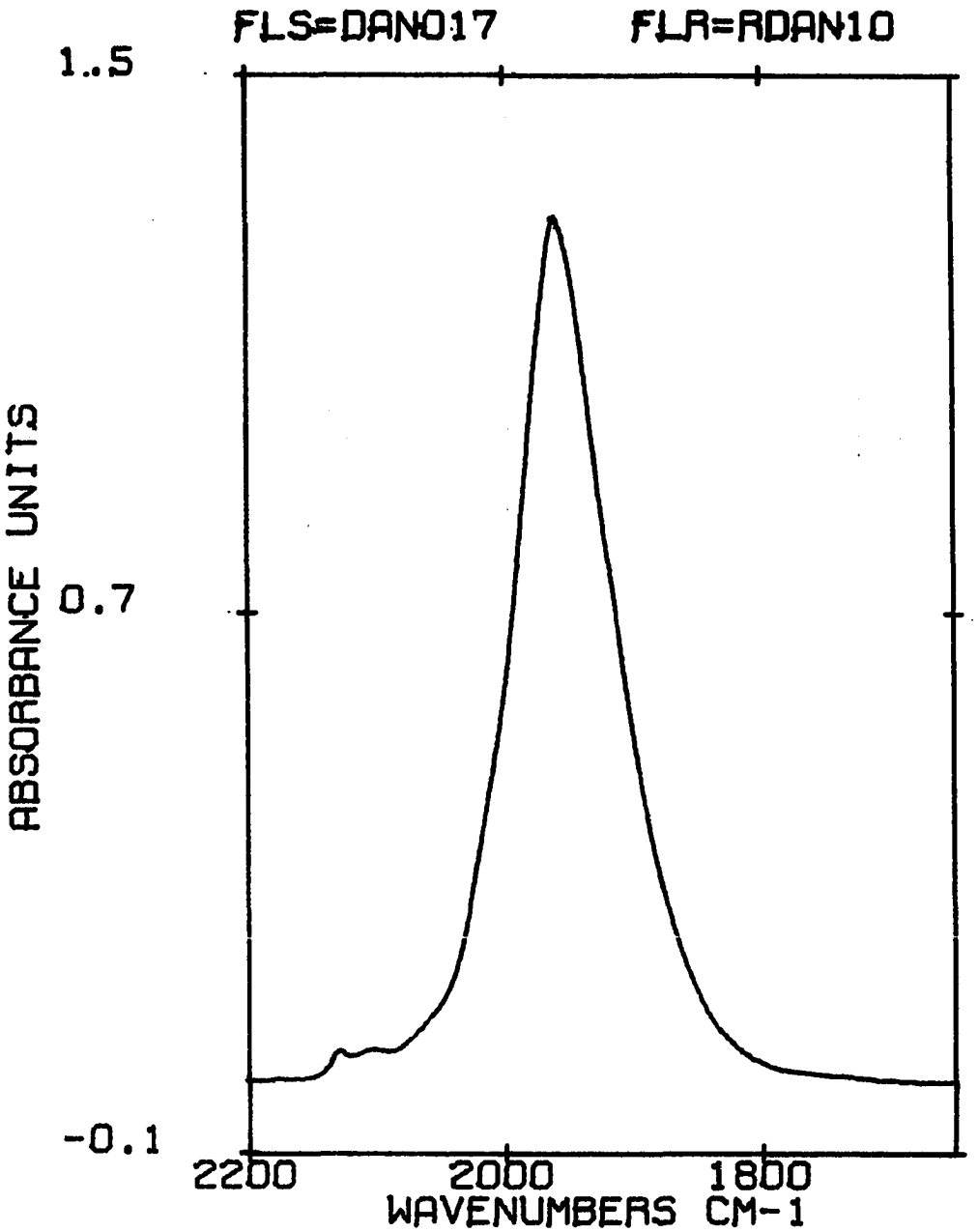

Figure 19. The infrared ν(CN) band of $Cr(t\text{-}BuDiNC)_3$ in CH_2Cl_2 solution

monodentate complexes are reported to show two or more major ν(NC) bands. In light of the known local O_h symmetry of $Cr(CNPh)_6$ based on a recent X-ray diffraction study,[216] it appears that these additional bands may be attributable to impurities rather than significant geometric distortions, as proposed.[107,178]

Repeated attempts to obtain ^1H NMR spectra of $Cr(t\text{-}BuDiNC)_3$ in the chlorinated solvents $CDCl_3$ and CD_2Cl_2 failed, giving spectra with very broad and often multiple resonances. Two likely processes could be in operation. The first is simple aerobic oxidation of the complex; the second is a photo-promoted oxidation reaction involving the chlorinated solvent, as observed for $Cr(CN\text{-}2,6\text{-}(i\text{-}Pr)_2\text{-}C_6H_3)_6$[265] (eq. XXX). The paramagnetism of the Cr(I) or other oxidized products

$$Cr(CNR)_6 \xrightarrow[h\nu]{CHCl_3} [Cr(CNR)_6]Cl \ (+ \ C_2H_2Cl_4?) \qquad \text{(XXX)}$$

in the case of $Cr(t\text{-}BuDiNC)_3$ would be expected to perturb the ^1H NMR spectrum of the complex through contact shifts and possibly, intermolecular electron exchange. Suitable ^1H and ^{13}C NMR are obtainable in C_6D_6 solvent, however, and indicate that the six CH_2 groups (and the six t-butyl groups) are chemically-equivalent, as expected in this and similar molecules of D_3 symmetry.

The next member of the homoleptic d^6 series is the cation $[Mn(t\text{-}BuDiNC)_3]^+$. This complex is obtained initially as its THF-insoluble Cl^- salt, in a reaction between $Mn(CO)_5Cl$ and t-BuDiNC (1:3

molar ratio, refluxing THF, 26 h) as shown in eq. XXXI. Metathesis with NH_4PF_6 in EtOH gives the cream-colored product, $[Mn(t\text{-}BuDiNC)_3]PF_6$, in 49% yield (eq. XXXII). A similar reaction between $Mn(CO)_5Br$ and t-BuDiNC

$$Mn(CO)_5Cl + 3\ t\text{-}BuDiNC \xrightarrow[\Delta]{THF} [Mn(t\text{-}BuDiNC)_3]Cl + 5\ CO \qquad (XXXI)$$

$$Mn(t\text{-}BuDiNC)_3]Cl + NH_4PF_6 \longrightarrow [Mn(t\text{-}BuDiNC)_3]PF_6 + NH_4Cl \qquad (XXXII)$$

(1:3 molar ratio) gives a lower (38%) yield of $[Mn(t\text{-}BuDiNC)_3]Br$ after a reaction time of 76 h, suggesting that $Mn(CO)_5Cl$ is the starting material of choice for such reactions. Similar methodologies have been employed for the synthesis of $[Mn(CNPh)_6]X$,[231,251] though high yields (>50%) are best obtained with a slight excess of PhNC.[231]

A seventeen-electron dication, $[Mn(t\text{-}BuDiNC)_3]^{2+}$, is readily obtainable via the HNO_3 oxidation[252] of $[Mn(t\text{-}BuDiNC)_3]^+$ as in equation XXXIII. Metathesis with KPF_6 in water gives the deep blue product in

$$3[Mn(t\text{-}BuDiNC)_3]^+ + 4HNO_3 \xrightarrow{HOAC} 3[Mn(t\text{-}BuDiNC)_3]^{2+} + 3NO_3^- + NO + 2H_2O \qquad (XXXIII)$$

93% yield, but this product is slightly contaminated by the Mn(I) starting material. Reprecipitation of the sample from CH_2Cl_2 in the presence of a drop of HNO_3 gives an analytically pure product. This oxidation from Mn(I) to Mn(II) is accompanied by an increase in the ν(CN) frequency from 2082 cm^{-1} to 2162 cm^{-1} (both in CH_2Cl_2 solutions)

as would be expected. In $CHCl_3$ (Fig. 20) or CH_2Cl_2 solution, the Mn(II) complex undergoes an apparent reduction over a period of 24 to 36 h. Spectra in CH_2Cl_2 solution show the growth of a small peak at ca. 2243 cm^{-1} which is due to an isocyanate or diisocyanate of t-BuDiNC. The isocyanate group can be generated independently by treating a hot $CHCl_3$ solution of t-BuDiNC with HgO and a small amount of I_2;[266] the isocyanate (ν(CNO) = 2243 cm^{-1}) as well as some isocyanide diiodide (ν(CN) = 1731 cm^{-1}) are both observed. Thus, it is quite possible that the isonitrile is the reductant in the conversion of $[Mn(t\text{-}BuDiNC)_3]^{2+}$ to $(Mn(t\text{-}BuDiNC)_3]^{+}$, though it is not clear what the oxide source is. Similar reductions have been observed for other $[Mn(CNAr)_6]^{2+}$ complexes in $CHCl_3$ solution.[252] In the case of $[Mn(CN\text{-}P\text{-}anisyl)_6](PF_6)_2$, a typical example, the reduction is nearly complete within 15 min, contrasting greatly with the much longer time period of 24-36 h required for the full reduction of the t-BuDiNC complex in $CHCl_3$ solution.

The iron(II) complex, $[Fe(t\text{-}BuDiNC)_3](PF_6)_2$, is prepared in a crude yield of 50% as shown in equation XXXIV. In the first step, both chloride

$$cis\text{-}FeCl_2(t\text{-}BuDiNC)_2 \xrightarrow{2\ AgPF_6} \xrightarrow{t\text{-}BuDiNC} [Fe(t\text{-}BuDiNC)_3](PF_6)_2 \quad \text{(XXXIV)}$$

ions are removed from $cis\text{-}FeCl_2(t\text{-}BuDiNC)_2$ by $AgPF_6$ in CH_2Cl_2, yielding AgCl quantitatively. The addition of t-BuDiNC then gives a brown solution of the crude product, which is isolated and purified by several recrystallizations. The presumed intermediate in the reaction, $[Fe(t\text{-}BuDiNC)_2](PF_6)_2$, is apparently quite acidic, since the odor of hydrogen fluoride

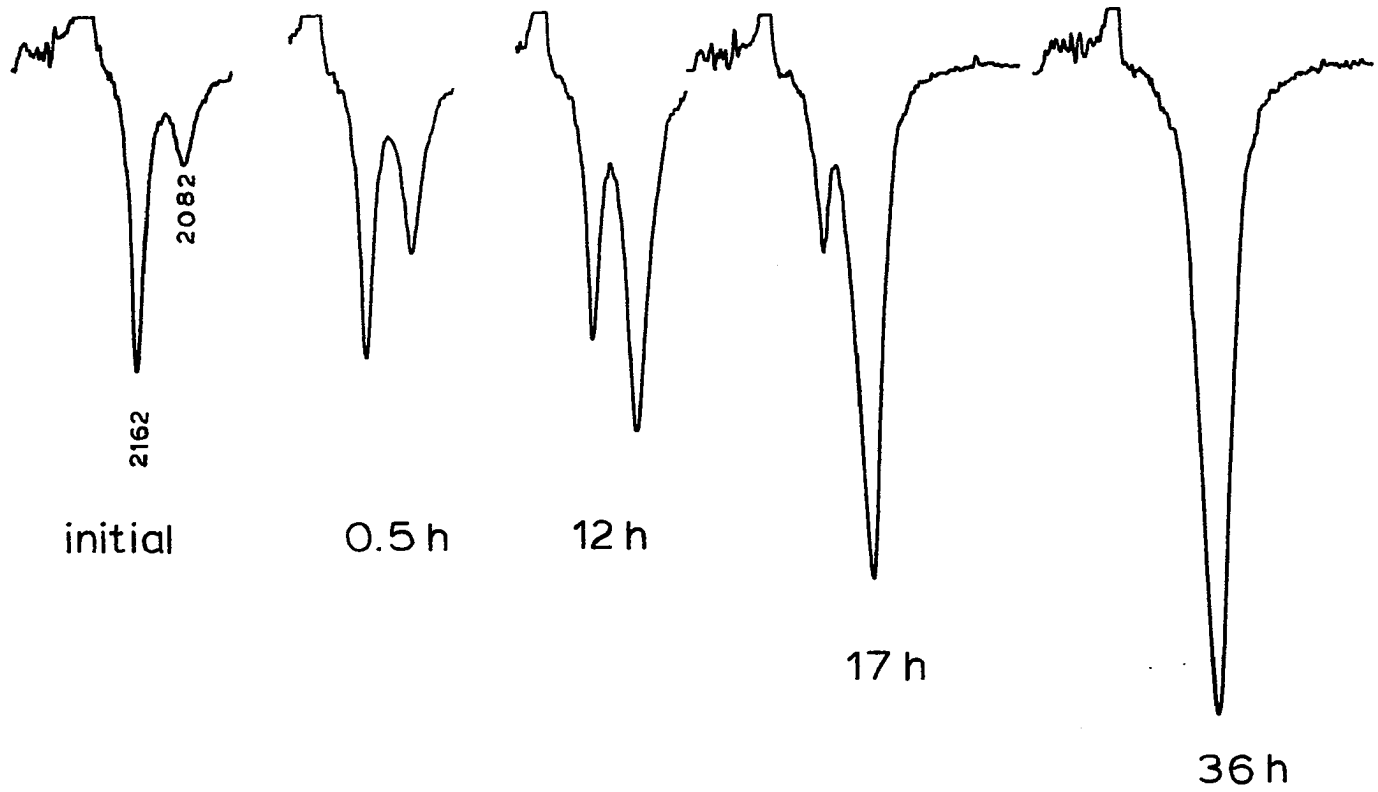

Figure 20. Reductive decomposition of $[Mn(t\text{-}BuDiNC)_3](PF_6)_2$ in $CHCl_3$ solution

(or PF_5) can be detected when N_2 gas is blown across the reaction mixture and vented to the atmosphere. Also in support of the acidity of the intermediate is the observation that only one chloride ion can be removed from cis-$FeCl_2$(t-BuDiNC)$_2$ in the presence of acetonitrile. Here, solvation of Ag^+ by CH_3CN may render it too weakly acidic to remove the second chloride ion. Padoa[267] long ago claimed to have isolated unreactive $[Fe(CNAr)_4](ClO_4)_2$ complexes by the reaction of $Fe(ClO_4)_2$ with aromatic isonitriles. A repetition of this work by Bonati and Minghetti, however, failed to support those results and led instead to the isolation of $[Fe(CN\text{-}P\text{-tolyl})_6](ClO_4)_2$,[189] the only monodentate aromatic isonitrile analog of $[Fe(t\text{-BuDiNC})_3](PF_6)_2$. Both complexes are off-white or ivory in color and have similar isonitrile stretching frequencies; $[Fe(t\text{-BuDiNC})_3](PF_6)_2$ has a single, strong band at 2195 cm^{-1} in Nujol mull (2194 cm^{-1} in CH_2Cl_2) and the p-tolylisonitrile derivative has a band at 2190 cm^{-1} in Nujol (2195 cm^{-1} in $CHCl_3$).[189] The formulation of $[Fe(t\text{-BuDiNC})_3](PF_6)_2$ is supported by elemental analysis, conductivity measurements (Λ_M = 156 Ω^{-1} cm^2 mol^{-1}) as well as ^1H and ^{13}C NMR (Tables 23 and 24).

The last member of the d^6 homoleptic series is the complex $[Co(t\text{-BuDiNC})_3](PF_6)_3$. It is prepared in a reaction (eq. XXXV) similar

$$\begin{array}{l} CoBr_2(t\text{-BuDiNC})_2 \xrightarrow{1/2\ Br_2} [CoBr_2(t\text{-BuDiNC})_2]Br \xrightarrow{3\ AgPF_6} \\ \xrightarrow{t\text{-BuDiNC}} [Co(t\text{-BuDiNC})_3](PF_6)_3 \end{array} \qquad \text{(XXXV)}$$

to that employed for the preceding Fe(II) compound. Oxidation of

$CoBr_2(t\text{-}BuDiNC)_2$ with 0.5 molar equivalents of Br_2 gives a homogeneous solution of the Co(III) derivative $[CoBr_2(t\text{-}BuDiNC)_2]Br$ (as discussed in Section III. 5. b). Reaction of this species in CH_2Cl_2 solution with three molar equivalents of $AgPF_6$ yields AgBr and a highly acidic intermediate, as in the Fe(II) reaction. Addition of t-BuDiNC forms the final product, which is isolated in low yield (22%) after precipitation from CH_2Cl_2 solution with Et_2O. As with $FeCl_2(t\text{-}BuDiNC)_2$, the abstraction of Br^- from $[CoBr_2(t\text{-}BuDiNC)_2]^+$ by $AgPF_6$ is hampered by the presence of acetonitrile and it is necessary to carry the reaction out in a non-coordinating solvent such as CH_2Cl_2. Sacco, in 1953, reported attempts to remove I^- from $[Co(CN\text{-}p\text{-}tolyl)_4I_2]I$ and $[Co(CNBz)_5I](ClO_4)_2$ with $AgClO_4$ in CH_2Cl_2/toluene solvent mixtures.[193] These reactions failed to remove the last I^-, however, and led to the isolation of $[Co(CN\text{-}P\text{-}tolyl)_5I](ClO_4)_2$ and unchanged $[Co(CNBz)_5I](ClO_4)_2$, respectively. These results suggest that I^- is tightly bound to the Co(III) center. The failure of $AgClO_4$ to abstract I^- here is not understood, though a possible explanation might be strong ion-pairing or covalent bonding (i.e. $Ag\text{-}OClO_3$) between Ag^+ and ClO_4^-.

In strong support of the proposed formulation as $[Co(t\text{-}BuDiNC)_3](PF_6)_3$ is a molar conductance of 229 Ω^{-1} cm^2 mol^{-1}, clearly indicative of a 1:3 electrolyte. The high symmetry of the complex is supported by the observation of a single, weak $\nu(CN)$ band in the infrared spectrum at 2259 cm^{-1} and by the ^1H NMR spectrum, which shows sharp, well-resolved resonances for each group of symmetry-related protons of the t-BuDiNC ligand (vide infra).

$[Co(t\text{-}BuDiNC)_3](PF_6)_3$ is quite sensitive to moisture and decomposes over a period of several hours when exposed to air. The decomposition is accompanied by a color change from yellow to tan, and when observed by IR, a decrease in the intensity of the initial, weak ν(CN) band at 2259 cm^{-1} at the expense of a more intense band at ca. 2225 cm^{-1} occurs. Wet solvents such as technical grade acetone decompose the complex immediately to give brown solutions; even with rigorous precautions against moisture, solutions for measurement of IR, NMR, UV-Vis spectra and conductivity (vide infra) usually underwent slow decomposition. The exact nature of the reaction with water is not known, though processes involving oxidation of the isonitrile, reduction of Co(III), isonitrile displacement and/or hydration could be all possible. It is probably this reactivity toward water which causes a slight discrepancy between calculated and observed values of % C, H and N in the compound's elemental analysis (Table 21).

The homoleptic d^6 series of complexes $[M(t\text{-}BuDiNC)_3]^{Z+}$ represents a wide range of bonding modes for the isonitrile ligand, from the electron-rich Cr(0) complex to the previously unknown and highly acidic Co(III) derivative. Perhaps the most obvious comparisons which might be made among all these complexes are those of the isonitrile infrared stretching frequencies of T_{1u} symmetry. Considering only spectra obtained in CH_2Cl_2 solution, the ν(CN) values range from 1958 cm^{-1} to 2256 cm^{-1} (from Cr(0) to Co(III)), thus spanning nearly 300 cm^{-1} in energy. These values are plotted vs. charge in Figure 21.

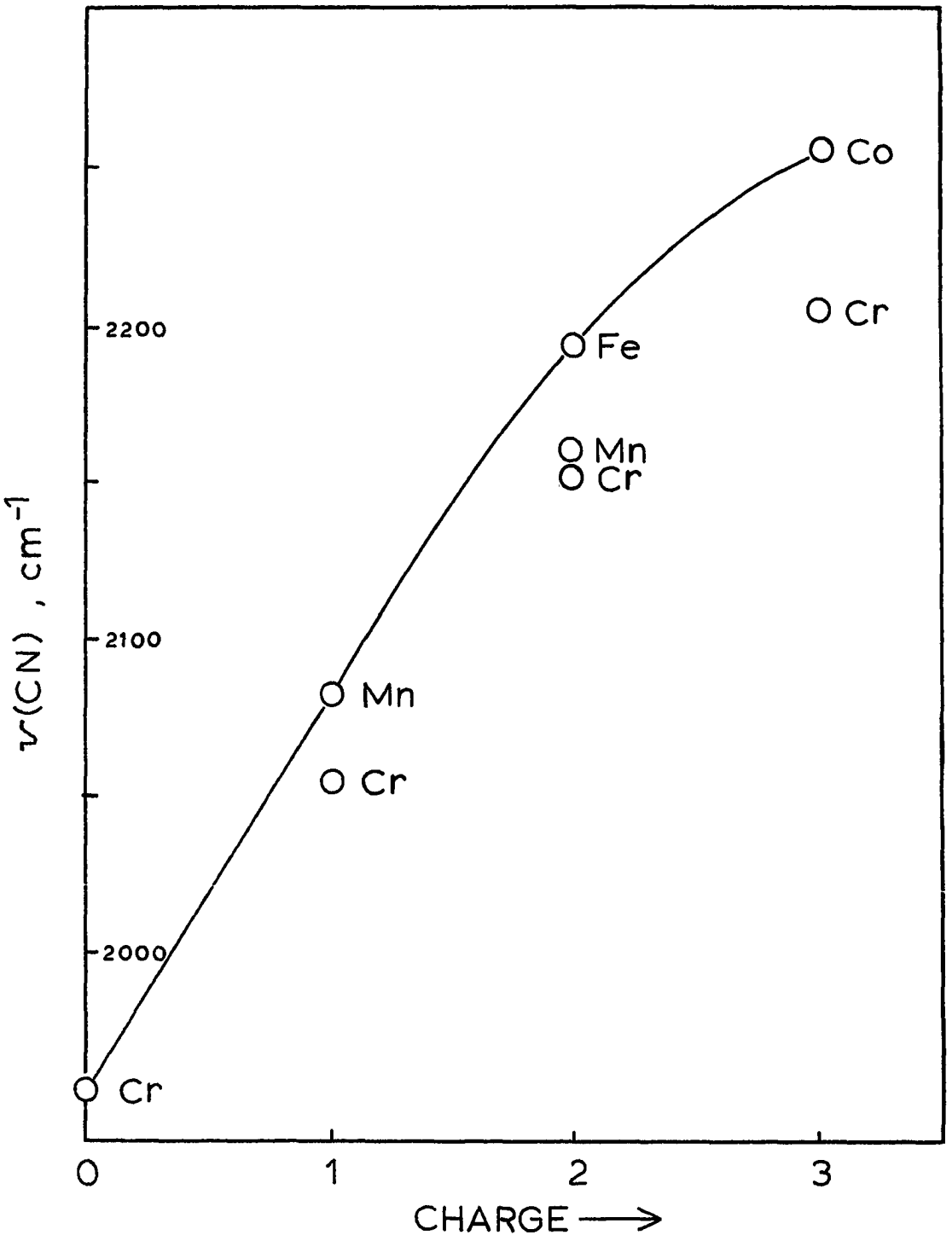

Figure 21. Isonitrile stretching frequency/charge relationships in $[M(t\text{-}BuDiNC)_3]^{Z+}$

There is no question that the low frequencies observed for the Cr(0) and Mn(I) complexes are due in large part to π-donation from metal t_{2g} orbitals into the π^*_{NC} system.[19, 148] Conversely, the very high value of ν(CN) for the Co(III) derivative suggests that such back-donation is of minor importance with respect to σ-donation from the isonitrile to the metal. Recall that such σ-donation involves a bonding interaction between the isonitrile C lone pair (which is antibonding with respect to C and N) and the metal; donation from this orbital strengthens the C-N bond and increases the stretching frequency. In fact, the value of 2256 cm^{-1} in $[Co(t\text{-}BuDiNC)_3](PF_6)_3$ appears to be the highest yet observed for a coordinated aromatic isonitrile, and this is not surprising in light of the fact that no other tricationic isonitrile complexes are known. Square-planar, dicationic complexes such as $[Pt(CN\text{-}p\text{-}tolyl)_4]PtCl_4$,[268] $[Pt(DiNC)_2]PtCl_4$[155] and $[Ni(t\text{-}BuDiNC)_2](BF_4)_2$ (vide supra) exhibit ν(CN) values (E_u mode) of 2248, 2238, and 2234 cm^{-1}, respectively, which are fairly close to the Co(III) stretching frequency. While it might be desirable to compare a more fundamental quantity such as the stretching force constant from one geometry to another, the frequencies of T_{1u} modes in O_h symmetry should be comparable to frequencies of E_u modes in D_{4h} symmetry, since the approximate secular equations relating the frequencies, stretching force constants, and interaction force constants for each case are the same.[269] Thus, the Co^{3+} ion appears to demand more electron density from each of its six isonitrile ligands than do the Pt^{2+} or Ni^{2+} ions

from each of their four ligands, based upon the infrared active isonitrile stretching frequencies. The existence of the $[Co(t\text{-}BuDiNC)_3]^{3+}$ trication, which represents an extreme in isonitrile-metal bonding, might be attributable to the chelate effect, which would keep the weakly-bound t-BuDiNC isonitrile groups bound to the metal in a situation where monodentate arylisonitriles would dissociate. However, a reinvestigation of analogous monodentate systems might be necessary in order to define the true role of the chelate effect here.

An examination of Figure 21 shows also that there are significant differences between ν(CN) values for complexes of the same charge. Thus, ν(CN) for the Mn(I) and Mn(II) complexes are higher than for the corresponding Cr(I) and Cr(II) complexes; $[Fe(t\text{-}BuDiNC)_3]^{2+}$ gives the highest ν(CN) of the divalent complexes. This trend is related to the regular stabilization of metal atom d orbitals as the first transition series is traversed, and is due to ineffective shielding of increasing nuclear charge.[270] The ionization potentials of the gaseous metal atoms are effected in a similar way by this phenomenon, though no linear correlation between ν(CN) and ionization potentials appears to hold. In terms of ν(CN), a lowering of the energy of the π-bonding t_{2g} orbitals gives rise to a weaker bonding interaction between these orbitals and the isonitrile π^* orbitals, increasing ν(CN).

The decreasing importance of π-backbonding across the homoleptic d^6 series is also born out by measurements of the absolute integrated intensities of their ν(CN) bands. Values determined by measurements

made with an IBM IR 98 Fourier Transform spectrometer are plotted as a function of the total charge on the complex in Figure 22. Also included in Figure 22 are values for an isoelectronic series of metal hexacarbonyls from $V(CO)_6^-$ to $Mn(CO)_6^+$, as determined by Noack.[109] Though there appear to be no examples in the literature of integrated intensity measurements of coordinated isonitriles, there are data available for a very large number of compounds containing coordinated CO.[271] Measurements have also been made for complexes containing coordinated N_2,[272] CS,[273] CN^-,[274] and benzonitrile ligands,[139] as well as for free isonitriles.[34,275]

Theory states[271,276] that the integrated intensity, A, of an infrared band is proportional to the quantity $(\frac{\partial\mu}{\partial Q_i})^2$, where μ is the molecular dipole moment and Q_i corresponds to the normal coordinate of interest. An approximation gives $A \propto (\frac{\partial\mu}{\partial r})^2$, where r is the bond length of the oscillator in question. The high intensities of coordinated CO and CNR are due to significant charge transfer from metal $d\pi$ to ligand π^* orbitals. As the C≡N (or C≡O) bond stretches, (i.e. as r increases) the energy of π^* orbitals on the ligand drops and the metal $d\pi \longrightarrow \pi^*$ bonding interaction increases. This transfers charge into the C≡N (or C≡O) group, changing its dipole moment, μ. The closer the $d\pi$ and π^* orbital energies, the more charge can be transferred into the ligand as the bond stretches. Hence, the integrated intensity of a coordinated ν(CO) or ν(CN) absorption is, to a large extent, a measure of the metal electron density available to the ligand. For CO, it is proposed that the π-bonding effects control the integrated intensity to a much greater

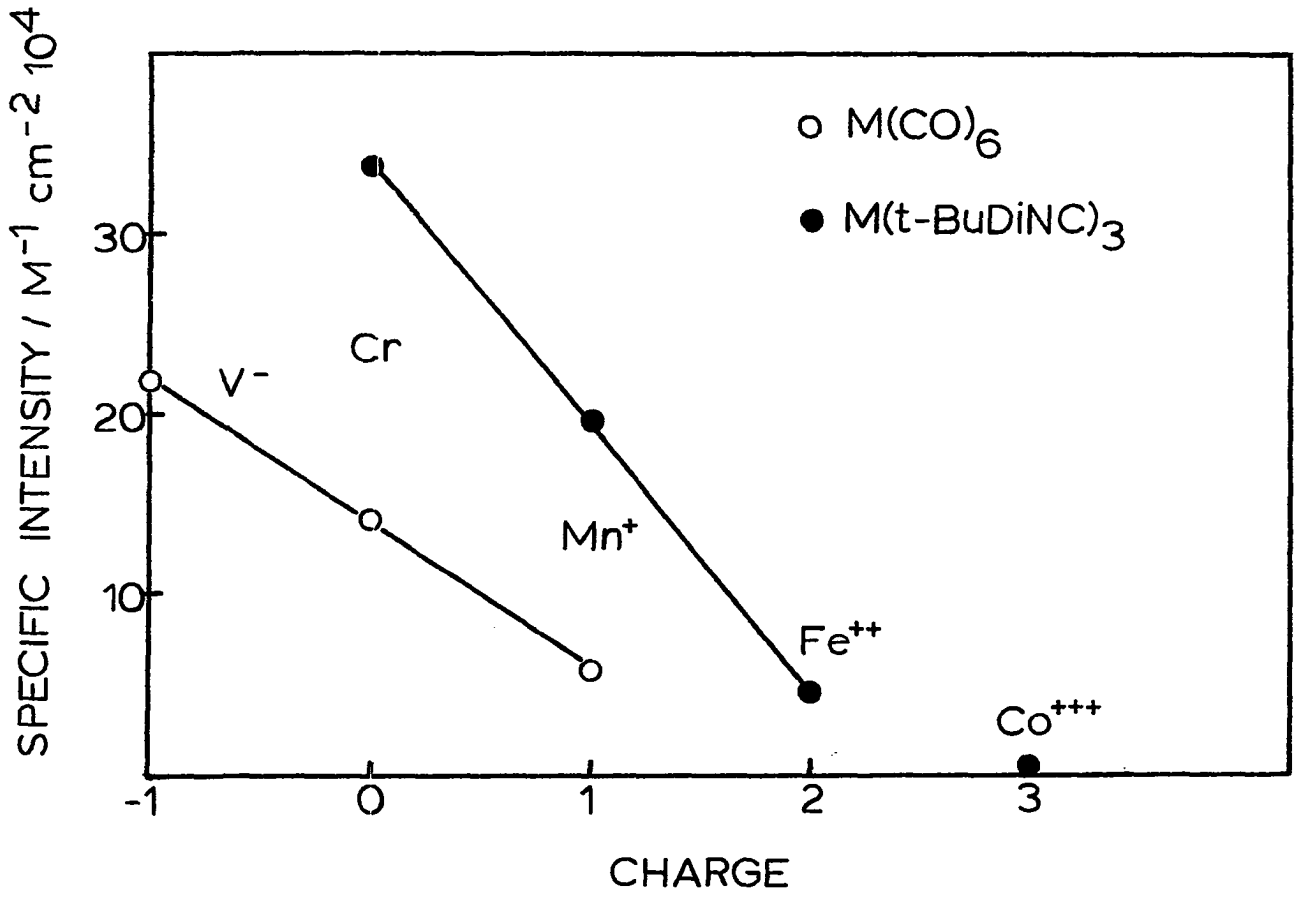

Figure 22. Specific integrated intensities of ν(CO) and ν(CN) in d^6 CO and t-BuDiNC complexes

extent than do σ-bonding effects, based upon the observation of weak ν(CO) bands for CO which is σ-bound to a metal or metal oxide surface.[276] Thus, where CO intensities, and presumably CNR intensities, are very large, π-bonding is assumed to be the major factor in determining the intensity. This method then, provides a way of evaluating the degree of π-bonding in a CNR or CO complex more or less independent of σ-bonding effects; both σ- and π-bonding make large contributions to the stretching frequency of the bound ligand and make this parameter less suitable for the evaluation of σ- or π-effects alone.

The intensity values plotted in Figure 22 are specific intensities, as defined by Noack,[109] and are obtained by dividing the total integrated intensity by the number of equivalent absorbing groups. The specific intensity for t-BuDiNC is not plotted, but has a value of 1.1×10^4 M^{-1} cm^{-2}, which is very near the value of 1.29×10^4 M^{-1} cm^{-2} reported by Gillis and Occolowitz[34] for PhNC in $CHCl_3$ solution. It is also known that electron-releasing substituents on the aromatic ring, will lower the isonitrile stretching band intensity somewhat,[275] and thus the t-BuDiNC value seems to be quite reasonable. As for the homoleptic $[M(CO)_6]^{Z+}$ series, the specific intensities of $[M(t\text{-BuDiNC})_3]^{Z+}$ form a linear plot vs. charge for the Cr(0), Mn(I), and Fe(II) compounds, while the Co(III) complex introduces a discontinuity. Even for $[Fe(t\text{-BuDiNC})_3]^{2+}$, whose specific intensity is ca. 4.2 times higher than that of t-BuDiNC, it could well be that π-backbonding is of some, though minor, importance in the Fe(II)-CNR bonding scheme. The cobalt(III)

compound, alternatively, has a specific intensity which is about half that of free t-BuDiNC and here, π-backbonding from Co(III) to the isonitrile π^* system is probably close to non-existent.

Proton NMR spectra of the homoleptic complexes are quite simple, due to the high (D_3) symmetry of the tris-chelates. These spectra resemble those of the free ligand in that single resonances are observed for the CH_2 and t-butyl protons. Figure 23 shows the 300 MHz ^1H NMR spectrum of $[Fe(t\text{-}BuDiNC)_3](PF_6)_2$ as an example. At 300 MHz, the aromatic proton signals of the Mn, Fe, and Co complexes in CD_2Cl_2 solution can be resolved well enough to assign the chemical shift of each proton. At 90 MHz, these signals appear in a first-order pattern only for the cobalt complex, as shown in Figure 24. Also shown in Figure 24 is the aromatic multiplet of t-BuDiNO$_2$ in $CDCl_3$ solution, which closely resembles the pattern of the Co(III) complex. This is taken as a qualitative indication that the $-N{\equiv}C-Co^{3+}$ unit is strongly electron-withdrawing, as is the NO_2 group. Chemical shifts of the three aromatic protons and the CH_2 protons for the Mn, Fe, and Co complexes are plotted in Figure 25. Unfortunately, $Cr(t\text{-}BuDiNC)_3$ cannot be included in these comparisons, since the C_6D_6 solvent (the only solvent in which decent spectra could be obtained) causes very large aromatic solvent-induced shifts in the resonances in this and other isonitrile complexes.[179] The CH_2 and H_c ring protons produce gradually sloping curves which tend to level off toward Co(III). The other two

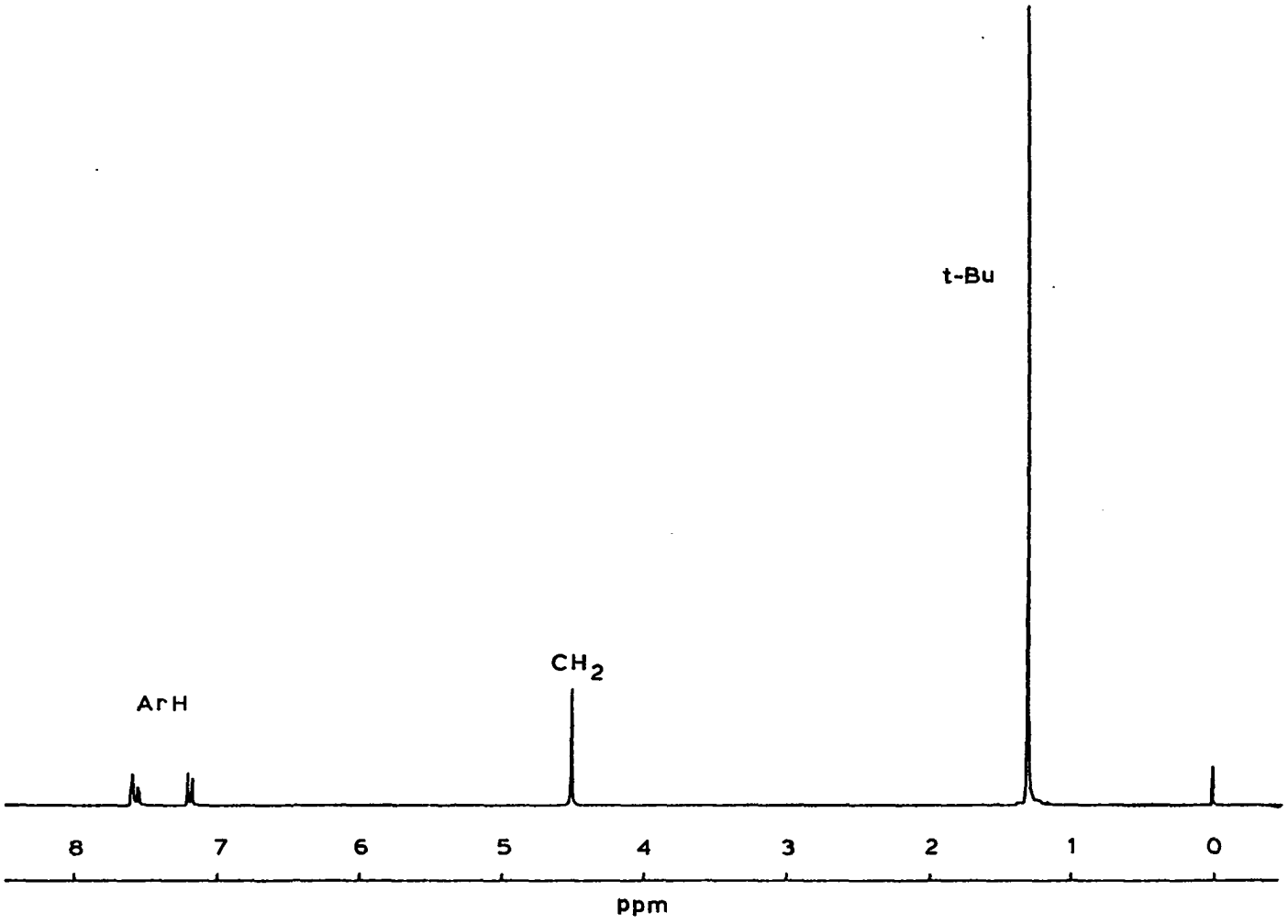

Figure 23. ^{1}H NMR spectrum of $[Fe(t\text{-}BuDiNC)_3](PF_6)_2$ (300 MHz) in CD_2Cl_2 solution

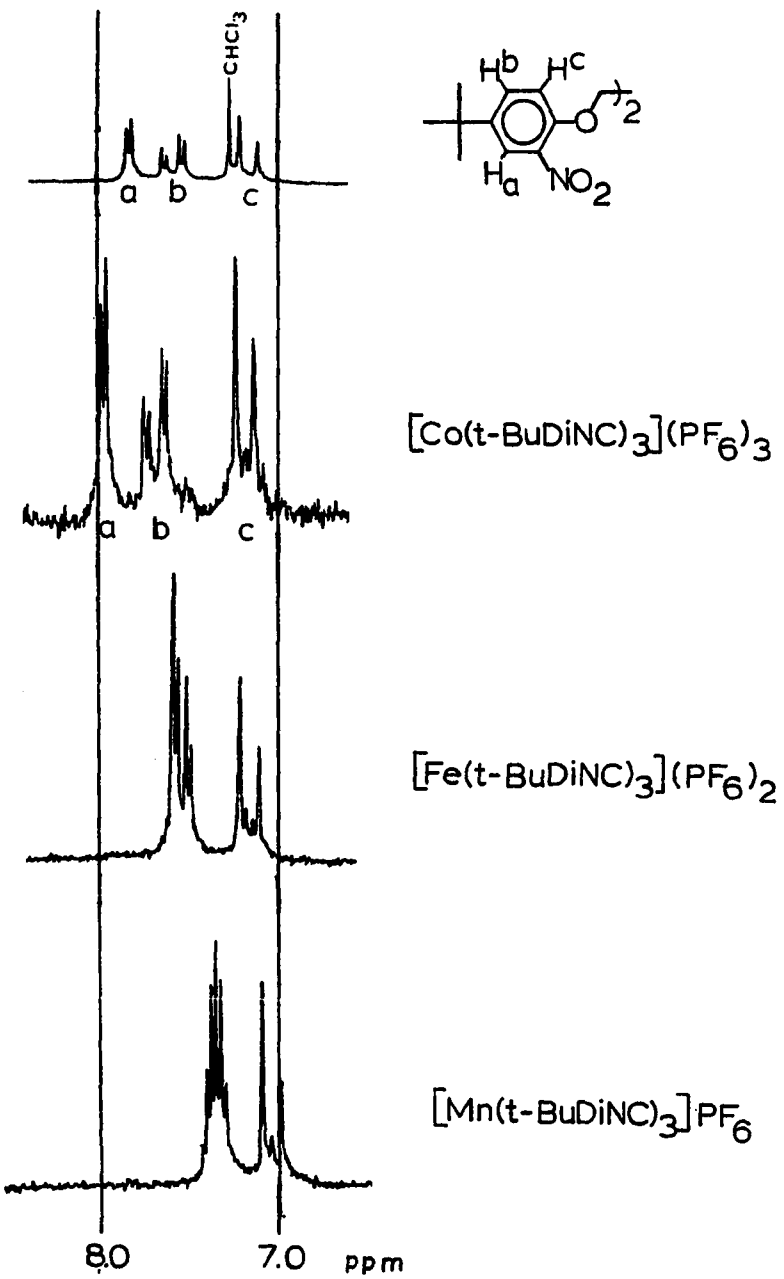

Figure 24. ^1H NMR spectra of aromatic protons of $[M(t\text{-}BuDiNC)_3]^{Z+}$ in CD_2Cl_2 solution and $t\text{-}BuDiNO_2$ in $CDCl_3$ solution

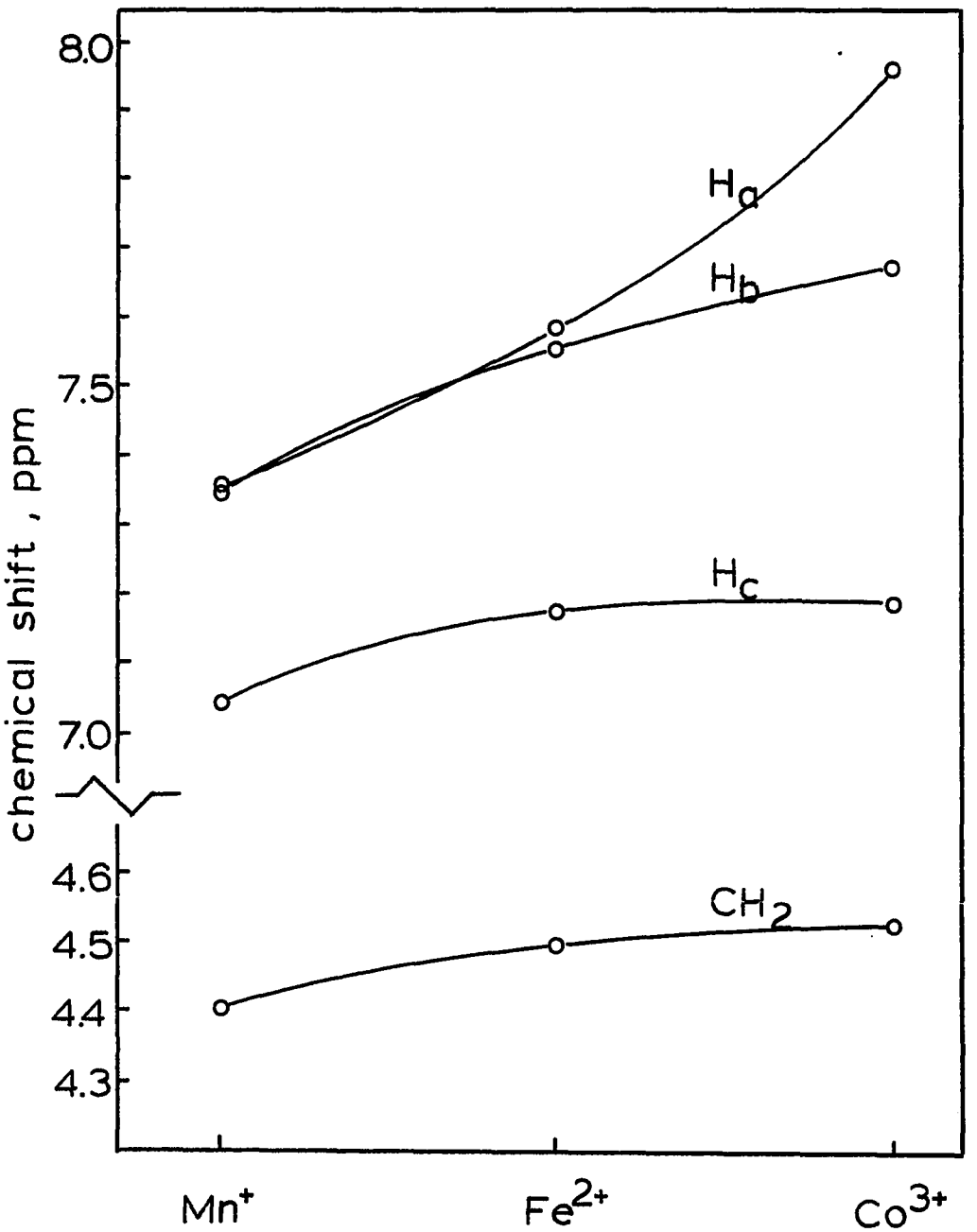

Figure 25. ^{1}H NMR chemical shifts of CH_2 and aromatic protons of $[M(t\text{-}BuDiNC)_3]^{2+}$ in CD_2Cl_2 solution

aromatic protons, H_a and H_b, (ortho and para to the isonitrile group, respectively) show more dramatic increases toward Co(III), especially H_a. That these protons shift more drastically than does the meta proton, H_c, might be taken as evidence that the aromatic ring is able to help stabilize the increasing positive charge on the metal through resonance interactions as shown below. The large separation of

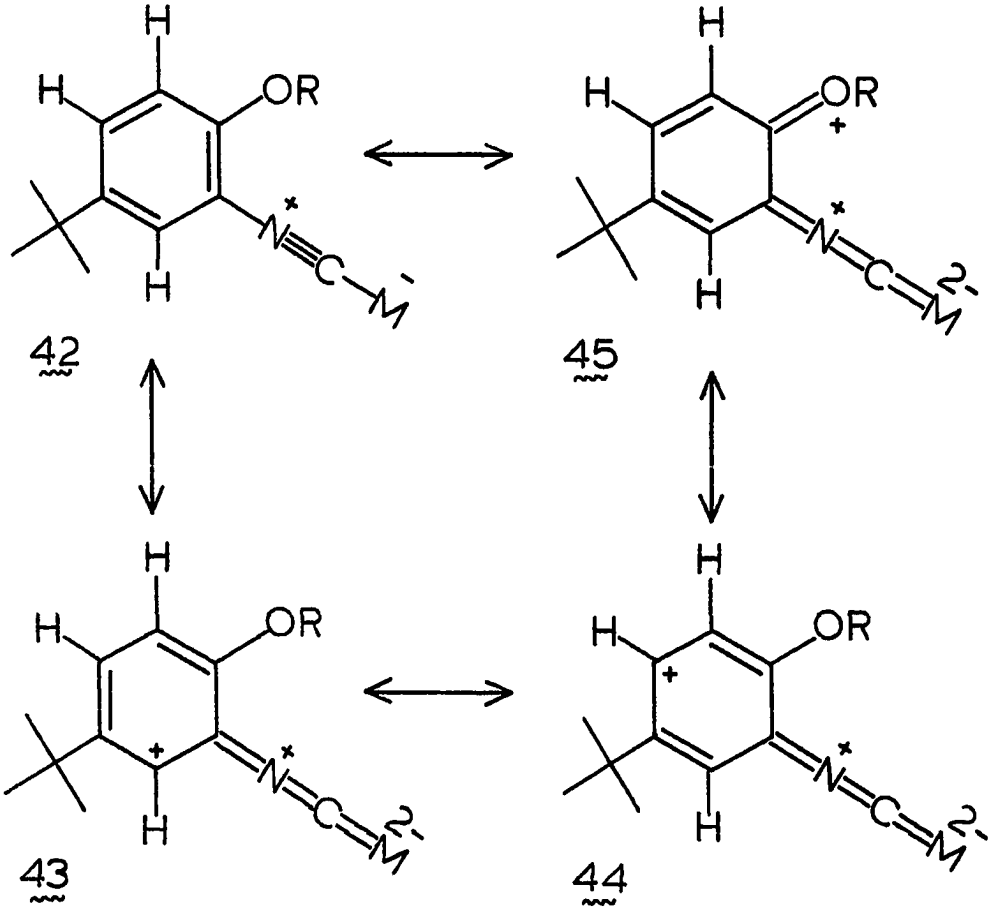

H_a and H_b in $[Co(t\text{-}BuDiNC)_3](PF_6)_3$ (and in $t\text{-}BuDiNO_2$) might be due to a number of electronic factors including strong σ-inductive effects, a strong weighting of structure 43, or magnetic anisotropic effects arising from electronic currents within the isonitrile group. Alternatively, the lower chemical shift differences and higher field resonances in $[Mn(t\text{-}BuDiNC)_3]PF_6$ might be considered as arising from delocalization of electron density from the metal into the aromatic ring's π^* system via the π^*_v orbital of the isonitrile group. Strong interactions between these orbitals are known to exist, through theoretical calculations[52] and experiment.[148]

Electronic spectra of the homoleptic $[M(t\text{-}BuDiNC)_3]^{Z+}$ complexes have been recorded and are tabulated in Table 25. Figure 26 contains traces of the four d^6 members of the series. Following assignments made by Mann et al[107] for homoleptic phenylisonitrile complexes of Cr and Mn, the lowest energy bands in each compound are assigned as the $d\pi \longrightarrow \pi^*_v$ MLCT transitions, which can be seen in the simple molecular orbital diagram of Figure 27. The spectrum of $Cr(t\text{-}BuDiNC)_3$, measured in THF solution, shows the two lowest energy bands at 468 (sh) nm and 420 nm, compared with 458 (sh) nm and 394 nm, reported for $Cr(CNPh)_6$.[107] The higher energy bands at 300 nm and 286 are assigned as $d\pi \longrightarrow \pi_h^*$ transitions, by analogy with $Cr(CNPh)_6$, which exhibits one such band at 310 nm.[107]

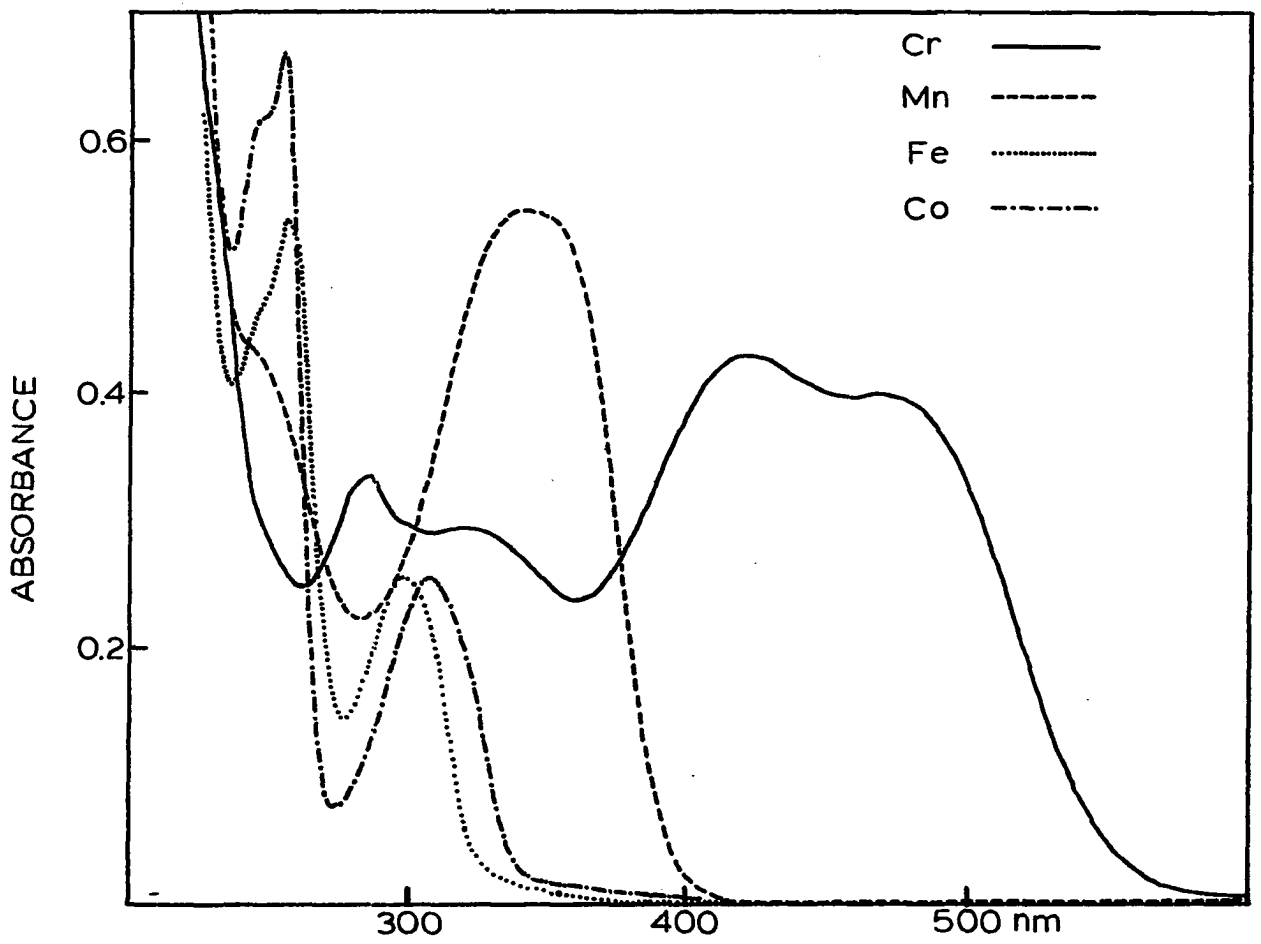

Figure 26. Electronic spectra of the d^6 complexes $[M(t\text{-}BuDiNC)_3]^{Z+}$, where $M^{Z+} = Cr^o$, Mn^+, Fe^{2+}, and Co^{3+}

Concentrations are ca. 9×10^{-5} M, b = 1 mm

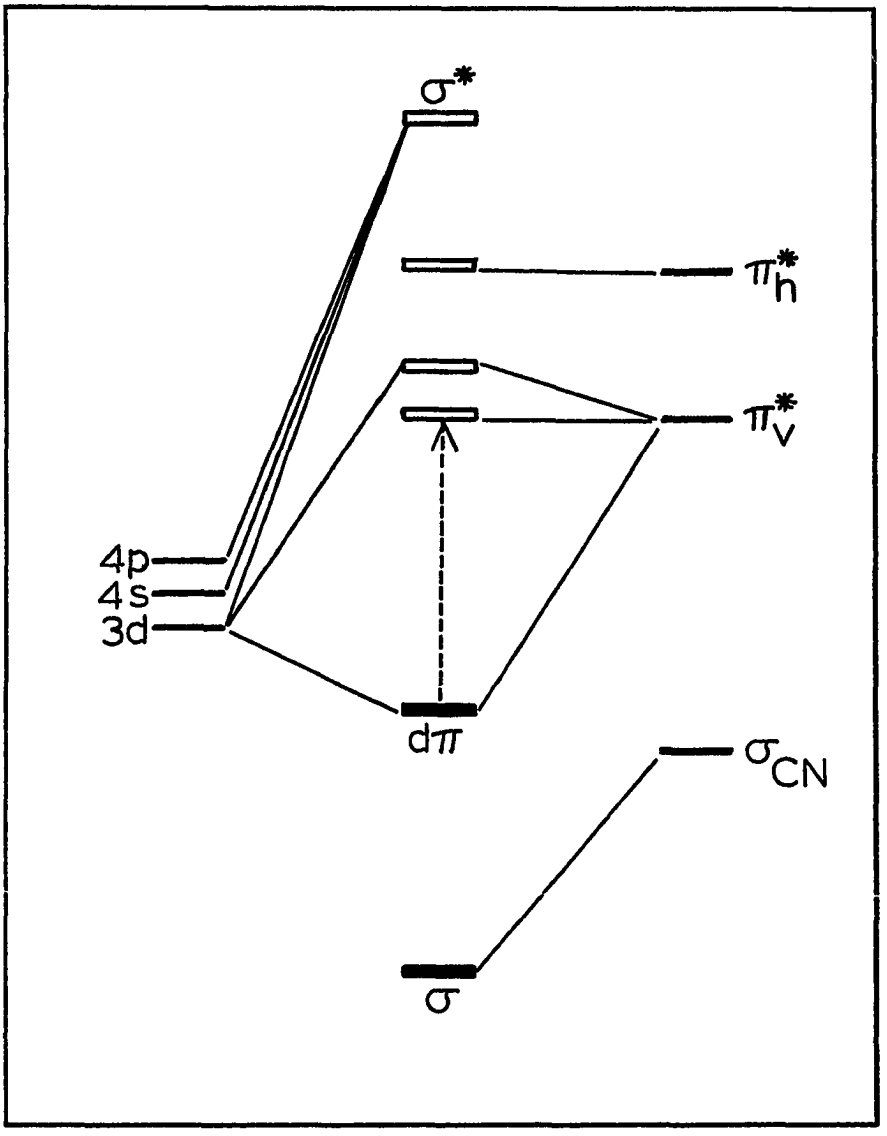

Figure 27. Qualitative molecular orbital diagram for d^6 $M(CNR)_6$ molecules

The single band at 341 nm for $[Mn(t\text{-}BuDiNC)_3]PF_6$ is similar in energy to the closely-spaced bands reported for the PhNC analog at 340 and 322 nm.[107] The Fe(II) complex shows two major bands at 298 nm and 258 nm, while the Co(III) analog has bands of slightly lower and higher energy at 307 nm and 255 nm. A shoulder at 247-249 nm for the Mn(I), Fe(II), and Co(III) complexes is thought to be attributable to an intraligand transition, shifted from its position of 225 nm in the free ligand. The steady increase in the MLCT energies from Cr(0) through Fe(II) is most likely due to a steady drop in $d\pi$ orbital energies as a result of the increasing charge on the complexes, and less effective nuclear charge screening, as discussed earlier. The close resemblance of the Fe(II) and Co(III) spectra is somewhat surprising, but might be due in part to a drop in the isonitrile π^* orbital energies through the inductive and/or resonance effects referred to in the discussion on ^1H NMR. Also, the low degree of $d\pi$-π^* backbonding in this complex would tend to not stabilize the $d\pi$ orbitals, as is expected where moderate or strong π-backbonding is taking place.

The 17-electron species $[Cr(t\text{-}BuDiNC)_3]PF_6$ shows an electronic spectrum similar to that of its neutral, 18-electron congener, with blue-shifted $d\pi \longrightarrow \pi_v^*$ bands at 443 (sh) nm and 365 nm. Similarly, the MLCT bands of the 17-electron complex $[Mn(t\text{-}BuDiNC)_3](PF_6)_2$ are seen at 303 nm and 282 (sh) nm, compared to 341 nm for the 18-electron parent compound. Weak, low energy bands are also seen in the spectrum

of $[Mn(t\text{-}BuDiNC)_3]^{2+}$ at 684 nm, 481 nm and 355 nm. These are thought to arise from transitions from the filled σ-bonding orbitals into the dπ orbitals, which have only five electrons.[107]

The electrochemistry of hexakis (isonitrile) chromium[227-230,232,233] and manganese[231-233] complexes has been studied with some enthusiasm for the last ten years. Generally, these compounds exhibit three or four closely-spaced redox processes which are interesting in themselves and also have provided some insight into the nature of the bonding between isonitriles and these metals.[277] Though the complexes $[Cr(t\text{-}BuDiNC)_3]^{Z+}$ (Z = 0-3) and $[Mn(t\text{-}BuDiNC)_3]^{Z+}$ (Z = 1,2) have been generated chemically (vide supra), the investigation of such complexes through cyclic voltammetry was undertaken to determine if the chelating t-BuDiNC ligand selectively stabilizes any particular oxidation states. Also of interest was the comparison of these electrochemical results with those in the literature. No complexes of the type $[Fe(CNAr)_6]^{2+}$ have been investigated by cyclic voltammetry, and so the investigation of this complex was carried out as well. All studies were carried out at 25°C in CH_2Cl_2 solution containing Bu_4NPF_6 at a concentration of 0.1 M as the supporting electrolyte. Other details are given in Section II.B.7.

The starting complex $[Cr(t\text{-}BuDiNC)_3]PF_6$ was used to study the interconversions of the various $[Cr(t\text{-}BuDiNC)_3]^{Z+}$ species. The electrochemical data are presented in Table 28. Figure 28 shows the cyclic voltammogram recorded at a scan rate of 20 mVs^{-1}. As can be seen from the figure, there are three distinct waves, due to the

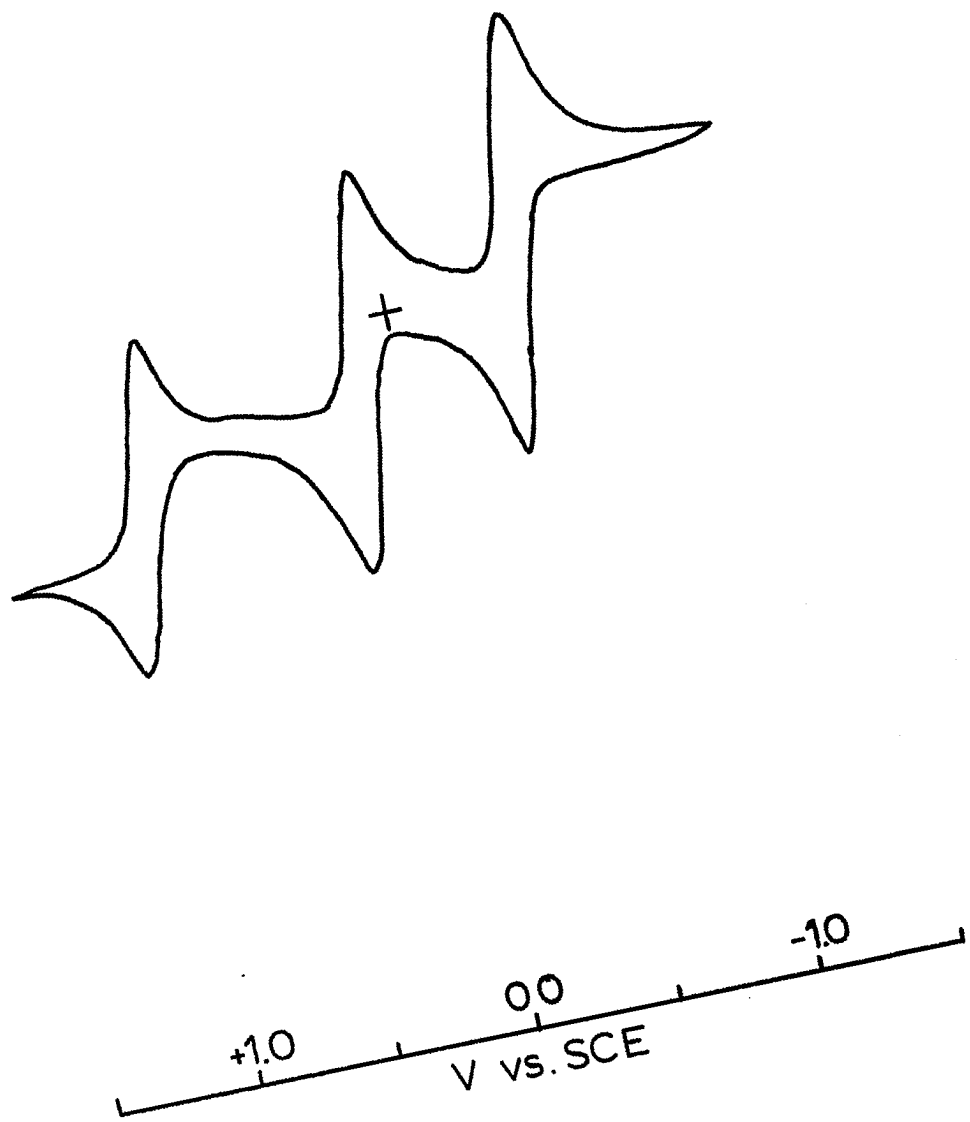

Figure 28. Cyclic voltammogram for $[Cr(t\text{-}BuDiNC)_3]PF_6$

interconversion of the four $[Cr(t\text{-}BuDiNC)_3]^{Z+}$ species for Z = 0-3. The chemical reversibility of all three processes is indicated by $i_{p,a}/i_{p,c}$ ratios of unity for each step. Half-wave potentials, $E_{1/2}$, calculated as $1/2(E_{p,a} + E_{p,c})$, are -0.50, +0.10, and +0.99 V vs. SCE. These potentials can be compared with those determined by Essenmacher and Treichel[227] for $Cr(CN\text{-}p\text{-}anisyl)_6$ under similar conditions: -0.44, +0.11, +0.84 V vs. SCE. The t-BuDiNC values are close to those of the CN-p-anisyl complex for the first two processes, which correspond to the $Cr^0 \longrightarrow Cr^+$ and $Cr^+ \longrightarrow Cr^{2+}$ conversions, respectively. The last process, $Cr^{2+} \longrightarrow Cr^{3+}$, is seen to be slightly less favorable for the t-BuDiNC case with respect to CN-p-anisyl. Bohling et al.[228] have observed a difference of 150 mV between the $Cr^{2+} \longrightarrow Cr^{3+}$ processes of $[Cr(CN\text{-}o\text{-}tolyl)_6]^{2+}$ and $[Cr(CN\text{-}p\text{-}tolyl)_6]^{2+}$; oxidation of the CN-o-tolyl derivative is more difficult. They have tentatively attributed the destabilization of $[Cr(CN\text{-}o\text{-}tolyl)_6]^{3+}$ to unfavorable steric interactions between ortho ligand substituents. In the case of t-BuDiNC, a similar explanation may be applicable; it is imaginable that as the charge of the chelated Cr ion is increased from +2 to +3, the attendant decrease in its ionic radius (due to d-orbital contraction) strains the chelate ring, destabilizing the complex.

Peak-to-peak separations for all three redox processes are found to vary with the scan rate. The separation is approximately 600 mV at 100 mVs^{-1} and 190 mV at 20 mVs^{-1}. The system is thus characterized

as quasi-reversible, where the rate of electron transfer is somewhat slow relative to the rate of potential change.[278] Other $Cr(CNAr)_6$ complexes exhibit similar behavior.[227,229]

The manganese complex, $[Mn(t\text{-}BuDiNC)_3]PF_6$, like other $[Mn(CNR)_6]^+$ systems,[231-233] shows only two waves, corresponding to the processes $Mn^+ \longrightarrow Mn^{2+}$ and $Mn^{2+} \longrightarrow Mn^{3+}$. No reduction processes are observed at potentials as low as -2.0 V vs. SCE. Figure 29 presents the cyclic voltammogram of the complex as recorded at a scan rate of 20 mVs^{-1}. The $E_{1/2}$ values for the equilibria are +0.86 and ca. +2.0 V vs. SCE, though the exact determination of the latter value is complicated by the onset of solvent decomposition. As in the Cr case, the ratio of the peak heights is unity for the clean $Mn^+ \rightleftharpoons Mn^{2+}$ equilibrium but the peak separations for both processes are large and dependent upon scan rate (see Table 28), indicative of quasi-reversibility. The $E_{1/2}$ values of +0.86 and +2.0 V can be compared with the values of +1.00 and +1.90 V vs. SCE reported by Treichel and coworkers[232] for $[Mn(CNPh)_6]PF_6$ in CH_2Cl_2 solution. Voltammetric data for $[Mn(CN\text{-}p\text{-}anisyl)_6]PF_6$, which is electronically similar to the t-BuDiNC complex, have only been reported in CH_3CN solution,[231] but these data show the first oxidation of $[Mn(CN\text{-}p\text{-}anisyl)_6]^+$ to take place at a potential 140 mV more negative than for the PhNC complex. If we assume a similar difference to exist between $[Mn(CNPh)_6]^+$ and $[Mn(CN\text{-}p\text{-}anisyl)_6]^+$ in CH_2Cl_2 solution, the latter would be expected to show a first oxidation wave at +0.86 V vs. SCE, which is just where the $E_{1/2}$ for oxidation of $[Mn(t\text{-}BuDiNC)_3]^+$ lies. However, the second wave, attributed to the $Mn^{2+} \longrightarrow Mn^{3+}$ process, is more positive for

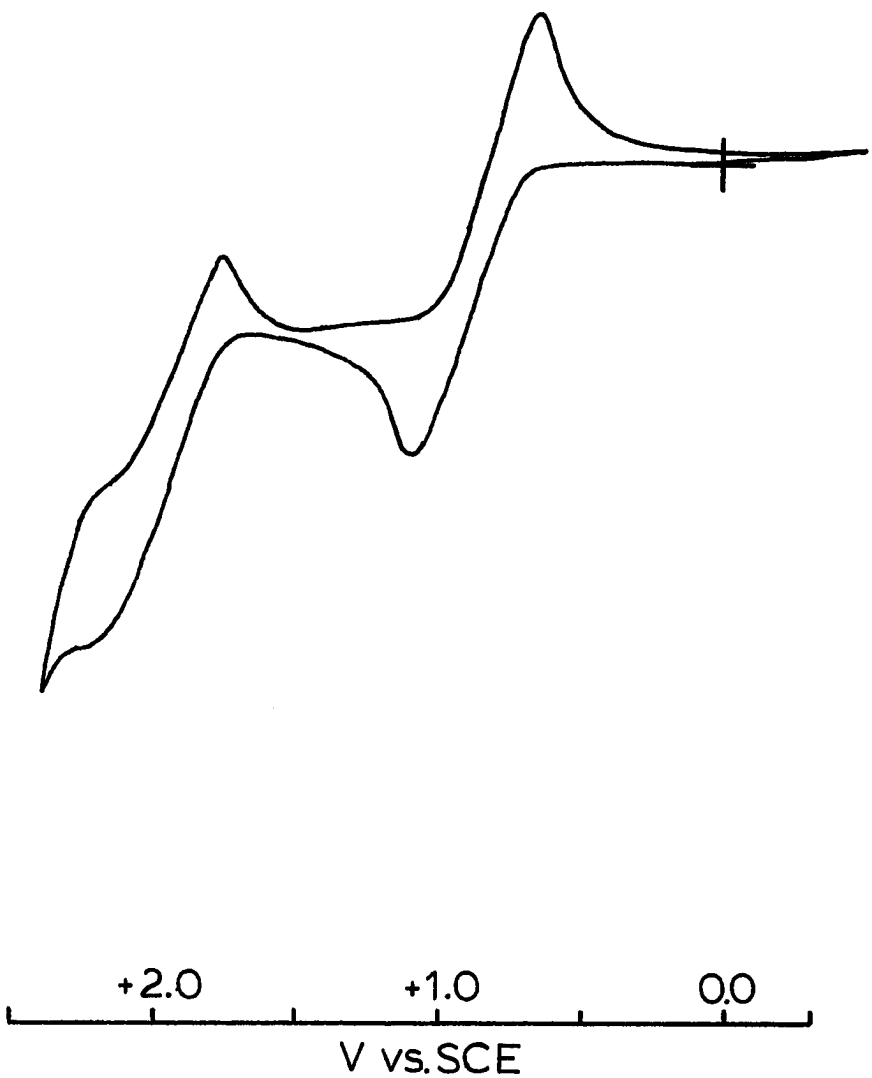

Figure 29. Cyclic voltammogram for $[Mn(t\text{-}BuDiNC)_3]PF_6$

$[Mn(t\text{-}BuDiNC)_3]^{2+}$ than for the PhNC analog (compare +2.00 V to +1.90 V) and certainly would be more positive than for the CN-p-anisyl complex in CH_2Cl_2 solution. As for $[Cr(t\text{-}BuDiNC)_3]^{3+}$, these observations indicate a slight destabilization of $[Mn(t\text{-}BuDiNC)_3]^{3+}$ with respect to the trivalent Mn complex containing the p-anisylisonitrile ligand.

Unlike its isoelectronic chromium and manganese analogs, $[Fe(t\text{-}BuDiNC)_3](PF_6)_2$ undergoes no chemically reversible redox processes when examined by cyclic voltammetry. Figure 30 shows traces recorded at scan rates of (a) 200 mVs^{-1} and (b) 20 mVs^{-1} with switching potentials of +1.5 V and -2.25 V vs. SCE. The most prominent feature in the voltammograms is a chemically and kinetically irreversible wave in the vicinity of -2 V. At 200 mVs^{-1}, two oxidation waves are produced on the return sweep from -2.25 V, one at ca. -0.2 V, the other at ca. +1.2 V. A lower scan rate shifts the cathodic wave from a position negative of -2.25 V to -1.84 V, indicating the kinetic irreversibility of the process. Only a very tiny anodic wave at ca. -0.5 V is observed on the return sweep, indicating that the product(s) of the reduction of $[Fe(t\text{-}BuDiNC)_3]^{2+}$ undergoes a relatively fast decomposition. With switching potentials of +1.50 V and -1.25 V, no waves are observed at all, indicating that the weak anodic waves are due to electrochemical activity of a reduction product of $[Fe(t\text{-}BuDiNC)_3]^{2+}$, and not $[Fe(t\text{-}BuDiNC)_3]^{2+}$ itself. Scans to the more positive potential of +2.25 V show some anodic current above +1.9 V, part of which is due to solvent decomposition, and a very slight cathodic wave at ca. +0.7 V,

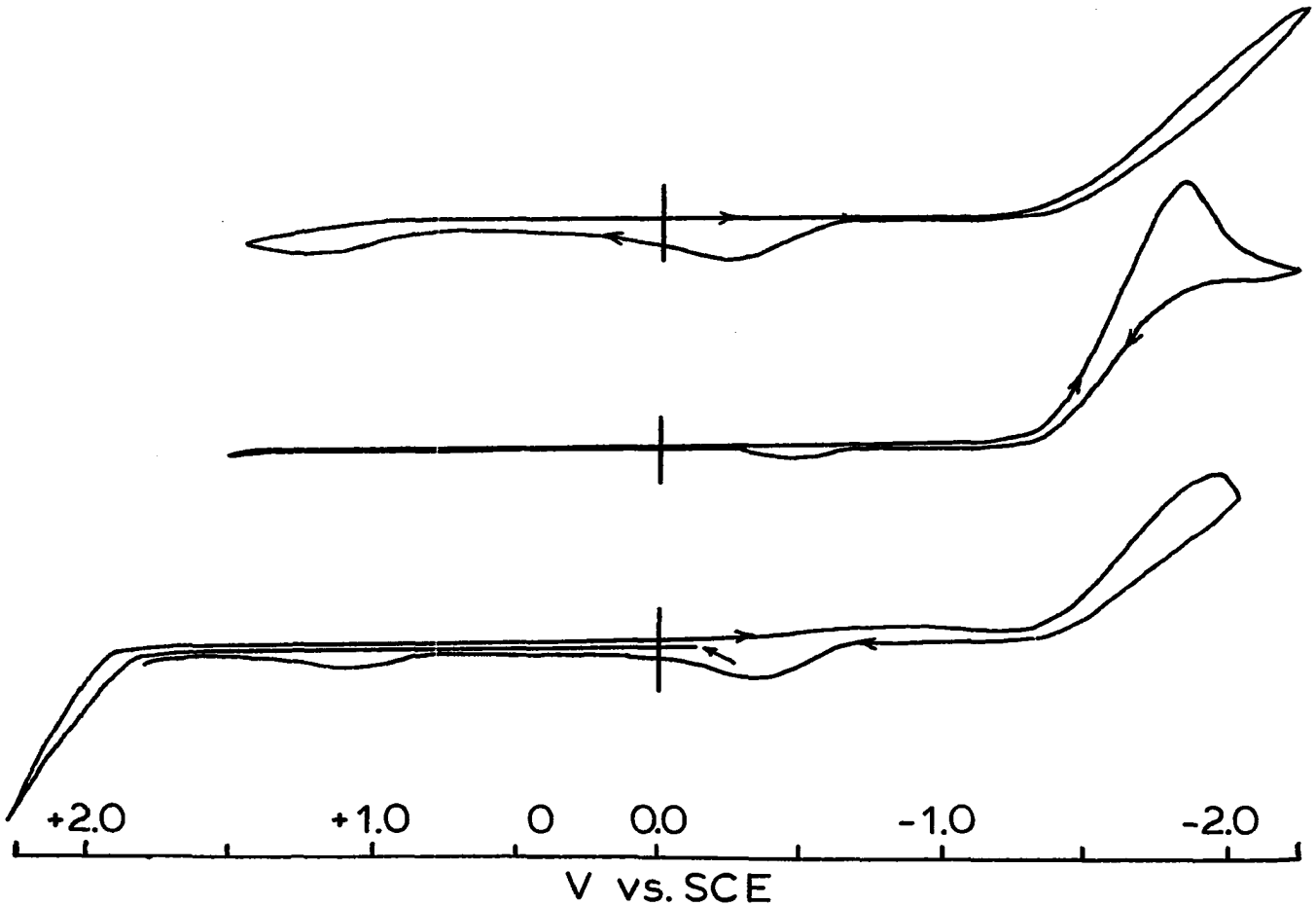

Figure 30. Cyclic voltammograms for $[Fe(t\text{-}BuDiNC)_3](PF_6)_2$

as shown in part c of Figure 30. This suggests that only a small amount of oxidation of the complex takes place, and that this process, like the reduction, is irreversible.

IV. CONCLUSION

This study of the coordination behavior of multidentate nitrile and isonitrile ligands was undertaken for several reasons. It was of interest to first characterize a number of pseudooctahedral chelate complexes, and to provide solid evidence that such structures are indeed capable of existence. A second area of investigation concerned other coordination modes, such as bridging or pseudotetrahedral chelating configurations, which these ligands might adopt. Finally, it was hoped that these ligands might form interesting complexes with unusual oxidation states or coordination numbers which have no analogs in the chemistry of the corresponding monodentate ligands. The chemical and spectroscopic properties of such molecules would be of interest from several points of view.

The bidentate nitrile ligands DiCN-3 and DiCN-4 are prepared in a manner identical to that previously reported[14,96] for the synthesis of DiCN-2. All three ligands react with $Mn(CO)_5Br$ to afford complexes of the type $Mn(CO)_3$(DiCN-n)Br. Where n = 2 and 3, the complexes appear to be mononuclear, and employ the DiCN-n ligands in their chelated forms. The structure of $Mn(CO)_3$(DiCN-4)Br remains questionable; the ligand might be either chelating or bridging. Competition experiments between the DiCN ligands and CH_3CN in the system $Mn_2(CO)_6(CH_3CN)_2(\mu\text{-}Br)_2$ show that DiCN-2 is a more efficient chelating agent than either DiCN-3 or DiCN-4. The DiCN ligands appear to constitute the first examples of

organodinitriles capable of chelating to a single metal center through the nitrogen lone pair. Further studies with the DiCN ligands would be useful in the determination of a quantitative measure of the chelate effect for these and ligands of similar structure.

The tridentate nitrile ligand, TriCN, is synthesized in six steps from 2-methylacetophenone in an overall yield of 12%. This ligand functions as either a bidentate ligand, as in $M(CO)_3(TriCN)Br$ (M = Mn or Re), or as a tridentate ligand, as in $[M(CO)_3(TriCN)]^+$ (M = Mn or Re). The rhenium complexes are fully characterized by ^1H and ^{13}C NMR spectrometry. Both methods distinguish between bidentate and tridentate binding modes of TriCN.

The bidentate isonitrile ligands SiNC-2 and SiNC-3 are synthesized in yields of 10% and 24%, respectively, from 2-nitroresorcinol. It was expected that these ligands would form 13- and 14-membered chelate rings, respectively, in reactions with $[Rh(COD)Cl]_2$. However, the SiNC-2 ligand affords a dinuclear dication, $[Rh_2(SiNC\text{-}2)_4]^{2+}$, which contains bridging SiNC-2 ligands. SiNC-3 yields the mononuclear cation, $[Rh(SiNC\text{-}3)_2]^+$. Steric interactions between bulky $-OSiMe_3$ groups are thought to preclude the formation of $[Rh(SiNC\text{-}2)_2]^+$, and may also prevent the oligomerization of $[Rh(SiNC\text{-}3)_2]^+$ in solution and the solid state. Both Rh complexes react very rapidly with halogen-containing substrates to give oxidative-addition products.

The synthesis of a macrocyclic tetraisonitrile complex of Rh(I) was not achieved when $[Rh_2(SiNC\text{-}2)_4](BPh_4)_2$ was treated with malonyl fluoride. However, mononuclear $[Rh(SiNC\text{-}3)_2]^+$ might be a promising starting material for the preparation of a macrocyclic complex.

An improved synthesis of the diisonitrile ligand t-BuDiNC is reported. This ligand and the non-butylated molecule, DiNC,[14,96] are seen to be capable of chelation at pseudooctahedral metal sites, as in $Cr(CO)_4(L\text{-}L)$, or at psuedotetrahedral sites, as in $Ni(CO)_2(L\text{-}L)$. In certain cases, these ligands will bridge between two metals, as in $[Cr(CO)_5]_2(\mu\text{-DiNC})$ and $\{[Co(t\text{-BuDiNC})_2]_2(\mu\text{-t-BuDiNC})\}(BF_4)_2$. Homoleptic d^6 complexes, $[M(t\text{-BuDiNC})_3]^{Z+}$ (M^{Z+} = Cr^o, Mn^+, Fe^{2+}, and Co^{3+}), have also been prepared. The Co(III) complex has no known analogs in isonitrile chemistry, while only one other homoleptic Fe(II) complex containing aromatic isonitriles is known. Spectroscopic investigations of this series of compounds show that there are large variations in the degree of $d\pi\text{-}\pi^*_{CN}$ back-bonding; such bonding is quite important for Cr^o and Mn^+, but is essentially nonexistent for Co^{3+}.

Thus, the multidentate ligands of the present research have shown themselves to possess rather rich coordination chemistries. While there appears to be no difficulty associated with the formation of chelate complexes in "normal" oxidation states and geometries, many reactions intended to form more unusual complexes were unsuccessful. The preparations of $[Fe(t\text{-BuDiNC})_3]^{2+}$ and $[Co(t\text{-BuDiNC})_3]^{3+}$ are exceptions, though the use of these synthetic methods with monodentate isonitriles remains untested.

Space-filling molecular models, which were used extensively in the design of all the ligands reported here, provide a reasonable picture of inter- and intramolecular interactions in these complexes. In certain cases, such as $Ni(CO)_2(DiNC)$ or $[Mn(CO)_3(TriCN)]^+$, the models appear to exaggerate the amount of strain which would be present in a molecule. On the other hand, the dinuclear structure of $[Rh_2(SiNC\text{-}2)_4]^{2+}$ was unexpected, even after the construction of molecular models. This latter failure suggests that the prediction of the products of such a reaction requires a prior consideration of alternate structures and the reaction mechanism.

V. REFERENCES

1. Jörgensen, S. M. J. Prakt. Chem. 1889, 39, 1.
2. Jörgensen, S. M. J. Prakt. Chem. 1890, 41, 440.
3. Werner, A. Z. Anorg. Allg. Chem. 1893, 3, 267.
4. Ley, H. Z. Elektrochem. 1904, 10, 954.
5. Spike, C. G.; Parry, R. W. J. Amer. Chem. Soc. 1953, 75, 2726.
6. Cotton, F. A.; Harris, F. E. J. Phys. Chem. 1955, 59, 1203.
7. Myers, R. T. Inorg. Chem. 1978, 17, 952.
8. Carrano, C. J.; Raymond, K. N. J. Amer. Chem. Soc. 1979, 101, 5401.
9. Durbin, P. W.; Jones, S.; Raymond, K. N.; Weitl, F. L. Rad. Res. 1980, 81, 170.
10. Langford, G. R.; Akhtar, M.; Ellis, P. D.; MacDiarmid, A. G.; Odom, J. D. Inorg. Chem. 1975, 14, 2937.
11. Chatt, J.; Watson, H. R. J. Chem. Soc. 1962, 2545.
12. Vineyard, B. D.; Knowles, W. S.; Sabacky, M. J.; Bachman, G. K.; Weinkauff, D. J. J. Amer. Chem. Soc. 1977, 99, 5946.
13. Williams, R. J. P. Inorg. Chim. Acta Revs. 1971, 5, 137.
14. Angelici, R. J.; Quick, M. H.; Kraus, G. A. Inorg. Chim. Acta 1980, 44, L137.
15. Kawakami, K.; Okajima, M.; Tanaka, T. Bull. Chem. Soc. Jpn. 1978, 51, 2327.
16. Yaneff, P. V.; Powell, J. J. Organomet. Chem. 1979, 179, 101.
17. Goddard, R.; Howard, J.; Woodward, P. J. Chem. Soc. Dalton Trans. 1974, 2025.
18. Storhoff, B. N.; Lewis, H. C., Jr. Coord. Chem. Revs. 1977, 23, 1.
19. Yamamoto, Y. Coord. Chem. Revs. 1980, 32, 193.

20. Bland, W. J.; Kemmitt, R. D. W.; Moore, R. D. J. Chem. Soc. Dalton Trans. 1973, 1292.

21. Krogmann, K.; Mattes, R. Angew. Chem. Int. Ed. Engl. 1966, 5, 1046.

22. Bock, H.; tom Dieck, H. Chem. Ber. 1966, 99, 213.

23. Sicher, J. Progr. Stereochem. 1962, 3, 202.

24. Eliel, E. L.; Allinger, N. L.; Angyal, S. J.; Morrison, G. A. "Conformational Analysis", Wiley-Interscience: New York, 1965; Chapter 4.

25. Ogino, H.; Fujita, J. Bull. Chem. Soc. Jpn. 1975, 48, 1836.

26. Dale, J. J. Chem. Soc. 1963, 93.

27. Adamson, A. W. J. Amer. Chem. Soc. 1954, 1578.

28. Al-Salem, N. A.; Empsall, H. D.; Markham, R.; Shaw, B. L., Weeks, B. J. Chem. Soc. Dalton Trans. 1979, 1972.

29. Schwarzenbach, G. Helv. Chim. Acta 1952, 35, 2344.

30. Smith, G. F.; Margerum, D. W. J. Chem. Soc. Chem. Comm. 1975, 807.

31. Hinz, F. P.; Margerum, D. W. Inorg. Chem. 1974, 13, 2941.

32. Hinz, F. P.; Margerum, D. W. J. Amer. Chem. Soc. 1974, 96, 4993.

33. Joris, L.; Mitsky, J.; Taft, R. W. J. Amer. Chem. Soc. 1972, 94, 3438.

34. Gillis, R. G.; Occolowitz, J. L. Spectrochim. Acta 1963, 19, 873.

35. Barnhart, D. M.; Caughlin, C. N.; ul-Haque, M. Inorg. Chem. 1969, 8, 2768.

36. Barnhart, D. M.; Caughlin, C. N.; ul-Haque, M. Inorg. Chem. 1968, 7, 1135.

37. Greene, D. L.; Sears, P. G. J. Inorg. Nucl. Chem. 1973, 35, 1471.

38. Walton, R. A. Quart. Rev. Chem. Soc. 1965, 19, 126.

39. Greene, D. L.; Sears, P. G.; Krippendorf, J. Inorg. Nuc. Chem. Lett. 1974, 10, 895.

40. Farona, M. F.; Bremer, N. J. J. Amer. Chem. Soc. 1966, 88, 3735.

41. Farona, M. F.; Kraus, K. F. Inorg. Chem. 1970, 9, 1700.

42. Dunn, J. G.; Edwards, D. A. Chem. Comm. 1971, 482.

43. Dunn, J. G.; Edwards, D. A. J. Organomet. Chem. 1975, 102, 199.

44. Payne, D. H.; Frye, H. Inorg. Nuc. Chem. Lett. 1973, 9, 2540.

45. Payne, D. H.; Payne, Z. A.; Rohmer, R. A.; Frye, H. Inorg. Chem. 1973, 12, 2540.

46. Storhoff, B. N.; Infante, A. J. Inorg. Chem. 1974, 13, 3043.

47. Storhoff, B. N. J. Organomet. Chem. 1972, 43, 197.

48. Hohmann, F.; tom Dieck, H. J. Organomet. Chem. 1975, 85, 47.

49. Davies, J. A.; Hartley, F. R.; Murray, S. G. J. Chem. Soc. Dalton Trans. 1980, 2246.

50. Usón, R.; Oro, L. A.; Artigas, J.; Sariego, R. J. Organomet. Chem. 1979, 179, 65.

51. Green, M.; Parker, G. J. J. Chem. Soc. Dalton Trans. 1974, 333.

52. Dart, J. W.; Lloyd, M. K.; Mason, R.; McCleverty, J. A. J. Chem. Soc. Dalton Trans. 1973, 2039.

53. Olmstead, M. O.; Balch, A. L. J. Organomet. Chem. 1978, 148, C15.

54. Balch, A. L.; Olmstead, M. O. J. Amer. Chem. Soc. 1979, 101, 3128.

55. Mann, K. R.; Lewis, N. S.; Miskowski, V. M.; Erwin, D. K.; Hammond, G. S.; Gray, H. B. J. Amer. Chem. Soc. 1977, 99, 5525.

56. Mann, K. R.; Lewis, N. S.; Williams, R. M.; Gray, H. B.; Gordon, J. G., II. Inorg. Chem. 1978, 17, 828.

57. Miskowski, V. M.; Nobinger, G. L.; Kliger, D. S.; Hammond, G. S.; Lewis, N. S.; Mann, K. R.; Gray, H. B. J. Amer. Chem. Soc. 1978, 100, 485.

58. Mann, K. R.; Thich, J. A.; Bell, R. A.; Coyle, C. L.; Gray, H. B. Inorg. Chem. 1980, 19, 2462.

59. Ohtani, Y.; Miya, S.; Yamamoto, Y.; Yamazaki, H. Inorg. Chim. Acta 1981, 53, 653.

60. Gladfelter, W. L.; Gray, H. B. J. Amer. Chem. Soc. 1980, 102, 5909.

61. Efraty, A.; Feinstein, I.; Wackerle, L.; Frolow, F. Ang. Chem. Int. Ed. Engl. 1980, 19, 633.

62. Efraty, A.; Feinstein, I.; Frolow, F.; Wackerle, L. J. Amer. Chem. Soc. 1980, 102, 6342.

63. Efraty, F.; Feinstein, I.; Frolow, F. Inorg. Chem. 1982, 21, 485.

64. Efraty, A.; Feinstein, I. Inorg. Chim. Acta 1981, 54, L211.

65. Howell, J. A. S.; Rowan, A. J. J. Chem. Soc. Dalton Trans. 1981, 297.

66. Michelin, R. A.; Angelici, R. J. Inorg. Chem. 1980, 19, 3853.

67. Ito, Y.; Kobayashi, K.; Seko, N.; Saegusa, T. Heterocycles 1981, 16, 181.

68. Stille, J. K.; Fritschel, S. J.; Takaishi, N.; Masuda, T. Ann. N. Y. Acad. Sci. 1980, 333, 35.

69. Nagel, U.; Menzel, H.; Lednor, P. W.; Beck, W.; Guyot, A.; Bartholin, M. Z. Naturforsch. 1981, 36b, 578.

70. Skorna, G.; Stemmer, R.; Ugi, I. Chem. Ber. 1978, 111, 806

71. Ugi, I.; Skorna, G. Chem. Ber. 1978, 111, 3965.

72. Howell, J. A. S.; Berry, M. J. Chem. Soc. Chem. Comm. 1980, 1039.

73. Evans, J.; Gracey, B. P. J. Organomet. Chem. 1982, 228, C4.

74. Menzel, H.; Fehlhammer, W. P.; Beck, W. Z. Naturforsch. 1982, 37b, 201.

75. Shriver, D. F. "The Manipulation of Air-sensitive Compounds"; McGraw-Hill: New York, 1969; pp. 141-158.

76. Gordon, A. J.; Ford, R. A. "The Chemist's Companion"; Wiley-Interscience: New York, 1972; p. 185.

77. Ramsay, D. A. J. Amer. Chem. Soc. 1952, 74, 72.

78. Russell, R. A.; Thompson, H. W. Spectrochim. Acta 1957, 9, 133.

79. Gansow, O. A.; Burke, A. R.; Lamar, G. N. J. Chem. Soc. Chem. Comm. 1972, 456.

80. Pretsch, E.; Clerc, T.; Seibl, J. "Strukturaufklärung Organischer Verbindungen"; Springer-Verlag: West Berlin, 1976; pp. C120, 125.

81. Silverstein, R. M.; Bassler, G. C.; Morrill, T. C. "Spectrometric Identification of Organic Compounds", 4th ed.; Wiley: New York, 1981; pp. 265-266.

82. Lind, J. E., Jr.; Abdel-Rahim, H. A. A.; Rudich, S. W.; J. Phys. Chem. 1966, 70, 3610.

83. Krimen, L. I. Org. Synth. 1970, 50, 1.

84. Landini, D.; Rolla, F. Chem. Ind. 1979, 213.

85. Althoff, W.; Fild, M. Z. Naturforsch. B 1973, 28, 98.

86. Raha, C. Org. Synth. 1953, 33, 20.

87. Reimer, K. J.; Shaver, A. Inorg. Synth. 1979, 19, 159.

88. Quick, M. H.; Angelici, R. J. Inorg. Synth. 1979, 19, 160.

89. Angelici, R. J.; Kruse, A. E. J. Organomet. Chem. 1970, 22, 461.

90. Dunn, J. G.; Edwards, D. A. J. Organomet. Chem. 1971, 27, 73.

91. Eisch, J. J.; King, R. B. "Organometallic Syntheses"; Academic Press: New York, 1965; Vol. 1, pp. 122-125.

92. Abel, E. W.; Butler, I. S.; Reid, J. G. J. Chem. Soc. 1963, 2068.

93. Busetto, L.; Angelici, R. J. Inorg. Chim. Acta 1968, 2, 391.

94. Knol, D.; Koole, N. J.; DeBie, M. J. A. Org. Mag. Res. 1976, 8, 213.

95. Chatt, J.; Venanzi, L. M. J. Chem. Soc. A 1957, 4735.

96. Angelici, R. J.; Quick, M. H.; Kraus, G. A.; Plummer, D. T. Inorg. Chem. 1982, 21, 2178.

97. Wirth, H. O.; Kern, W.; Schmitz, E. Makromol. Chem. 1963, 68, 69.

98. DeStefano, N. J.; Johnson, D. K.; Lane, R. M.; Venanzi, L. M. Helv. Chim. Acta 1976, 59, 2674.

99. Bentley, T. J.; McGhie, J. F.; Barton, D. H. R. Tetrahedron Lett. 1965, 2497.

100. Schnekenburger, J. Fresenius' Z. Anal. Chem. 1973, 263, 23.

101. Spurlock, L. A.; Schultz, R. J. J. Amer. Chem. Soc. 1970, 92, 6302.

102. Sorkin, E.; Roth, W.; Erlenmeyer, H. Helv. Chim. Acta 1952, 35, 1736.

103. Jenkins, G. L.; Knevel, A. M.; Davis, C. S. J. Org. Chem. 1961, 26, 274.

104. Lane, E. S.; Williams, C. W. J. Chem. Soc. 1956, 569.

105. Lewis, N. S.; Mann, K. R.; Gordon, J. G., II; Gray, H. B. J. Amer. Chem. Soc. 1976, 98, 7461.

106. Nakanishi, H.; Yamamoto, O. Chem. Lett. 1974, 521.

107. Mann, K. R.; Cimolino, M.; Geoffroy, G. L.; Hammond, G. S.; Orio, A. A.; Albertin, G.; Gray. H. B. Inorg. Chim. Acta 1976, 16, 97.

108. Geary, W. J. Coord. Chem. Rev. 1971, 7, 81.

109. Noack, K. Helv. Chim. Acta 1962, 45, 1847.

110. Coerver, H. J.; Curran, C. J. Amer. Chem. Soc. 1958, 80, 3522.

111. Emeléus, H. J.; Rao, G. S. J. Chem. Soc. 1958, 4245.

112. VanDriel, C. A. A.; Groeneveld, W. L. Rec. Trav. Chim. 1971, 90, 389.

113. Strohmeier, W.; Guttenberger, J. F.; Müller, F. J. Z. Naturforsch. 1967, 22B, 1091.

114. Clarke, R. E.; Ford, P. C. Inorg. Chem. 1970, 9, 227.

115. Reedijk, J.; Groenevald, W. L. Rec. Trav. Chim. 1968, 87, 1079.

116. Reedijk, J.; Zuur, A. P.; Groeneveld, W. L. Rec. Trav. Chim. 1967, 86, 1127.

117. Sen, A.; Lai, T-W. J. Amer. Chem. Soc. 1981, 103, 4627.

118. Dobson, G. R.; ElSayed, M. F. A.; Stolz, I. W.; Sheline, R. K. Inorg. Chem. 1962, 1, 526.

119. Farona, M. F.; Grasselli, J. G.; Ross, B. L. Spectrochim. Acta Part A 1967, 23, 1875.

120. Riemann, R. H.; Singleton, E. J. Organomet. Chem. 1973, 59, C24.

121. Gill, T. P.; Mann, K. R. Organomet. 1982, 1, 485.

122. Fairhurst, G.; White, C. J. Chem. Soc. Dalton Trans. 1979, 1524.

123. White, C.; Thompson, S. J.; Maitlis, P. M. J. Chem. Soc. Dalton Trans. 1977, 1654.

124. Bennett, M. A.; Smith, A. K. J. Chem. Soc. Dalton Trans. 1974, 233.

125. Mortenson, C. W.; Spielman, H. A. J. Amer. Chem. Soc. 1940, 62, 1609.

126. Angelici, R. J.; Blacik, J. L. Inorg. Chem. 1972, 11, 1754.

127. Issleib, K.; Tzschach, A. Chem. Ber. 1959, 92, 1118.

128. Nesmeyanov, A. N.; Struchkov, Y. T.; Andrianov, V. G.; Krivykh, V. V.; Rybinskaya, M. I. J. Organomet. Chem. 1979, 166, 211.

129. Adams, D. M. "Metal-Ligand and Related Vibrations"; Edward Arnold: London, 1967.

130. Bamford, C. H.; Burley, J. W.; Coldbeck, M. J. Chem. Soc. Dalton Trans. 1972, 1846.

131. Drew, D.; Darensbourg, D. J.; Darensbourg, M. Y. Inorg. Chem. 1975, 1579.

132. Usón, R.; Riera, V.; Gimeno, J.; Laguna, M.; Gamasa, P. M. J. Chem. Soc. Dalton Trans. 1979, 996.

133. Todd, L. J.; Wilkinson, J. R. J. Organomet. Chem. 1974, 80, C31.

134. Casey, C. P.; Neumann, S. M. J. Amer. Chem. Soc. 1978, 100, 2545.

135. Mann, B. E.; Taylor, B. F. "^{13}C NMR Data for Organometallic Compounds" Academic Press: New York, 1981; Chapter 2.

136. Collman, J. P.; Kittleman, E. T. Inorg. Synth. 1966, VIII, 150.

137. Kern, R. J. J. Inorg. Nucl. Chem. 1963, 25, 5.

138. Brown, T. L.; Kubota, M. J. Amer. Chem. Soc. 1961, 83, 331.

139. Brown, T. L.; Kubota, M. J. Amer. Chem. Soc. 1961, 83, 4175.

140. Ulich, E.; Hertel, E.; Nespital, W. Z. Physik. Chem. 1932, B17, 21.

141. DeHand, J.; Rosé, J. J. Chem. Res. (S) 1979, 155.

142. Ugi, I., ed. "Isonitrile Chemistry"; Academic Press: New York, 1971.

143. Malatesta, L.; Bonati, F. "Isocyanide Complexes of Metals"; Wiley-Interscience: New York, 1969.

144. Treichel, P. M. Adv. Organomet. Chem. 1973, 11, 21.

145. Bonati, F.; Minghetti, G. Inorg. Chim. Acta 1974, 9, 95.

146. Meyer, E. J. Prakt. Chem. 1856, 68, 279.

147. Fantucci, P.; Naldini, L.; Cariati, F.; Valenti, V.; Bussetto, C. J. Organomet. Chem. 1974, 64, 109.

148. Bursten, B. E.; Fenske, R. F. Inorg. Chem. 1977, 16, 963.

149. Adams, R. D. J. Amer. Chem. Soc. 1980, 102, 7476, and references cited therein.

150. Novotny, M.; Lewis, D. F.; Lippard, S. J. J. Amer. Chem. Soc. 1972, 94, 6961.

151. Lux, F.; Bufe, U. E. Ang. Chem. Int. Ed. Engl. 1971, 10, 274.

152. Schröder, R.; Schöllkopf, U.; Blüme, E.; Hoppe, I. Liebigs Ann. Chem. 1975, 533.

153. Geoffroy, G. L.; Isci, H.; Litrenti, J.; Mason, W. R. Inorg. Chem. 1977, 16, 1950.

154. Mann, K. R.; Gordon, J. G. II; Gray, H. B. J. Amer. Chem. Soc. 1975, 97, 3553.

155. Winzenburg, M. L.; Kargol, J. A.; Angelici, R. J. manuscript in preparation. Department of Chemistry, Iowa State University.

156. Endres, H.; Gottstein, N.; Keller, H. J.; Martin, W. R.; Steiger, W. Z. Naturforsch. 1979, 34b, 827.

157. Yamamoto, Y.; Aoki, K.; Yamazaki, H. Inorg. Chem. 1979, 18, 1681.

158. Plummer, D. T.; Karcher, B. A.; Jacobson, R. A.; Angelici, R. J. manuscript in preparation.

159. Parish, R. V.; Simms, P. G. J. Chem. Soc. Dalton Trans. 1972, 809.

160. Balch, A. L.; Olmstead, M. M. J. Amer. Chem. Soc. 1976, 98, 2354.

161. Kuwae, R.; Tanaka, T. Bull. Chem. Soc. Jpn. 1979, 52, 1067.

162. Corey, E. J.; Vankateswarlu, A. J. Amer. Chem. Soc. 1972, 94, 6190.

163. Badley, E. M.; Chatt, J.; Richards, R. L. J. Chem. Soc. A 1971, 21.

164. Andrianov, K. A.; Dabagova, A. K.; Shokina, V. V.; Knunyants, I. L. Izv. Akad. Nauk SSSR Ser. Khim. 1974, 2063; Chem. Abstr. 1975, 82, 43505d.

165. Gibson, J. A.; Janzen, A. F. Can. J. Chem. 1972, 50, 3087.

166. Junek, H.; Ziegler, E.; Herzog, U.; Krobarth, H. Synthesis 1976, 332.

167. Nikolenko, L. N.; Karpova, E. N.; Vorozhtsov, G. N.; Sergeev, V. A.; Ivanova, M. E. Zhur. Obsch. Khim. 1960, 30, 1336; Chem. Abstr. 1961, 55, 426b.

168. Cannon, R. D.; Chiswell, B.; Venanzi, L. M. J. Chem. Soc. A 1967, 1277.

169. Freifelder, M. "Catalytic Hydrogenation in Organic Synthesis"; Wiley: New York, 1978.

170. Huffman, C. W. J. Org. Chem. 1958, 23, 727.

171. Siddall, T. H.; Stewart, W. E.; Marston, A. L. J. Phys. Chem. 1968, 72, 2135.

172. Ugi, I.; Fetzer, U.; Erholzer, U.; Knupfer, H.; Offerman, K. Angew. Chem. Int. Ed. Engl. 1965, 4, 472.

173. Appel, R.; Kleinstück, R.; Ziehn, K.-D. Angew. Chem. Int. Ed. Engl. 1971, 10, 132.

174. Hieber, W.; vonPigeot, D. Chem. Ber. 1956, 89, 616.

175. Bigorgne, M. Bull. Soc. Chim. (France) 1963, 295.

176. King, R. B.; Saran, M. S. Inorg. Chem. 1974, 13, 74.

177. Hieber, W.; Abeck, W.; Platzer, H. K. Z. Anorg. Allgem. Chem. 1955, 252, 280.

178. Cotton, F. A.; Zingales, F. J. Amer. Chem. Soc. 1961, 83, 351.

179. Connor, J. A.; Jones, E. M.; McEwen, G. K.; Lloyd, M. K.; McCleverty, J. A. J. Chem. Soc. Dalton Trans. 1972, 1246.

180. Murdoch, H. D.; Henzi, R. J. Organomet. Chem. 1966, 5, 166.

181. Albers, M. D.; Coville, N. J.; Ashworth, T. V.; Singleton, E.; Swanepoel, H. E. J. Organomet. Chem. 1980, 199, 55.

182. Coville, N. J.; Albers, M. O. Inorg. Chim. Acta 1982, 65, L7.

183. King, R. B. Inorg. Chem. 1963, 2, 936.

184. Darensbourg, D. J.; Kump, R. L. Inorg. Chem. 1978, 17, 2680.

185. Cronin, D. L.; Wilkinson, J. R.; Todd, L. J. J. Magn. Reson. 1975, 17, 353.

186. Kargol, J. A.; Angelici, R. J. manuscript in preparation.

187. Taylor, R. C.; Horrocks, W. D., Jr. Inorg. Chem. 1964, 3, 584.

188. Mays, M. J.; Prater, B. E. J. Chem. Soc. A. 1969, 2525.

189. Bonati, F.; Minghetti, G. J. Organomet. Chem. 1970, 22, 195.

190. Schindler, J. W.; Luoma, J. R.; Cusick, J. P. Inorg. Chim. Acta 1974, 10, 203.

191. Albertin, G.; Bordignon, E.; Orio, A. A.; Troilo, G. Inorg. Chem. 1975, 14, 238.

192. Canziani, F.; Cariati, F.; Sartorelli, U. 1st. Lombardo (Rend. Sci.) A 1964, 98, 564.

193. Sacco, A. Atti. Acad. naz. Lincei. Rend. Classe Sci. Fis. Mat. [VIII] 1953, 15, 82.

194. Albers, M. O.; Coville, N. J.; Ashworth, T. V.; Singleton, E.; Swanepoel, H. E. J. Chem. Soc. Chem. Comm. 1980, 489.

195. Klein, H. F.; Karsch, H. H. Inorg. Chem. 1975, 14, 473.

196. Aresta, M.; Rossi, M.; Sacco, A. Inorg. Chim. Acta 1969, 3, 227.

197. Powell, E. W.; Mays, M. J. J. Organomet. Chem. 1974, 66, 137.

198. Becker, C. A. L. J. Inorg. Nucl. Chem. 1975, 37, 703.

199. Kawakami, K.; Okajima, M. J. Inorg. Nucl. Chem. 1979, 41, 1501.

200. Feltham, R. D.; Hayter, R. G. J. Chem. Soc. 1964, 4587.

201. King, R. B.; Saran, M. S. Inorg. Chem. 1972, 11, 2112.

202. Hieber, W.; Böckly, E. Z. Anorg. Chem. 1950, 262, 344.

203. Klages, F.; Mönkemeyer, K. Chem. Ber. 1950, 83, 501.

204. Otsuka, S.; Nakamura, A.; Tatsuno, Y. J. Amer. Chem. Soc. 1969, 91, 6994.

205. Thomas, M. G.; Pretzer, W. R.; Beier, B. F.; Hireskorn, F. J.; Muetterties, E. L. J. Amer. Chem. Soc. 1977, 99, 743.

206. Behrens, H.; Meyer, K. Z. Naturforsch. 1966, 21B, 489.

207. Nast, R.; Schultz, H. Chem. Ber. 1970, 103, 785.

208. Band, E.; Pretzer, W. R.; Thomas, M. G.; Muetterties, E. L. J. Amer. Chem. Soc. 1977, 99, 7380.

209. Nolte, R. J. M.; Stephany, R. W.; Drenth, W. Rec. Trav. Chim. 1973, 92, 83.

210. Stephany, R. W.; Nolte, R. J. M.; Dreuth, W. Rec. Trav. Chim. 1973, 92, 275.

211. Stephany, R. W.; Drenth, W. Rec. Trav. Chim. 1972, 91, 1453.

212. Miller, J. S.; Balch, A. L. Inorg. Chem. 1972, 11, 2069.

213. Otsuka, S.; Nakamura, A.; Tatsuno, Y.; Miki, M. J. Amer. Chem. Soc. 1972, 94, 3761.

214. Cherwinski, W. J.; Clark, H. C.; Manzer, L. E. Inorg. Chem. 1972, 11, 1511.

215. van Hecke, G. R.; Horrocks, W. D. Inorg. Chem. 1966, 5, 1960.

216. Ljungström, E. Acta Chem. Scand. 1978, 32A, 47.

217. Otsuka, S.; Nakamura, A.; Yoshida, T. J. Chem. Soc. Chem. Comm. 1967, 836.

218. Gill, N. S.; Taylor, F. B. Inorg. Synth. 1967, 9, 136.

219. a) Otsuka, S.; Nakamura, A.; Yoshida, T. J. Amer. Chem. Soc. 1969, 91, 7196;

b) Otsuka, S.; Nakamura, A.; Yoshida, T.; Naruto, M.; Ataka, K. J. Amer. Chem. Soc. 1975, 95, 3180.

220. Klages, F.; Mönkemeyer, K.; Heinle, R. Chem. Ber. 1952, 85, 109.

221. Bailey, J.; Mays, M. J. J. Organomet. Chem. 1973, 47, 217.

222. Stephany, R.; Drenth, W. Rec. Trav. Chim. 1970, 89, 305.

223. Saegusa, T.; Ho, Y.; Kinoshita, H.; Tomita, S. J. Org. Chem. 1971, 36, 3316.

224. Saegusa, T.; Ho, Y.; Tomita, S.; Kinoshita, H. J. Org. Chem. 1970, 35, 670.

225. Saegusa, T.; Ho, Y.; Tomita, S. J. Amer. Chem. Soc. 1971, 93, 5656.

226. Speck, A. L. Cryst. Struct. Comm. 1982, 11, 413.

227. Essenmacher, G. J.; Treichel, P. M. Inorg. Chem. 1977, 16, 800.

228. Bohling, D. A.; Evans, J. F.; Mann, K. R. Inorg. Chem. 1982, 21, 3546.

229. Treichel, P. M.; Essenmacher, G. J. Inorg. Chem. 1976, 15, 146.

230. a) Mialki, W. S.; Wigley, D. E.; Wood, T. E.; Walton, R. A. Inorg. Chem. 1982, 21, 480;

b) Mialki, W. S.; Wood, T. E.; Walton, R. A. J. Amer. Chem. Soc. 1980, 102, 7105.

231. Treichel, P. M.; Dirreen, G. E.; Mueh, H. J. J. Organomet. Chem. 1972, 44, 339.

232. Treichel, P. M.; Firsich, D. W.; Essemacher, G. P. Inorg. Chem. 1979, 18, 2405.

233. Treichel, P. M.; Dirreen, G. E. J. Organomet. Chem. 1972, 39, C20.

234. Mann, K. R.; Gray, H. B.; Hammond, G. S. J. Amer. Chem. Soc. 1977, 99, 306.

235. a) Iuchi, K.; Asada, S.; Sugimori, A. Chem. Lett. 1974, 801;

b) Iuchi, K.; Asada, S.; Kinugasa, T.; Kanamori, K.; Sugimori, A. Bull. Chem. Soc. Jpn. 1976, 49, 577.

236. Gray, H. B.; Mann, K. R.; Lewis, N. S.; Thich, J. A.; Richman, R. M. Adv. Chem. Ser. 1978, 168, 44.

237. Bamford, C. H.; Eastmond, G. O.; Hargreaves, K. Nature 1965, 205, 385.

238. a) Brit. Patent 854,615; Chem. Abstr. 1961, 55, 10977i;

b) Ital. Patent 599,661; Chem. Abstr. 1961, 55, 18193c.

239. Silverman, L. D.; Dewan, J. C.; Giandomenico, C. M., Lippard, S. J. Inorg. Chem. 1980, 19, 3379.

240. Silverman, L. D.; Corfield, P. W. R.; Lippard, S. J. Inorg. Chem. 1981, 20, 3106.

241. Malatesta, L.; Sacco, A.; Ghielmi, S. Gazz. Chim. Ital. 1952, 82, 516.

242. Timms, P. L.; Turney, T. W. J. Chem. Soc. Dalton Trans. 1976, 2021.

243. Müller, J.; Holzinger, W. Z. Naturforsch. B., 1978, 33B, 1309.

244. Malatesta, L.; Sacco, A.; Gabaglio, M. Gazz. Chim. Ital. 1952, 82, 548.

245. Malatesta, L.; Sacco, A. Ann. Chim. (Italy) 1953, 43, 622.

246. a) Klendworth, D. D.; Welters, W. W., III; Walton, R. A. Organomet. 1982, 1, 336;

b) Klendworth, D. D.; Welters, W. W. III; Walton, R. A. J. Organomet. Chem. 1981, 213, C13.

247. Giandomenico, C. M.; Hanau, L. H.; Lippard, S. J. Organomet. 1982, 1, 142.

248. Brant, P.; Cotton, F. A.; Sekutowski, J. C.; Wood, T. E.; Walton, R. A. J. Amer. Chem. Soc. 1979, 101, 6588.

249. Mialki, W. S.; Wild, R. E.; Walton, R. A. Inorg. Chem. 1981, 20, 1380.

250. a) Sacco, A. Gazz. Chim. Ital. 1956, 86, 201.

b) Sacco, A.; Naldini, L. Gazz. Chim. Ital. 1956, 86, 207.

251 Joshi, K. K.; Pauson, P. L.; Stubbs, W. H. J. Organomet. Chem. 1963, 1, 51.

252. Naldini, L. Gazz. Chim. Ital. 1960, 90, 871.

253. Matteson, D. S.; Bailey, R. A. J. Amer. Chem. Soc. 1969, 91, 1975.

254. Sacco, A. Ann. Chim. (Italy) 1958, 48, 225; Chem. Abstr. 1959, 53, 204g.

255. Freni, M.; Valenti, V. Gazz. Chim. Ital. 1961, 91, 1352.

256. Treichel, P. M.; Williams, J. P. J. Organomet. Chem. 1977, 135, 39.

257. Allison, J. D.; Wood, T. E.; Wild, R. E.; Walton, R. A. Inorg. Chem. 1982, 21, 3540.

258. Girolami, G. S.; Anderson, R. A. Inorg. Chem. 1981, 20, 2040.

259. a) Hartley, E. G. J. J. Chem. Soc. 1910, 97, 1066;

b) Hartley, E. G. J. J. Chem. Soc. 1912, 101, 705;

c) Hartley, E. G. J.; Powell, H. M. J. Chem. Soc. 1933, 101.

260. Heldt, W. Z. J. Inorg. Nucl. Chem. 1961, 22, 305.

261. Malhotra, S. C. J. Inorg. Nucl. Chem. 1963, 25, 971.

262. Doonan, D. J.; Balch, A. L. Inorg. Chem. 1974, 13, 921.

263. Schaal, M.; Beck, W. Ang. Chem. Int. Ed. Engl. 1972, 11, 527.

264. a) King, R. B. Accts. Chem. Res. 1980, 13, 243.

b) Mann, K. R. personal communication, Department of Chemistry, University of Minnesota.

265. Mann, K. R.; Gray, H. B.; Hammond, G. S. J. Amer. Chem. Soc. 1977, 99, 306.

266. Johnson, H. W., Jr.; Krutzsch, H. J. Org. Chem. 1967, 32, 1939.

267. Padoa, G. Ann. Chim. (Italy) 1955, 45, 28.

268. Bonati, F.; Minghetti, G. J. Organomet. Chem. 1970, 24, 251.

269. Braterman, P. S. "Metal Carbonyl Spectra", Academic Press: New York, 1975.

270. Huheey, J. E. "Inorganic Chemistry", 2nd ed.; Harper and Row: New York, 1978; Chapter 2.

271. Kettle, S. F. A.; Paul, I. Advan. Organomet. Chem. 1972, 10, 199.

272. Darensbourg, D. J.; Hyde, C. L. Inorg. Chem. 1971, 10, 431.

273. Butler, I. S.; Johansson, D. A. Inorg. Chem. 1975, 14, 701.

274. Oehme, G.; Modler, A. Z. Anorg. Allg. Chem. 1979, 449, 157.

275. Ugi, I.; Meyr, R. Chem. Ber. 1960, 93, 239.

276. Brown, T. L.; Darensbourg, D. J. Inorg. Chem. 1967, 6, 971.

277. Bursten, B. E. J. Amer. Chem. Soc. 1982, 104, 1299.

278. Nicholson, R. S. Anal. Chem. 1965, 37, 1351.

VI. ACKNOWLEDGEMENTS

I am deeply indebted to Dr. Robert J. Angelici for his guidance, encouragement, and support throughout the course of this work. I wish to thank Dr. James H. Espenson, Dr. George A. Kraus, Dr. Robert E. McCarley, and Dr. Bernard J. White for their assistance over the years, their service on the committee, and their review of this dissertation. I wish also to thank Dr. Owen L. York, Dr. James A. Pappenhagen and Dr. Gordon L. Johnson for their fine introductions to chemistry and their personal guidance. I gratefully acknowledge the efforts of Lynn Moore, who typed this manuscript. Finally, I'd like to express my gratitude toward my family and friends, who, being there more often than needed, made all the difference.